

# LOAN DOCUMENT

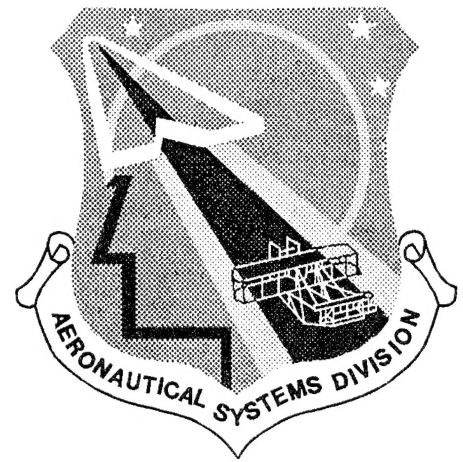
DTIC ACCESSION NUMBER	PHOTOGRAPH THIS SHEET																		
	LEVEL																		
	INVENTORY																		
DOCUMENT IDENTIFICATION																			
DISTRIBUTION STATEMENT																			
<table border="1"><tr><td colspan="2">ACCESSION FOR</td></tr><tr><td>NTIS</td><td>GRAB</td></tr><tr><td>DTIC</td><td>TRAC</td></tr><tr><td>UNANNOUNCED</td><td></td></tr><tr><td>JUSTIFICATION</td><td></td></tr><tr><td colspan="2">BY</td></tr><tr><td colspan="2">DISTRIBUTION/</td></tr><tr><td colspan="2">AVAILABILITY CODES</td></tr><tr><td>DISTRIBUTION</td><td>AVAILABILITY AND/OR SPECIAL</td></tr></table>	ACCESSION FOR		NTIS	GRAB	DTIC	TRAC	UNANNOUNCED		JUSTIFICATION		BY		DISTRIBUTION/		AVAILABILITY CODES		DISTRIBUTION	AVAILABILITY AND/OR SPECIAL	DATE ACCESSIONED
ACCESSION FOR																			
NTIS	GRAB																		
DTIC	TRAC																		
UNANNOUNCED																			
JUSTIFICATION																			
BY																			
DISTRIBUTION/																			
AVAILABILITY CODES																			
DISTRIBUTION	AVAILABILITY AND/OR SPECIAL																		
DISTRIBUTION STAMP																			
DATE RECEIVED IN DTIC																			
REGISTERED OR CERTIFIED NUMBER																			
PHOTOGRAPH THIS SHEET AND RETURN TO DTIC-FDAC																			

H  
A  
N  
D  
L  
E  
  
W  
I  
T  
H  
  
C  
A  
R  
E

1000

**ASD-TR-90-5002**

**EVALUATION OF THE F/FB/EF-111  
GROUND COLLISION AVOIDANCE  
SYSTEM (GCAS)**



**John A. Hassoun  
G. Fred Ward, Capt., USAF  
James M. Barnaba  
Donald L. McCarthy, C1C, USAFA**

**CREW STATION EVALUATION FACILITY  
HUMAN FACTORS BRANCH  
ASD/ENECH  
WRIGHT-PATTERSON AFB, OHIO 45433**

**DECEMBER 1989**

**FINAL COPY FOR THE PERIOD MAY 1988 THROUGH JUNE 1989**

Approved for public release; distribution is unlimited.


**DCS FOR INTEGRATED ENGINEERING AND TECHNICAL MANAGEMENT  
AERONAUTICAL SYSTEMS DIVISION  
AIR FORCE SYSTEMS COMMAND  
WRIGHT-PATTERSON AFB, OHIO 45433-6503**

## NOTICE

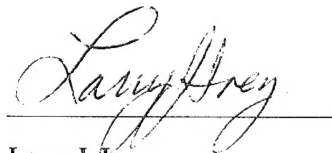
When Government drawings, specifications, or other data are used for any purpose other than in connection with a definitely Government-related procurement, the United States Government incurs no responsibility or any obligation whatsoever. The fact that the government may have formulated or in any way supplied the said drawings, specifications, or other data, is not to be regarded by implication, or otherwise in any manner construed, as licensing the holder, or any other person or corporation; or as conveying any rights or permission to manufacture, use, or sell any patented invention that may in any way be related thereto.

This report is releasable to the National Technical Information Service (NTIS). At NTIS, it will be available to the general public, including foreign nations.

This technical report has been reviewed and is approved for publication.

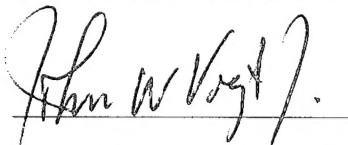


John A. Hassoun  
Program Manager  
Crew Station Evaluation Facility



Larry J. Ivey  
Technical Specialist  
Human Factors Branch

FOR THE COMMANDER



John W. Vogt, Jr., Lt Col, USAF  
Acting Director, Support Systems Engrg

If your address has changed, if you wish to be removed from our mailing list, or if the addressee is no longer employed by your organization, please notify ASD/ENECH, Wright-Patterson AFB, Ohio 45433-6503 to help maintain a current mailing list.

Copies of this report should not be returned unless return is required by security considerations, contractual obligations, or notice on a specific document.

UNCLASSIFIED

SECURITY CLASSIFICATION OF THIS PAGE

REPORT DOCUMENTATION PAGE				Form Approved OMB No. 0704-0188	
1a. REPORT SECURITY CLASSIFICATION UNCLASSIFIED			1b. RESTRICTIVE MARKINGS		
2a. SECURITY CLASSIFICATION AUTHORITY			3. DISTRIBUTION/AVAILABILITY OF REPORT Approved for public release, distribution unlimited.		
2b. DECLASSIFICATION/DOWNGRADING SCHEDULE					
4. PERFORMING ORGANIZATION REPORT NUMBER(S) ASD-TR-90-5002			5. MONITORING ORGANIZATION REPORT NUMBER(S)		
6a. NAME OF PERFORMING ORGANIZATION Crew Station Design Facility		6b. OFFICE SYMBOL (If applicable) ASD/ENECH	7a. NAME OF MONITORING ORGANIZATION		
6c. ADDRESS (City, State, and ZIP Code) Wright Patterson AFB  Ohio, 45433-6503			7b. ADDRESS (City, State, and ZIP Code)		
8a. NAME OF FUNDING/SPONSORING - ORGANIZATION F/FB/EF-111 DFCS SPO		8b. OFFICE SYMBOL (If applicable) ASD/SDFP	9. PROCUREMENT INSTRUMENT IDENTIFICATION NUMBER		
8c. ADDRESS (City, State, and ZIP Code) Wright Patterson AFB  Ohio, 45433-6503			10. SOURCE OF FUNDING NUMBERS		
			PROGRAM ELEMENT NO.	PROJECT NO.	TASK NO.
			WORK UNIT ACCESSION NO.		
11. TITLE (Include Security Classification) Evaluation of the F/FB/EF-111 Ground Collision Avoidance System (GCAS)					
12. PERSONAL AUTHOR(S) J.A. Hassoun; G.F. Ward, Capt, USAF; J.M. Barnaba; D.L. McCarthy, ClC, USAFA					
13a. TYPE OF REPORT Final		13b. TIME COVERED FROM May 88 TO Jun 89		14. DATE OF REPORT (Year, Month, Day) October, 1989	
				15. PAGE COUNT 165	
16. SUPPLEMENTARY NOTATION					
17. COSATI CODES			18. SUBJECT TERMS (Continue on reverse if necessary and identify by block number)		
FIELD	GROUP	SUB-GROUP	Ground Collision Avoidance System (GCAS) Human Engineering (HE)		
			Ground Proximity Warning System (GPWS) Simulation		
19. ABSTRACT (Continue on reverse if necessary and identify by block number) In support of the F/FB/EF-111 Digital Flight Control System Program Office, subjective and performance data were collected in order to provide the Government and contractor engineers with information needed in the design of a Ground Collision Avoidance system (GCAS) for all F/FB/EF-111 aircraft. The GCAS, one of the new safety of flight systems, is being included as part of the Digital Flight Control Computer. The GCAS will serve to alert the crew of an impending ground impact. This decision will be based on sensor data collected mainly from the Combined Altitude Radar Altimeter (CARA). The GCAS, due to the down looking nature of the CARA will not be as effective as the forward looking Terrain Following Radar (TFR) and will only serve to complement this system. Its efficacy will be emphasized in non-TFR modes of flight. The evaluation was comprised of three phases. All were conducted using the simulation and computation capabilities of the ASD/ENECH Crew Station Design Facility. The Phase I evaluation focused primarily on two main efforts related to the prediction power of individual equations within the					
20. DISTRIBUTION/AVAILABILITY OF ABSTRACT <input checked="" type="checkbox"/> UNCLASSIFIED/UNLIMITED <input type="checkbox"/> SAME AS RPT. <input type="checkbox"/> DTIC USERS			21. ABSTRACT SECURITY CLASSIFICATION UNCLASSIFIED		
22a. NAME OF RESPONSIBLE INDIVIDUAL John A. Hassoun			22b. TELEPHONE (Include Area Code) (513) 255-4109		22c. OFFICE SYMBOL ASD/ENECH



Continued from Block 19.

GCAS algorithm. The first effort involved identifying critical parameters and their associated critical windows which influenced the use of one set of coefficients over another (changing paths). The second effort examined the break points between the different paths in an attempt to describe the continuity (or discontinuity) between the different sets of coefficients, and whether or not a dramatic step existed between the paths. The Phase II evaluation used a simple pilot model to place the FB-111 simulator in specific flight configurations (based on roll angle, flight path angle, wing sweep angle, initial air speed, release altitude, and terrain slope), release the simulator, fly until a GCAS warning, and execute a proper ground collision avoidance maneuver. The main objective of Phase II was to identify gross areas of concern that could be corrected by General Dynamics before any man-in-the-loop evaluation was executed. Phase III introduced the pilot factor and replicated a subset of the runs flown by the pilot model throughout Phase II, with a strong emphasis on standard flying configuration. Phase III allowed F/FB/EF-111 operational users to fly a GCAS equipped FB-111 simulator in order to evaluate and critique the most current version of the GCAS algorithm. The critique, as well as the performance and subjective results, were then shared with the SPO and the contractor for further modifications of the algorithm.

## TABLE OF CONTENTS

<u>Section</u>	<u>Page</u>
F/FB/EF-111 GCAS EVALUATION . . . . .	1
Introduction . . . . .	1
Introductory Note: Report Terminology . . . . .	2
F/FB/EF-111 GCAS Description . . . . .	2
Overall GCAS Evaluation Procedure . . . . .	3
PHASE I EVALUATION . . . . .	4
Phase I Introduction . . . . .	4
Phase I Results . . . . .	5
HGAMMA Sub-Algorithm . . . . .	5
H Evaluation . . . . .	5
Breakpoint Evaluation. . . . .	9
HTERR Sub-Algorithm . . . . .	12
H Evaluation. . . . .	12
Breakpoint Evaluation . . . . .	17
HPHI Sub-Algorithm . . . . .	18
H Evaluation. . . . .	18
Breakpoint Evaluation. . . . .	23
HPILOT Sub-Algorithm . . . . .	23
Phase I Discussion . . . . .	24
PHASE II EVALUATION . . . . .	30
Phase II Introduction . . . . .	30
Phase II Method . . . . .	30
Apparatus . . . . .	30
Facility. . . . .	30
Simulator. . . . .	30
Computer Complex. . . . .	32
Design . . . . .	32

<u>Section</u>	<u>Page</u>
Procedure . . . . .	33
Phase II Results . . . . .	34
Low Airspeed -- 350 Knots . . . . .	34
Medium Airspeed -- 500 Knots . . . . .	58
High Airspeed -- 650 Knots . . . . .	73
Phase II Discussion . . . . .	88
PHASE III EVALUATION . . . . .	89
Phase III Introduction . . . . .	89
Phase III Method . . . . .	89
Subjects . . . . .	89
Apparatus . . . . .	89
Facility . . . . .	89
Computer Complex . . . . .	89
Simulator . . . . .	89
Experimenter's Console . . . . .	89
VMU Mechanization . . . . .	90
Audio Systems . . . . .	90
Design . . . . .	91
Procedure . . . . .	92
Phase III Results . . . . .	93
Performance Data Results . . . . .	93
Low Airspeed--350 Knots/26 Degrees Wing Sweep . . . . .	94
Medium Airspeed--475 Knots/45 Degrees Wing Sweep . . . . .	107
High Airspeed--600 Knots/55 Degrees Wing Sweep . . . . .	120
Performance Data Discussion . . . . .	133
Pilot Reaction Time Results . . . . .	133
Pilot Reaction Time Discussion . . . . .	138
Pilot Ratings Results . . . . .	138

<u>Section</u>	<u>Page</u>
Pilot Ratings Discussion . . . . .	.149
Pilots Preferences on the Proposed GCAS Mechanization . . . . .	.149
CONCLUSION . . . . .	.149
REFERENCES . . . . .	.151

## List of Figures

Figure	Page
1. Example depicting a step increase for a given breakpoint.	5
2. List of paths for the HGAMMA sub-algorithm.	6
3. Predicted altitude loss (HGAMMA) as a function of flight path angle for airspeeds of 500, 900, 1100, and 1300 feet/second at a wing sweep of 60 degrees.	7
4. Predicted altitude loss (HGAMMA) as a function of flight path angle for airspeeds of 500, 900, 1100, and 1300 feet/second at a wing sweep of 30 degrees.	9
5. List of paths for the HTERR sub-algorithm.	13
6. Predicted altitude loss (HTERR) as a function of terrain slope for GAMMA of -45, -25, and -05 degrees at an airspeed of 300 feet/second.	15
7. Predicted altitude loss (HTERR) as a function of terrain slope for GAMMA of -45, -25, and -05 degrees at an airspeed of 900 feet/second.	16
8. Predicted altitude loss (HTERR) as a function of terrain slope for GAMMA of -45, -25, and -05 degrees at an airspeed of 1100 feet/second.	17
9. List of paths for the HPHI sub-algorithm.	18
10. Predicted altitude loss (HPHI) as a function of roll attitude for GAMMA of -45, -25, and -05 degrees at a wing sweep of 25 degrees.	19
11. Predicted altitude loss (HPHI) as a function of roll attitude for GAMMA of -45, -25, and -05 degrees at a wing sweep of 35 degrees.	20
12. Predicted altitude loss (HPHI) as a function of roll attitude for GAMMA of -45, -25, and -05 degrees at a wing sweep of 45 degrees.	21
13. Predicted altitude loss (HPHI) as a function of roll attitude for GAMMA of -45, -25, and -05 degrees at a wing sweep of 65 degrees.	22
14 (a). RTIMA calculations as a function of Gs.	25
14 (b). RTIMB calculations as a function of Gamma.	25
14 (c). RTIMC calculations as a function of Gs.	26
14 (d). RTIMD calculations as a function of Altitude.	26
15. Predicted pilot reaction time (RTIME) as a function of Gs for GAMMA of -45, -25, and -5 degrees at an altitude of 80 feet.	27
16. Predicted pilot reaction time (RTIME) as a function of Gs for GAMMA of -45, -25, and -5 degrees at an altitude of 300 feet.	28
17. Predicted pilot reaction time (RTIME) as a function of Gs for GAMMA of -45, -25, and -5 degrees at an altitude of 1000 feet.	29
18. Picture depicting the FB-111 simulator.	31
19. Typical output plot available for quick look evaluations.	35
20 (a). Minimum clearance as a function of flight path angle for pilot model at slope = 0 speed = 350 wsweep = 25.	37
20 (b). Minimum clearance as a function of flight path angle for pilot model at slope = 0 speed = 350 wsweep = 45.	38
20 (c). Minimum clearance as a function of flight path angle for pilot model at slope = 0 speed = 350 wsweep = 65.	39

Figure	Page
21 (a). Minimum clearance as a function of flight path angle for pilot model at slope = 3 speed = 350 wsweep = 25.	.40
21 (b). Minimum clearance as a function of flight path angle for pilot model at slope = 3 speed = 350 wsweep = 45.	.41
21 (c). Minimum clearance as a function of flight path angle for pilot model at slope = 3 speed = 350 wsweep = 65.	.42
22 (a). Minimum clearance as a function of flight path angle for pilot model at slope = 6 speed = 350 wsweep = 25.	.43
22 (b). Minimum clearance as a function of flight path angle for pilot model at slope = 6 speed = 350 wsweep = 45.	.44
22 (c). Minimum clearance as a function of flight path angle for pilot model at slope = 6 speed = 350 wsweep = 65.	.45
23 (a). Minimum clearance as a function of flight path angle for pilot model at slope = 9 speed = 350 wsweep = 25.	.46
23 (b). Minimum clearance as a function of flight path angle for pilot model at slope = 9 speed = 350 wsweep = 45.	.47
23 (c). Minimum clearance as a function of flight path angle for pilot model at slope = 9 speed = 350 wsweep = 65.	.48
24 (a). Minimum clearance as a function of flight path angle for pilot model at slope = 12 speed = 350 wsweep = 25.	.49
24 (b). Minimum clearance as a function of flight path angle for pilot model at slope = 12 speed = 350 wsweep = 45.	.50
24 (c). Minimum clearance as a function of flight path angle for pilot model at slope = 12 speed = 350 wsweep = 65.	.51
25 (a). Minimum clearance as a function of flight path angle for pilot model at slope = 15 speed = 350 wsweep = 25.	.52
25 (b). Minimum clearance as a function of flight path angle for pilot model at slope = 15 speed = 350 wsweep = 45.	.53
25 (c). Minimum clearance as a function of flight path angle for pilot model at slope = 15 speed = 350 wsweep = 65.	.54
26 (a). Minimum clearance as a function of flight path angle for pilot model at slope = 18 speed = 350 wsweep = 25.	.55
26 (b). Minimum clearance as a function of flight path angle for pilot model at slope = 18 speed = 350 wsweep = 45.	.56
26 (c). Minimum clearance as a function of flight path angle for pilot model at slope = 18 speed = 350 wsweep = 65.	.57
27 (a). Minimum clearance as a function of flight path angle for pilot model at slope = 0 speed = 500 wsweep = 45.	.59
27 (b). Minimum clearance as a function of flight path angle for pilot model at slope = 0 speed = 500 wsweep = 65.	.60
28 (a). Minimum clearance as a function of flight path angle for pilot model at slope = 3 speed = 500 wsweep = 45.	.61
28 (b). Minimum clearance as a function of flight path angle for pilot model at slope = 3 speed = 500 wsweep = 65.	.62
29 (a). Minimum clearance as a function of flight path angle for pilot model at slope = 6 speed = 500 wsweep = 45.	.63

Figure	Page
29 (b). Minimum clearance as a function of flight path angle for pilot model at slope = 6 speed = 500 wsweep = 65.	.64
30 (a). Minimum clearance as a function of flight path angle for pilot model at slope = 9 speed = 500 wsweep = 45.	.65
30 (b). Minimum clearance as a function of flight path angle for pilot model at slope = 9 speed = 500 wsweep = 65.	.66
31 (a). Minimum clearance as a function of flight path angle for pilot model at slope = 12 speed = 500 wsweep = 45.	.67
31 (b). Minimum clearance as a function of flight path angle for pilot model at slope = 12 speed = 500 wsweep = 65.	.68
32 (a). Minimum clearance as a function of flight path angle for pilot model at slope = 15 speed = 500 wsweep = 45.	.69
32 (b). Minimum clearance as a function of flight path angle for pilot model at slope = 15 speed = 500 wsweep = 65.	.70
33 (a). Minimum clearance as a function of flight path angle for pilot model at slope = 18 speed = 500 wsweep = 45.	.71
33 (b). Minimum clearance as a function of flight path angle for pilot model at slope = 18 speed = 500 wsweep = 65.	.72
34 (a). Minimum clearance as a function of flight path angle for pilot model at slope = 0 speed = 650 wsweep = 45.	.74
34 (b). Minimum clearance as a function of flight path angle for pilot model at slope = 0 speed = 650 wsweep = 65.	.75
35 (a). Minimum clearance as a function of flight path angle for pilot model at slope = 3 speed = 650 wsweep = 45.	.76
35 (b). Minimum clearance as a function of flight path angle for pilot model at slope = 3 speed = 650 wsweep = 65.	.77
36 (a). Minimum clearance as a function of flight path angle for pilot model at slope = 6 speed = 650 wsweep = 45.	.78
36 (b). Minimum clearance as a function of flight path angle for pilot model at slope = 6 speed = 650 wsweep = 65.	.79
37 (a). Minimum clearance as a function of flight path angle for pilot model at slope = 9 speed = 650 wsweep = 45.	.80
37 (b). Minimum clearance as a function of flight path angle for pilot model at slope = 9 speed = 650 wsweep = 65.	.81
38 (a). Minimum clearance as a function of flight path angle for pilot model at slope = 12 speed = 650 wsweep = 45.	.82
38 (b). Minimum clearance as a function of flight path angle for pilot model at slope = 12 speed = 650 wsweep = 65.	.83
39 (a). Minimum clearance as a function of flight path angle for pilot model at slope = 15 speed = 650 wsweep = 45.	.84
39 (b). Minimum clearance as a function of flight path angle for pilot model at slope = 15 speed = 650 wsweep = 65.	.85
40 (a). Minimum clearance as a function of flight path angle for pilot model at slope = 18 speed = 650 wsweep = 45.	.86
40 (b). Minimum clearance as a function of flight path angle for pilot model at slope = 18 speed = 650 wsweep = 65.	.87

Figure	Page
41. Head-Up Display (HUD)	.90
42 (a). Minimum clearance as a function of flight path angle for all pilots at speed = 350 slope = 0 roll = 0.	.95
42 (b). Minimum clearance as a function of flight path angle for all pilots at speed = 350 slope = 0 roll = 30.	.96
42 (c). Minimum clearance as a function of flight path angle for all pilots at speed = 350 slope = 0 roll = 60.	.97
43 (a). Minimum clearance as a function of flight path angle for all pilots at speed = 350 slope = 6 roll = 0.	.98
43 (b). Minimum clearance as a function of flight path angle for all pilots at speed = 350 slope = 6 roll = 30.	.99
43 (c). Minimum clearance as a function of flight path angle for all pilots at speed = 350 slope = 6 roll = 60.	100
44 (a). Minimum clearance as a function of flight path angle for all pilots at speed = 350 slope = 12 roll = 0.	101
44 (b). Minimum clearance as a function of flight path angle for all pilots at speed = 350 slope = 12 roll = 30.	102
44 (c). Minimum clearance as a function of flight path angle for all pilots at speed = 350 slope = 12 roll = 60.	103
45 (a). Minimum clearance as a function of flight path angle for all pilots at speed = 350 slope = 18 roll = 0.	104
45 (b). Minimum clearance as a function of flight path angle for all pilots at speed = 350 slope = 18 roll = 30.	105
45 (c). Minimum clearance as a function of flight path angle for all pilots at speed = 350 slope = 18 roll = 60.	106
46 (a). Minimum clearance as a function of flight path angle for all pilots at speed = 475 slope = 0 roll = 0.	108
46 (b). Minimum clearance as a function of flight path angle for all pilots at speed = 475 slope = 0 roll = 30.	109
46 (c). Minimum clearance as a function of flight path angle for all pilots at speed = 475 slope = 0 roll = 60.	110
47 (a). Minimum clearance as a function of flight path angle for all pilots at speed = 475 slope = 6 roll = 0.	111
47 (b). Minimum clearance as a function of flight path angle for all pilots at speed = 475 slope = 6 roll = 30.	112
47 (c). Minimum clearance as a function of flight path angle for all pilots at speed = 475 slope = 6 roll = 60.	113
48 (a). Minimum clearance as a function of flight path angle for all pilots at speed = 475 slope = 12 roll = 0.	114
48 (b). Minimum clearance as a function of flight path angle for all pilots at speed = 475 slope = 12 roll = 30.	115
48 (c). Minimum clearance as a function of flight path angle for all pilots at speed = 475 slope = 12 roll = 60.	116
49 (a). Minimum clearance as a function of flight path angle for all pilots at speed = 475 slope = 18 roll = 0.	117



<b>Figure</b> . . . . .	<b>Page</b>
49 (b). Minimum clearance as a function of flight path angle for all pilots at speed = 475 slope = 18 roll = 30. . . . .	118
49 (c). Minimum clearance as a function of flight path angle for all pilots at speed = 475 slope = 18 roll = 60. . . . .	119
50 (a). Minimum clearance as a function of flight path angle for all pilots at speed = 600 slope = 0 roll = 0. . . . .	121
50 (b). Minimum clearance as a function of flight path angle for all pilots at speed = 600 slope = 0 roll = 30. . . . .	122
50 (c). Minimum clearance as a function of flight path angle for all pilots at speed = 600 slope = 0 roll = 60. . . . .	123
51 (a). Minimum clearance as a function of flight path angle for all pilots at speed = 600 slope = 6 roll = 0. . . . .	124
51 (b). Minimum clearance as a function of flight path angle for all pilots at speed = 600 slope = 6 roll = 30. . . . .	125
51 (c). Minimum clearance as a function of flight path angle for all pilots at speed = 600 slope = 6 roll = 60. . . . .	126
52 (a). Minimum clearance as a function of flight path angle for all pilots at speed = 600 slope = 12 roll = 0. . . . .	127
52 (b). Minimum clearance as a function of flight path angle for all pilots at speed = 600 slope = 12 roll = 30. . . . .	128
52 (c). Minimum clearance as a function of flight path angle for all pilots at speed = 600 slope = 12 roll = 60. . . . .	129
53 (a). Minimum clearance as a function of flight path angle for all pilots at speed = 600 slope = 18 roll = 0. . . . .	130
53 (b). Minimum clearance as a function of flight path angle for all pilots at speed = 600 slope = 18 roll = 30. . . . .	131
53 (c). Minimum clearance as a function of flight path angle for all pilots at speed = 600 slope = 18 roll = 60. . . . .	132
54. Frequency distribution representing pilots' reaction times to the GCAS warnings. . . . .	135
54-1. Predicted versus actual . . . . .	136
54-2. Reaction time as a function of warning altitude . . . . .	137
55. Minimum clearance altitude as a function of vertical velocity for pilots' subjective rating of 1 (too high). . . . .	139
56. Minimum clearance altitude as a function of vertical velocity for pilots' subjective rating of 2 (slightly too high). . . . .	140
57. Minimum clearance altitude as a function of vertical velocity for pilots' subjective rating of 3 (about right). . . . .	141
58. Minimum clearance altitude as a function of vertical velocity for pilots' subjective rating of 4 (slightly low). . . . .	142
59. Minimum clearance altitude as a function of vertical velocity for pilots' subjective rating of 5 (too low). . . . .	143
60. Predicted function lines for minimum clearance altitude as a function of vertical velocity for pilots' subjective ratings of 1 through 5. . . . .	145
61. Minimum clearance altitude as a function of vertical velocity for pilots' subjective ratings of 1 and 2 combined. . . . .	146

<u>Figure</u> . . . . .	<u>Page</u>
62. Pilots' Window of Acceptability based on pilots' subjective ratings. . . . .	147
63. Function lines from the four terrain slope conditions overlayed on top of the Window of Acceptability. . . . .	148

## List of Tables

<u>Table</u> . . . . .	<u>Page</u>
1. Breakpoint evaluation for HGAMMA at a wing sweep of 50 degrees. . . . .	10
2. Breakpoint evaluation for HGAMMA at airspeeds of 800, 1000, and 1200 feet/second. . . . .	11
3. Breakpoint evaluation for HGAMMA. The following is a list of the maximum step values for HGAMMA at each of the breakpoints shown in Table 1. . . . .	12
4. Breakpoint evaluation for HGAMMA. The following is a list of the maximum step values for HGAMMA at each of the breakpoints shown in Table 2. . . . .	12
5. Breakpoint evaluation for HTERR at airspeeds of 600 and 1000 feet/second. . . . .	14
6. Breakpoint evaluation for HTERR. The following is a list of the maximum step values for HTERR at each of the breakpoints shown in Table 5. . . . .	14
7. Breakpoint evaluation for HPHI at airspeeds of 600 and 1000 feet/second. . . . .	23
8. Breakpoint evaluation for HPHI. The following is a list of the maximum step values for HPHI at each of the breakpoints shown in Table 7. . . . .	23
9. An example of the pilot model set-up page. . . . .	33
10. An example of the data display page available to the experimenter. . . . .	34
11. Man-in-the-loop design matrix. . . . .	91
12. Correlation coefficients for predicted and actual reaction times over the entire range of data. . . . .	134
13. Correlation coefficients for predicted and actual reaction times for recoveries less than 500 feet. . . . .	134
14. Rating criteria for each minimum recovery (or clearance) altitude. . . . .	138

## Introduction

Between 1970 and 1984, the statistics for combined Air Force and Navy accident mishaps related to Controlled Flight Into Terrain (CFIT) have involved approximately 400 aircraft and many lives. The installation of a forward looking Terrain Following Radar (TFR) system would greatly reduce the number of mishaps. However, such a solution may be prohibitively expensive, and would make the aircraft more susceptible to detection by enemy radars. A Ground Collision Avoidance System (GCAS) on the other hand, while not as reliable as a forward looking TFR, provides an alternative yet beneficial solution.

In 1976, the Federal Aviation Administration mandated the use of a Ground Proximity Warning System (GPWS) on commercial airliners. The algorithm was mainly designed to promote safety in final approach. Since that period, the number of commercial CFIT accidents has dropped to virtually zero. In the case of commercial aircraft, the algorithm need not be extremely sophisticated. In the tactical and strategic environments, however, such simplicity may be unacceptable. The SAC and TAC aircraft will be operating in a totally different regime than the commercial and some wide body military transports. The highly maneuverable TAC and SAC aircraft need a GCAS algorithm that will function consistently in low level missions, over diverse terrain.

In general, GCAS systems rely on a software algorithm with the appropriate parameters being drawn from existing aircraft sensors, to present the pilot with an emergency warning that requires immediate reaction to avoid impending ground impact. The design philosophy of a GCAS is that (1) if a pilot does not commit a ground clearance error, he should never receive a warning to pullup (otherwise considered to be a nuisance warning or a false alarm), and (2) if he receives a warning, the pilot may be assured that he has committed a ground clearance error. Nuisance warnings may be caused by three factors. In the first case, erroneous sensor data input into the algorithm may cause an unwarranted GCAS warning. The level of sophistication exhibited by the algorithm dictates such nuisance warnings. The second type of nuisance warning is related to the algorithm's ability to predict pilot reaction time. Reaction time is defined as the interval of time beginning at the moment the system recognizes a ground clearance error (and subsequently initiating a warning) until the pilot begins the recovery maneuver. In high vertical velocity conditions (for example 750 feet per second), a minimum pilot reaction time differential (such as 500 versus 1500 milliseconds) could add an additional 750 feet to the total loss of altitude exhibited during the pullup maneuver. The third type of nuisance warnings is attributed to the algorithm's inability to predict, calculate, and extrapolate. The present evaluation focused on the last two types of nuisance warnings.

Several aircraft in the SAC and TAC fleets are in the process of implementing or have already implemented some type of a GCAS algorithm (F-16, A-10, A-7, KC-135, C-130, B-1, F/FB/EF-111). Many algorithms are presently competing for installation in these aircraft. Some of the algorithms, such as Cubic's Ground Collision Avoidance System (Cubic, 1985) and Fairchild's Low Altitude Warning

System (Shah, 1988), attempt to calculate the maximum loss of altitude based on a set of generic aerodynamic equations. The algorithms differ greatly in some of the assumptions being considered throughout the calculations (such as the number of G's available, altitude loss based on pilot reaction time, and altitude loss due to sloping terrain). Other algorithms, such as the General Dynamics' (GD) Enhanced Ground Clobber, is based on form functions empirically derived using off-line simulation. Two recent studies at the Crew Station Design Facility (Orr, 1986; Di Padua, 1988) have evaluated the above mentioned algorithms. The discrepancies between the algorithms seem to give each strengths in some areas and weaknesses in others. For example, Cubic's algorithm offered a selectable warning altitude which was considered a positive feature. As judged by the minimum recovery altitude, LAWS provided the least amount of nuisance warnings. All three algorithms seem to provide poor warnings in near level flight into rising terrain and in shallow descents.

As part of the Digital Flight Control System (DFCS) development for the F/FB/EF-111, GD is in the process of designing and developing such a GCAS algorithm. The F/FB/EF-111 is currently equipped with a forward looking TFR, therefore the efficacy of this GCAS system will be emphasized when the aircraft is in non-terrain following mode.

### **Introductory Note: Report Terminology**

The terms "Gamma" and "Flight Path Angle" are used interchangeably throughout the document, and mean exactly the same thing. Furthermore, the reader should assume that, every time "Gamma" or "Flight Path Angle" are used, it is in reference to the simulator's negative attitude even when positive values are used, except when the value is preceded by the word "positive" or the "+" sign.

### **F/FB/EF-111 GCAS Description**

The present GD algorithm warns the pilot, through an aural voice warning, of an impending ground collision in one of three separate modes: (1) sink rate monitoring mode, (2) normal mode, and (3) dive angle monitoring mode for Terrain Following (TF). Only the normal mode was of interest in the present evaluation. A complete description of the algorithm may be found in GD's top level software document FZM-12-31017B (GD, 1988).

Based on form functions empirically derived using off-line simulation, the GCAS normal mode calculates an estimated recovery altitude, referred to as HTOTAL, based on several variables including true airspeed, dive angle, wing sweep, gross weight, roll attitude, and terrain slope. Due to the complexity of the algorithm, GD has separated HTOTAL into four smaller algorithms (HGAMMA, HPHI, HTERR, and HPILOT). A warning is initiated when the algorithm encounters one of two conditions: (1) the terrain slope compensated vertical velocity is less than zero and HTOTAL is greater than or equal to the altitude above ground level for two consecutive frames (data are collected at a rate of 50 frames per second), or (2) the digital altitude above ground level is less than 90 feet.

The following paragraph describes the relationship between HTOTAL and the four sub-algorithms.

$$\text{HTOTAL} = \text{HGAMMA} + \text{HPhi} + \text{HTERR} + \text{HPILOT} + \text{BUFFER}$$

HTOTAL = Total estimated recovery altitude

HGAMMA = Estimated recovery altitude due to dive angle

HPhi = Estimated recovery altitude due to roll angle

HTERR = Estimated recovery altitude due to sloping terrain

HPILOT = Estimated recovery altitude due to pilot reaction time

BUFFER = Current buffer zone is set at 50 feet

The design of the system was based on the following conditions:

1. Roll angles up to 60 degrees (CARA coverage)
2. Dive angles up to 45 degrees (CARA coverage)
3. Velocities up to 800 KIAS (1350 feet/second)
4. Terrain slope angles up to 18 degrees
5. A minimum recovery altitude of 90 feet
6. A recovery maneuver using a 5 G pullout or maximum available Gs at 14 degrees Angle of Attack (AOA).

### **Overall GCAS Evaluation Procedure**

The GD algorithm was evaluated in three separate phases. Through discussions with the System Program Office (SPO) and the contractor (GD), the results and recommendations of each phase influenced the modification of the algorithm prior to the execution of the following phase.

Throughout the first phase of the evaluation, efforts focused primarily on the verification and validation of the algorithm in the FB-111 simulator and the individual equations pertinent to the normal mode (HGAMMA, HPhi, HTERR, HPILOT), and their relationship to HTOTAL.

Phase II of the evaluation involved testing the GCAS algorithm in an FB-111 simulator using a simple pilot model to perform the recovery maneuvers. This preliminary setup allowed the Crew Station Design Facility (CSDF) engineers to collect a large amount of data without subjecting the pilots to a highly time consuming activity. The objective for Phase II was to identify gross problem areas and correct them before the man-in-the-loop, phase III evaluation.

During Phase III, only a subset of the conditions flown in Phase II required pilot participation and evaluation. Formal statistical analyses were conducted in an attempt to (1) describe the trend of the collected data, and (2) identify the acceptable and non-acceptable conditions from the users' perspective.

# PHASE I EVALUATION

## Phase I Introduction

During the development of the GCAS algorithm, GD derived several equations in order to compute the recovery altitudes required for dive recovery (HGAMMA), roll out (HPHI), terrain rise (HTERR), and pilot reaction time (HPILOT). An off-line simulation to calculate aircraft performance data based on various parameters such as gamma (flight path angle), wing sweep, airspeed, roll, etc... These data were used to curve-fit different sets of coefficients for the various recovery altitude equations. Furthermore, the configuration of the aircraft, dictates the selection of a specific equation set, or path, allowing for case oriented, derived coefficients.

The Phase I evaluation focused primarily on two main efforts related to the prediction power of the individual equations (or sub-algorithms). The first effort, referred to as the H EVALUATION, involved identifying critical parameters and their associated critical windows which influenced the use of one set of coefficients over another (changing paths). Plots were generated for each of the sub-algorithms depicting the calculated recovery altitude (such as HGAMMA) as a function of the parameters of interest.

Throughout the second effort, referred to as the BREAKPOINT EVALUATION, the breakpoints between the different paths were examined in an attempt to describe the continuity (or discontinuity) between the different sets of coefficients, and whether or not a dramatic step increase existed between the paths. Figure 1 depicts a graphic representation of the breakpoint phenomenon. To test the equations at the various breakpoints, two values per parameter of interest were calculated. The first value was computed at one delta less than the breakpoint, while the second value was calculated at one delta greater than the breakpoint value. The delta used was equal to 0.01 percent of the breakpoint value. The two values were then used to calculate the size of the step. This process was performed repeatedly with all other input parameters varying across their ranges. These ranges were limited so as to not allow the parameters to cross another breakpoint and consequently select another set of coefficients. For HGAMMA, the calculations were replicated at five levels of aircraft gross weight: 50,000; 60,000; 70,000; 80,000; and 90,000 pounds.

The following sections will describe each of the four sub- algorithms, along with the results of the evaluation.

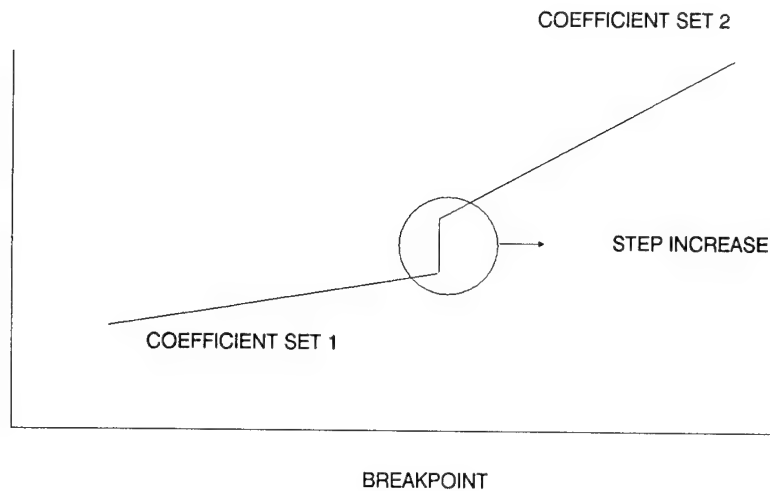


Figure 1. Example depicting a step increase for a given breakpoint.

## Phase I Results

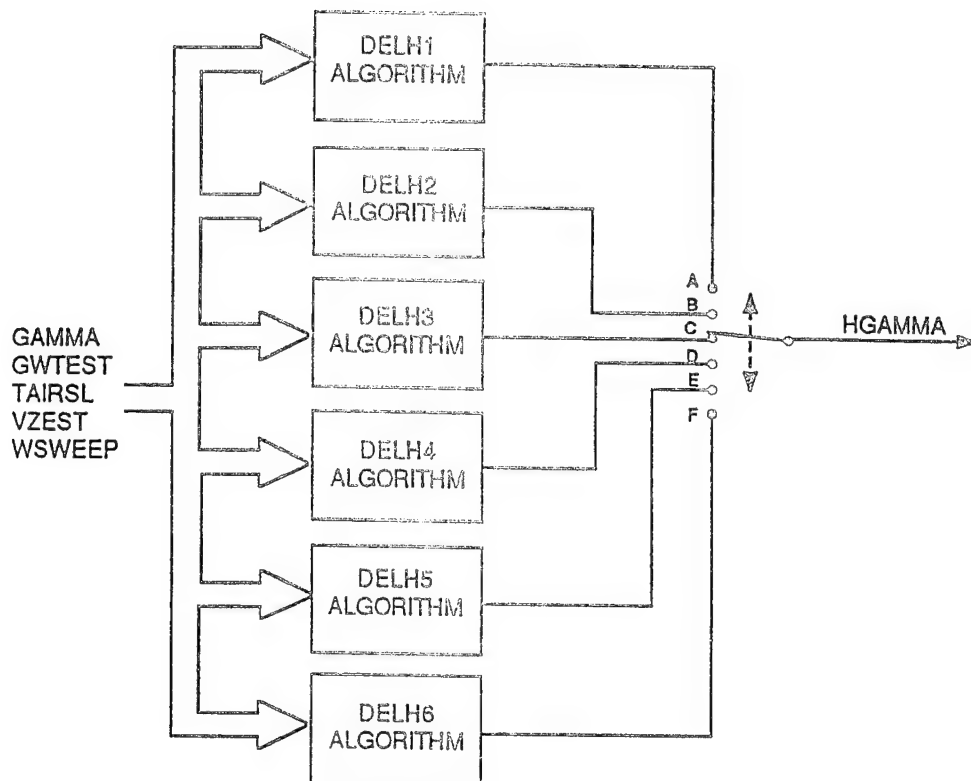
### HGAMMA Sub-Algorithm

#### **H Evaluation**

Five variables were identified as critical to the HGAMMA sub-algorithm. These were dive angle, true airspeed, vertical velocity, wing sweep, and gross weight. Along with these variables, six sets of coefficients (or paths) were developed by GD to satisfy breakpoints associated with airspeed and wing sweep. A representation of the different paths is shown in Figure 2 (borrowed from FZM-12-31017B).

The calculated recovery altitude (HGAMMA) data were plotted as a function of Gamma (0 through -45 degrees) for two different wing sweep conditions (30 and 60 degrees) and four levels of airspeed (1300, 1100, 900, and 500 feet/second), and are shown in Figures 3 and 4. An inspection of the figures suggested that the calculated recovery altitude varied from zero to approximately 4,500 feet, with more altitude predicted as a function of higher Gamma and higher airspeed. However, a discrepancy appeared to exist between wing sweep and airspeed. At a wing sweep of 30 degrees, the HGAMMA algorithm calculated the lowest recovery altitudes at 500 feet/second. When wing sweep was set at 60 degrees however, and airspeed was at 500 feet/second, HGAMMA was shown to have predicted the second highest recovery altitudes (second curve from the top). No clear explanation of the discrepancy is currently available, however, GD is in the process of investigating the issue.





PATH A IS ACTIVE WHEN  
 $\text{TAIRSL} \leq 800 \text{ ft/s}$  AND  $\text{WSWEEP} \leq 50 \text{ DEG}$

PATH B IS ACTIVE WHEN  
 $800 \text{ ft/s} < \text{TAIRSL} \leq 1000 \text{ ft/s}$  AND  $\text{WSWEEP} \leq 50 \text{ DEG}$

PATH C IS ACTIVE WHEN  
 $\text{TAIRSL} \leq 800 \text{ ft/s}$  AND  $\text{WSWEEP} > 50 \text{ DEG}$

PATH D IS ACTIVE WHEN  
 $800 \text{ ft/s} < \text{TAIRSL} \leq 1000 \text{ ft/s}$  AND  $\text{WSWEEP} > 50 \text{ DEG}$

PATH E IS ACTIVE WHEN  
 $1000 \text{ ft/s} < \text{TAIRSL} \leq 1200 \text{ ft/s}$

PATH F IS ACTIVE WHEN  
 $\text{TAIRSL} > 1200 \text{ ft/s}$

Figure 2. List of paths for the HGAMMA sub-algorithm.

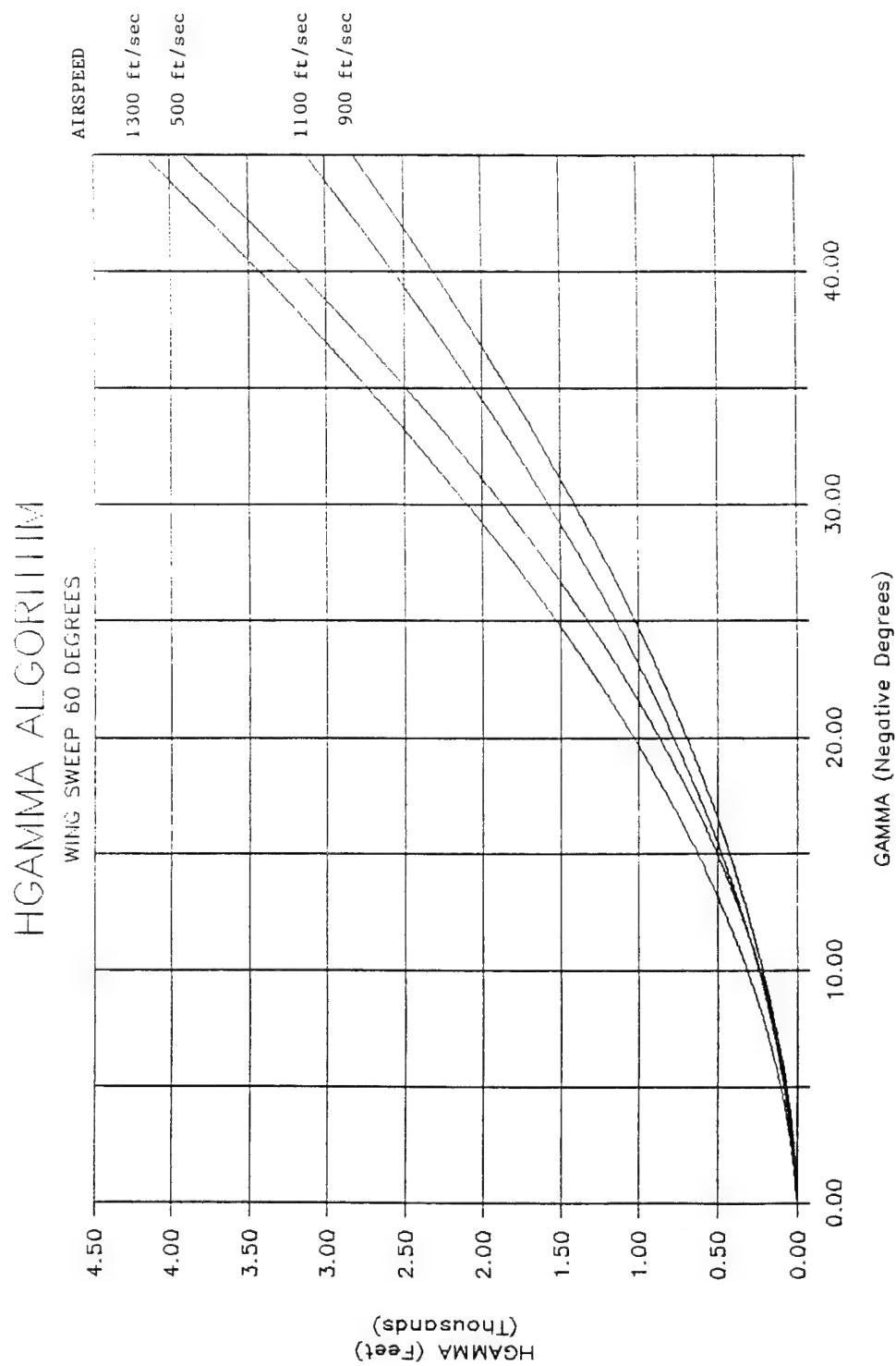


Figure 3. Predicted altitude loss (HGAMMA) as a function of flight path angle for airspeeds of 500, 900, 1100, and 1300 feet/second at a wing sweep of 60 degrees.

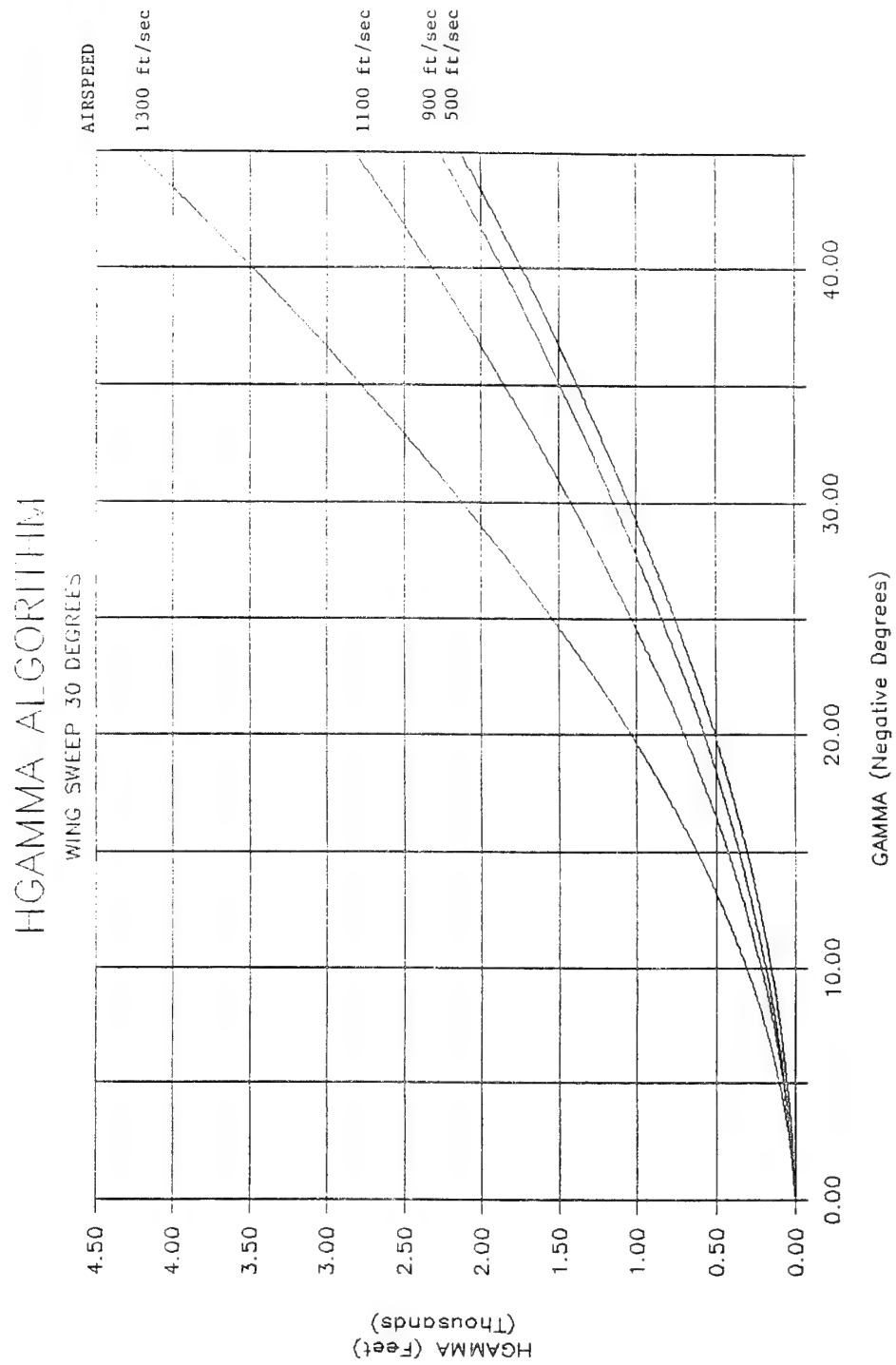


Figure 4. Predicted altitude loss (HGAMMA) as a function of flight path angle for airspeeds of 500, 900, 1100, and 1300 feet/second at a wing sweep of 30 degrees.

### **Breakpoint Evaluation.**

The critical variables for switching paths within the HGAMMA sub-algorithm were identified as wing sweep and airspeed. The wing sweep path-breakpoint occurs at 50 degrees, while the airspeed breakpoints take place at 800, 1000, and 1200 feet/second. The following tables contain the ranges around which the input parameters were varied for a given breakpoint being tested, along with the maximum, average of the absolute values, and the standard deviations of the step sizes. Table 1 contains the data for the wing sweep breakpoint at 50 degrees. The HGAMMA steps were calculated as a function of Gamma (5 through 45 degrees, at 5 degree increments) and three levels of varying airspeed ( [1] 400 through 800, with 10 feet/second increments; [2] 810 through 1000, with 10 feet/second increments; and [3] 1010 through 1200, with 10 feet/second increments). These three levels of airspeed were selected to insure that the variables would not cross into a second set of coefficients.

Results indicated that as gross weight increased, at airspeeds of 400 to 800 Knots and flight path angles between 5 and 45 degrees, step sizes also increased dramatically from 7.3 (at 50,000 lbs.) to 117 feet (at 90,000 lbs.).

Table 2 represents three different airspeed (800, 1000, and 1200 feet/second) breakpoints, while preventing wing sweep from crossing into a second path. Both Gamma and wing sweep were manipulated, with Gamma varying from 5 through 45 degrees with an increment of 5 degrees, and wing sweep varying at two different levels (20 through 50 degrees, by increments of one; and 51 through 70 degrees, also by increments of one).

An examination of the data yielded a problem at the 1,000 feet/second airspeed condition with wing sweeps of 20 through 50 degrees. Step size decreased dramatically at higher gross weight conditions with worst case sceario (-579 feet) at 90,000 lbs. Finally, Tables 3 and 4 list the conditions at which the maximum step values were calculated for each of the breakpoints listed in Tables 1 and 2. A complete listing of the data may be requested from the Crew Station Design Facility (ASD/ENECH-CSDF, Wright-Patterson AFB, OH 45433-6503).

TABLE 1. Breakpoint evaluation for HGAMMA at a wing sweep of 50 degrees.

GROSS WEIGHT = 50,000 LBS.				
GAMMA	AIRSPEED	MAX STEP SIZE	ABSOLUTE AVE.	STANDARD DEV.
5 TO 45	400 TO 800	28.6	5.8	7.3
5 TO 45	810 TO 1000	-7.6	1.7	2.1
5 TO 45	1010 TO 1200	-0.0	0.0	0.0

GROSS WEIGHT = 60,000 LBS.				
GAMMA	AIRSPEED	MAX STEP SIZE	ABSOLUTE AVE.	STANDARD DEV.
5 TO 45	400 TO 800	137.0	32.7	34.6
5 TO 45	810 TO 1000	18.8	4.7	4.3
5 TO 45	1010 TO 1200	0.1	0.0	0.0

GROSS WEIGHT = 70,000 LBS.				
GAMMA	AIRSPEED	MAX STEP SIZE	ABSOLUTE AVE.	STANDARD DEV.
5 TO 45	400 TO 800	245.0	60.2	62.2
5 TO 45	810 TO 1000	35.6	10.0	8.2
5 TO 45	1010 TO 1200	0.1	0.0	0.0

GROSS WEIGHT = 80,000 LBS.				
GAMMA	AIRSPEED	MAX STEP SIZE	ABSOLUTE AVE.	STANDARD DEV.
5 TO 45	400 TO 800	353.0	87.8	89.7
5 TO 45	810 TO 1000	52.3	15.3	12.3
5 TO 45	1010 TO 1200	0.2	0.0	0.0

GROSS WEIGHT = 90,000 LBS.				
GAMMA	AIRSPEED	MAX STEP SIZE	ABSOLUTE AVE.	STANDARD DEV.
5 TO 45	400 TO 800	462.0	115.0	117.0
5 TO 45	810 TO 1000	69.1	20.6	16.4
5 TO 45	1010 TO 1200	0.2	0.1	0.1

TABLE 2. Breakpoint evaluation for HGAMMA at airspeeds of 800, 1000, and 1200 feet/second.

GROSS WEIGHT = 50,000

GAMMA	WING SWEEP	AIRSPPEED	MAX STEP SIZE	ABSOLUTE AVE.	STANDARD DEV.
5 TO 45	20 TO 50	800	0.1	0.0	0.0
5 TO 45	51 TO 70	800	-0.3	0.1	0.1
5 TO 45	20 TO 50	1000	87.3	16.9	18.7
5 TO 45	51 TO 70	1000	-6.8	1.9	2.4
5 TO 45	20 TO 50	1200	0.8	0.3	0.2
5 TO 45	51 TO 70	1200	0.7	0.3	0.2

GROSS WEIGHT = 60,000

GAMMA	WING SWEEP	AIRSPPEED	MAX STEP SIZE	ABSOLUTE AVE.	STANDARD DEV.
5 TO 45	20 TO 50	800	-0.2	0.1	0.0
5 TO 45	51 TO 70	800	-0.8	0.2	0.2
5 TO 45	20 TO 50	1000	-79.2	14.3	17.5
5 TO 45	51 TO 70	1000	-7.0	1.9	2.4
5 TO 45	20 TO 50	1200	1.0	0.3	0.3
5 TO 45	51 TO 70	1200	0.7	0.2	0.2

GROSS WEIGHT = 70,000

GAMMA	WING SWEEP	AIRSPPEED	MAX STEP SIZE	ABSOLUTE AVE.	STANDARD DEV.
5 TO 45	20 TO 50	800	-0.5	0.1	0.1
5 TO 45	51 TO 70	800	-1.3	0.4	0.3
5 TO 45	20 TO 50	1000	-246.0	42.6	52.4
5 TO 45	51 TO 70	1000	-7.2	1.9	2.4
5 TO 45	20 TO 50	1200	1.1	0.4	0.3
5 TO 45	51 TO 70	1200	0.7	0.2	0.2

GROSS WEIGHT = 80,000

GAMMA	WING SWEEP	AIRSPPEED	MAX STEP SIZE	ABSOLUTE AVE.	STANDARD DEV.
5 TO 45	20 TO 50	800	-0.7	0.2	0.2
5 TO 45	51 TO 70	800	-1.8	0.6	0.4
5 TO 45	20 TO 50	1000	-412.0	71.4	87.7
5 TO 45	51 TO 70	1000	-7.4	1.9	2.4
5 TO 45	20 TO 50	1200	1.2	0.4	0.3
5 TO 45	51 TO 70	1200	0.7	0.2	0.2

TABLE 2 (Cont.). Breakpoint evaluation for HGAMMA at airspeeds of 800, 1000, and 1200 feet/second.

GROSS WEIGHT = 90,000					
GAMMA	WING SWEEP	AIRSPEED	MAX STEP SIZE	ABSOLUTE AVE.	STAND. DEV.
5 TO 45	20 TO 50	800	-0.9	0.3	0.2
5 TO 45	51 TO 70	800	-2.3	0.7	0.6
5 TO 45	20 TO 50	1000	-579.0	100.0	123.0
5 TO 45	51 TO 70	1000	-7.7	1.9	2.5
5 TO 45	20 TO 50	1200	1.4	0.4	0.3
5 TO 45	51 TO 70	1200	0.7	0.2	0.2

TABLE 3. Breakpoint evaluation for HGAMMA. The following is a list of the maximum step values for HGAMMA at each of the breakpoints shown in Table 1.

GAMMA	WING SWEEP	AIRSPEED	-1H	+1H	MAX STEP	WEIGHT
45	50	400	3023	3485	462	90,000
45	50	1000	2507	2576	69	90,000
45	50	1080	2620	2620	0	90,000

TABLE 4. Breakpoint evaluation for HGAMMA. The following is a list of the maximum step values for HGAMMA at each of the breakpoints shown in Table 2.

GAMMA	WING SWEEP	AIRSPEED	-1H	+1H	MAX STEP	WEIGHT
45	50	800	2756	2755	-1	90,000
45	70	800	3725	3725	-2	90,000
45	20	1000	2423	1845	-579	90,000
45	70	1000	3060	3053	-8	90,000
45	20	1200	3623	3625	2	90,000
45	51	1200	3690	3691	1	90,000

## HTERR Sub-Algorithm

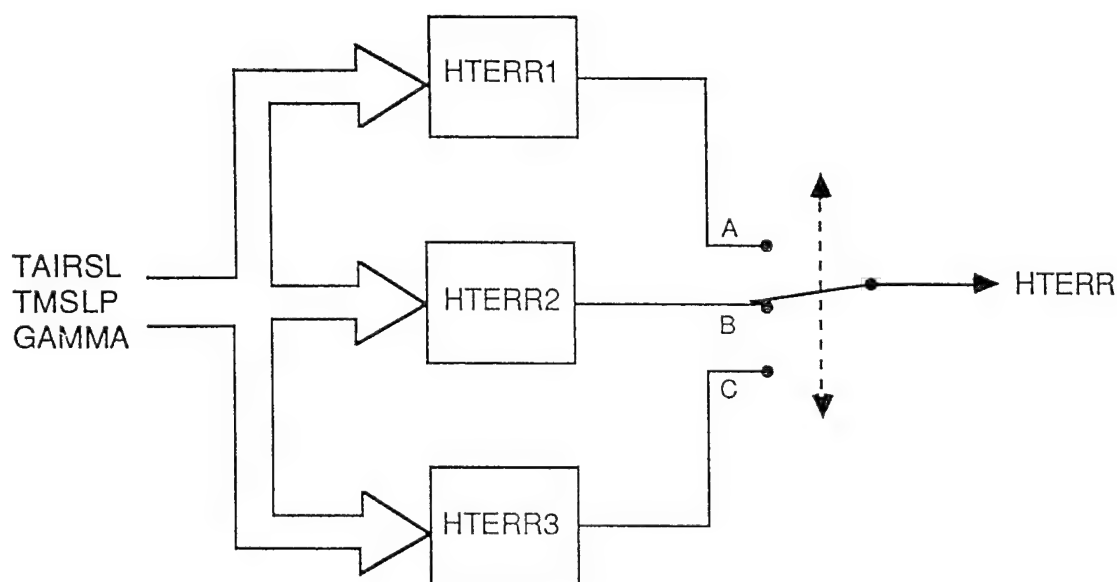
### H Evaluation.

Three variables were identified as critical to the HTERR sub-algorithm. These were Gamma, airspeed, and terrain slope. Along with the above mentioned variables, three sets of coefficients were used to satisfy breakpoints associated with airspeed. A representation of the three paths is shown in Figure 5 (borrowed from GD document FZM-12-31017B).

The recovery altitude data (HTERR) were plotted as a function of terrain slope (zero through 18 degrees) for three different Gamma conditions (-5, -25, and -45 degrees) and three airspeed conditions (300, 900, and 1100 feet/second). The data are shown in Figures 6, 7, and 8.

An inspection of the figures suggested the following trends. As terrain slope increased (at 300

feet/second airspeed), the recovery altitude curve appeared to reach an asymptote with the higher Gammas. However, this asymptote, which was more apparent at the higher airspeeds (900 and 1100 feet/second), began a decreasing trend above 15 degrees of terrain slope.



PATH A IS ACTIVE WHEN  $TAIRSL \leq 600$   
 PATH B IS ACTIVE WHEN  $TAIRSL \leq 1000$   
 PATH C IS ACTIVE WHEN  $TAIRSL > 1000$

HTERR = Compensated Altitude Due to Gradually Sloping Terrain  
 TAIRSL = True Airspeed  
 TMSLP = Terrain Model Slope  
 GAMMA = Dive Angle

Figure 5. List of paths for the HTERR sub-algorithm.



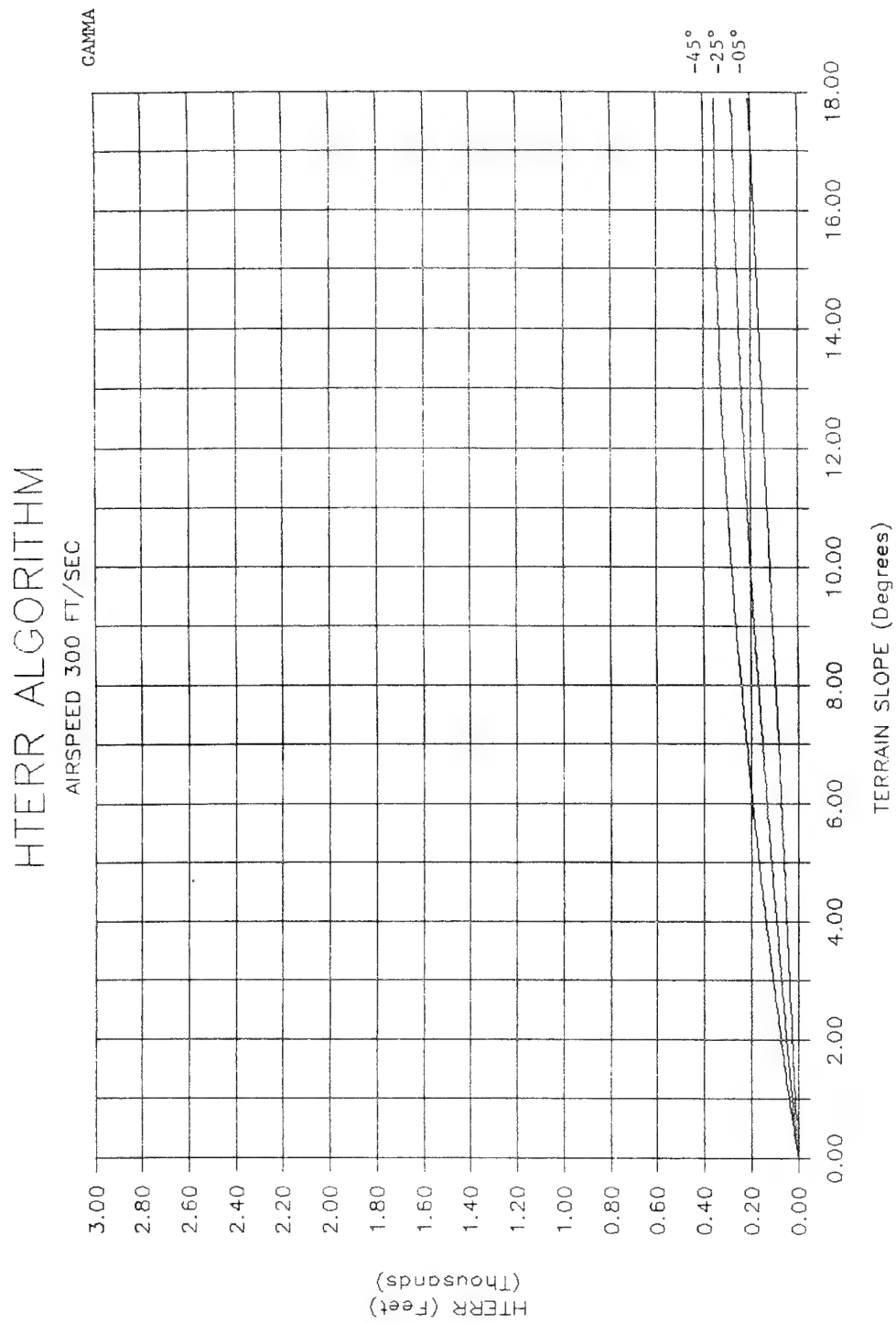


Figure 6. Predicted altitude loss (HTERR) as a function of terrain slope for GAMMA of -45, -25, and -05 degrees at an airspeed of 300 feet/second.

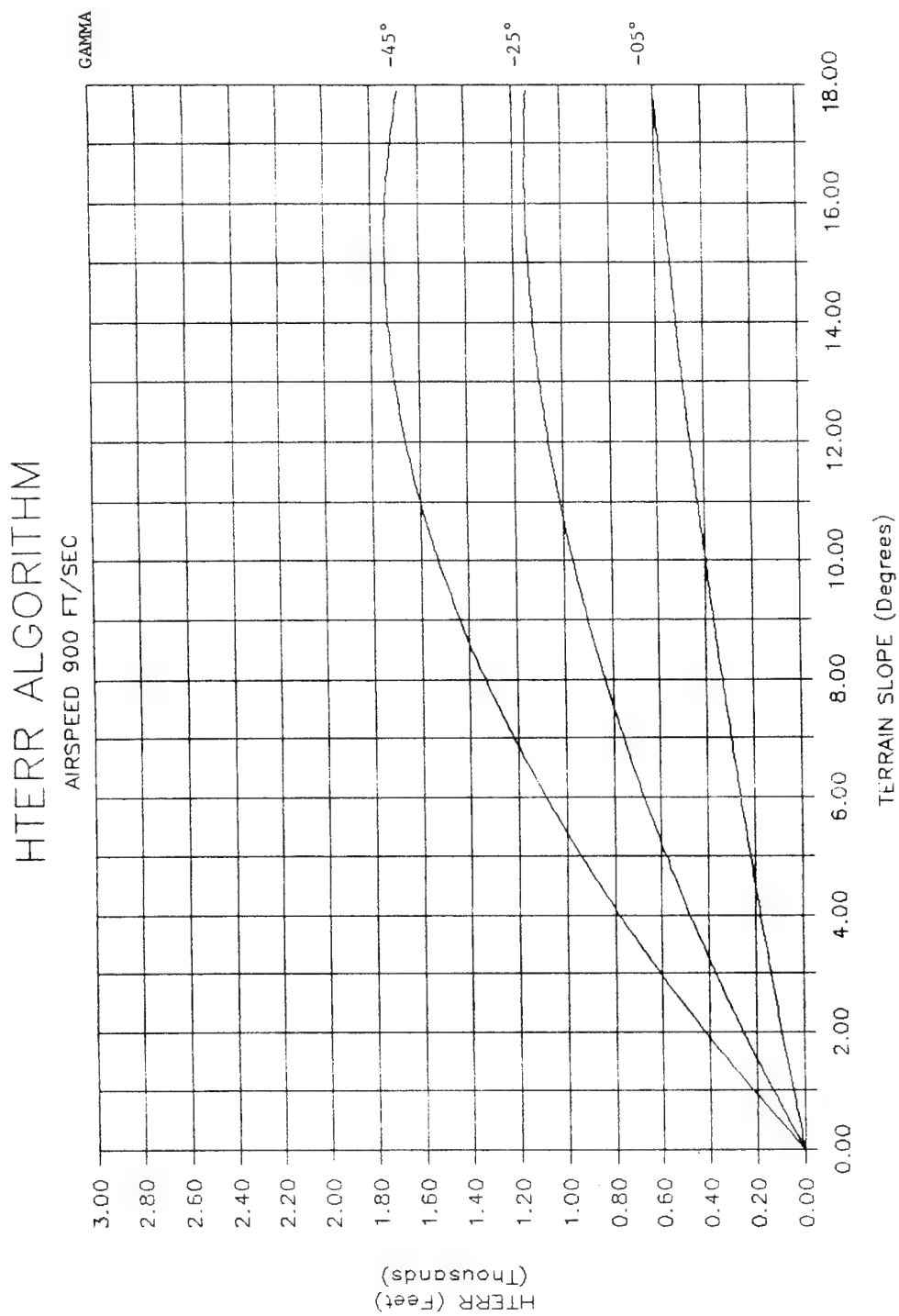


Figure 7. Predicted altitude loss (HTERR) as a function of terrain slope for GAMMA of -45, -25, and -05 degrees at an airspeed of 900 feet/second.

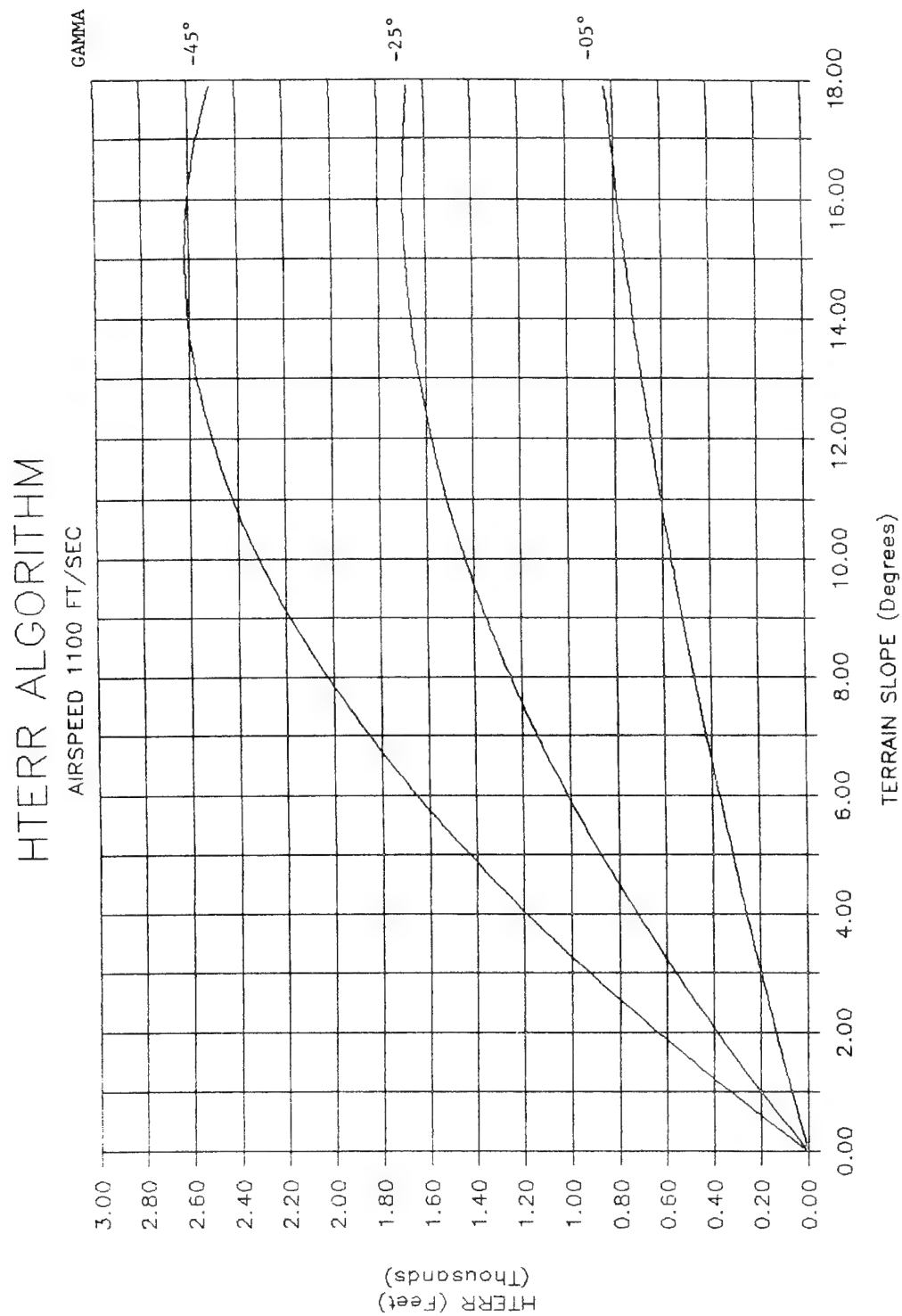


Figure 8. Predicted altitude loss (HTERR) as a function of terrain slope for GAMMA of -45, -25, and -05 degrees at an airspeed of 1100 feet/second.

### Breakpoint Evaluation

The critical variable associated with switching paths was identified as airspeed. The sub-algorithm switched from the first to the second set of coefficients at 600 feet/second, and switched again at 1000 feet/second. Therefore, Gamma and terrain slope, the other two variables affecting HTERR calculations, were manipulated in order to identify the maximum step size at each breakpoint. Gamma was changed from 5 to 45 degrees, with an increment of 5 degrees, while terrain slope (zero through 18 degrees) was incremented every degree. The design of the evaluation is shown in Table 5. Table 6 lists the conditions at which the maximum step values were calculated for each of the breakpoints listed in Table 5. A complete listing of the data may be requested from the Crew Station Design Facility (ASD/ENECH-CSDF, Wright-Patterson AFB, OH 45433-6503).

An examination of Tables 5 and 6 showed no significant changes in step size for either of the airspeed conditions (zero and one foot).

TABLE 5. Breakpoint evaluation for HTERR at airspeeds of 600 and 1000 feet/second.

GAMMA	TERR SLOPE	AIRSPPEED	MAX STEP SIZE	ABS AVE.	STAND DEV.
5 TO 45	0 TO 18	600	0.3	0.1	0.1
5 TO 45	0 TO 18	1000	0.9	0.4	0.2

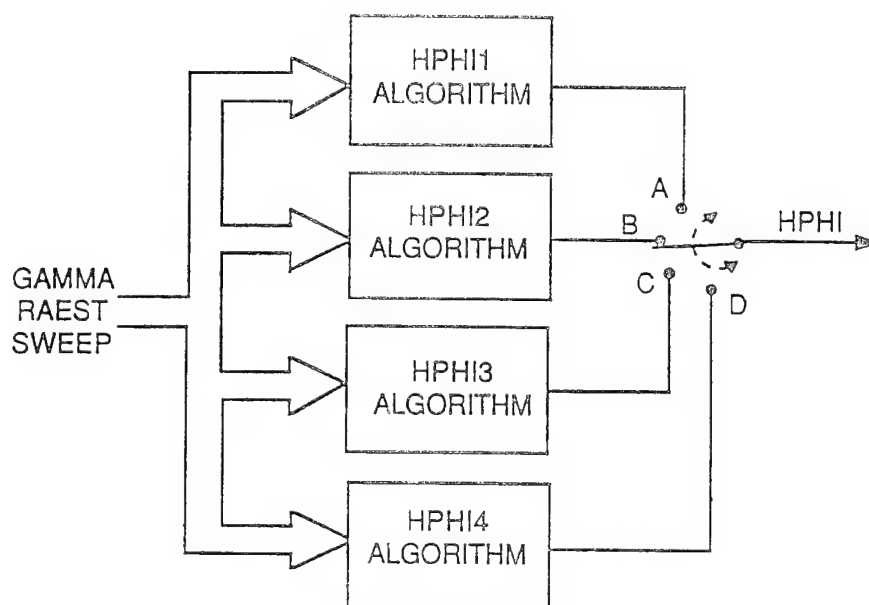
TABLE 6. Breakpoint evaluation for HTERR. The following is a list of the maximum step values for HTERR at each of the breakpoints shown in Table 5.

GAMMA	TERRAIN	AIRSPPEED	-1H	+1H	MAX STEP
45	15	600	688	688	0
45	14	1000	2083	2084	1

### HPHI Sub-Algorithm

#### **H Evaluation.**

Gamma, roll attitude, and wing sweep were identified as critical factors affecting the HPHI equations, which were based on four sets of coefficients. Three breakpoints were controlled by the aircraft's wing sweep angle. A representation of the four paths is shown in Figure 9 (borrowed from GD document FZM-12- 31017B).



PATH A IS ACTIVE WHEN  
 $WSWEEP \leq 26 \text{ DEG}$

PATH B IS ACTIVE WHEN  
 $26 \text{ DEG} < WSWEEP \leq 35 \text{ DEG}$

PATH C IS ACTIVE WHEN  
 $35 \text{ DEG} < WSWEEP \leq 50 \text{ DEG}$

PATH D IS ACTIVE WHEN  
 $WSWEEP > 50 \text{ DEG}$

Figure 9. List of paths for the HPHI sub-algorithm.

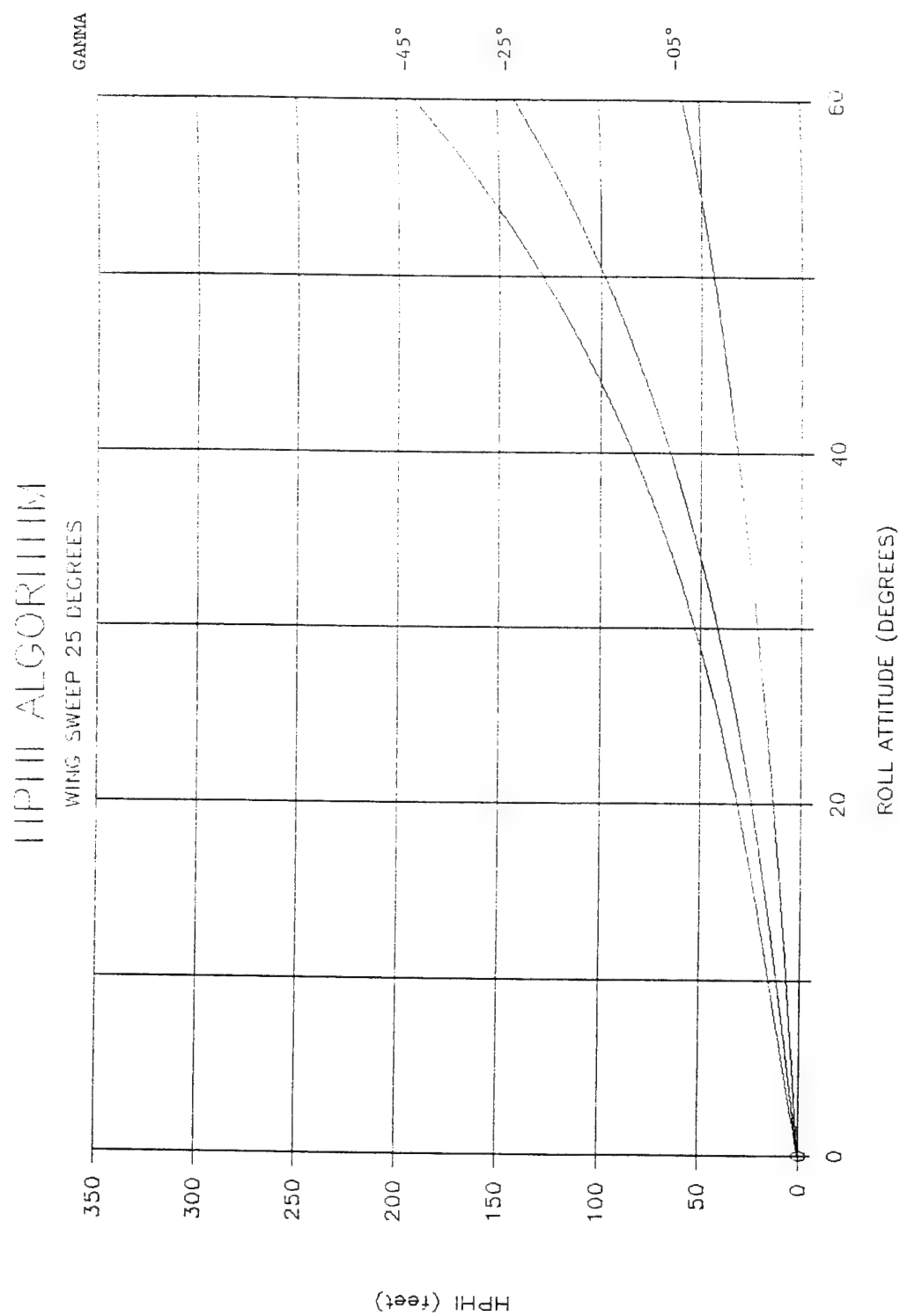


Figure 10. Predicted altitude loss (HPHI) as a function of roll attitude for GAMMA of -45, -25, and -05 degrees at a wing sweep of 25 degrees.

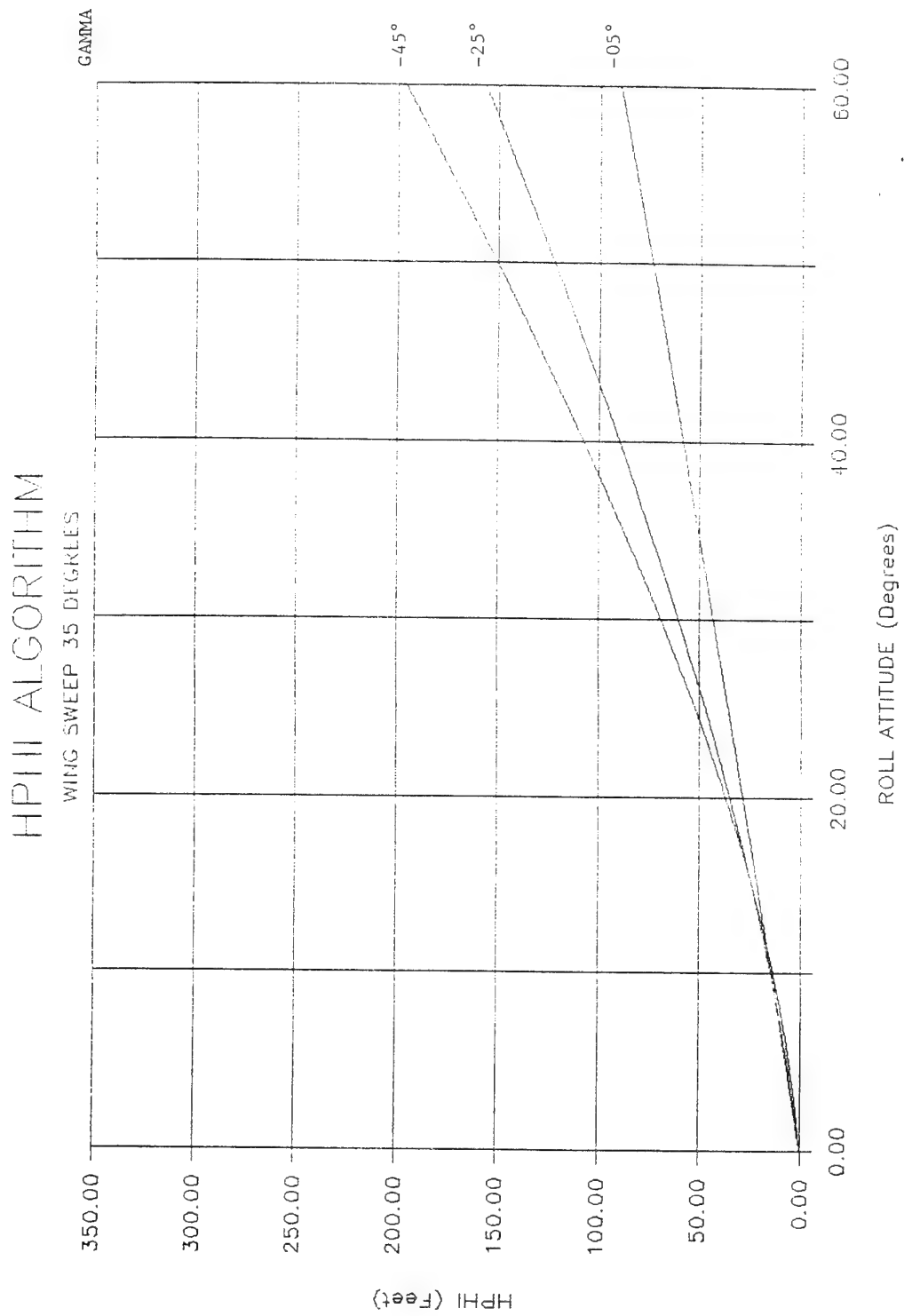


Figure 11. Predicted altitude loss (HPII) as a function of roll attitude for GAMMA of -45, -25, and -05 degrees at a wing sweep of 35 degrees.

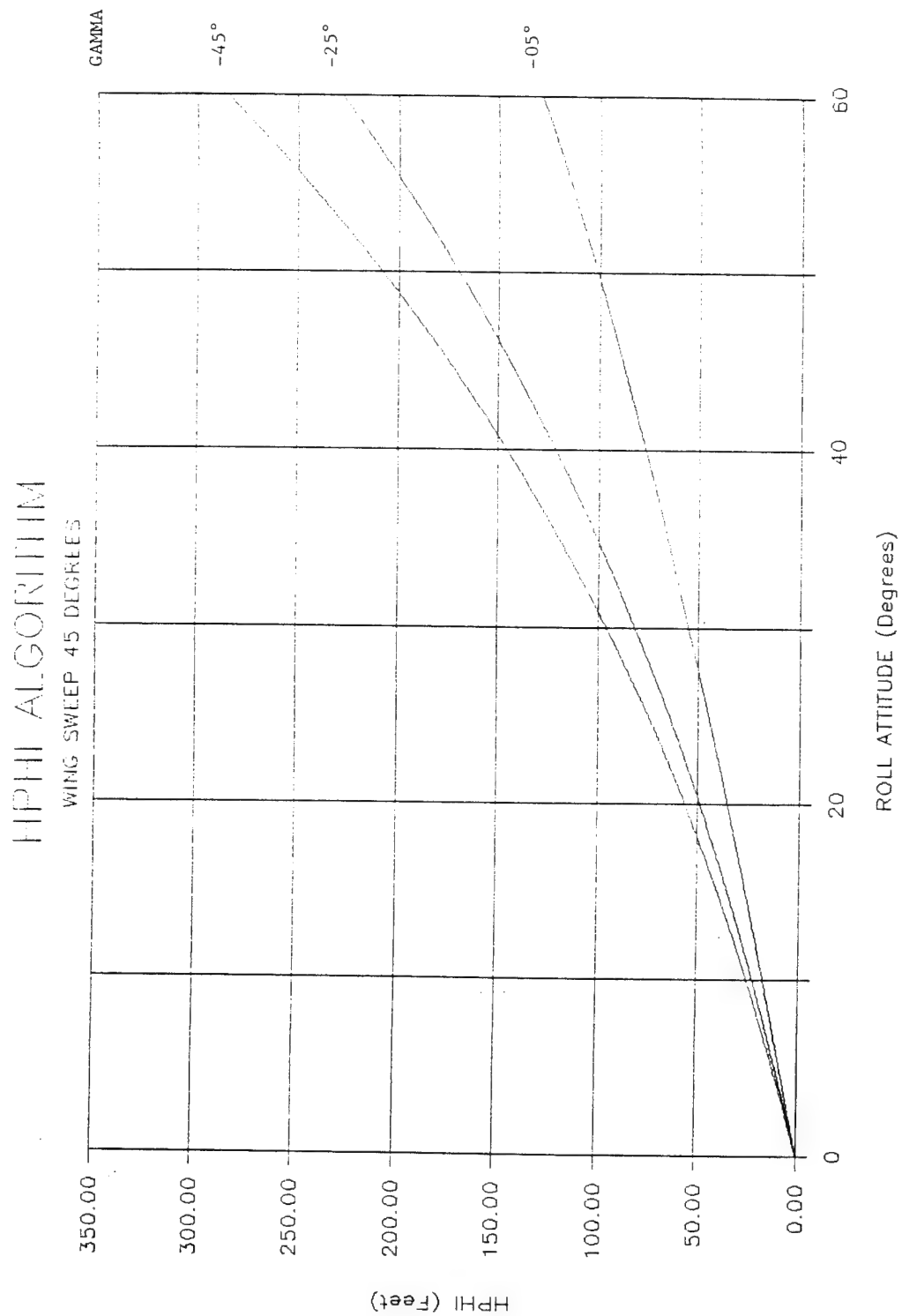


Figure 12. Predicted altitude loss (HPHI) as a function of roll attitude for GAMMA of -45, -25, and -05 degrees at a wing sweep of 45 degrees.



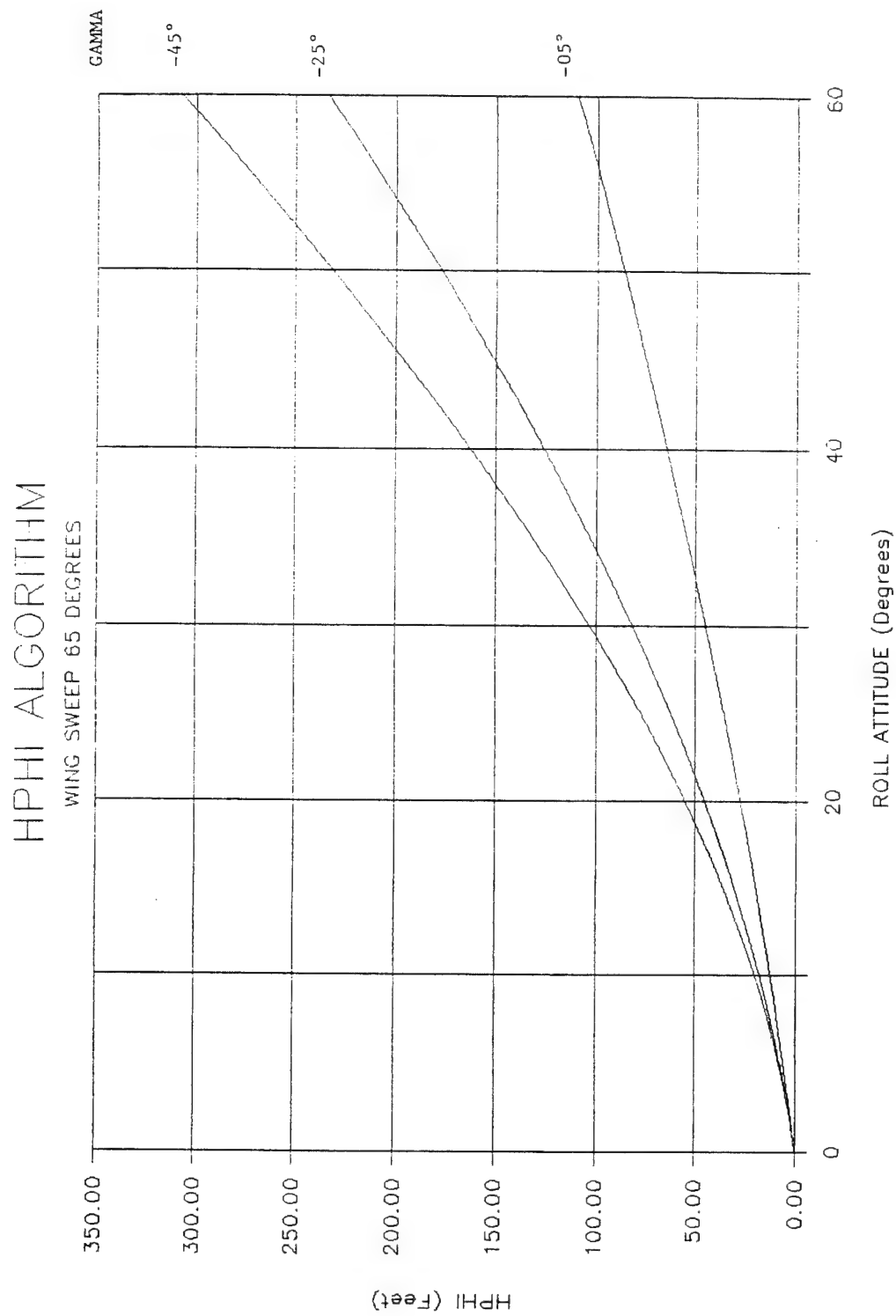


Figure 13. Predicted altitude loss (HPHI) as a function of roll attitude for GAMMA of -45, -25, and -05 degrees at a wing sweep of 65 degrees.

The predicted recovery altitude data (HPHI) were plotted as a function of roll angle (zero through 60 degrees) for three different Gamma conditions (-5, -25, and -45 degrees), and four wing sweep conditions (25, 35, 45, and 65 degrees). The plots are shown in Figures 10 through 13.

An inspection of the figures indicated an increase in predicted recovery altitude as a function of all three independent variables: roll attitude, Gamma, and wing sweep. The range of recovery altitude varied from zero to 310 feet. No obvious deficiencies appear to exist with the HPHI algorithm.

#### **Breakpoint Evaluation.**

The critical variable associated with switching paths was identified as wing sweep. The sub-algorithm switched from the first to the second set of coefficients at 27 degrees, and switched again at 36, and at 51 degrees. Furthermore, since roll angle and Gamma were the other two variables affecting HPHI, they were varied with an increment of one at the three breakpoints of 26, 35, and 50 degree wing sweep. The design of the HPHI breakpoint evaluation is shown in Table 7. Table 8 lists the conditions at which the maximum step values were calculated for each of the breakpoints listed in Table 7. A complete listing of the data may be requested from the Crew Station Design Facility (ASD/ENECH-CSDF, Wright-Patterson AFB, OH 45433-6503).

Similar to the HTERR breakpoint evaluation, no significant changes in step size were found in the HPHI evaluation.

TABLE 7. Breakpoint evaluation for HPHI at airspeeds of 600 and 1000 feet/second.

GAMMA	WING SWEEP	ROLL ANGLE	MAX STEP SIZE	ABS AVE.	STAND DEV.
5 TO 45	26	0 TO 60	43.7	21.4	12.5
5 TO 45	35	0 TO 60	27.8	11.9	6.7
5 TO 45	50	0 TO 60	-23.0	6.6	6.5

TABLE 8. Breakpoint evaluation for HPHI. The following is a list of the maximum step values for HPHI at each of the breakpoints shown in Table 7.

GAMMA	WING SWEEP	ROLL ANGLE	-1H	+1H	MAX STEP
24	26	60	158	201	44
18	35	60	136	164	28
5	50	60	129	106	-23

#### **HPILOT Sub-Algorithm**

The estimated recovery altitude due to pilot reaction time is calculated by multiplying pilot reaction time by the terrain slope compensated vertical velocity. While the algorithm does not rely on any sets of curve-fit coefficients, the predicted pilot reaction time varies as a function of three

independent variables: flight path angle, gravitational force (G), and radar altitude. The effects of all three variables on the predicted pilot reaction time, shown in Figure 14, are considered in the following equation:  $RTIME = RTIMD * MAX [MIN[RTIMA, RTIMB], RTIMC]$

The data from RTIME are shown in Figures 15, 16, and 17. Predicted pilot reaction time is calculated as a function of Gs (-4 through +5) for three levels of Gamma (-5, -25, and -45 degrees), at 80 feet, 300 feet, and 1000 feet altitude.

Overall, predicted pilot reaction time data seem to vary between 500 and 2500 milliseconds, with predicted pilot reaction times increasing as a function of higher flight path angles, higher altitudes, and lower Gs (negative Gs).

### Phase I Discussion

From the Phase I evaluation, CSDF engineers examined whether the predictive powers of HGAMMA, HPHI, HTERR, and HPILOT were sufficient. For each sub-algorithm, specific shortcomings were apparent. The recovery altitude generated by HGAMMA at an airspeed of 500 ft/sec for the two wing sweep conditions (30 and 60 degrees) was inconsistent. At 30 degrees of wing sweep, the predicted altitude loss increased linearly as airspeed increased. However, at 60 degrees of wing sweep, the predicted altitude loss, for the 500 ft/sec airspeed condition, was higher than for the 900 ft/sec or 1,100 ft/sec airspeed condition. One could infer from this that the pilot would receive the "pull-up" warning later at an airspeed of 500 ft/sec than at airspeeds of 900 ft/sec or 1,100 ft/sec. With such low airspeed and high wing sweep, the altitude loss would be greater in this case.

The asymptotic altitude loss lines found on the HTERR graphs are a major concern. The implication here is that at higher terrain slope conditions (greater than 15 degrees), the altitude loss becomes unpredictable, particularly at high flight path angles. The pilot's ability to rely on the algorithm when flying over rough terrain becomes questionable.

There is no clear definition of why or how pilot reaction time would be influenced by the three variables used in the algorithm (Gamma, altitude, Gs).

The breakpoint evaluation focused on whether or not a dramatic step size change occurred between paths. Each path defines a different set of coefficients to be used by the algorithm. These coefficients were selected as a function of wing sweep, true air speed, vertical velocity, dive angle and so on. Step size is the predicted altitude differential as a function of changing from one path (set of parameters) to another. At 1,100 ft/sec of airspeed (HGAMMA), for wing sweep conditions between 20 and 50 degrees, the step size decreased dramatically. Such a large change in step size leaves doubts concerning the reliability of the algorithm. When the flight parameters change, resulting in a path change within the algorithm, the pilot needs to know that the algorithm will respond appropriately.

The algorithm should be capable of transitioning from one path to another in a much smoother fashion.

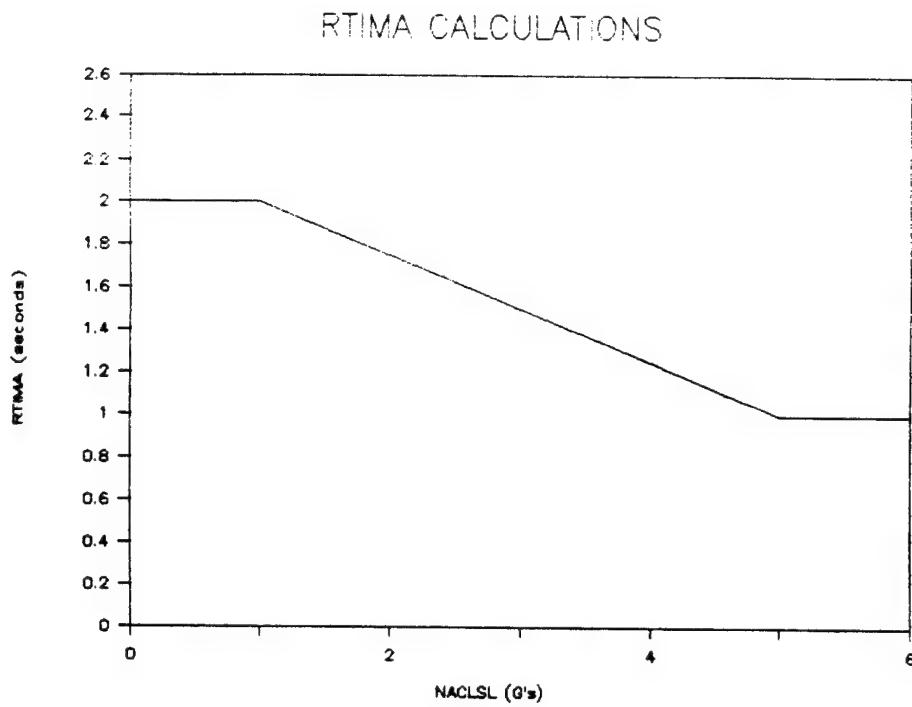


Figure 14 (a). RTIMA calculations as a function of Gs. ( $G \geq 0.0$ )

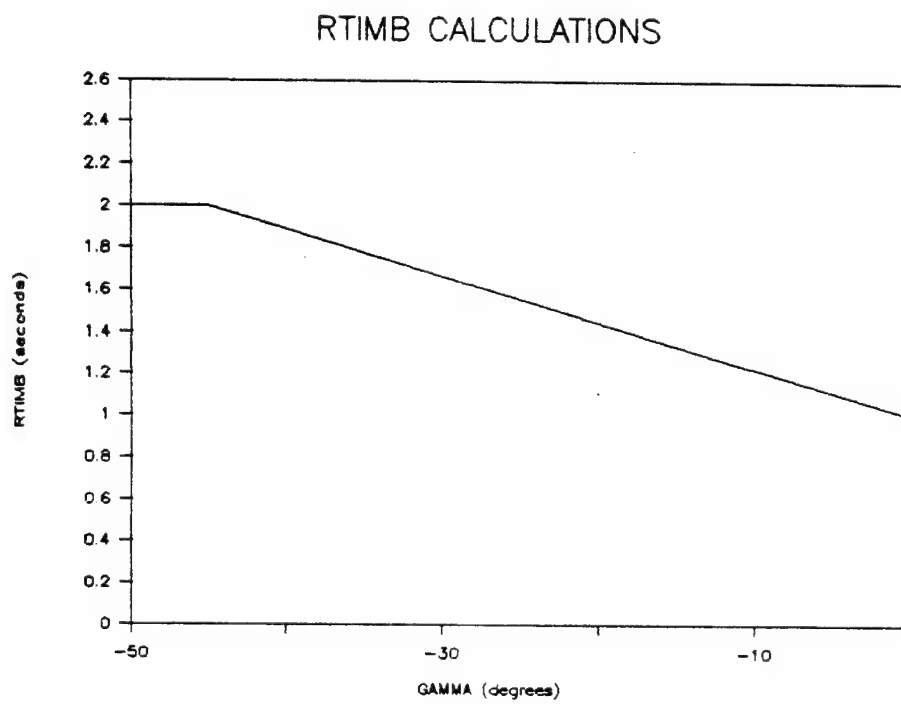


Figure 14 (b). RTIMB calculations as a function of Gamma.

### RTIMC CALCULATIONS

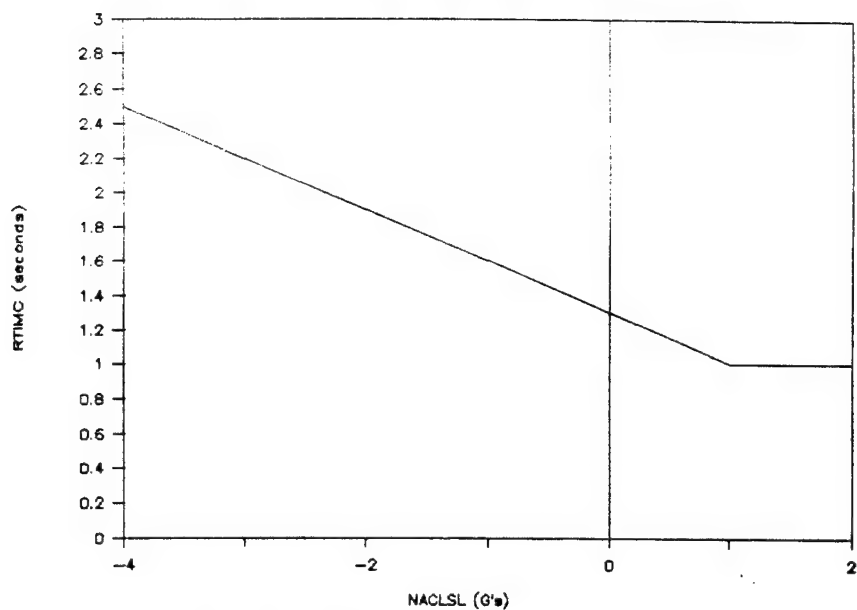


Figure 14 (c). RTIMC calculations as a function of Gs ( $G < 2$ ).

### RTIMD CALCULATIONS

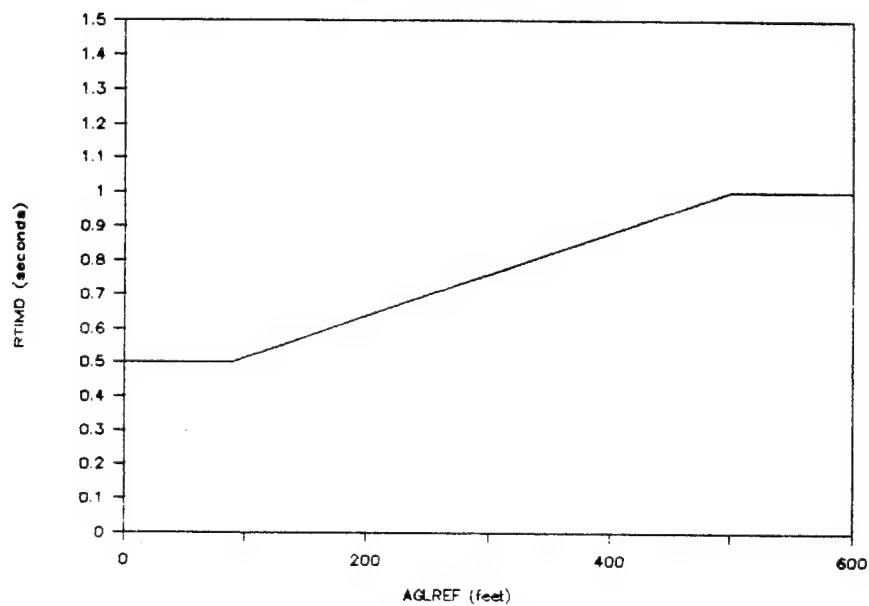


Figure 14 (d). RTIMD calculations as a function of Altitude.

# RTIME ALGORITHM (FROM HPILOT)

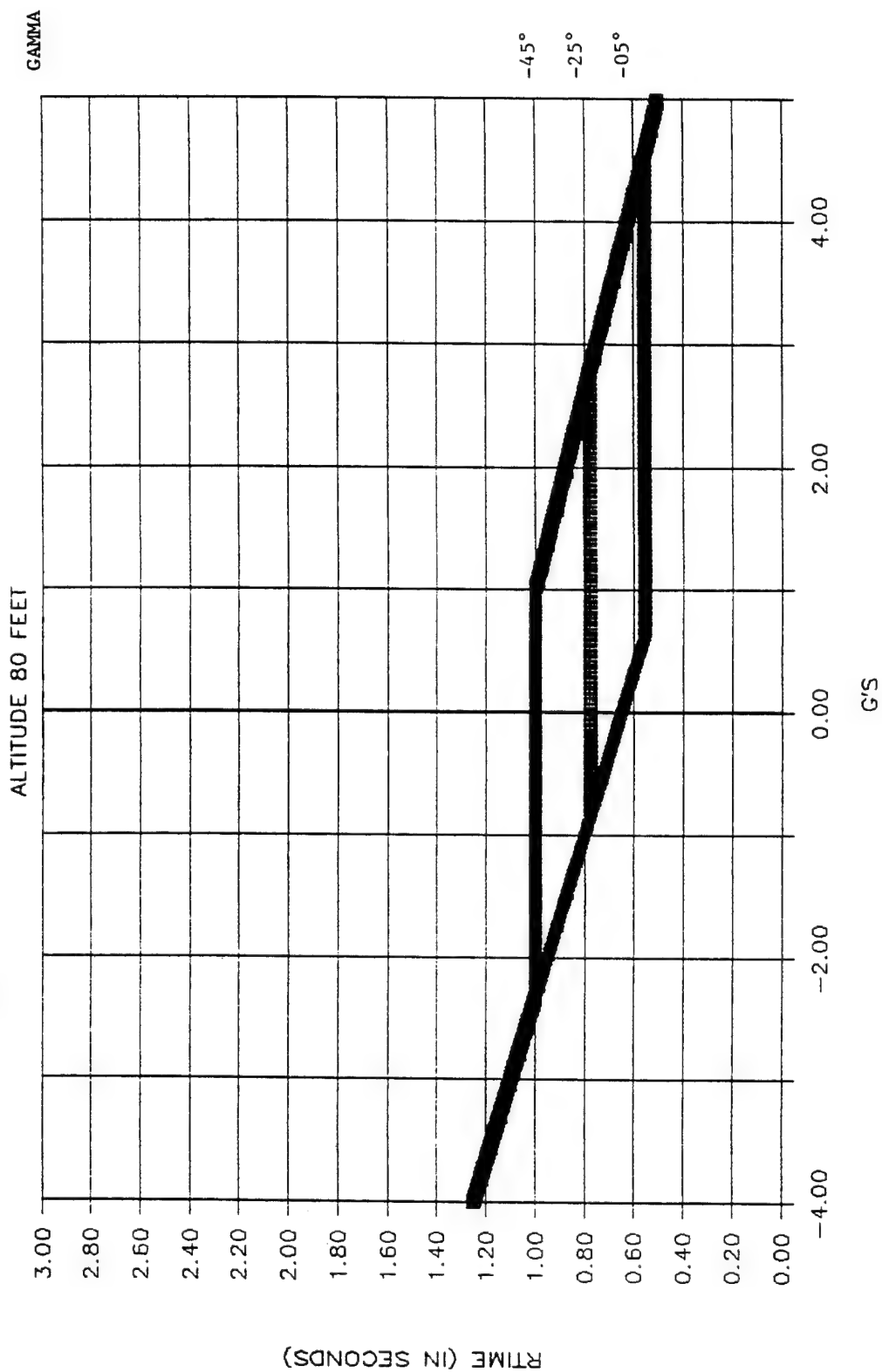


Figure 15. Predicted pilot reaction time (RTIME) as a function of Gs for GAMMA of -45, -25, and -5 degrees at an altitude of 80 feet.

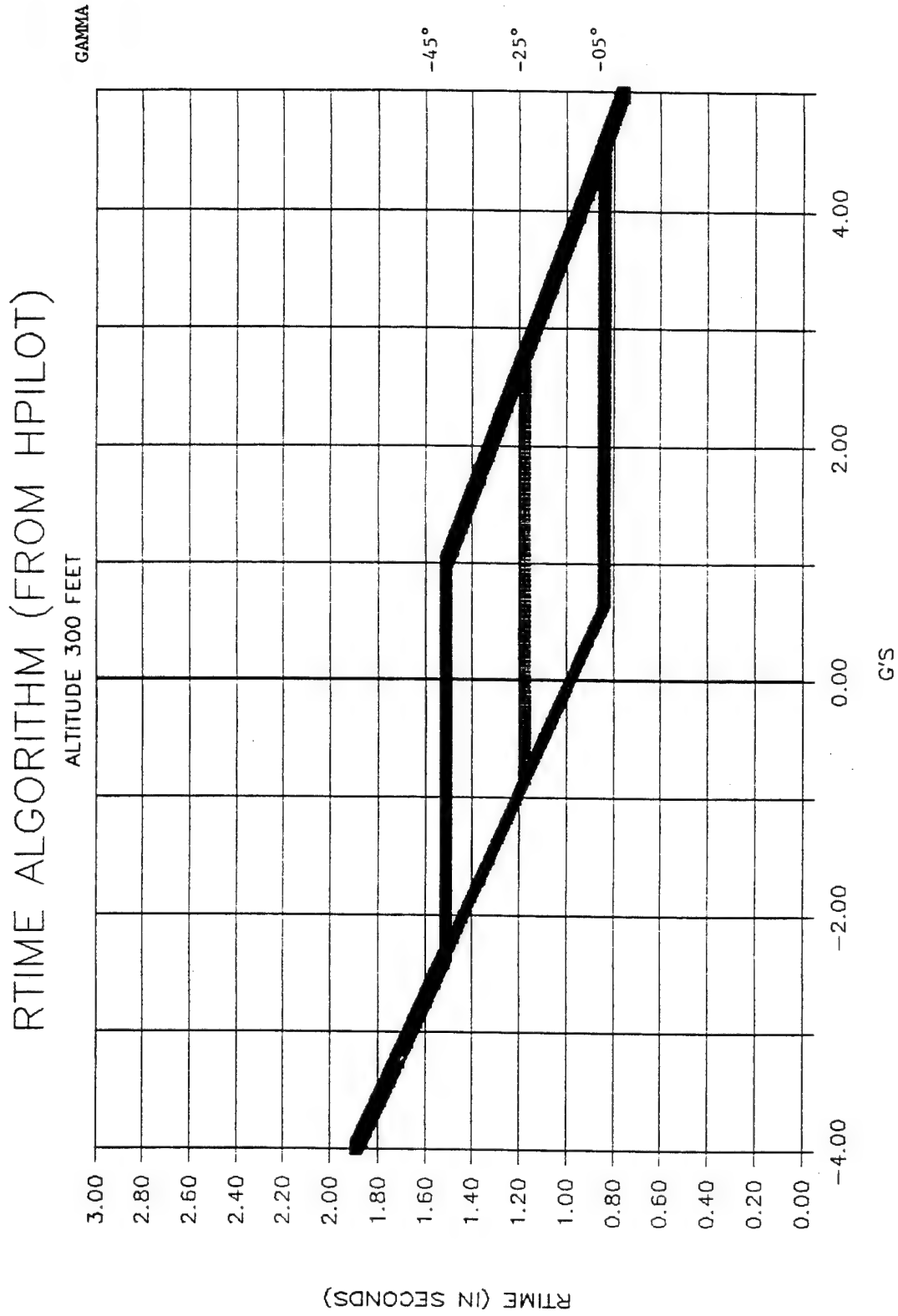


Figure 16. Predicted pilot reaction time (RTIME) as a function of Gs for GAMMA of -45, -25, and -5 degrees at an altitude of 300 feet.

# RTIME ALGORITHM (FROM HPILOT)

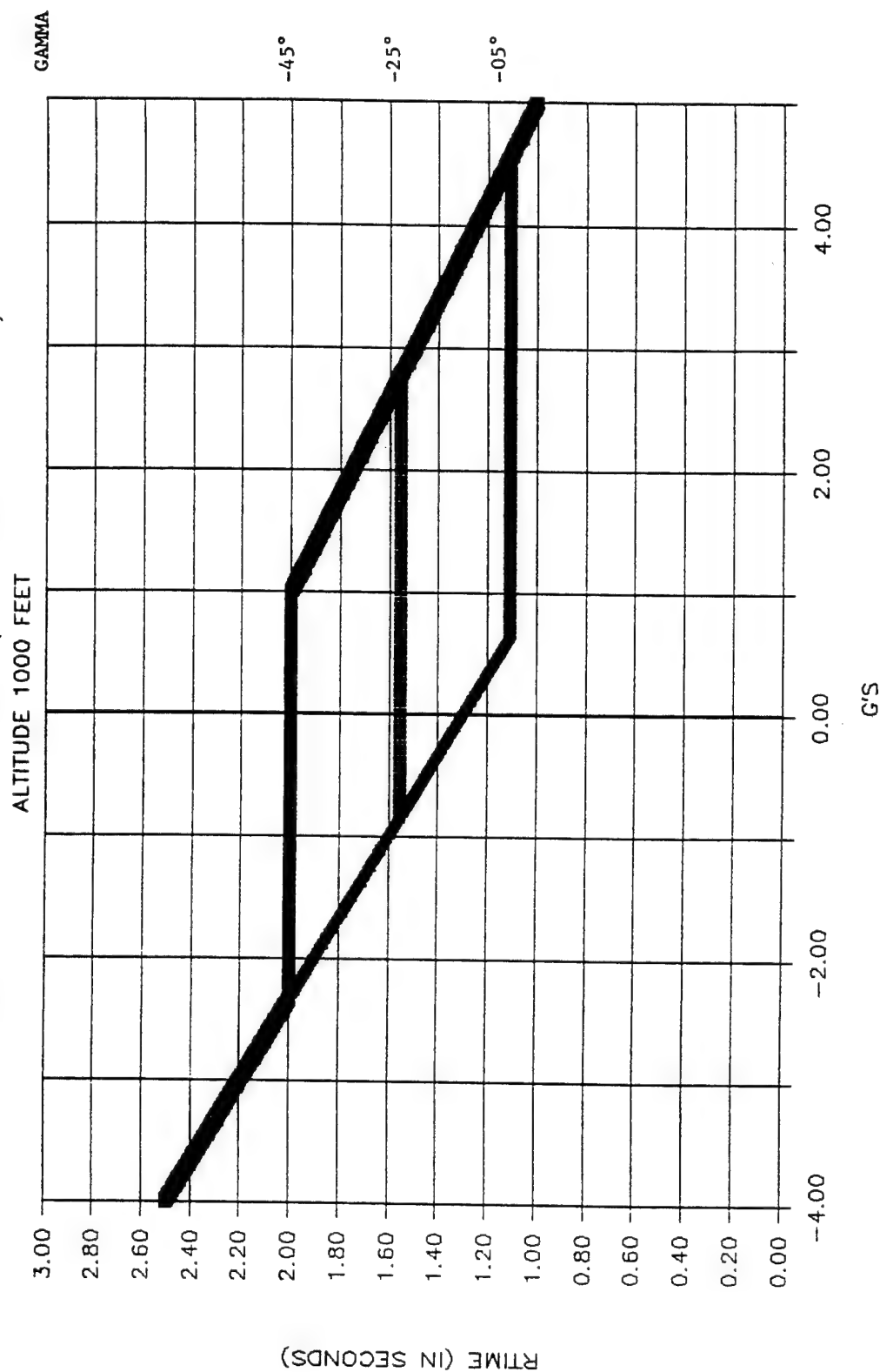


Figure 17. Predicted pilot reaction time (RTIME) as a function of Gs for GAMMA of -45, -25, and -5 degrees at an altitude of 1000 feet.



# **PHASE II EVALUATION**

## **Phase II Introduction**

Phase II of the evaluation used a simple pilot model to place an FB-111 simulator in a specific flight configuration (based on roll angle, flight path angle, wing sweep angle, initial air speed, release altitude, and terrain slope), release the simulator while attempting to stabilize it at one "G," and maintain that condition until a pull-up warning was initiated. Following a predetermined delay, based on the algorithm's calculations for predicted pilot reaction time, the pull-up maneuver was then performed by the pilot model based on the following criteria: Roll and pull simultaneously to a maximum of five Gs or 14 degrees Angle of Attack (AOA). This condition was maintained until the flight path angle of the aircraft became greater than that of the terrain.

The main objective of Phase II was to identify gross areas of concern that could be corrected by GD before the man-in-the-loop evaluation. This was not to be the case however. Due to the dynamic nature of software development, a copy of the GCAS algorithm was received too late to influence additional updates prior to Phase III. Despite its failure to satisfy its main objective, Phase II was still performed in order to examine a broad range of variables and conditions.

## **Phase II Method**

### **Apparatus**

#### **Facility.**

The study was conducted at the Crew Station Design Facility (CSDF), which is a U.S. Air Force simulation facility that belongs to the Aeronautical Systems Division (ASD) of Air Force Systems Command. The CSDF government personnel are assigned by the Human Factors Branch (ASD/ENECH). The facility is used to perform human engineering experiments in support of a variety of System Program Offices.

#### **Simulator.**

The FB-111 simulator, shown in Figure 18, is resting on a three degree-of-freedom motion platform, and includes such major components as the control loading assemblies, seats, canopies, and visual window. An Advanced Simulator Technology interface cabinet is mounted on the nose of the cockpit to interface the simulator with the Systems Engineering Labs computer complex. A walkway with railings is installed around the simulator to insure pilots' safety and allow for easy access in and out of the cockpit. The majority of the instrumentation on the left side of the cockpit are available to the pilot. The FB-111 software package contains all flight, engine, atmosphere, weights and balances modules, a dictionary of all FB-111 data variables, and several other specific commons and datapools.



Figure 18. Picture depicting the FB-111 simulator.

### Computer Complex.

The simulator is connected to a series of large and small computer systems. This computer complex includes five Gould series 32/7780, one Gould concept 32/8780, two PDP 11/34, three PDP 11/35, and two Silicon Graphics Iris Computer Aided Design Stations.

### Design

The objective of the evaluation was to assess the GCAS algorithm response characteristics as a function of five independent variables. These independent variables were: Roll angle, flight path angle (FPA), wing sweep angle, true air speed, and terrain slope. The following table lists the levels for each of the independent variables. These levels were purposely selected in order to test for the algorithm's consistency in predicting required altitude as it changed paths. Each path, in turn, defines a separate list of coefficients to be used by the algorithm.

<u>INDEPENDENT VARIABLES</u>				
ROLL	FPA	WING SWEEP	AIRSPEED	SLOPE
0	-5	25	350	0
30	-10	45	500	3
60	-15	65	650	6
	-20			9
	-25			12
	-30			15
	-35			18
	-40			
	-45			

Four ground dependent measures of interest were recorded for subsequent data analysis. These were: maximum Gs, maximum AOA, minimum clearance, and altitude loss. Maximum Gs and maximum AOA were used as criterion levels for accepting or rejecting each of the completed trials (the acceptable maximum G value was set at six Gs, while the acceptable maximum AOA value was set at 18 degrees). The reason our criterion levels were a little higher than the values assumed in the design of the GCAS algorithm (five Gs or 14 degrees AOA) is that these maximum values normally reflected a momentary spike in stick-pull force as opposed to an average value throughout the recovery maneuver.

Minimum clearance was the primary dependent variable of interest. The overall experimental design was comprised of a single run per condition for a total of 1,701 trials (three Roll X nine FPA X three wing sweep X three air speed X seven slope). Of the 1,701 trials, the simulator failed to fly 567 conditions, which reduced the total number of trials to 1,134. The failed conditions accounted for the following configurations: (1) 189 failed runs at 500 knots with a wing sweep of 25 degrees. This desired airspeed was too high for the 25 degree wing sweep, which caused the aircraft to experience what is referred to as "Mach Tuck." A "Mach Tuck" condition may occur when the aircraft is flying in an

incorrect wing sweep configuration. The air flows over the wings incorrectly forcing down the nose of the aircraft until it slows down to an acceptable airspeed; (2) 189 failed runs at 650 knots with a wing sweep of 25 degrees. The aircraft tended to experience the same response as in the above condition (Mach Tuck); and finally, (3) 189 failed runs at 350 knots and 60 degrees of roll for all wing sweep and terrain slope conditions. The simulator failed to hold the high roll angle at this low airspeed.

## Procedure

A set-up control interface program was developed in order to simplify user-computer interaction and allow the experimenter to monitor the real-time performance characteristics of the simulator as it flew each configuration. As presented in Table 9, the computer program provided the experimenter with the capability to manipulate a number of variables related to the simulator, the terrain it flew over, and the response characteristics of the pilot model.

Upon releasing the aircraft, the experimenter was presented with a new data page that allowed the monitoring of real time simulator performance characteristics (a sample of what is referred to as the "DATA PAGE" is shown in Table 10).

The pilot model attempted to stabilize and maintain the simulator at one G, until the warning signal was initiated. The response delay of the model was configured in such a way that it delayed the pullup maneuver by approximately the same time as the calculated reaction time variable (RTIME) found in the HPILOT sub-algorithm. Rolling and pulling back were executed simultaneously with a maximum of six Gs or 18 degrees AOA. The Gs and AOA were thereafter adjusted to five Gs and 14 degrees AOA. The pullup maneuver continued until the flight path angle of the aircraft became greater than that of the terrain.

TABLE 9. An example of the pilot model set-up page.

```
RECORD GCAS ROBOT AIRPLANE
1. ROLL ANGLE:  30.00
2. GAMMA:  -45.00
3. WING SWEEP:  65.00
4. AIR SPEED:  350.00
5. TERRAIN SLOPE:  15.00
6. TERRAIN SLOPE MINIMUM:  500.00
7. TERRAIN SLOPE MAXIMUM:  8000.00
8. RELEASE ALTITUDE:  8000.00
9. REACTION TIME:  -1.00
A. DESIRED G'S:  5.00
B. REACTION TIME:  1.00
```

PRESS 'R' TO RUN

TABLE 10. An example of the data display page available to the experimenter.

#### DATA DISPLAY PAGE

MACH 0.0    PITCH 0.0    ALT 0  
IAS 0    ROLL 0.0    VVI .0    AOA 0.00

MISSION #: 0

SUBJECT #: 0

DATA COL: (OFF)

RECORD: (OFF) NO WARNING

GAMMA 0.0    WING SWEEP 0.0

PHI 0.0    TERR SLOPE 0.0

SPEED 0.0

Once the maneuver had been completed, the experimenter was given the opportunity to plot, as shown in Figure 19, the course and performance characteristics exhibited throughout the pull-up maneuver.

### Phase II Results

No formal statistical analyses were performed on the data since only one subject (the robot aircraft) existed. However, the data from all 1,134 runs were sorted by airspeed, terrain slope, and wing sweep, and graphed for minimum clearance as a function of flight path angle (or gamma) for all the levels of roll angle. A description of the data will be given for each airspeed (350, 500, and 650 knots) separately.

#### Low Airspeed -- 350 Knots

The plots from the low airspeed runs are presented in Figures 20 through 26. Each figure contains three plots of minimum clearance as a function of flight path angle (-5, -10, -15, -20, -25, -30, -35, -40, and -45 degrees) and roll angle (0 and 30 degrees). The 60 degree roll at 350 knots could not be flown by the simulator (there was difficulty in the pilot model holding the 60 degree roll up in the air before releasing the simulator), and were therefore deleted from the evaluation. Each figure represents one slope condition for all three wing sweep configurations (25, 45, and 65 degrees). The 25 degree wing sweep configuration was defined as standard for the 350 knot airspeed, while the 45 and 65 degree wing sweeps were defined as nonstandard configurations. Four areas of concern arose from examining the data.

The first and most obvious concern was related to terrain slope. When terrain slope increased beyond zero degrees, the algorithm's ability to predict diminished. This trend occurred under all configurations of wing sweep and roll.



The second area of concern was related to the estimations for required altitude to roll the aircraft back to wings level. The algorithm's ability to predict altitude loss for the different roll angle conditions was more consistent at a wing sweep of 25 degrees (standard configuration) than at 45 and 60 degrees (nonstandard configurations). Variability between zero-degree roll and 60 degree roll, at 45 degree wing sweep, began appearing when the slope of the terrain was at zero, and increased significantly at nine, 12, 15, and 18 degrees. For the 65 degree wing sweep and 60 degree roll conditions, the algorithm consistently appeared to underestimate the needed altitude for a safe recovery.

The third area of concern was related to the 65 degree wing sweep configuration. The algorithm consistently failed to predict in all roll and slope conditions with the exception of zero-degree roll at zero-degree slope. While the authors understood this was a nonstandard configuration (65 degree wing sweep at 350 knots), the algorithm was written in such a way that it would be responsive under all configurations.

Finally, the algorithm's ability to predict weakened, as a function of flight path angle, with increasing terrain slopes. This phenomenon was demonstrated when the line slopes for minimum clearance changed from a negative to a positive relationship, as a function of flight path angle for all wing sweep and roll angle conditions.

SLOPE=0 SPEED=350 WSWEEP=25

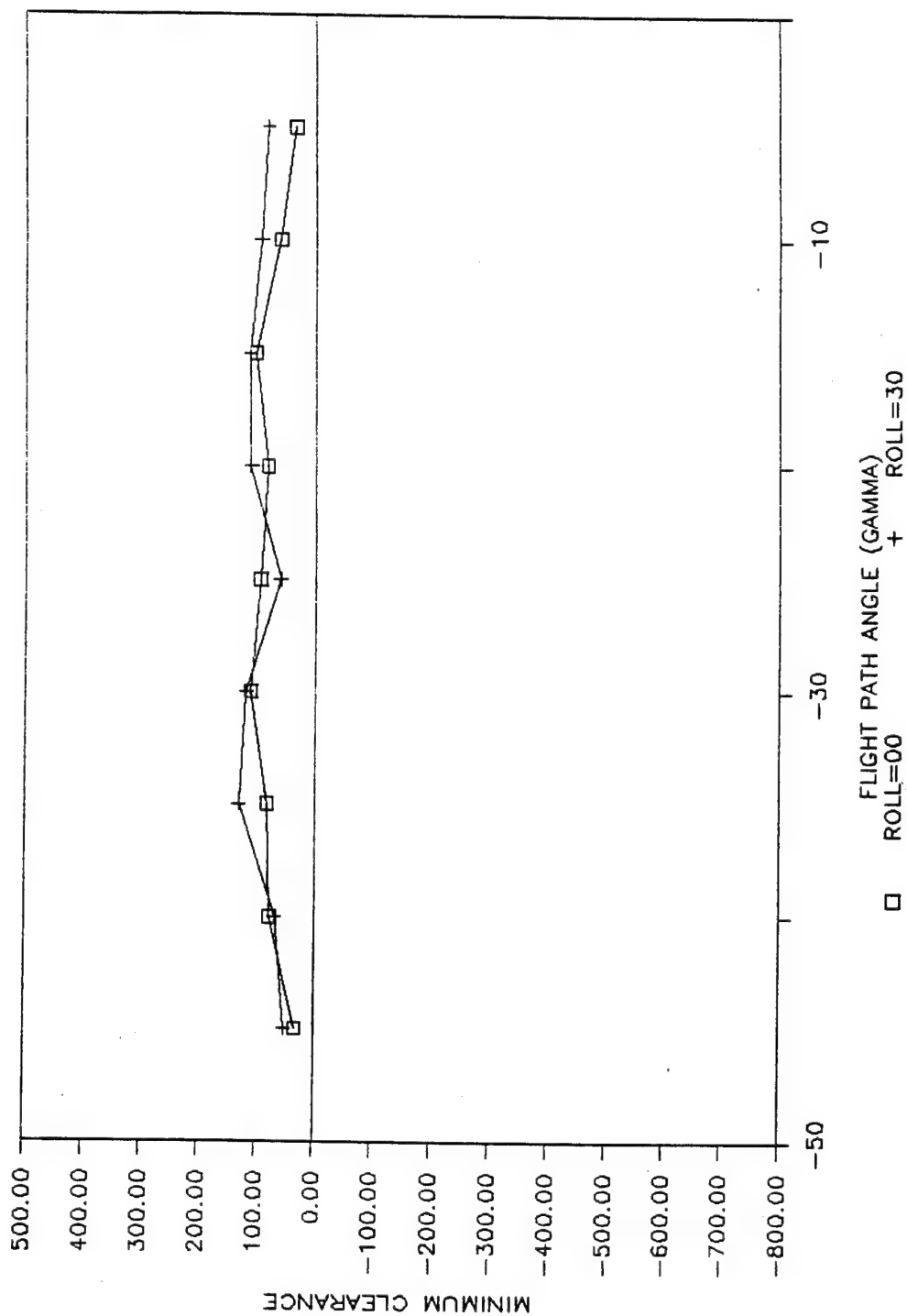


Figure 20 (a). Minimum clearance as a function of flight path angle for pilot model at slope=0 speed=350 wsweep=25.



SLOPE=0 SPEED=350 WSWEEP=45

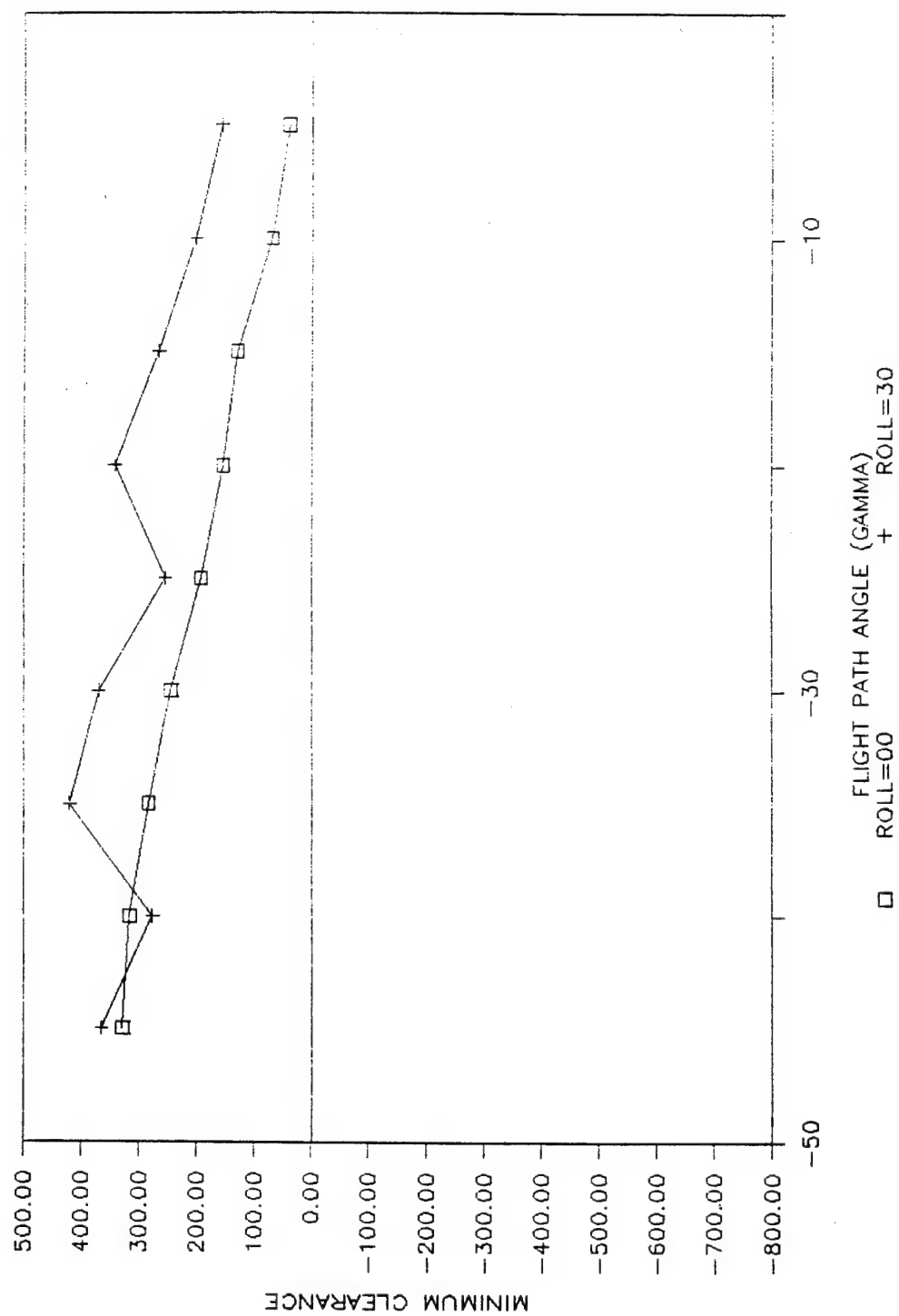


Figure 20 (b). Minimum clearance as a function of flight path angle for pilot model at slope=0 speed=350 wsweep=45.

SLOPE=0 SPEED=350 WSWEEP=65

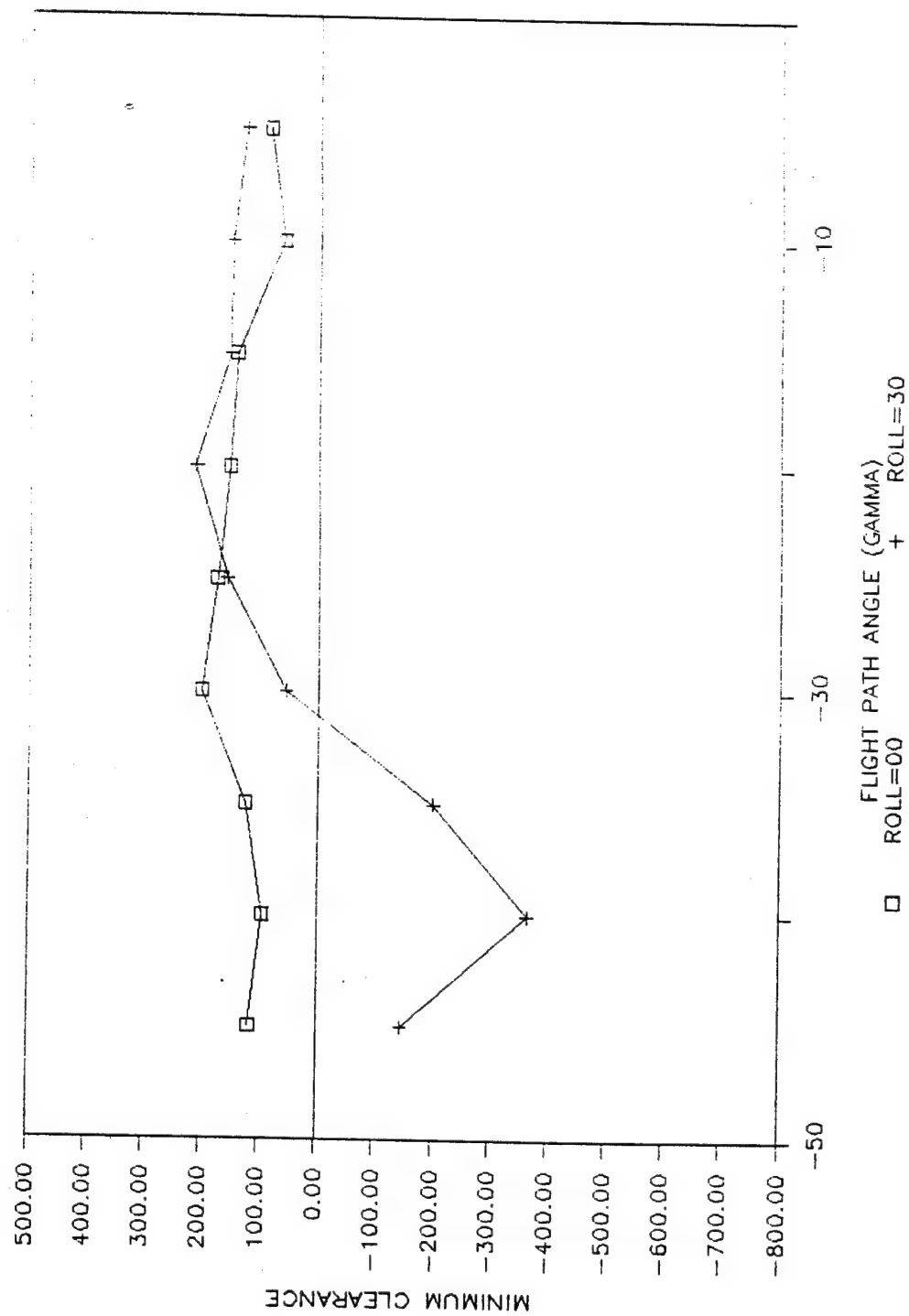


Figure 20 (c). Minimum clearance as a function of flight path angle for pilot model at slope = 0 speed = 350 wsweep = 65.

SLOPE=3 SPEED=350 WSWEEP=25

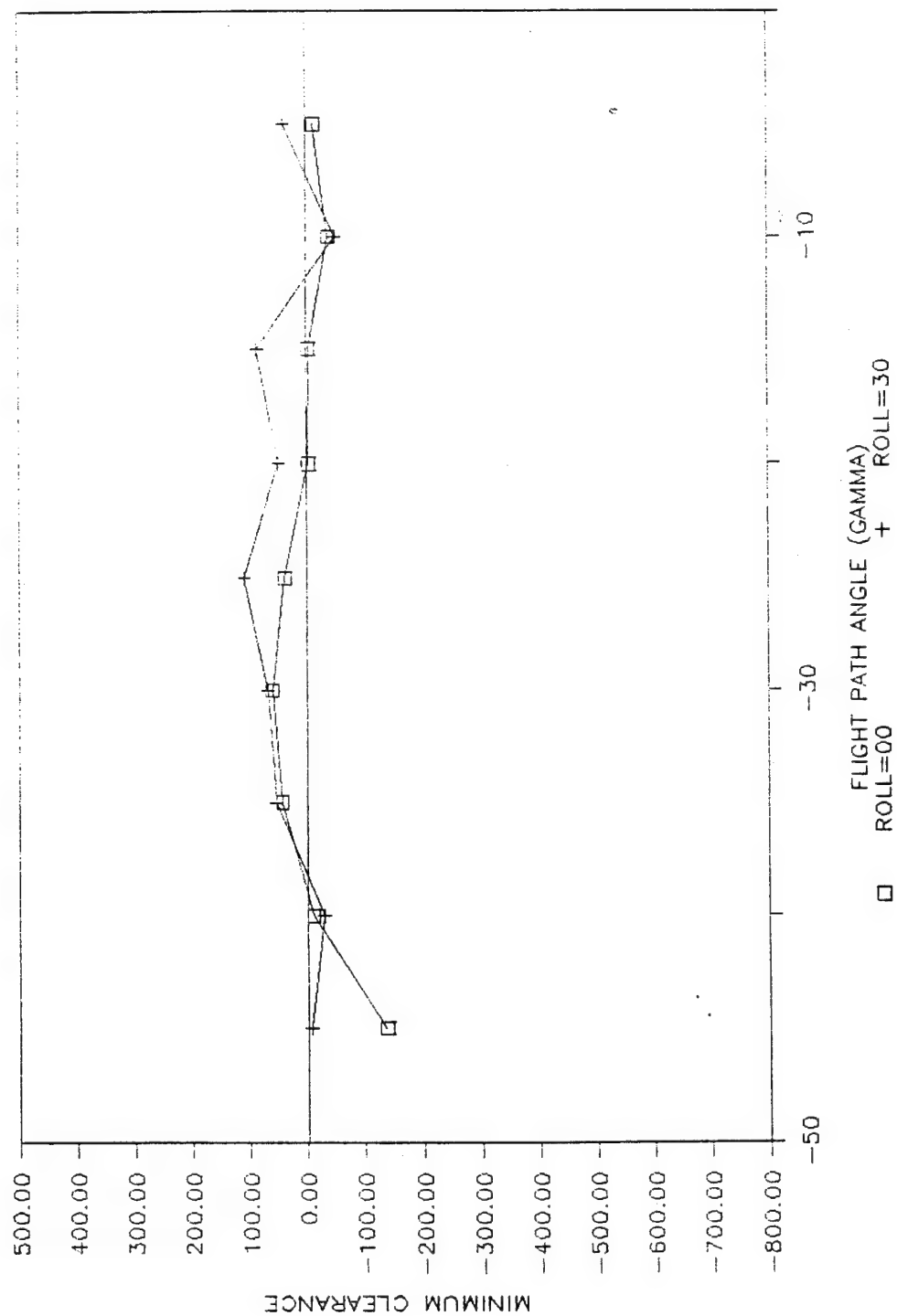


Figure 21 (a). Minimum clearance as a function of flight path angle for pilot model at slope=3 speed=350 wsweep=25.

SLOPE=3 SPEED=350 WSWEEP=45

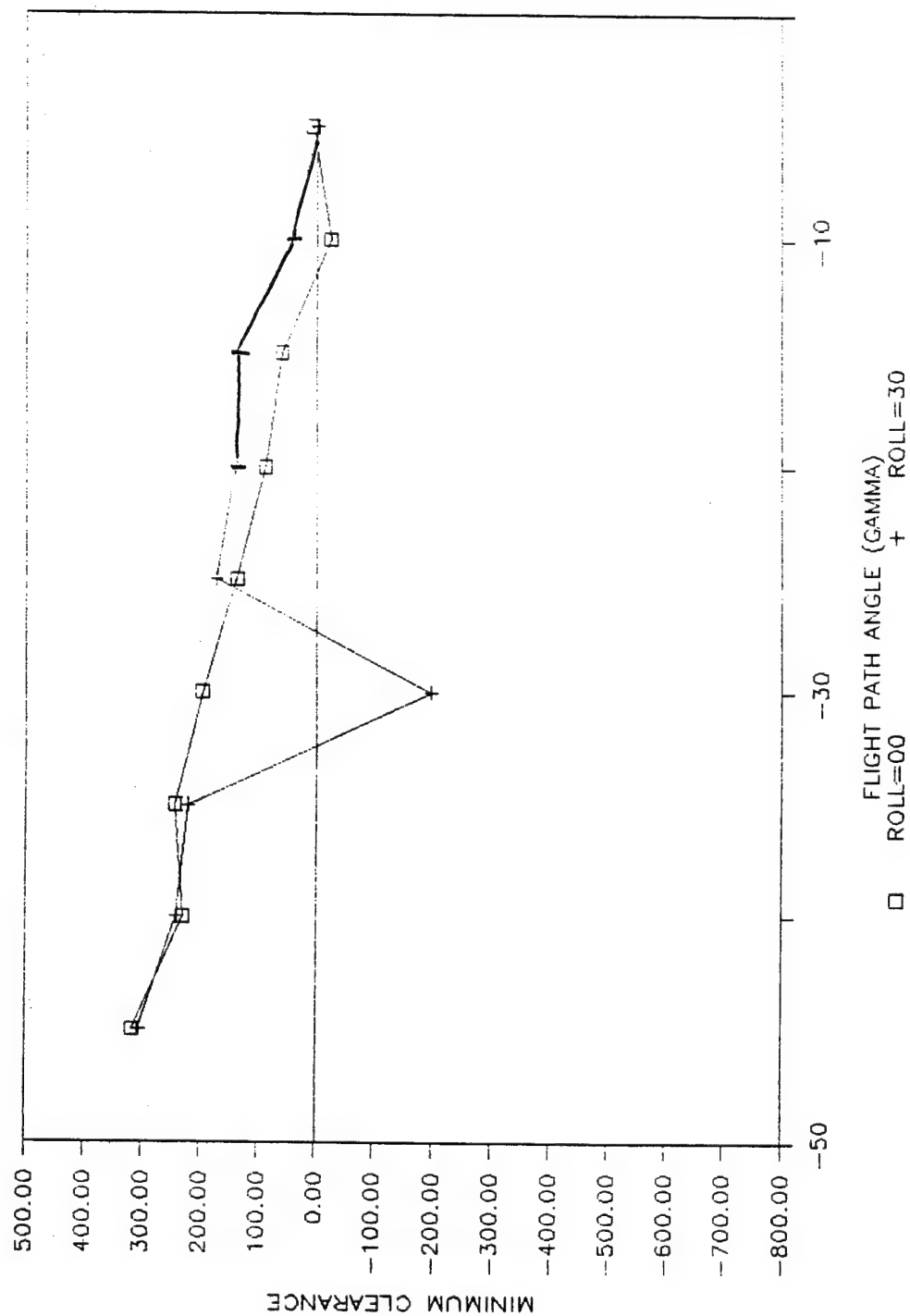


Figure 21 (b). Minimum clearance as a function of flight path angle for pilot model at slope = 3 speed = 350 wsweep = 45.

SLOPE=3 SPEED=350 WSWEEP=65

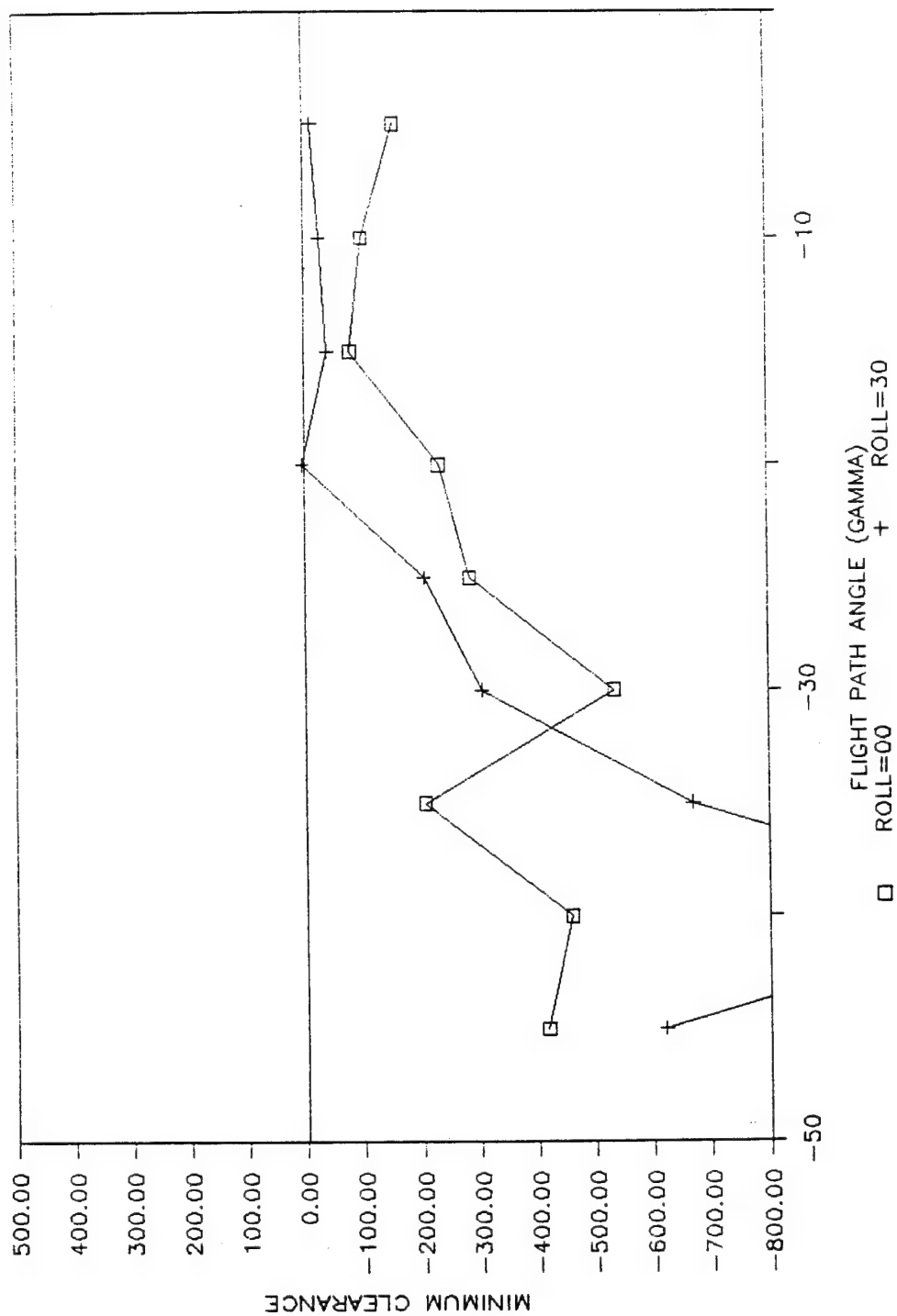


Figure 21 (c). Minimum clearance as a function of flight path angle for pilot model at slope = 3 speed = 350 wsweep = 65.

SLOPE=6 SPEED=350 WSWEEP=25

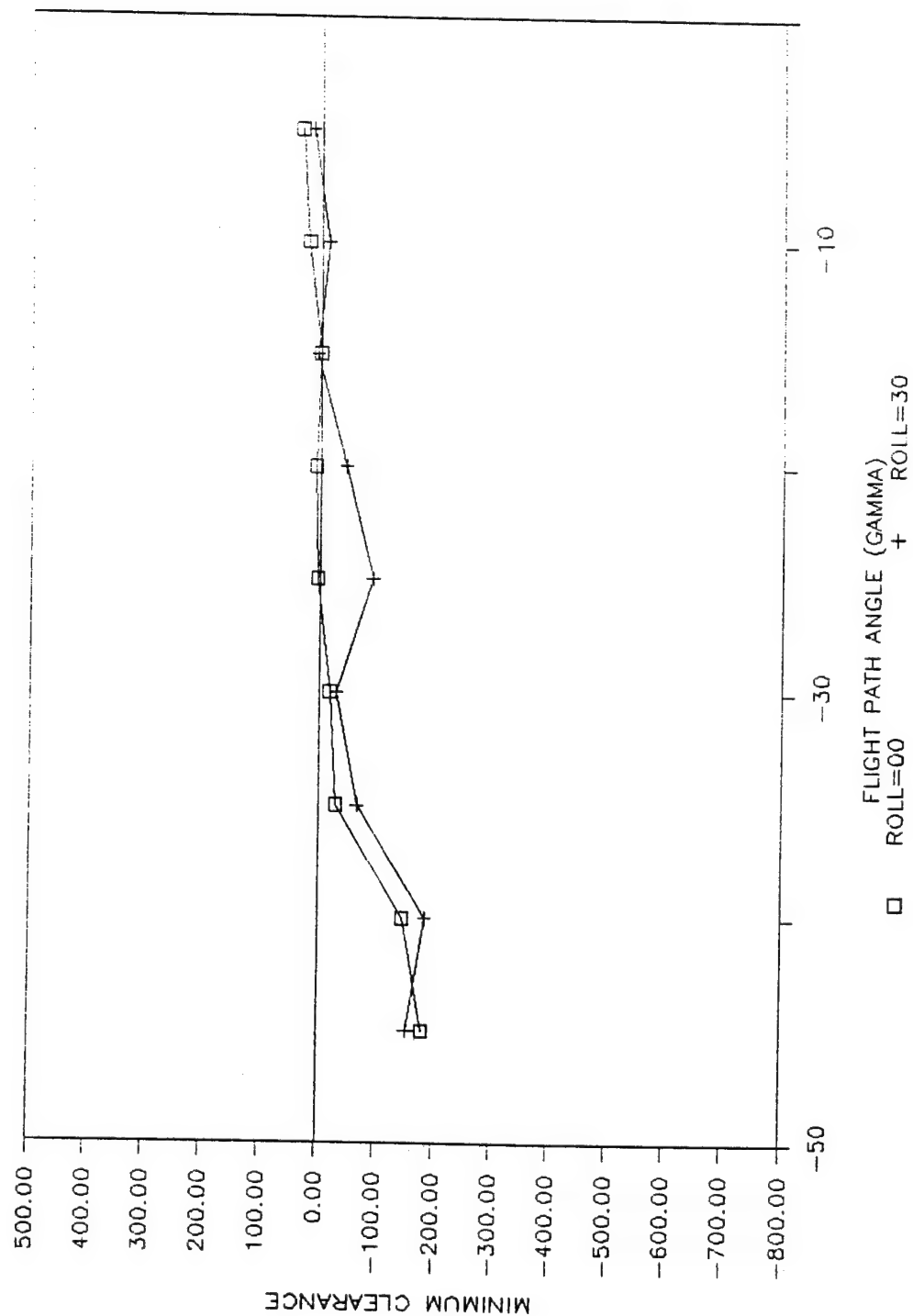


Figure 22 (a). Minimum clearance as a function of flight path angle for pilot model at slope = 6 speed = 350 wsweep = 25.

SLOPE=6 SPEED=350 WSWEEP=45

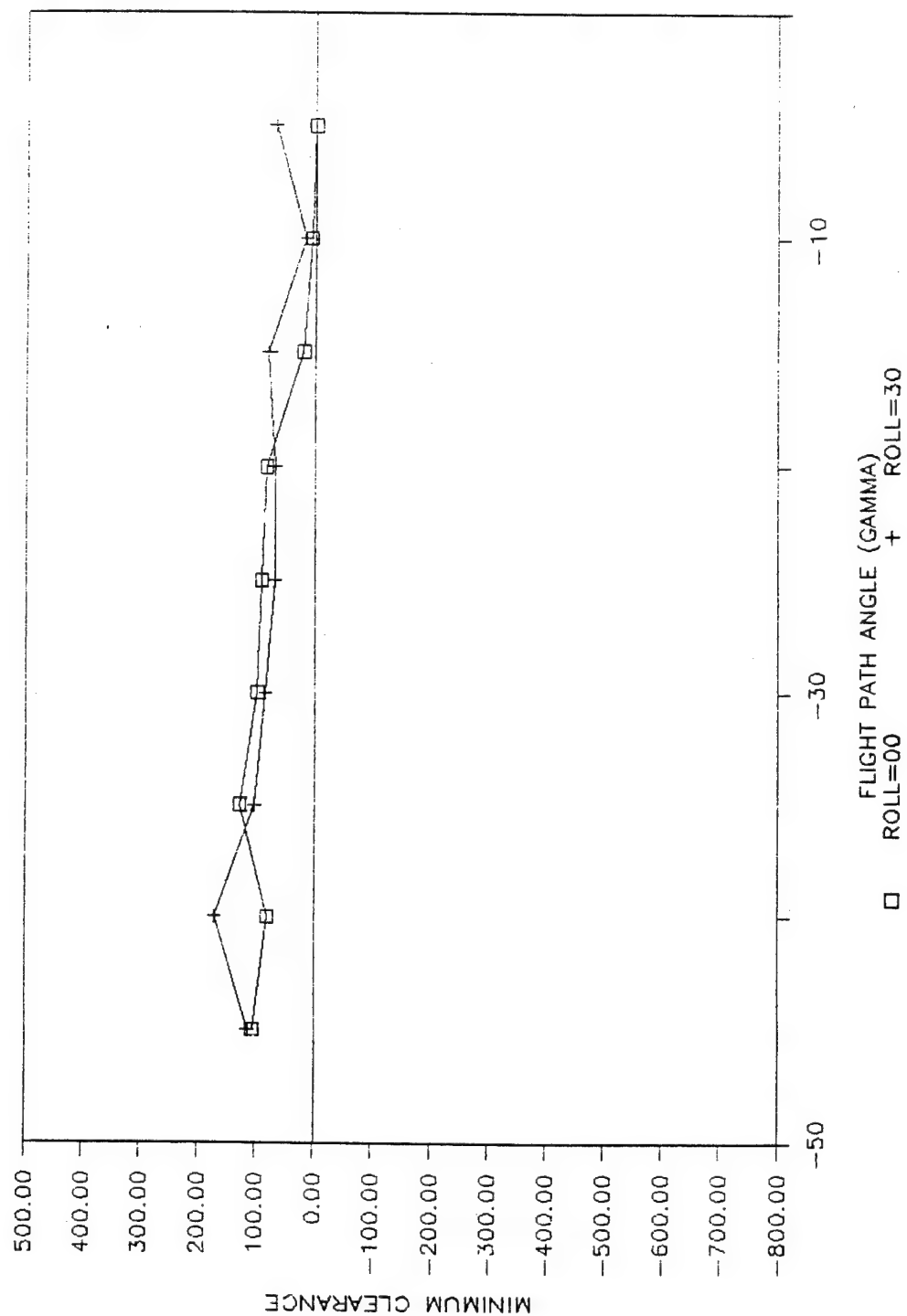


Figure 22 (b). Minimum clearance as a function of flight path angle for pilot model at slope = 6 speed = 350 wsweep = 45.

SLOPE=6 SPEED=350 WSWEEP=65

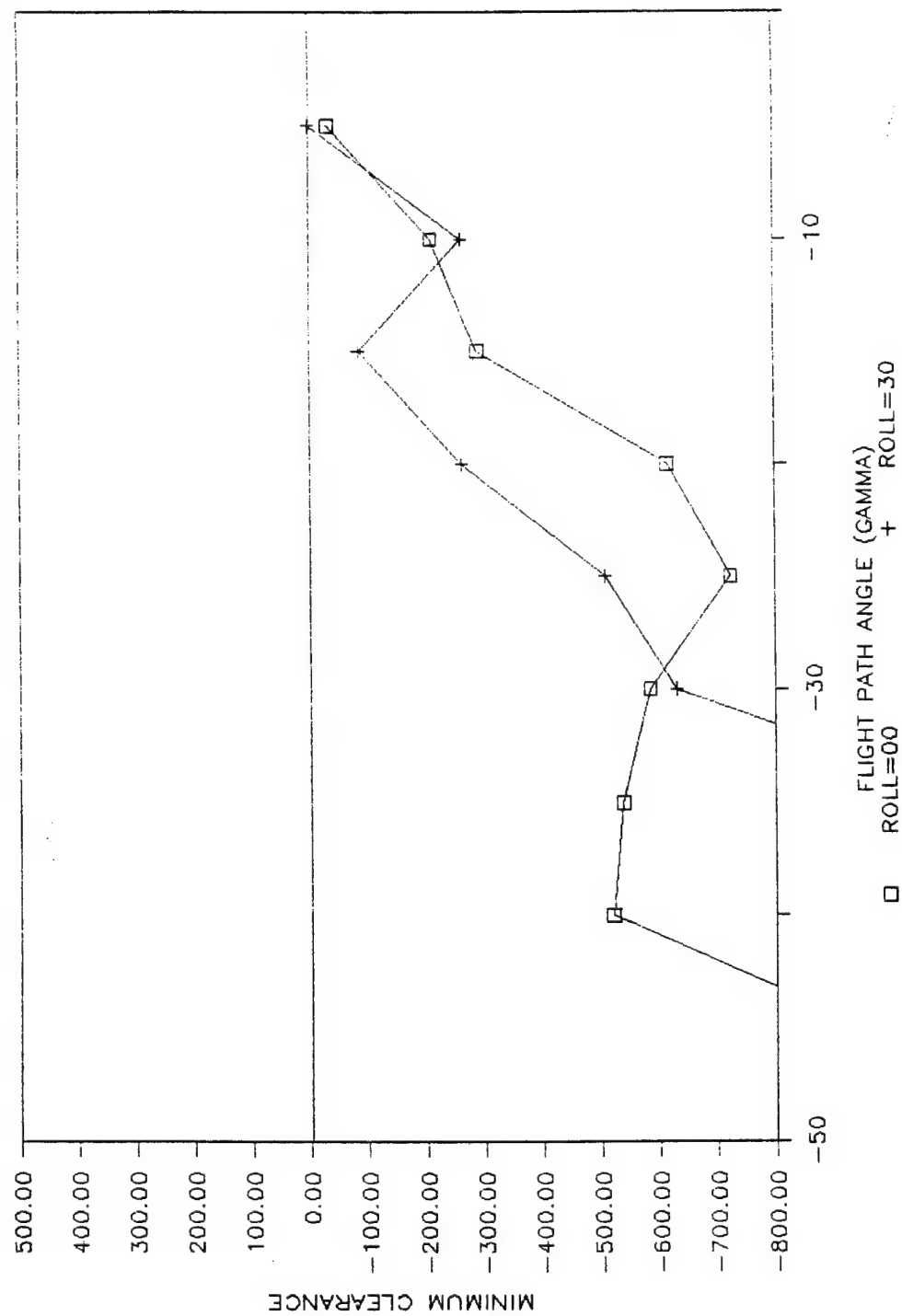


Figure 22 (c). Minimum clearance as a function of flight path angle for pilot model at slope=6 speed=350 wsweep=65.



SLOPE=9 SPEED=350 WSWEEP=25

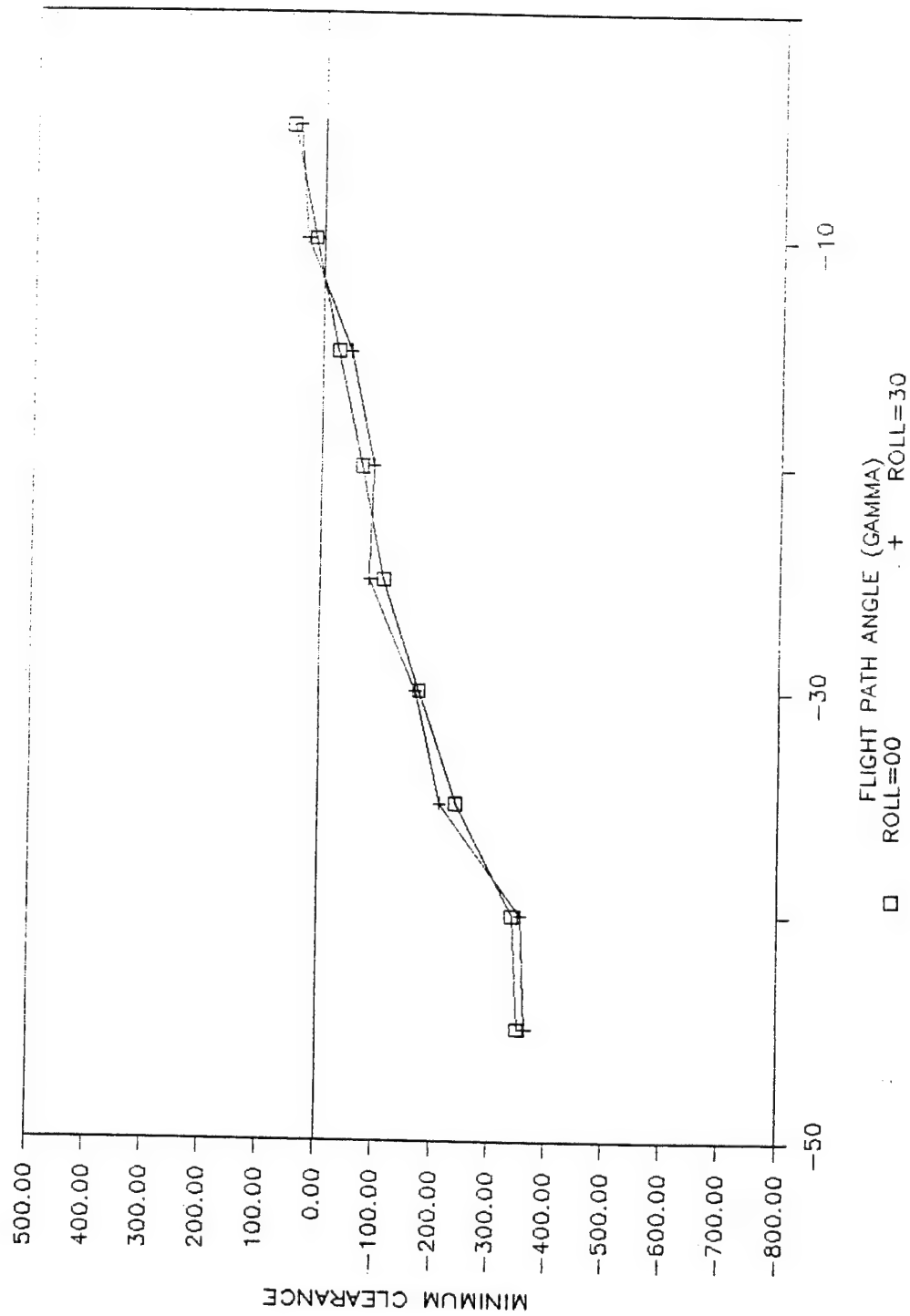


Figure 23 (a). Minimum clearance as a function of flight path angle for pilot model at slope=9 speed=350 wsweep=25.

SLOPE=9 SPEED=350 WSWEEP=45

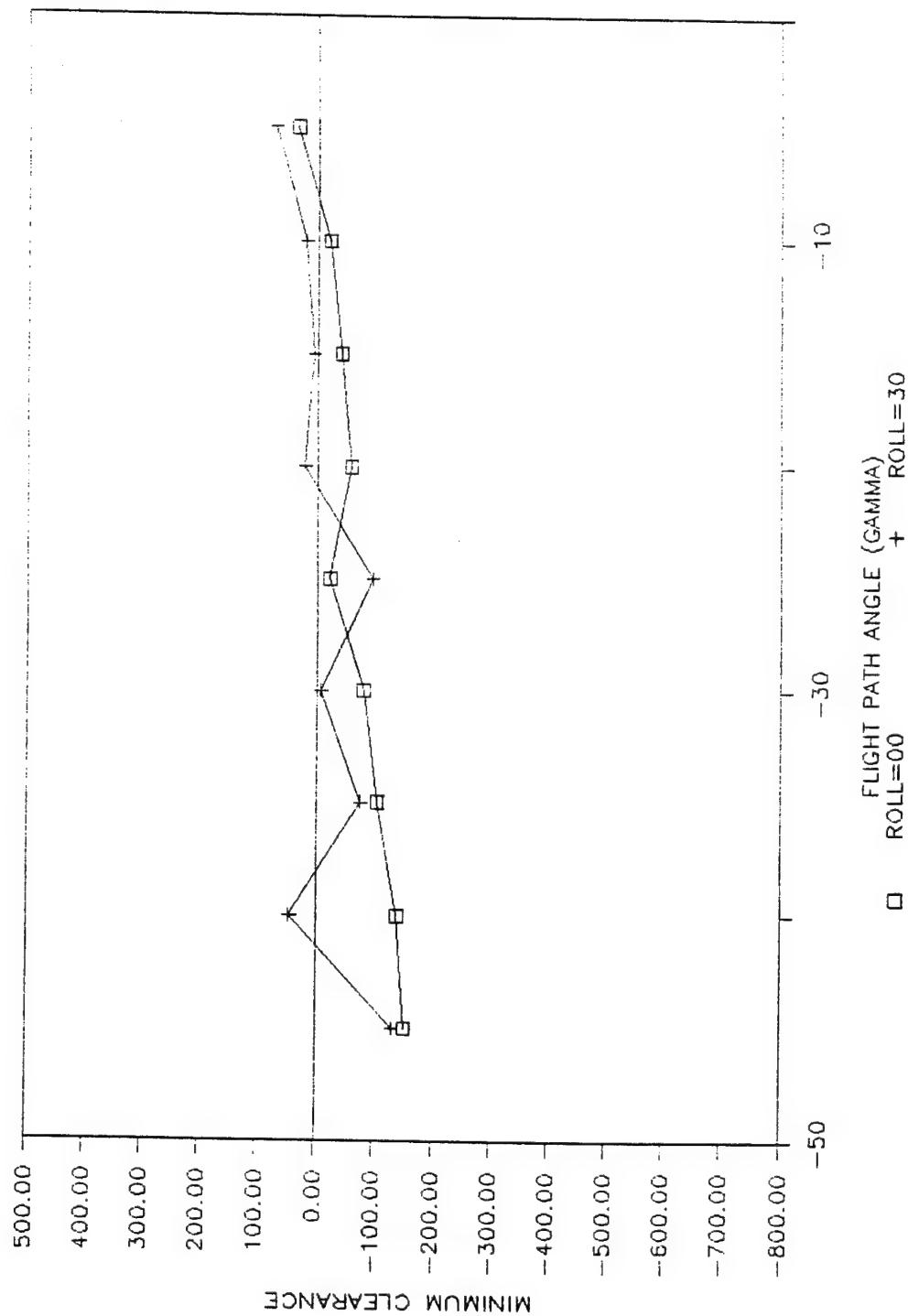


Figure 23 (b). Minimum clearance as a function of flight path angle for pilot model at slope=9 speed=350 wsweep=45.

SLOPE=9 SPEED=350 WSWEEP=65

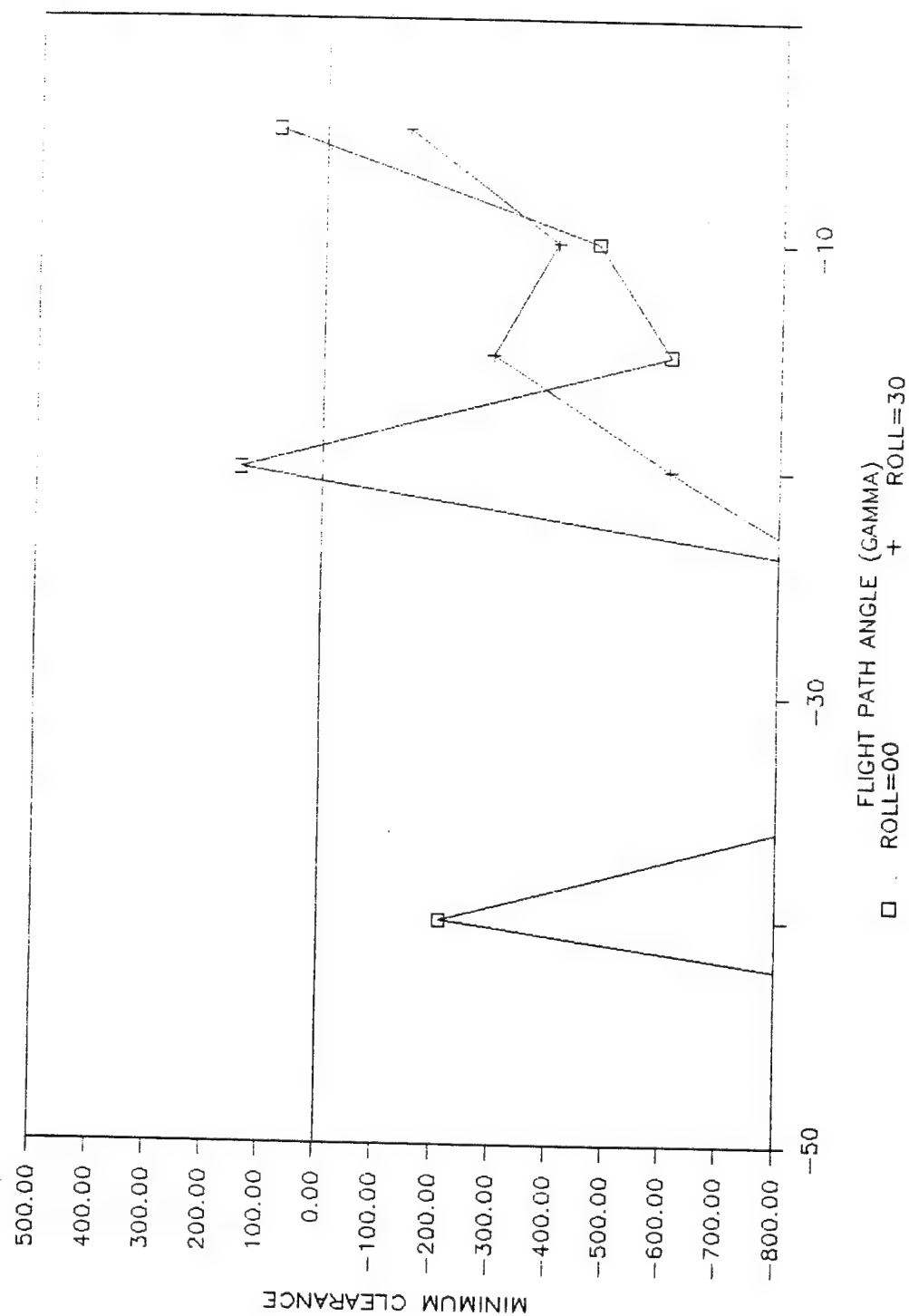


Figure 23 (c). Minimum clearance as a function of flight path angle for pilot model at slope=9 speed=350 wsweep=65.

SLOPE=12 SPEED=350 WSWEEP=25

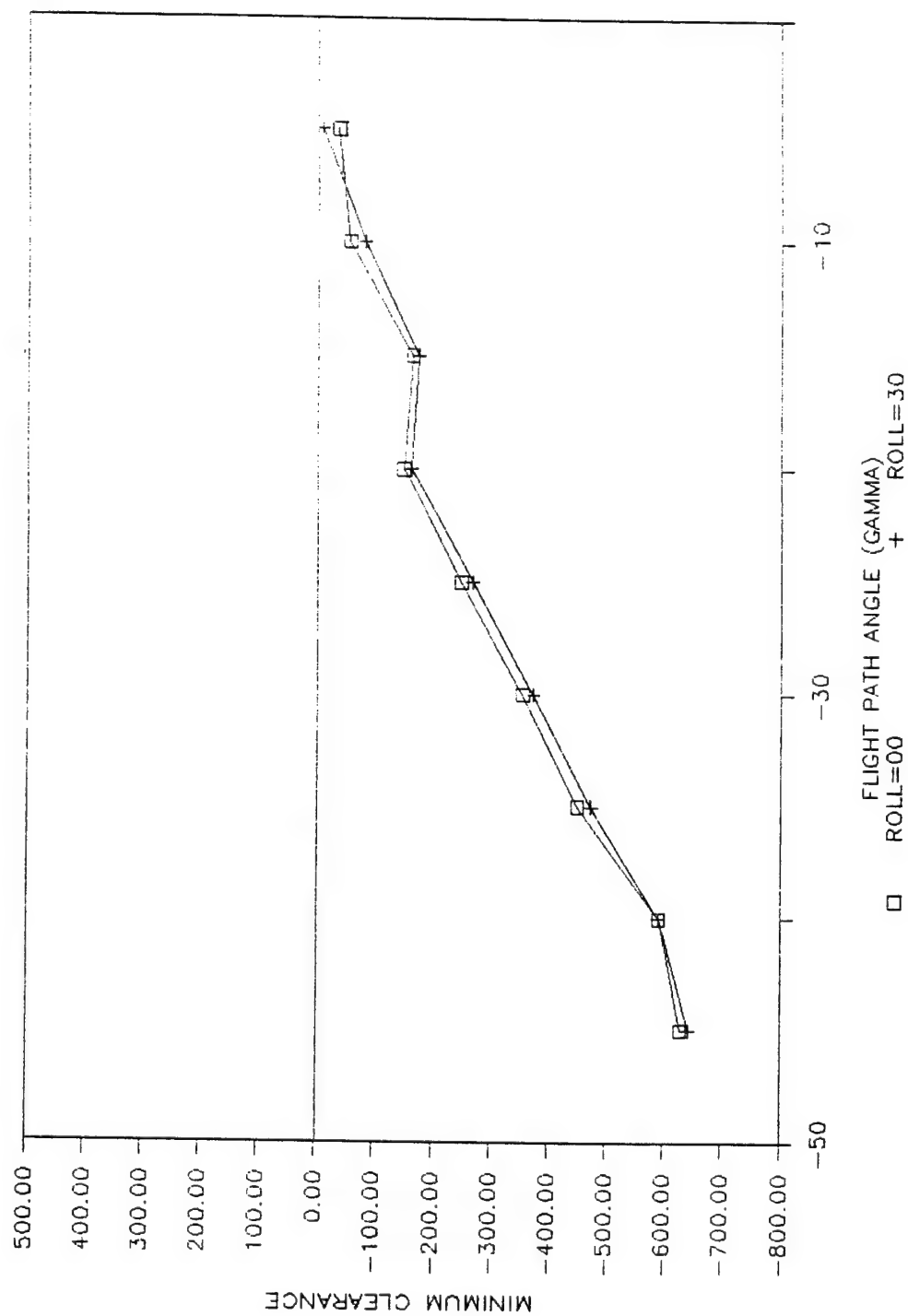


Figure 24 (a). Minimum clearance as a function of flight path angle for pilot model at slope = 12 speed = 350 wsweep = 25.

SLOPE=12 SPEED=350 WSWEEP=45

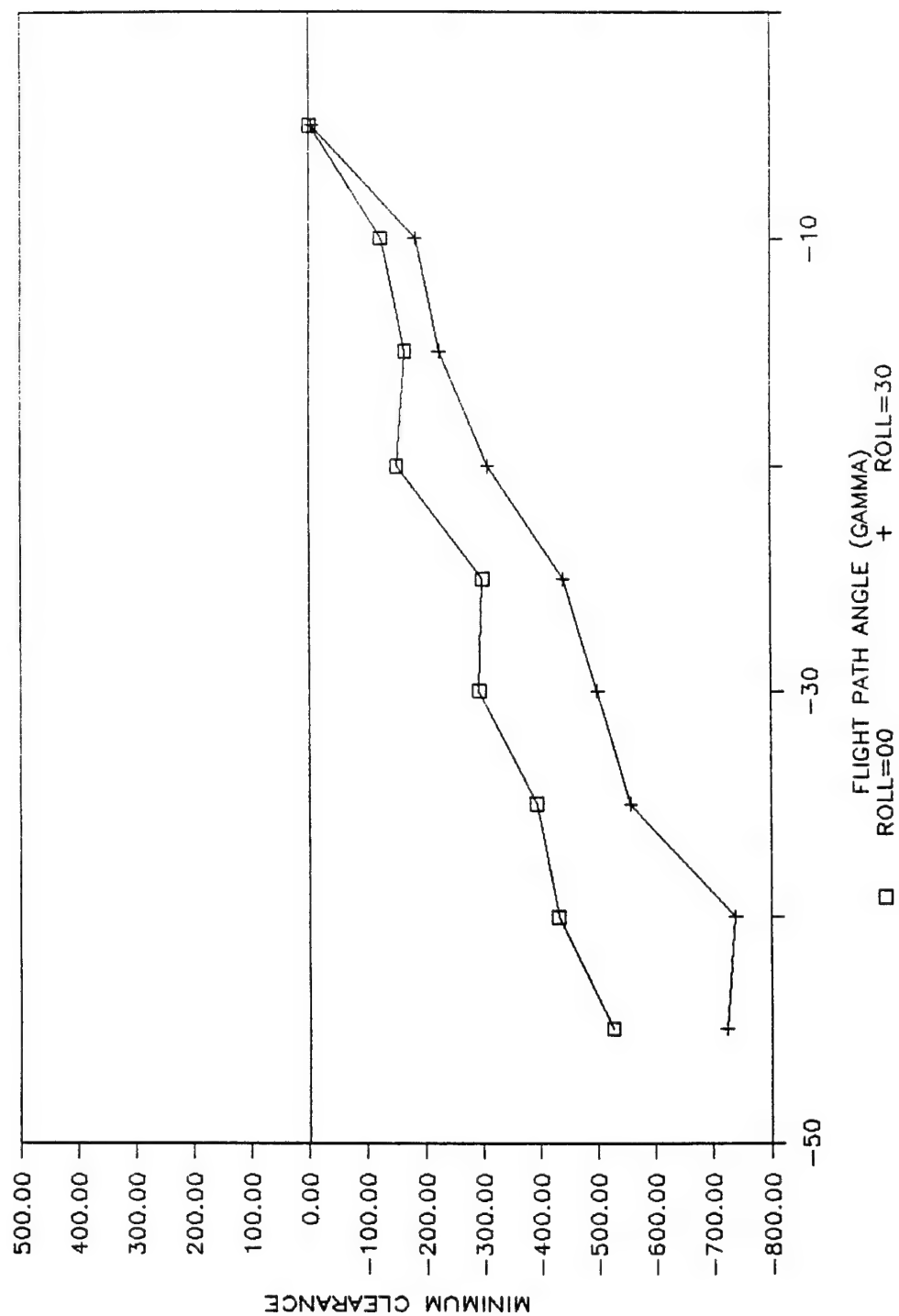


Figure 24 (b). Minimum clearance as a function of flight path angle for pilot model at slope = 12 speed = 350 wswEEP = 45.

SLOPE=12 SPEED=350 WSWEEP=65

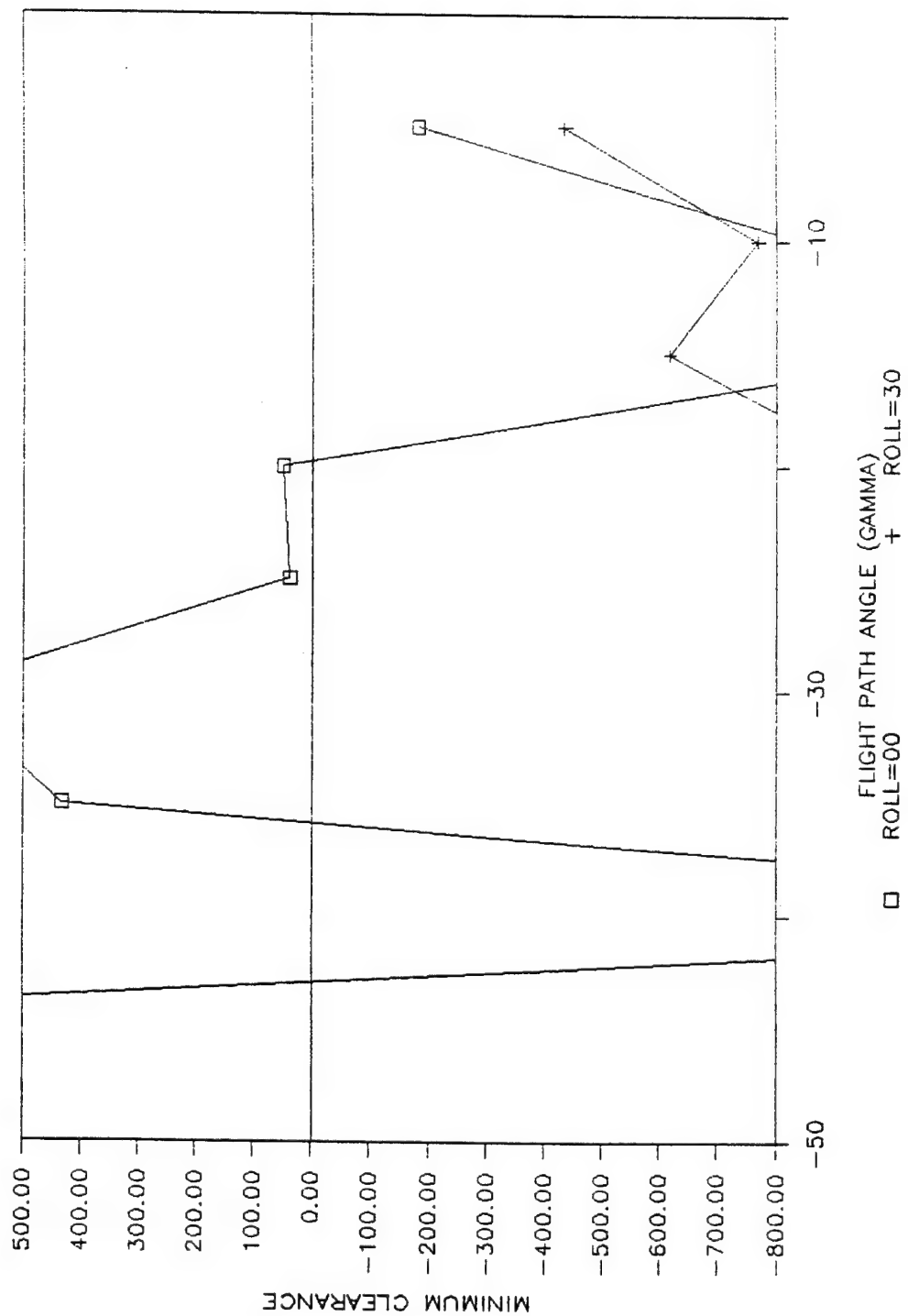


Figure 24 (c). Minimum clearance as a function of flight path angle for pilot model at slope = 12 speed = 350 wsweep = 65.

SLOPE=15 SPEED=350 WSWEEP=25

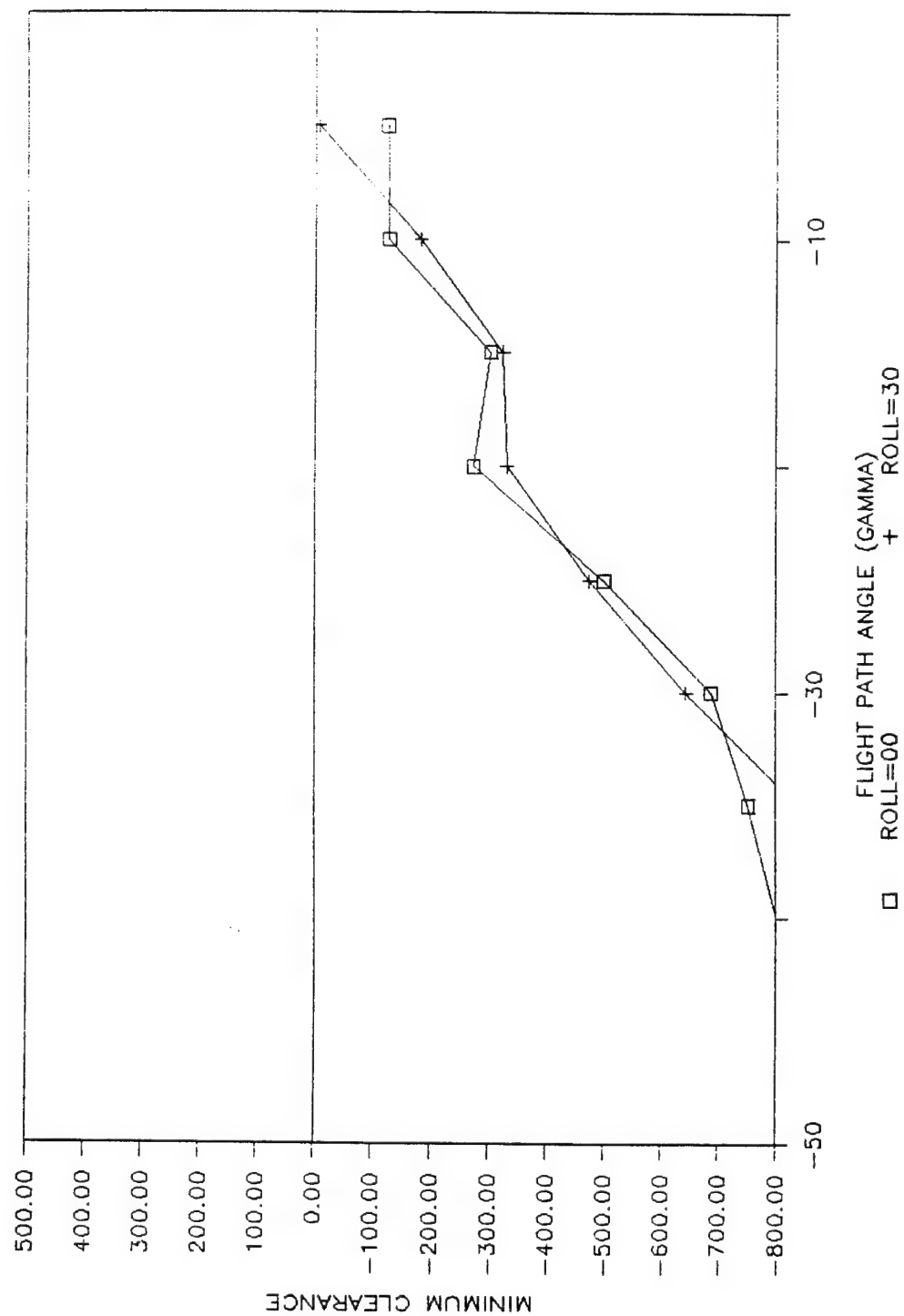


Figure 25 (a). Minimum clearance as a function of flight path angle for pilot model at slope = 15 speed = 350 wsweep = 25.

SLOPE=15 SPEED=350 WSWEEP=45

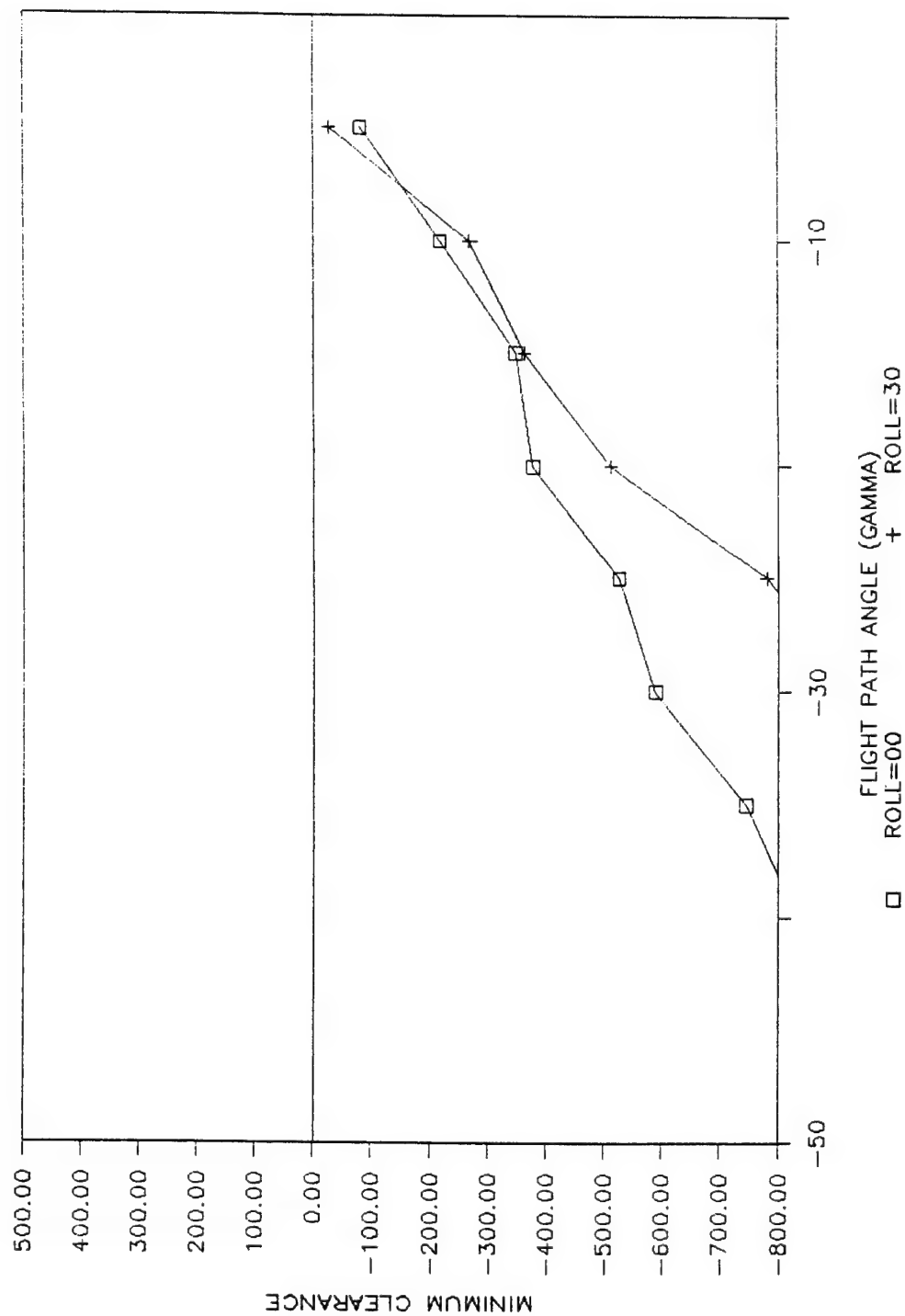


Figure 25 (b). Minimum clearance as a function of flight path angle for pilot model at slope = 15 speed = 350 wsweep = 45.



SLOPE=15 SPEED=350 WSWEEP=65

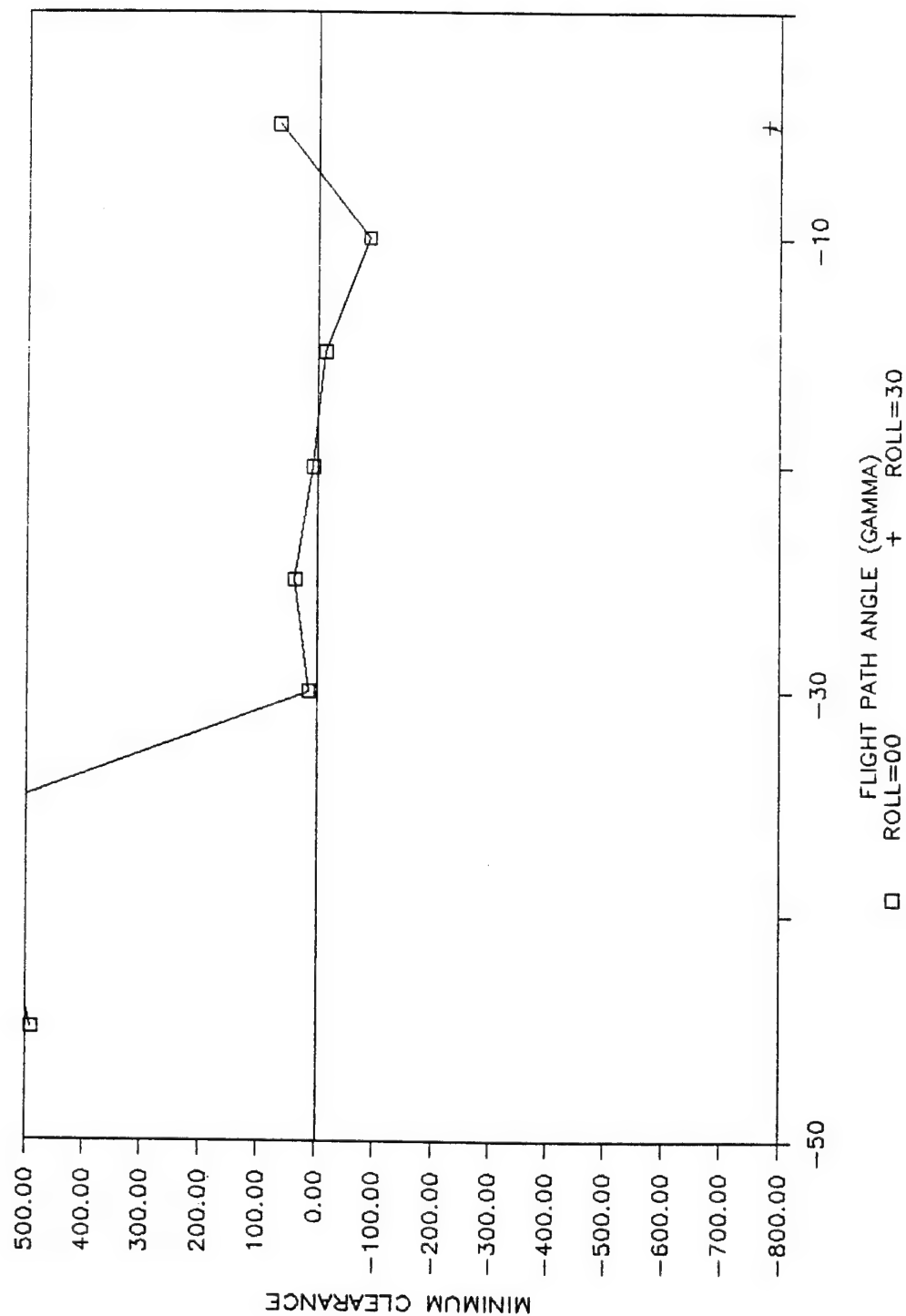


Figure 25 (c). Minimum clearance as a function of flight path angle for pilot model at slope = 15 speed = 350 wsweep = 65.

SLOPE=18 SPEED=350 WSWEEP=25

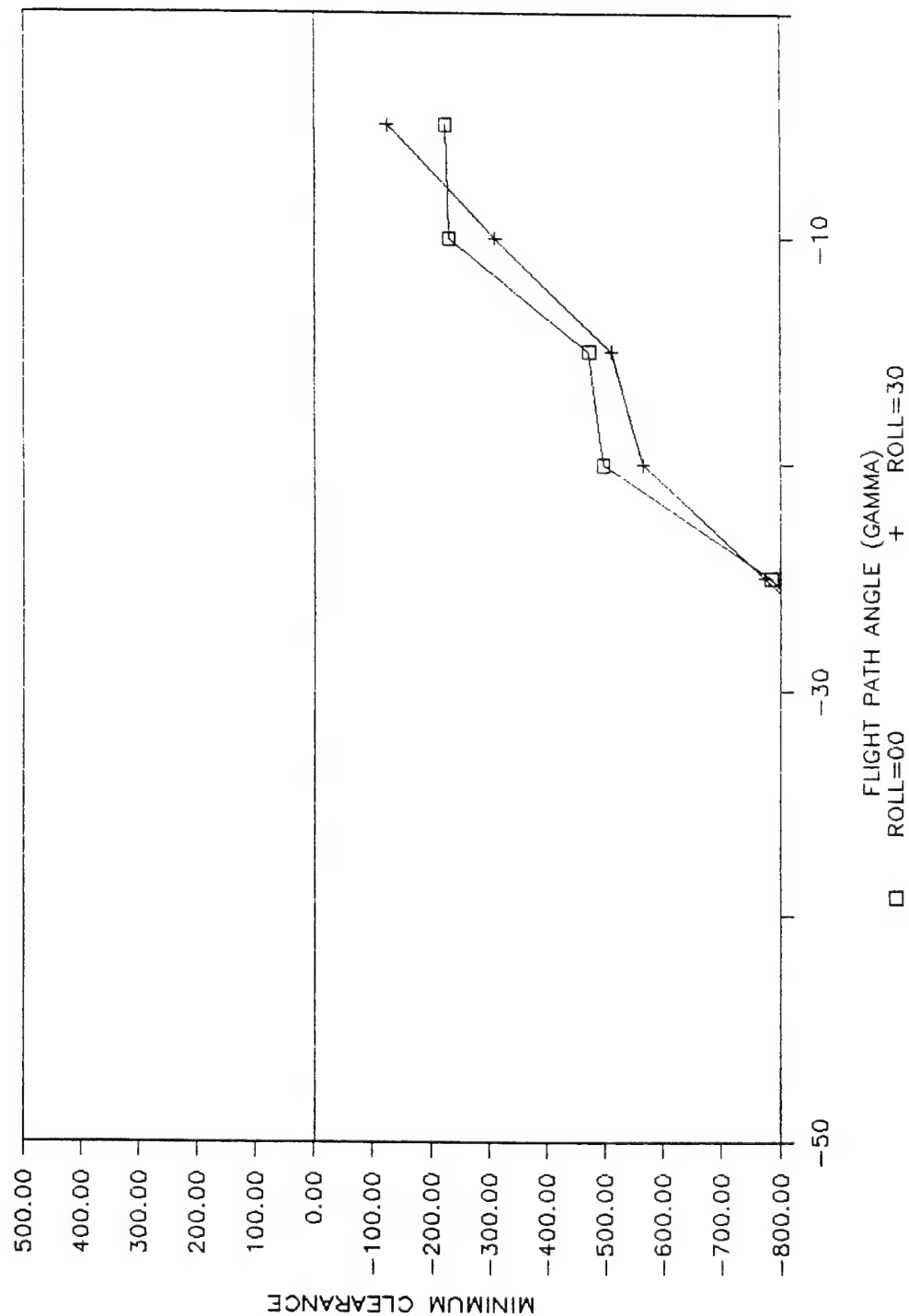


Figure 26 (a). Minimum clearance as a function of flight path angle for pilot model at slope = 18 speed = 350 wsweep = 25.

SLOPE=18 SPEED=350 WSWEEP=45

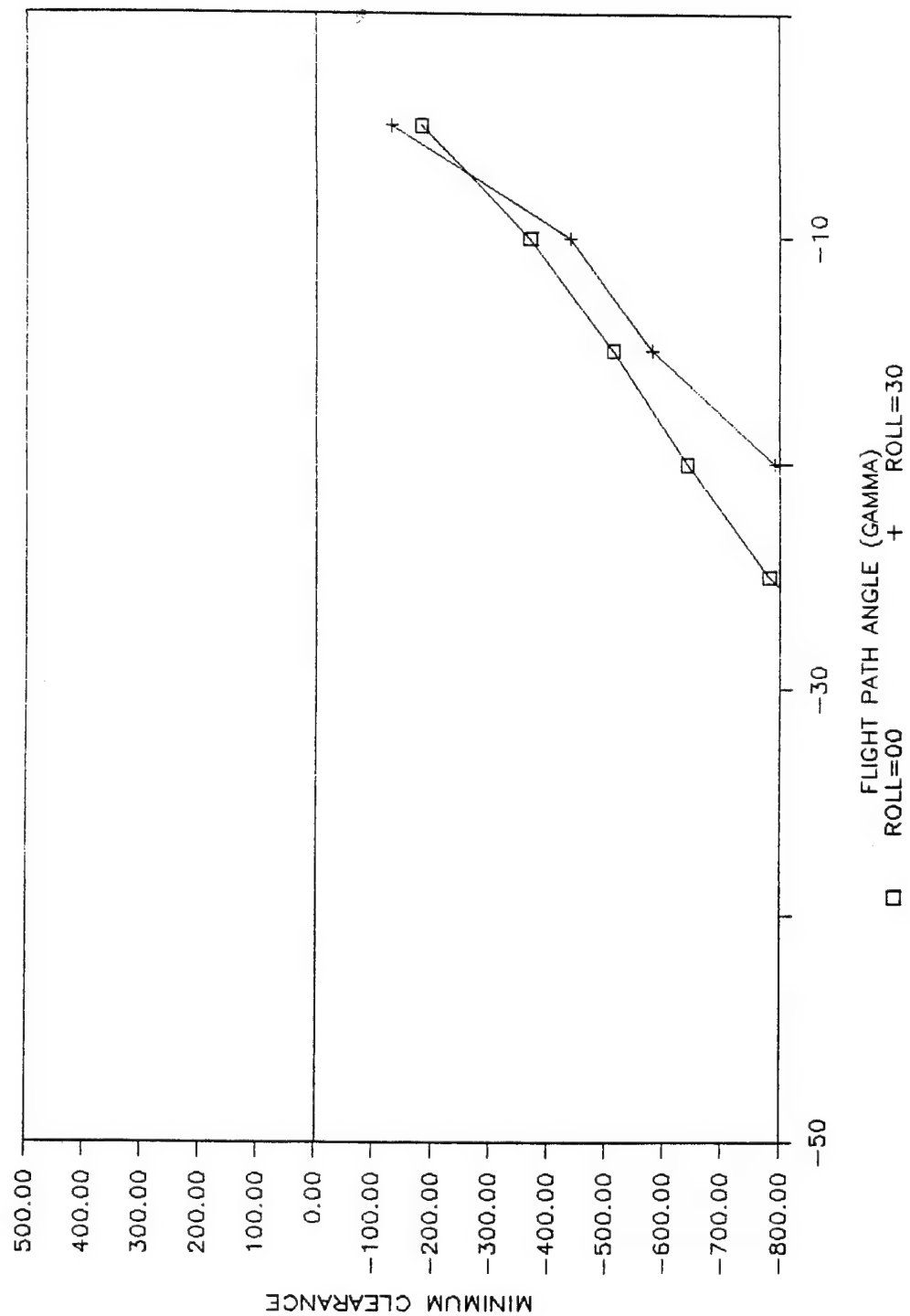


Figure 26 (b). Minimum clearance as a function of flight path angle for pilot model at slope = 18 speed = 350 wsweep = 45.

SLOPE=18 SPEED=350 WSWEEP=65

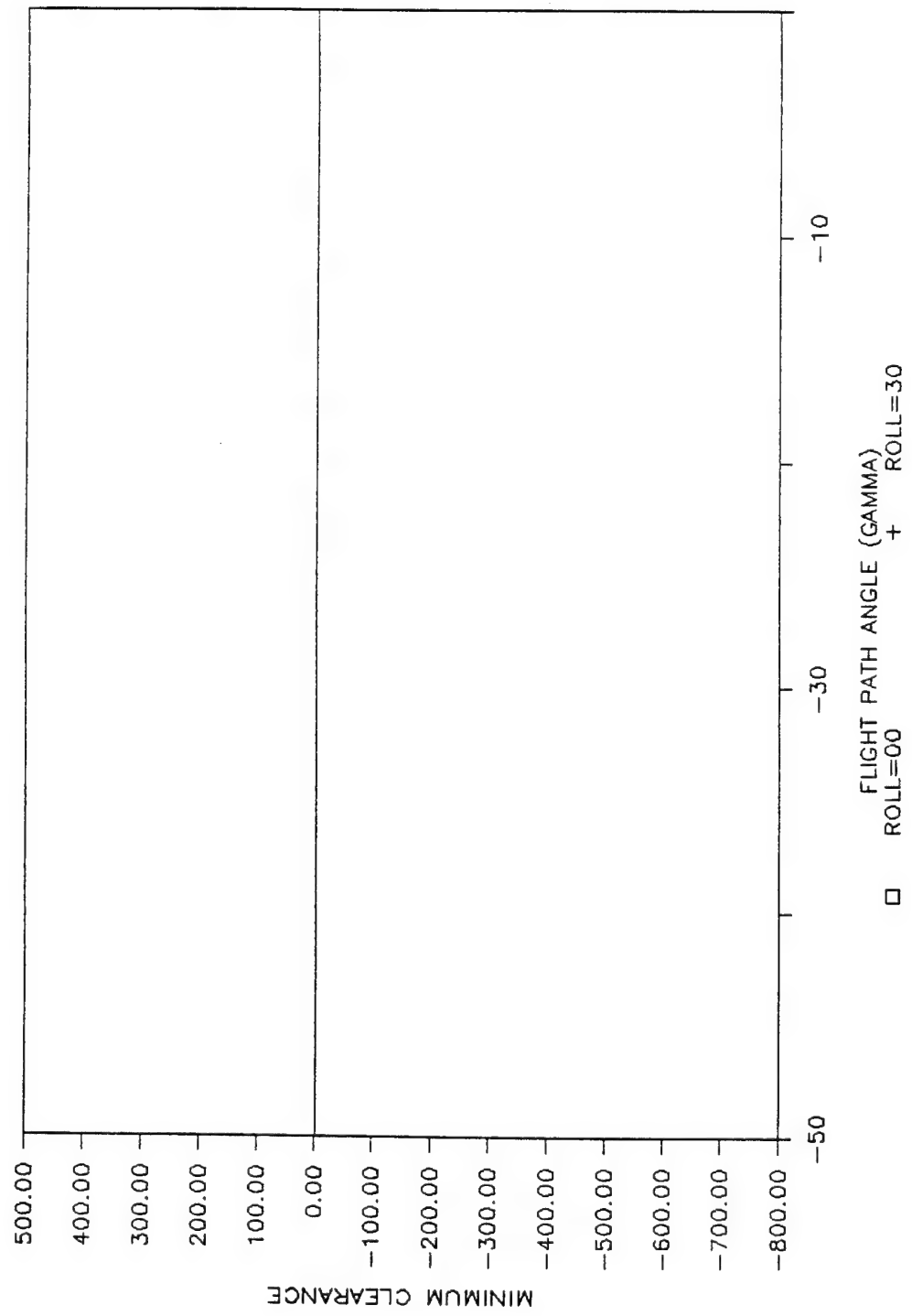


Figure 26 (c). Minimum clearance as a function of flight path angle for pilot model at slope = 18 speed = 350 wsweep = 65.

## Medium Airspeed -- 500 Knots

The plots from the medium airspeed conditions are shown in Figures 27 through 33. Each figure contains two graphs of minimum clearance as a function of flight path angle (-5, -10, -15, -20, -25, -30, -35, -40, and -45 degrees) and roll angle (0, 30, and 60 degrees). Also, each figure represents one terrain slope condition and two wing sweep configurations (45 and 65 degrees). Wing sweep of 25 degrees could not be flown by the simulator due to the "Mach Tuck" phenomenon, which was described previously. The 45 degree wing sweep configuration was defined as standard for the 500 knot airspeed condition, while 65 degree wing sweep was defined as a nonstandard configuration. An examination of the data revealed two main areas of concern.

As in the low airspeed condition, performance seemed to worsen as a function of sloping terrain. The algorithm's deficiencies were seen at 18 degrees of sloping terrain with a wing sweep of 45 degrees, and were apparent at 12, 15, and 18 degrees of slope with a wing sweep of 65 degrees. At the higher wing sweep configuration (65 degrees), it appeared that the slopes of the lines for minimum clearance changed from a negative to a positive relationship as a function of flight path angle. This phenomenon may have been caused by the simulator "running out" of energy during the recovery maneuver.

The other main area of concern was related to the 60 degree roll condition, at 65 degrees of wing sweep. During these trials, it was concluded from the figures that minimum clearance altitude decreased, when it should have increased, as a function of flight path angle. More specifically, the problem became noticeable at flight path angles greater than 20 degrees.

SLOPE=0 SPEED=500 WSWEEP=45

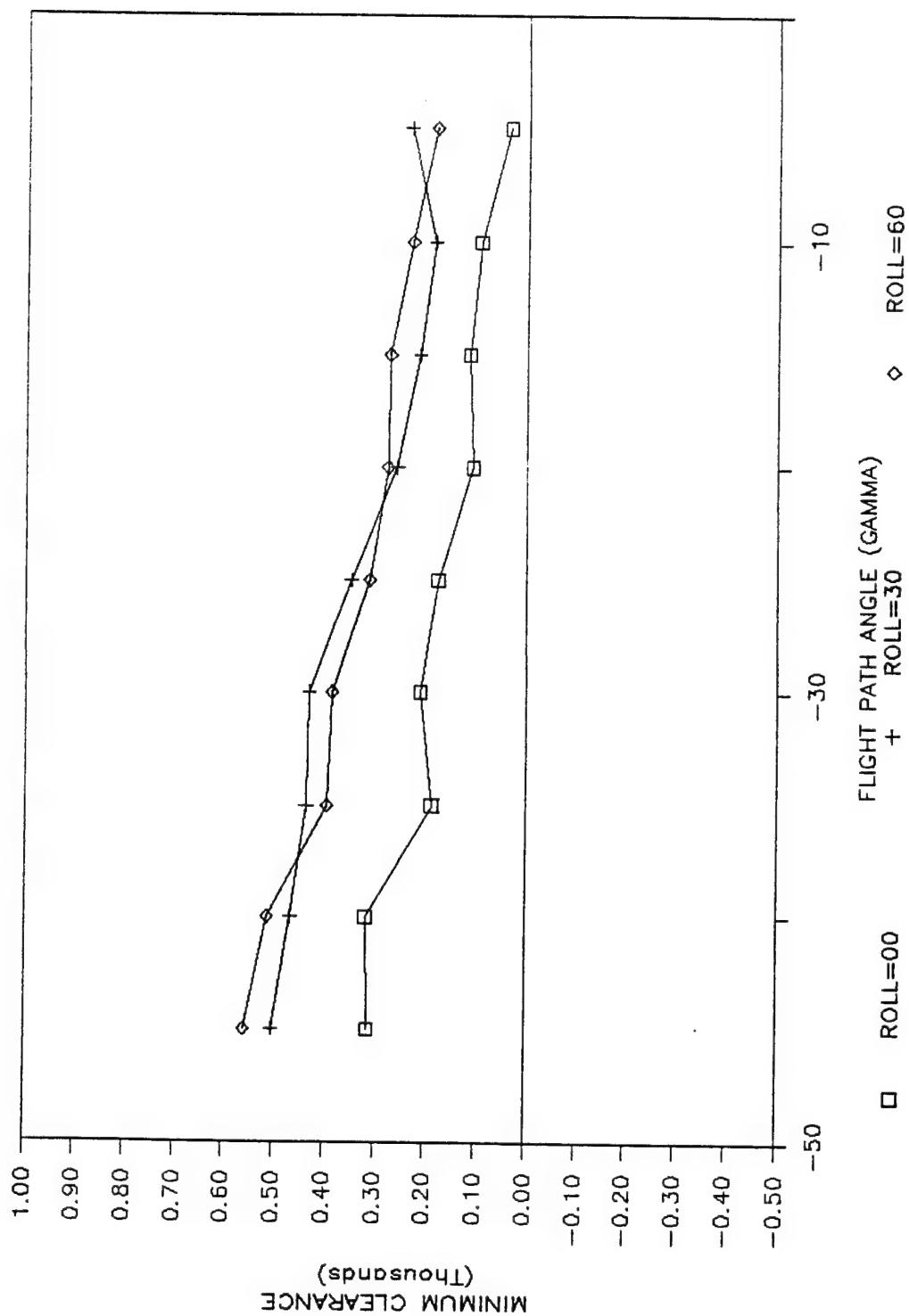


Figure 27 (a). Minimum clearance as a function of flight path angle for pilot model at slope=0 speed=500 wswEEP=45.

SLOPE=0 SPEED=500 WSWEEP=65

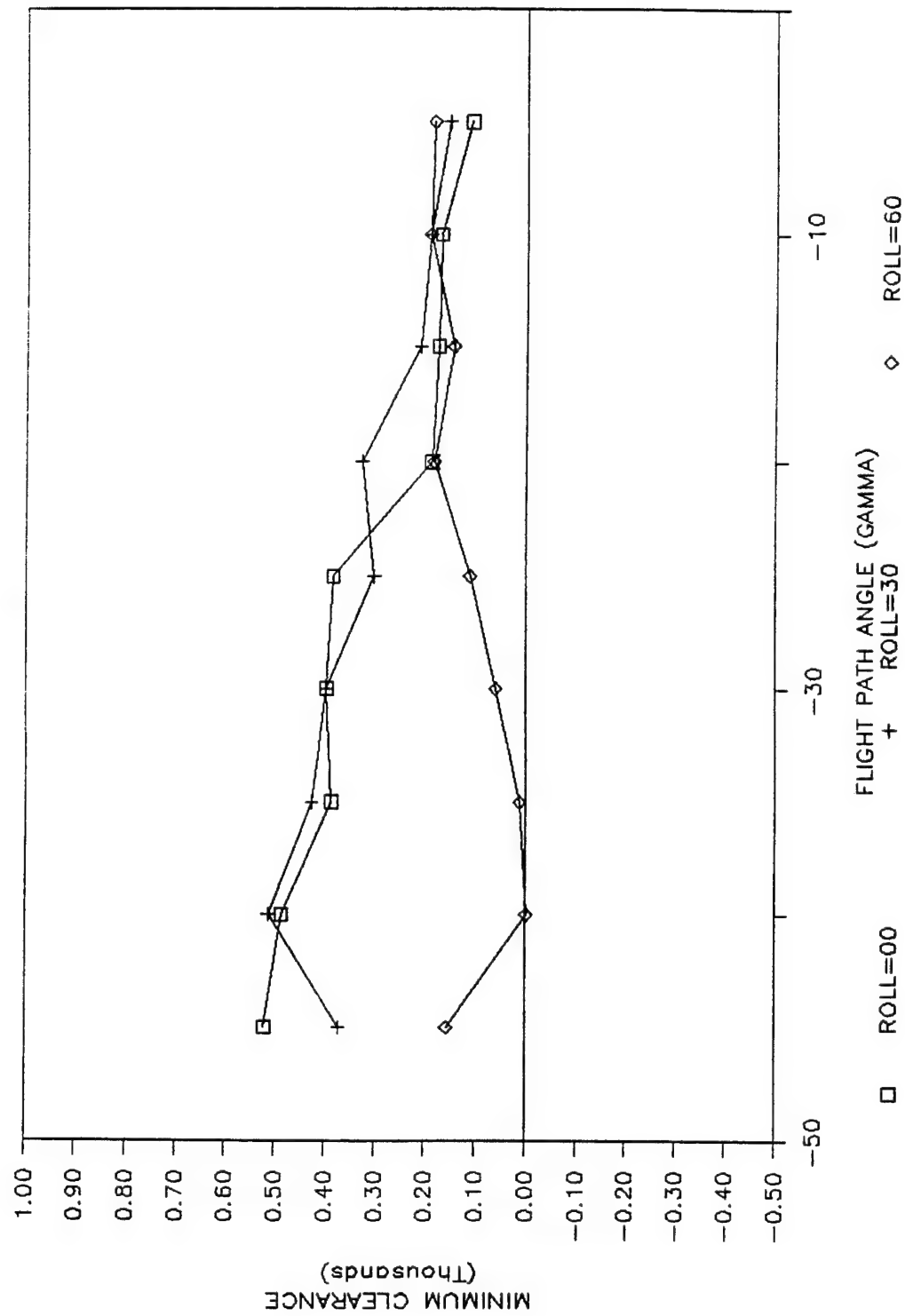


Figure 27 (b). Minimum clearance as a function of flight path angle for pilot model at slope=0 speed=500 wswEEP=65.

SLOPE=3 SPEED=500 WSWEEP=45

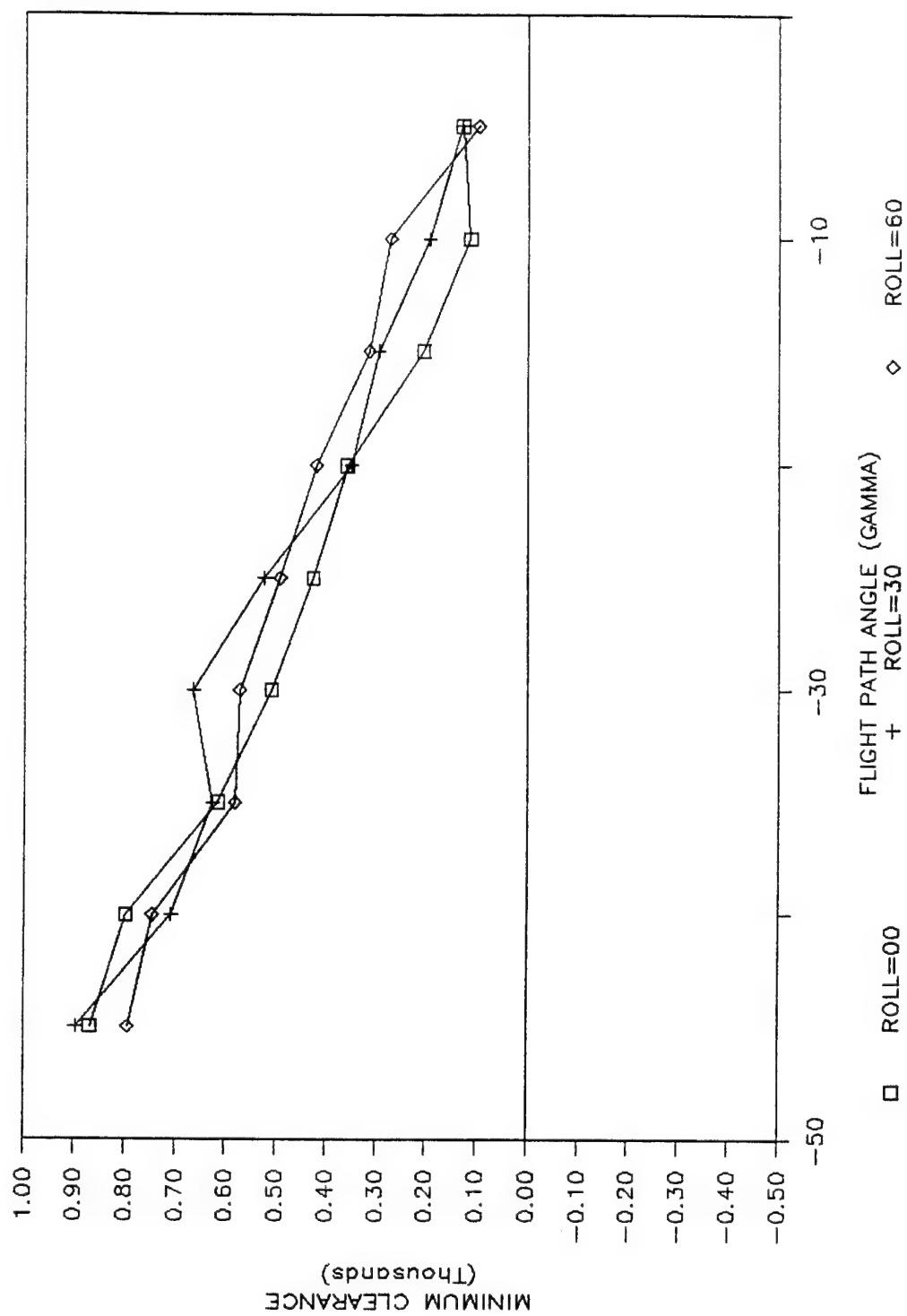


Figure 28 (a). Minimum clearance as a function of flight path angle for pilot model at slope=3 speed=500 wsweep=45.



SLOPE=3 SPEED=500 WSWEEP=65

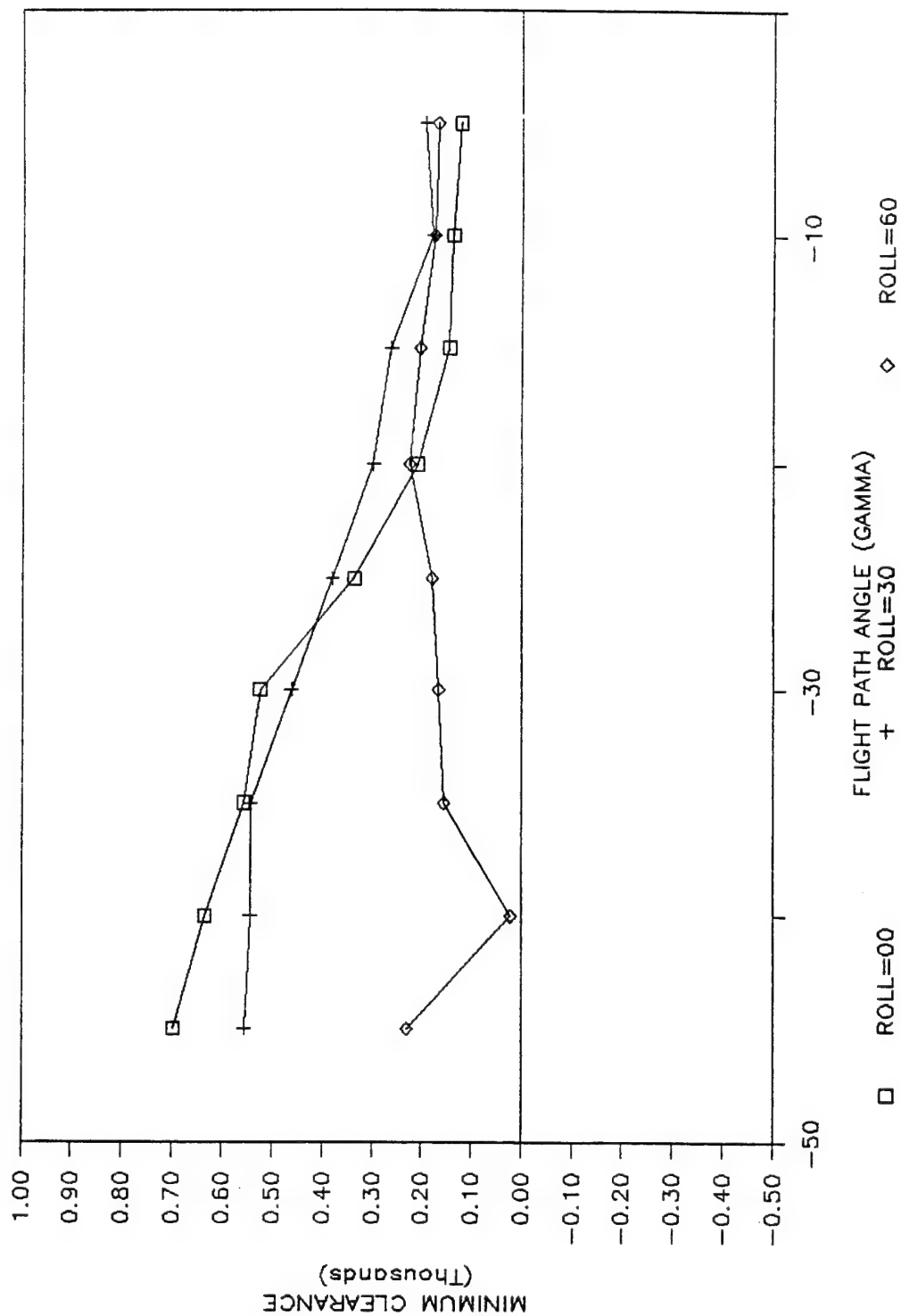


Figure 28 (b). Minimum clearance as a function of flight path angle for pilot model at slope=3 speed=500 wsweep=65.

SLOPE=6 SPEED=500 WSWEEP=45

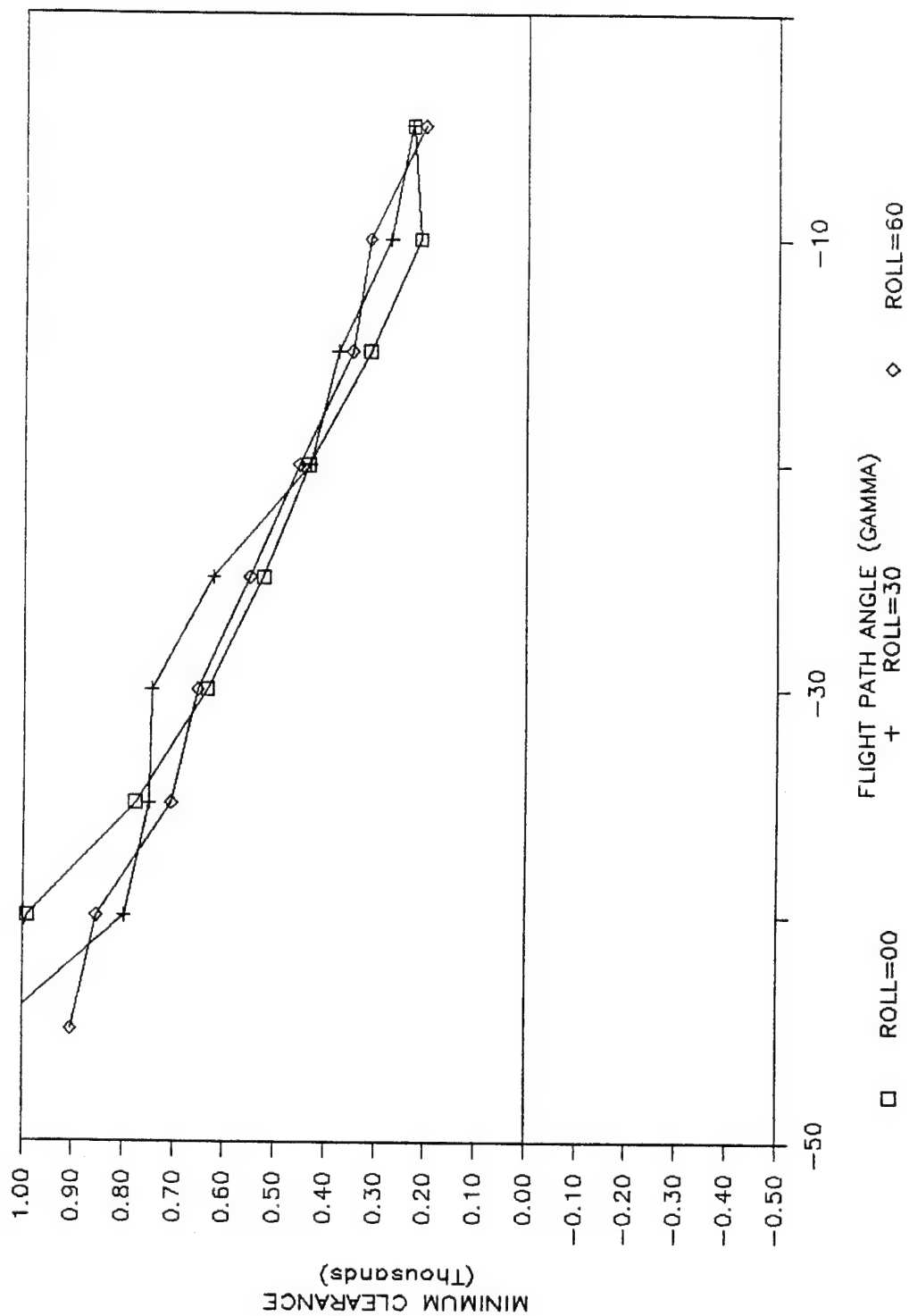


Figure 29 (a). Minimum clearance as a function of flight path angle for pilot model at slope=6 speed=500 wswEEP=45.

SLOPE=6 SPEED=500 WSWEEP=65

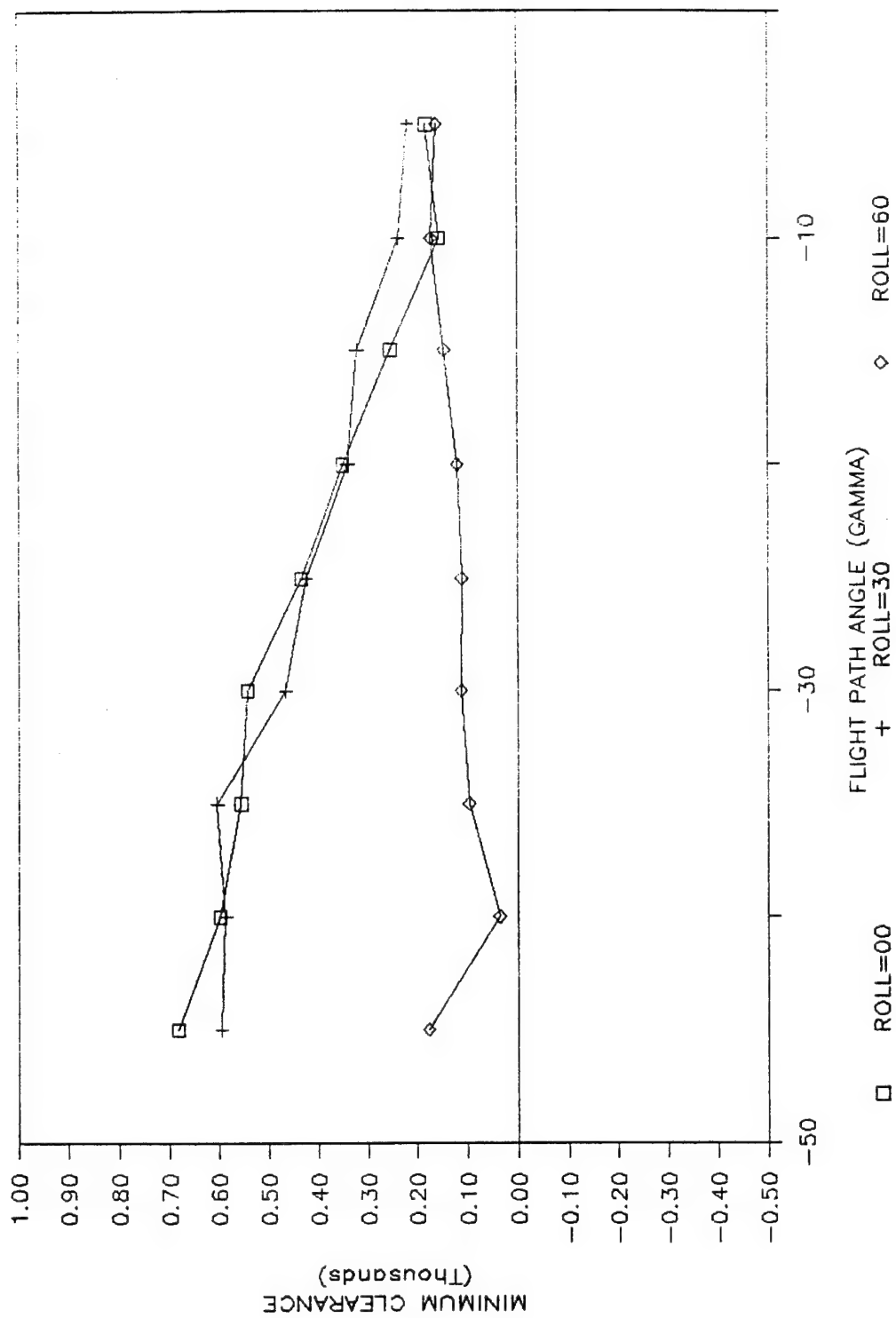


Figure 29 (b). Minimum clearance as a function of flight path angle for pilot model at slope = 6 speed = 500 wsweep = 65.

SLOPE=9 SPEED=500 WSWEEP=45

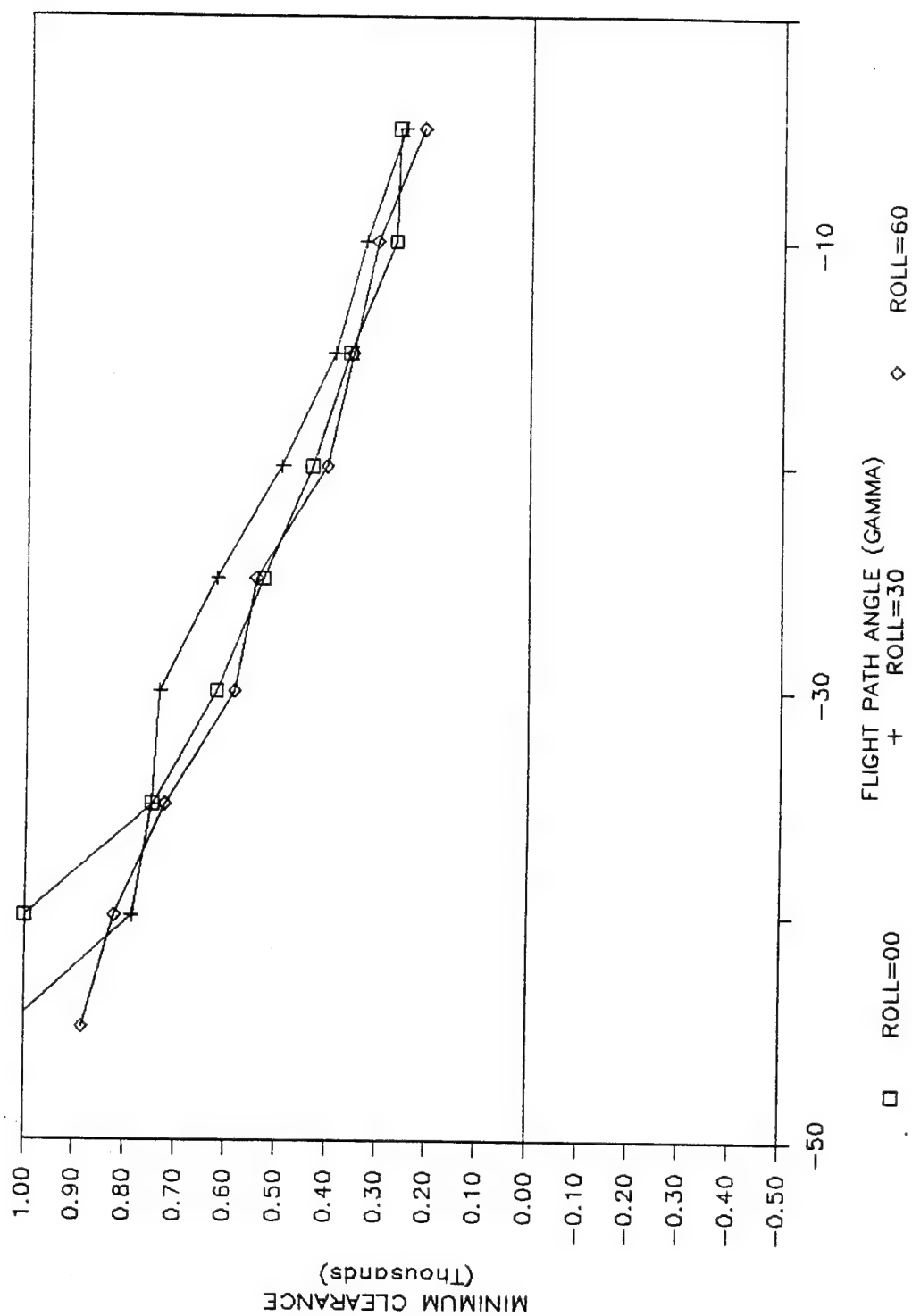


Figure 30 (a). Minimum clearance as a function of flight path angle for pilot model at slope = 9 speed = 500 wsweep = 45.

SLOPE=9 SPEED=500 WSWEEP=65

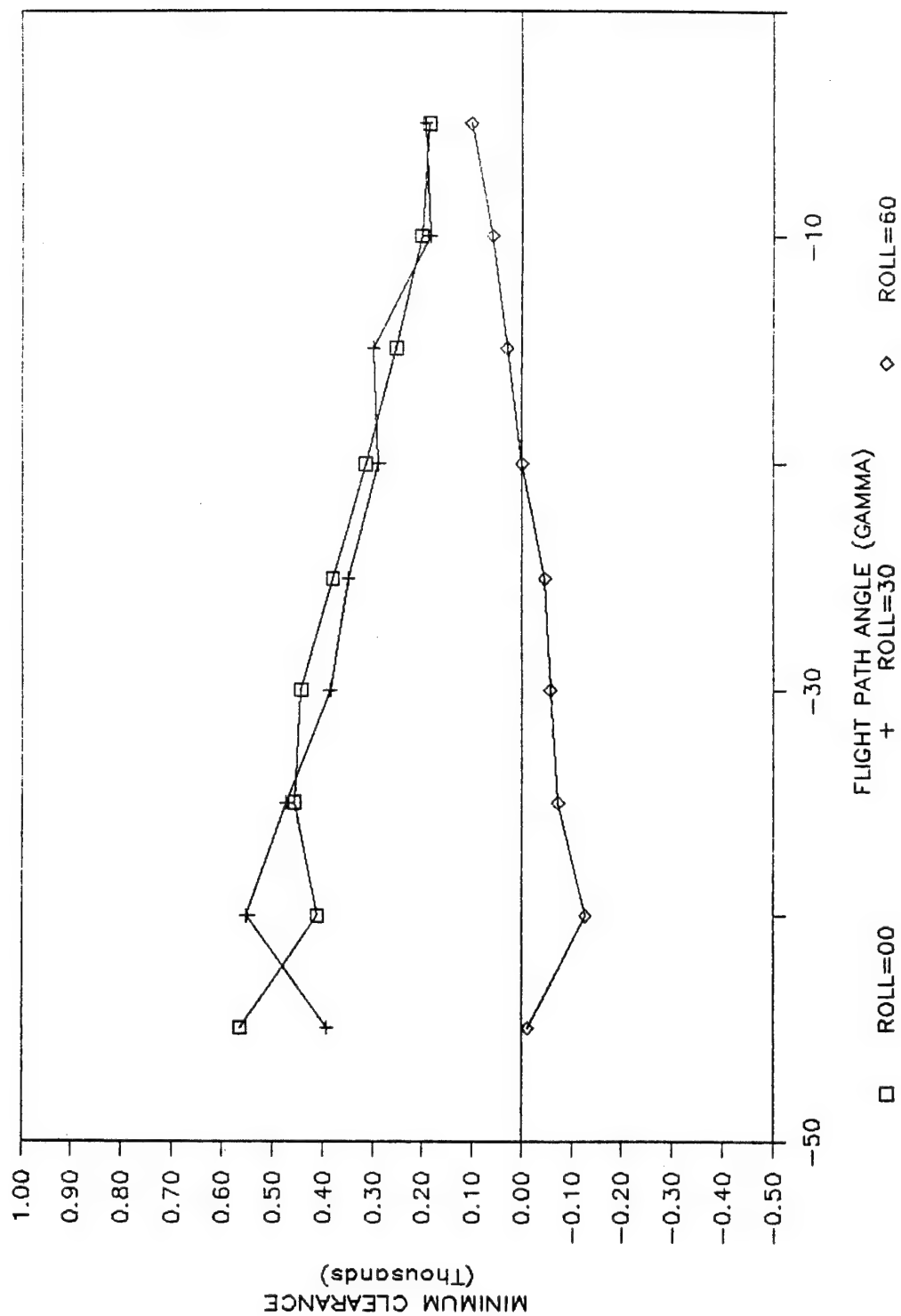


Figure 30 (b). Minimum clearance as a function of flight path angle for pilot model at slope=9 speed=500 wswEEP=65.

SLOPE=12 SPEED=500 WSWEEP=45

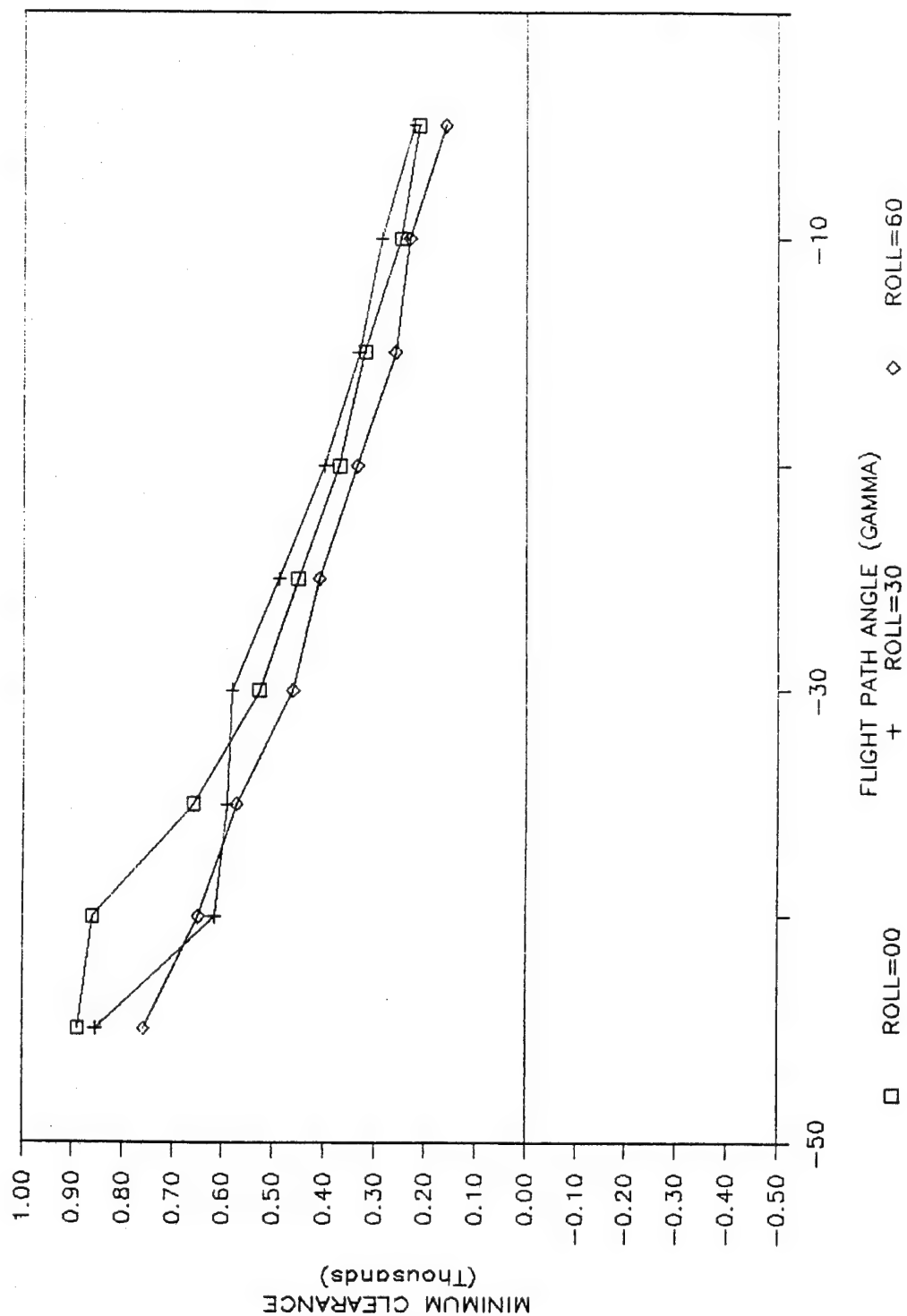


Figure 31 (a). Minimum clearance as a function of flight path angle for pilot model at slope = 12 speed = 500 wsweep = 45.

SLOPE=12 SPEED=500 WSWEEP=65

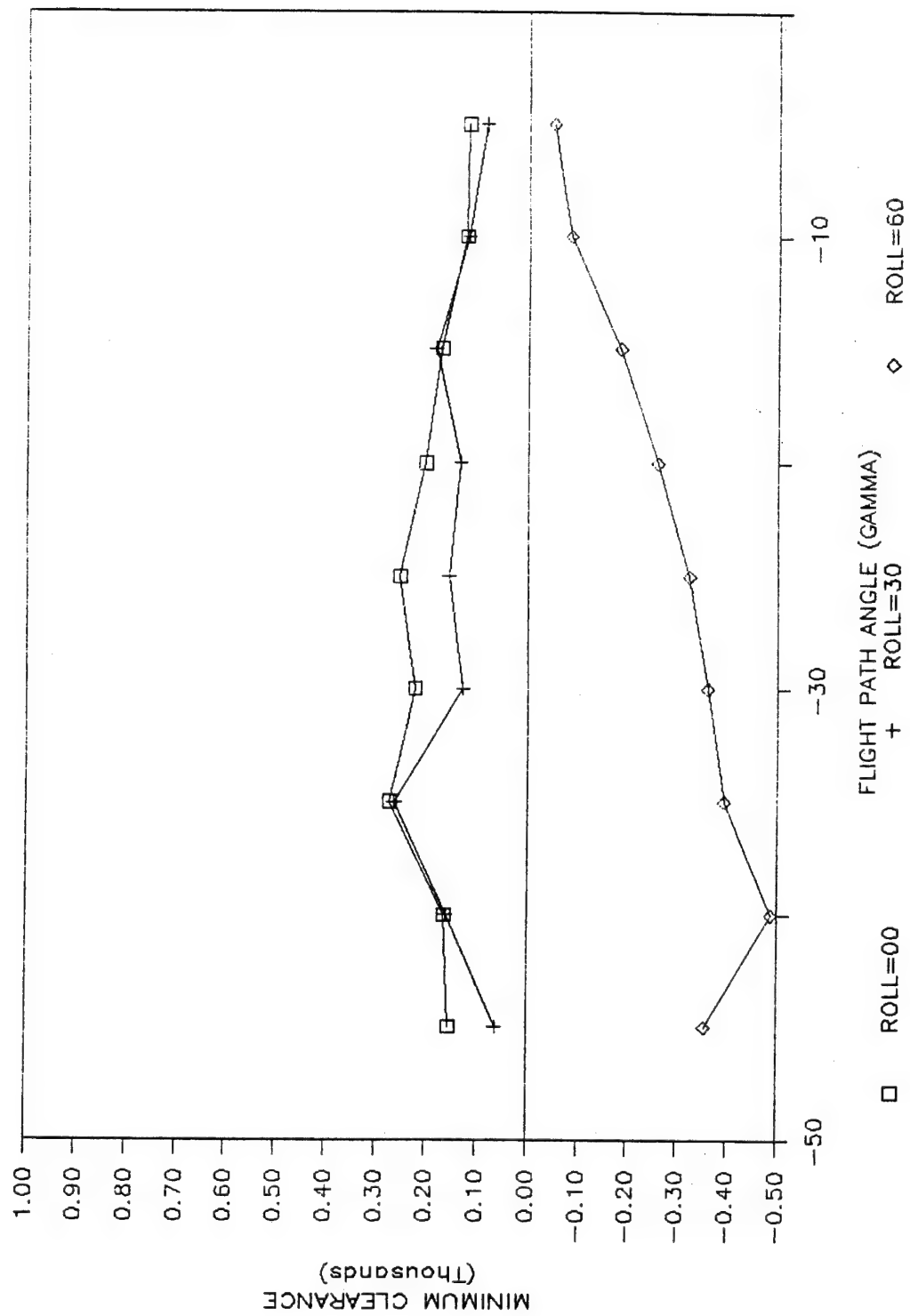


Figure 31 (b). Minimum clearance as a function of flight path angle for pilot model at slope=12 speed = 500 wsweep = 65.

SLOPE=15 SPEED=500 WSWEEP=45

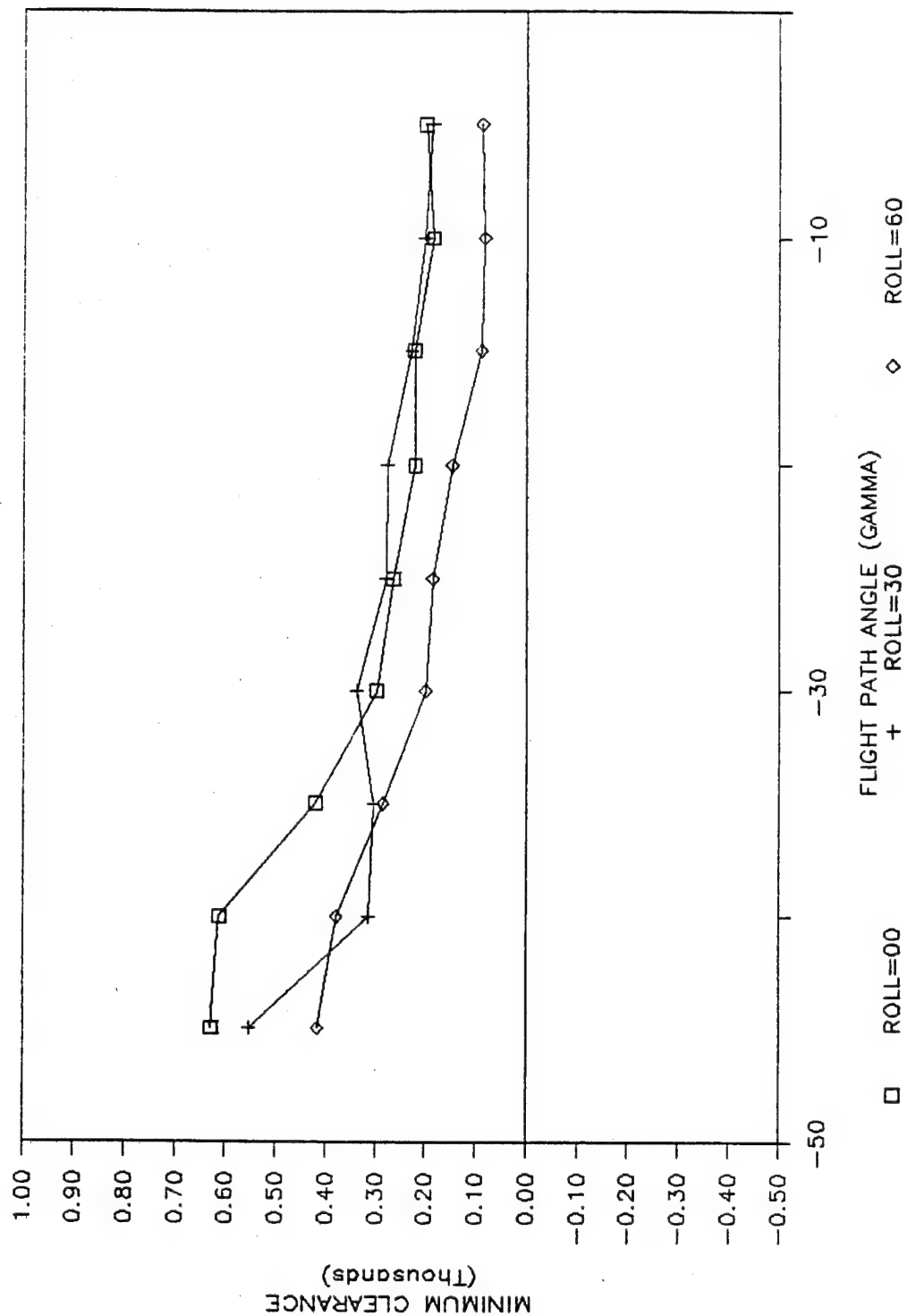


Figure 32 (a). Minimum clearance as a function of flight path angle for pilot model at slope=15 speed=500 wsweep=45.



SLOPE=15 SPEED=500 WSWEEP=65

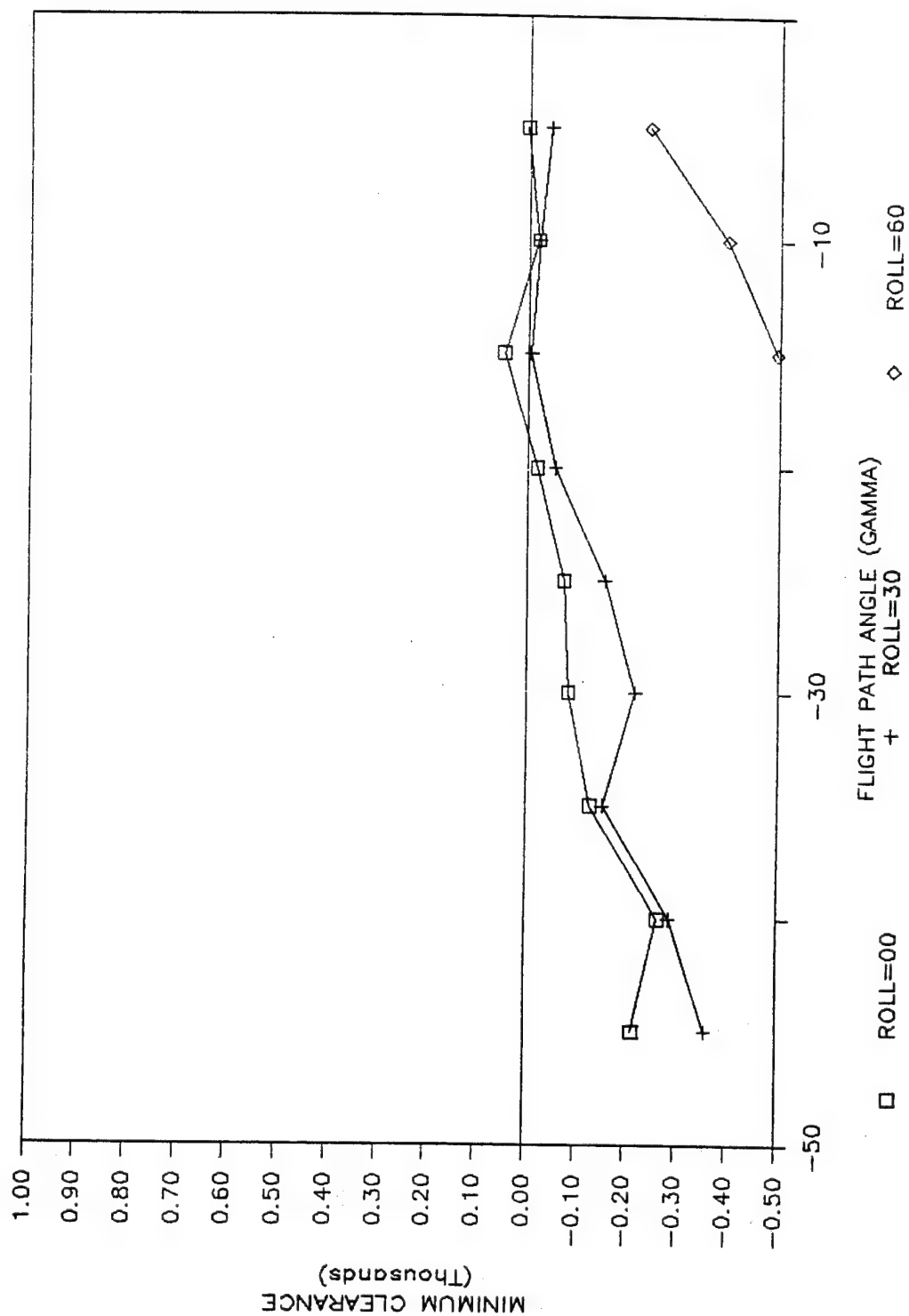


Figure 32 (b). Minimum clearance as a function of flight path angle for pilot model at slope=15 speed=500 wswEEP=65.

SLOPE=18 SPEED=500 WSWEEP=45

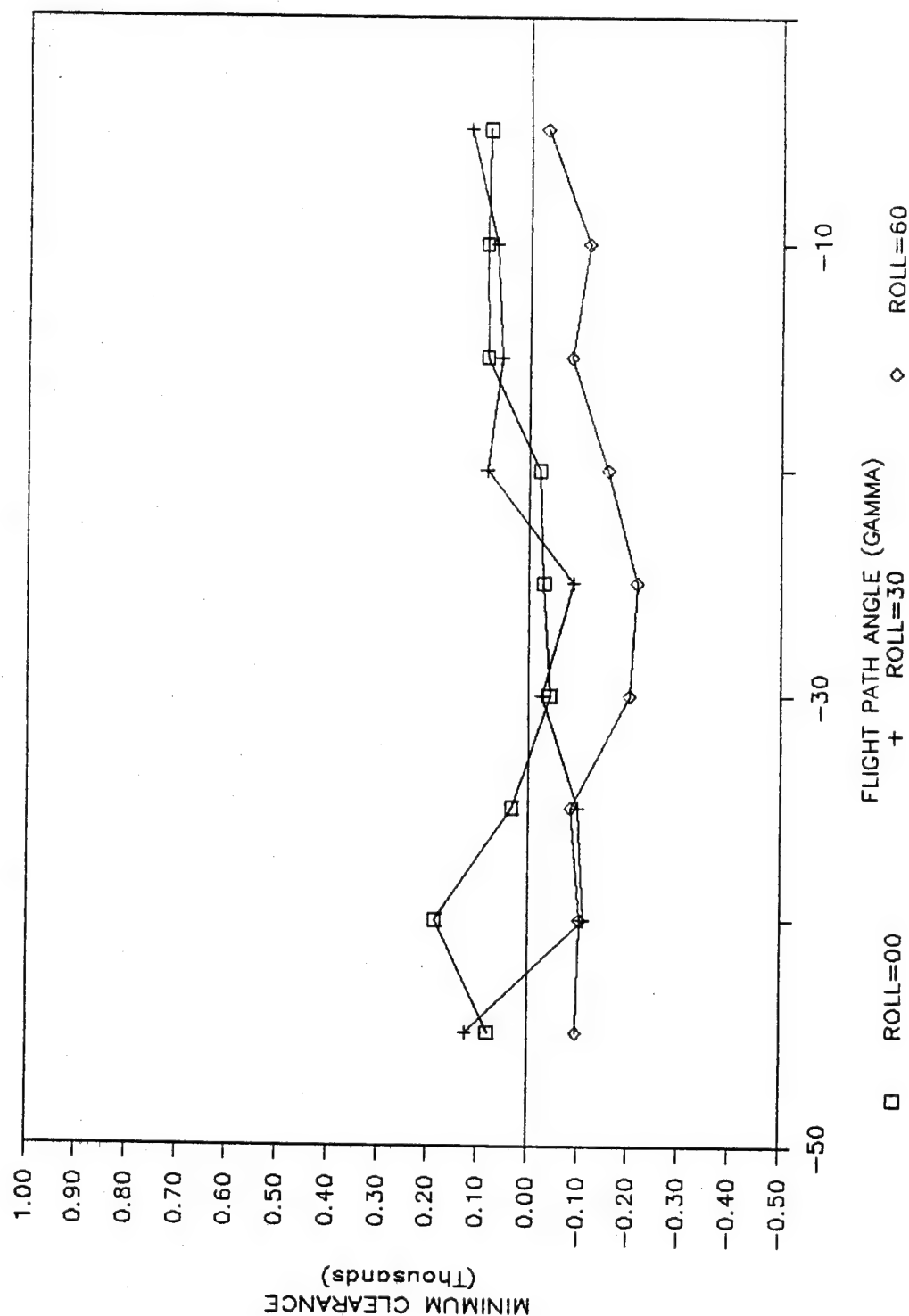


Figure 33 (a). Minimum clearance as a function of flight path angle for pilot model at slope = 18 speed = 500 wsweep = 45.

SLOPE=18 SPEED=500 WSWEEP=65

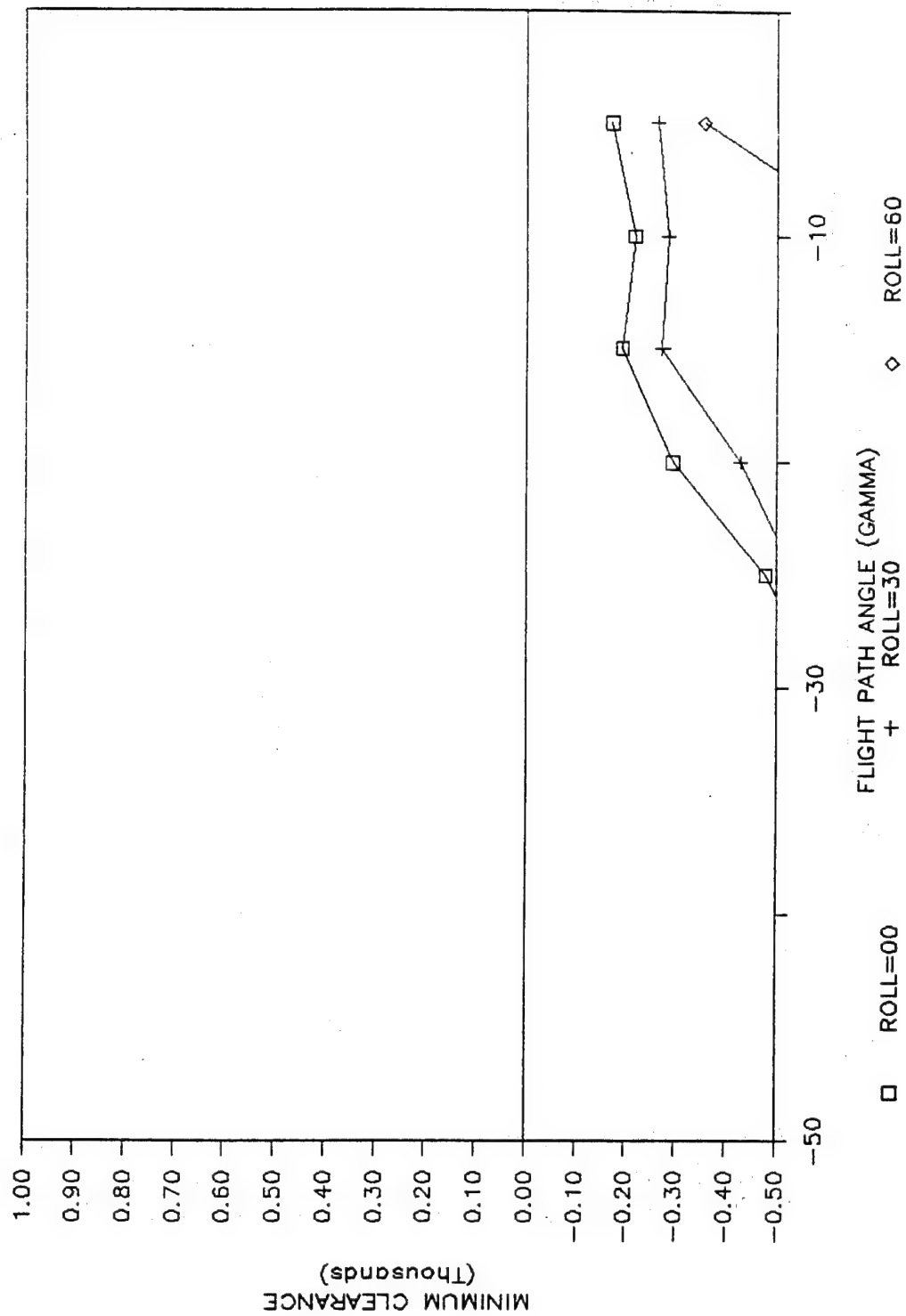


Figure 33 (b). Minimum clearance as a function of flight path angle for pilot model at slope = 18 speed = 500 wswEEP = 65.

## High Airspeed -- 650 Knots

The graphs from the high airspeed conditions are shown in Figures 34 through 40. As with the medium airspeed condition, each figure contains two graphs of minimum clearance as a function of flight path angle (5, 10, 15, 20, 25, 30, 35, 40, and 45 degrees) and roll angle (0, 30, and 60 degrees). In addition, each figure represents one terrain slope condition and two wing sweep configurations (45 and 65 degrees). Again, wing sweep of 25 degrees could not be flown by the simulator because of the "Mach Tuck" phenomenon. The 65 degree wing sweep was defined as standard for the 650 knots airspeed condition, while 45 degree wing sweep was defined as nonstandard configuration. The major areas of concern are presented in the following paragraphs.

An inspection of the figures suggested that minimum clearance as a function of flight path angle, for all roll and wing sweep configurations, increased as terrain slope was elevated from zero to nine degrees. However, once terrain slope became greater than nine degrees, minimum clearance tended to decrease with the worst effect demonstrated at 18 degrees of slope. Furthermore, for the terrain slope conditions between six and 12 degrees, the algorithm appeared to have overestimated the necessary altitude for a safe recovery. This was highlighted by minimum clearance values greater than 2,100 feet above ground for certain conditions.

As with the medium airspeed conditions which included the configuration for roll of 60 degrees and wing sweep of 65 degrees, the algorithm's ability to predict falters beyond 20 degrees of flight path angle. This trend was consistently seen across the different terrain slopes.

SLOPE=0 SPEED=650 WSWEEP=45

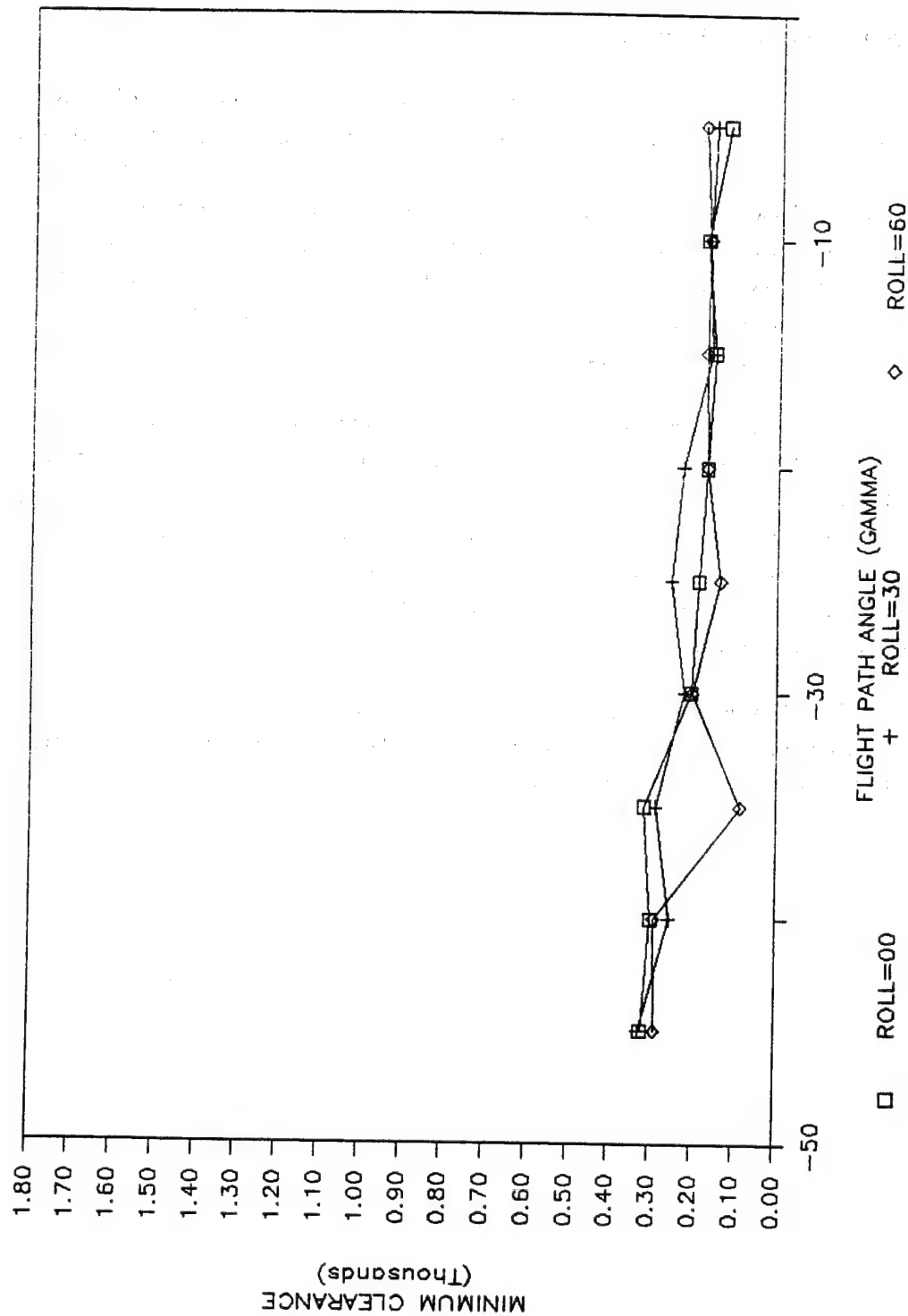


Figure 34 (a). Minimum clearance as a function of flight path angle for pilot model at slope=0 speed=650 wsweep=45.

SLOPE=0 SPEED=650 WSWEEP=65

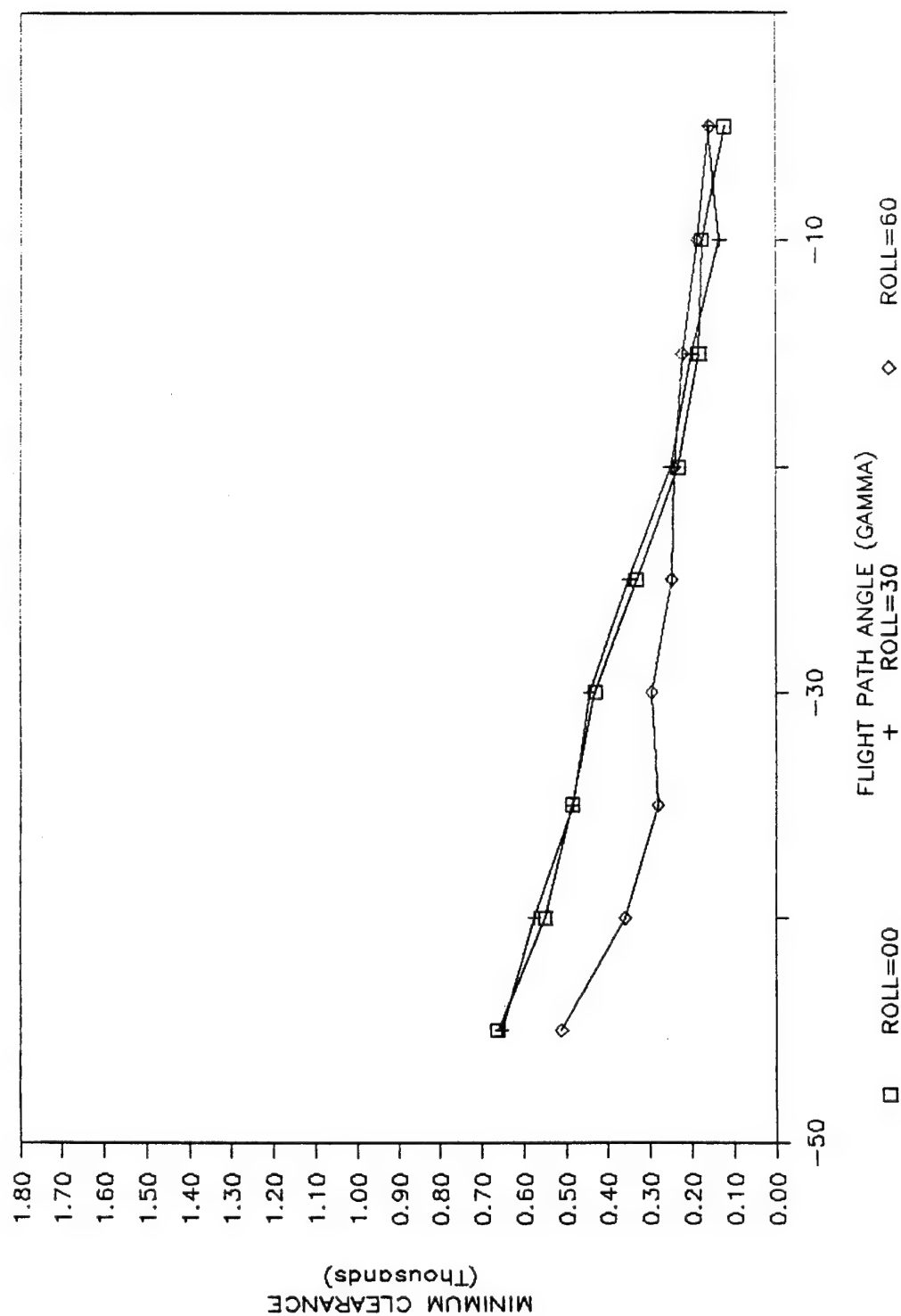


Figure 34 (b). Minimum clearance as a function of flight path angle for pilot model at slope=0 speed=650 wsweep=65.

SLOPE=3 SPEED=650 WSWEEP=45

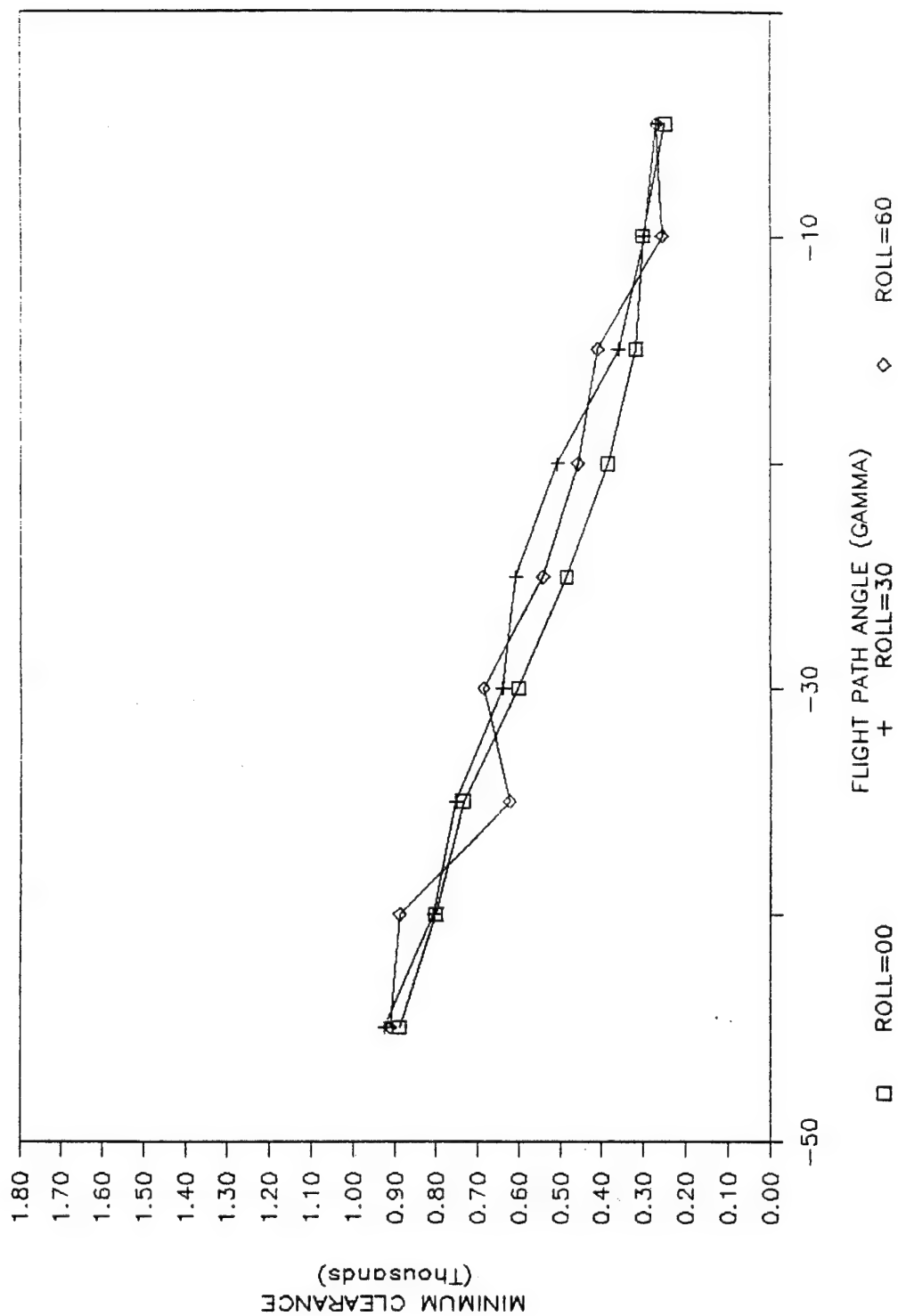


Figure 35 (a). Minimum clearance as a function of flight path angle for pilot model at slope=3 speed=650 wsweep=45.

SLOPE=3 SPEED=650 WSWEEP=65

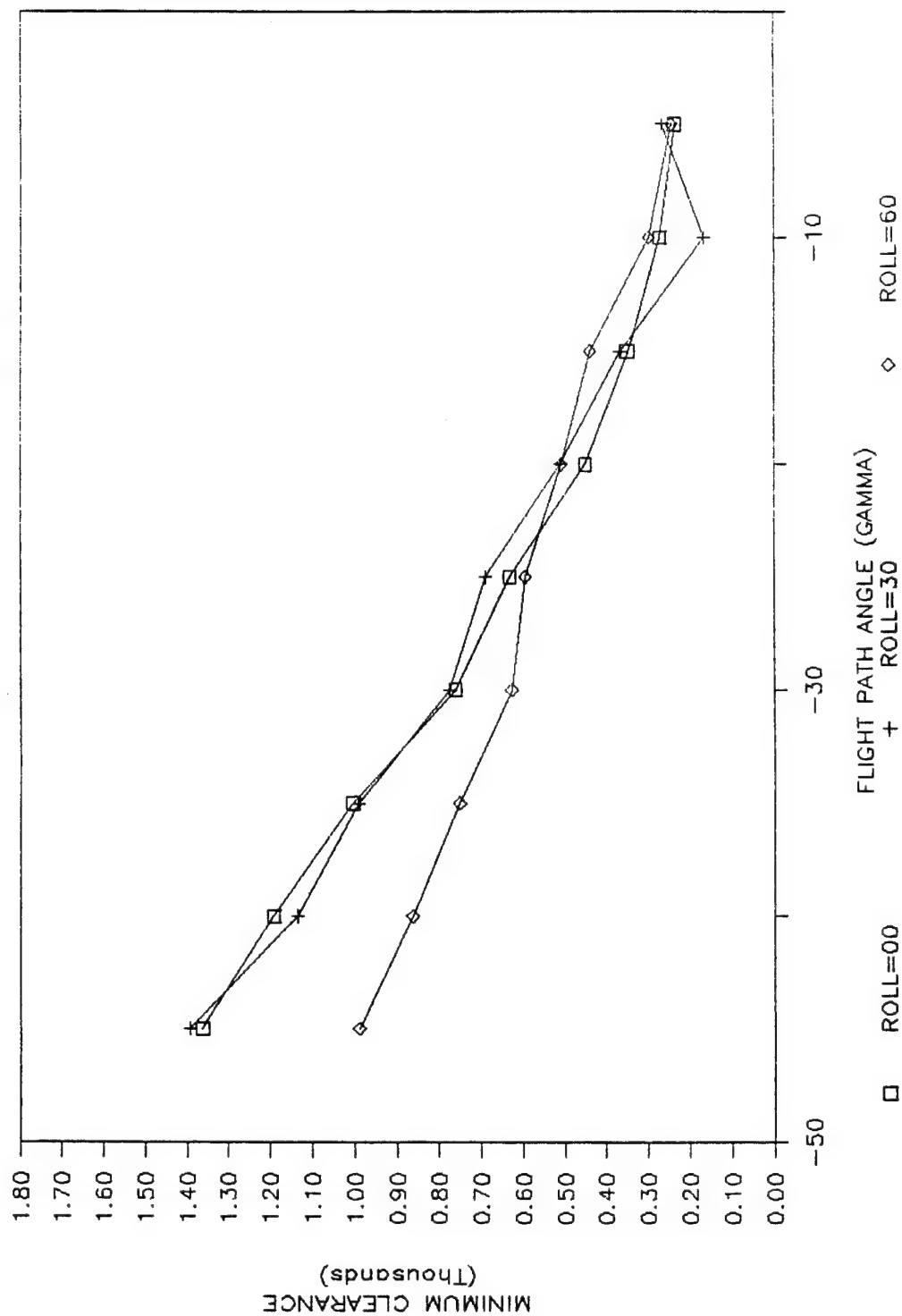


Figure 35 (b). Minimum clearance as a function of flight path angle for pilot model at slope=3 speed=650 wsweep=65.



SLOPE=6 SPEED=650 WSWEEP=45

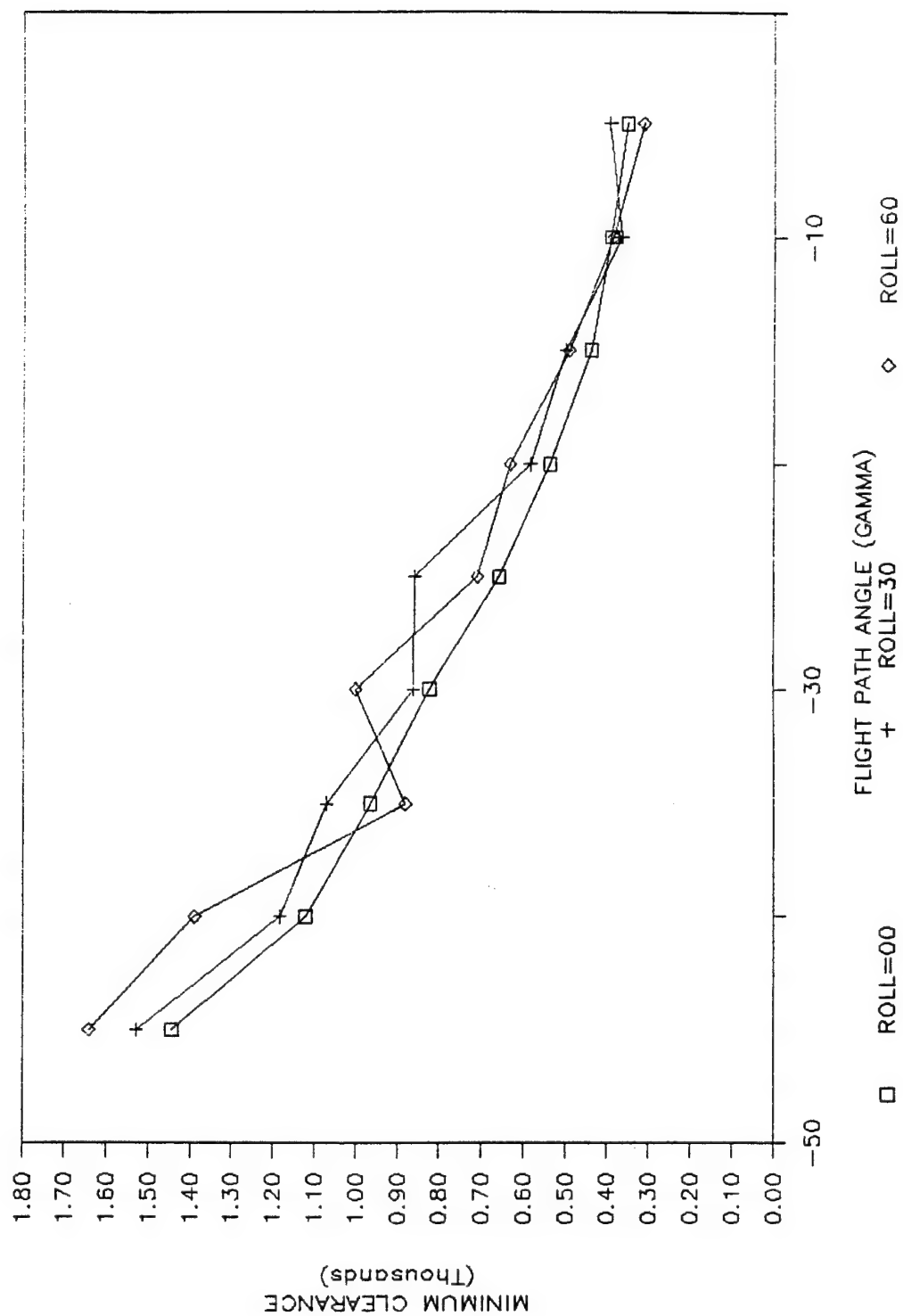


Figure 36 (a). Minimum clearance as a function of flight path angle for pilot model at slope=6 speed=650 wsweep=45.

SLOPE=6 SPEED=650 WSWEEP=65

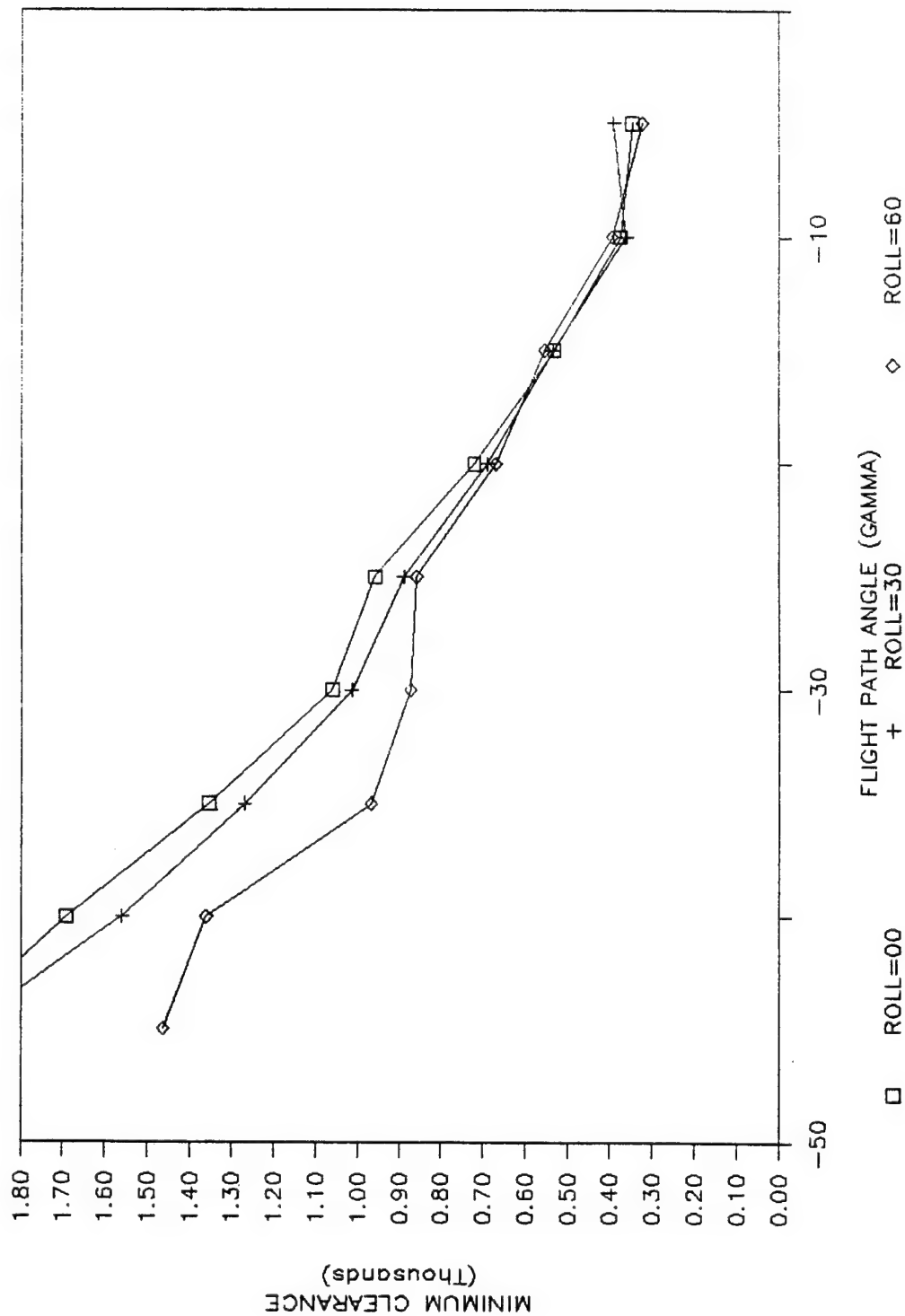


Figure 36 (b). Minimum clearance as a function of flight path angle for pilot model at slope=6 speed=650 wsweep=65.

SLOPE=9 SPEED=650 WSWEEP=45

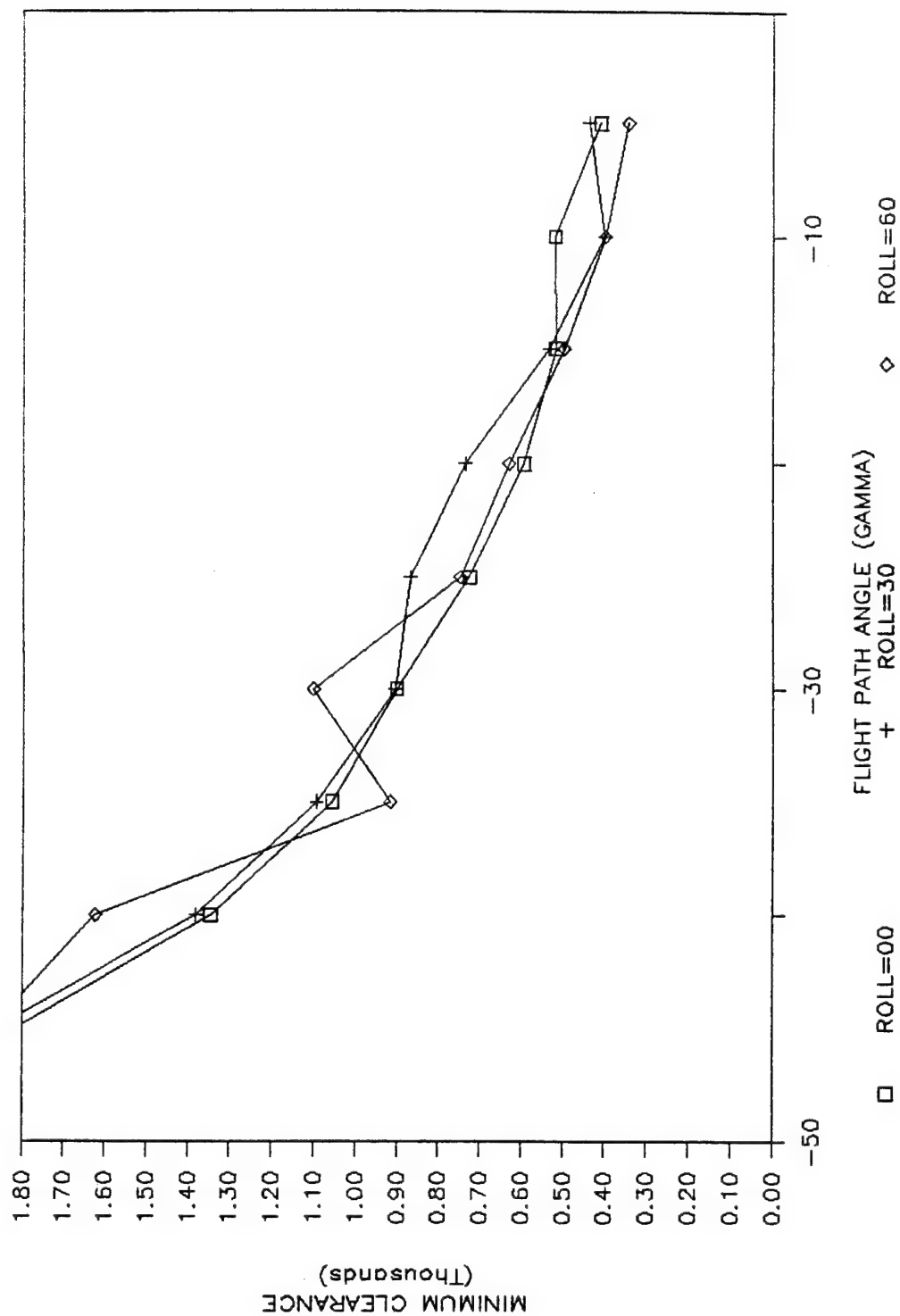


Figure 37 (a). Minimum clearance as function of flight path angle for pilot model at slope = 9 speed = 650 wsweep = 45.

SLOPE=9 SPEED=650 WSWEEP=65

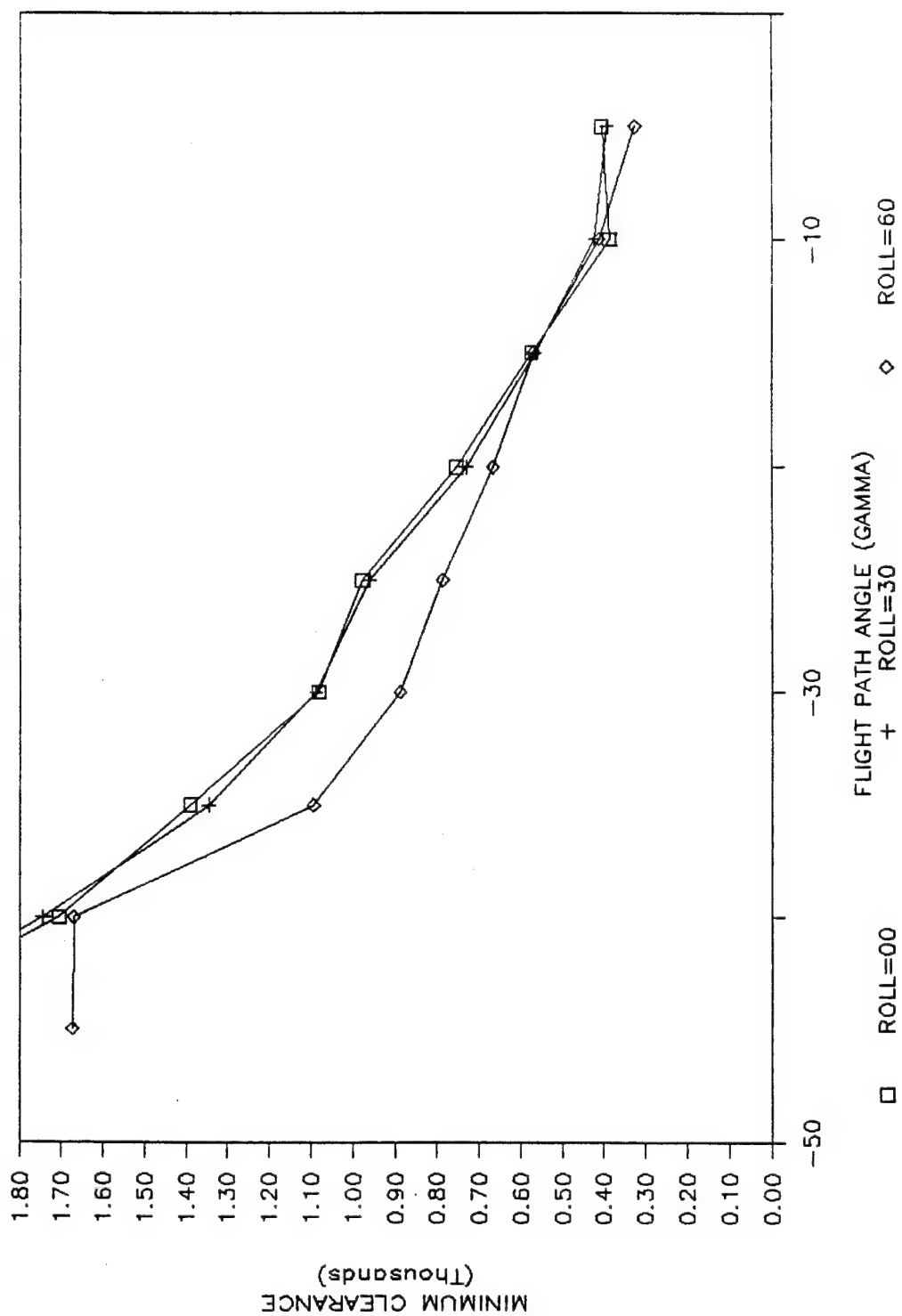


Figure 37 (b). Minimum clearance as a function of flight path angle for pilot model at slope = 9 speed = 650 wsweep = 65.

SLOPE=12 SPEED=650 WSWEEP=45

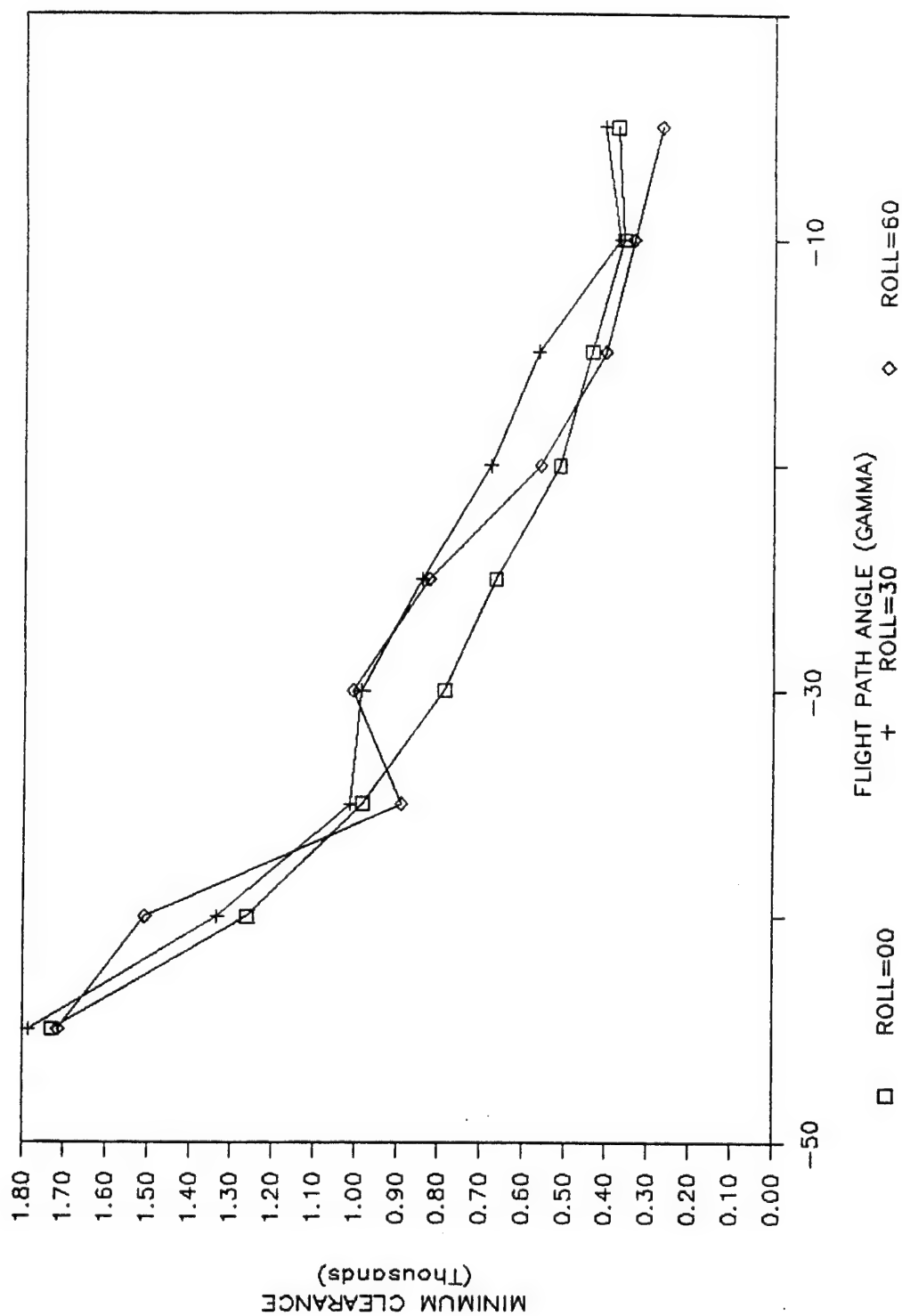


Figure 38 (a). Minimum clearance as a function of flight path angle for pilot model at slope = 12 speed = 650 wswEEP = 45.

SLOPE=12 SPEED=650 WSWEEP=65

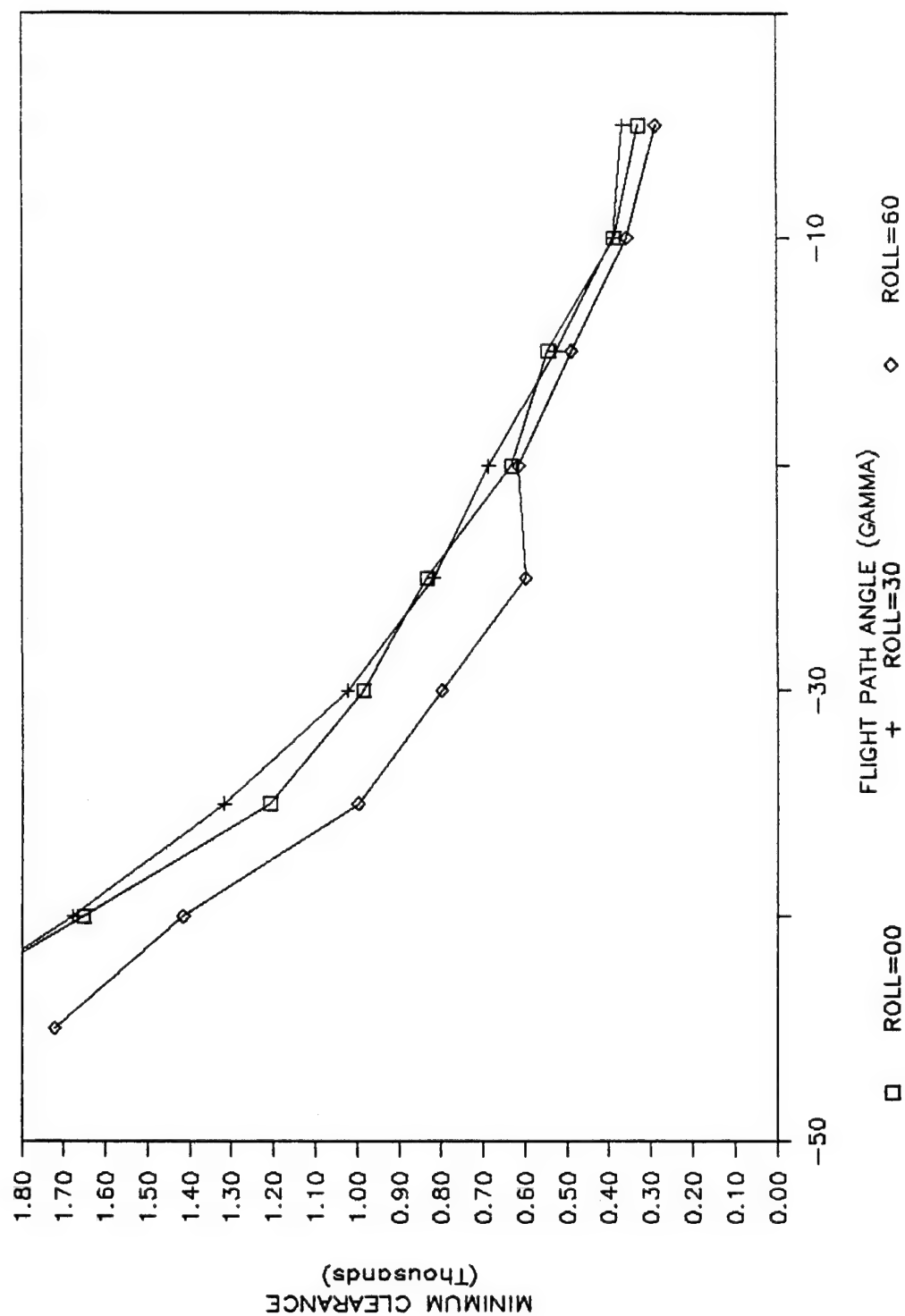


Figure 38 (b). Minimum clearance as a function of flight path angle for pilot model at slope = 12 speed = 650 wsweep = 65.

SLOPE=15 SPEED=650 WSWEEP=45

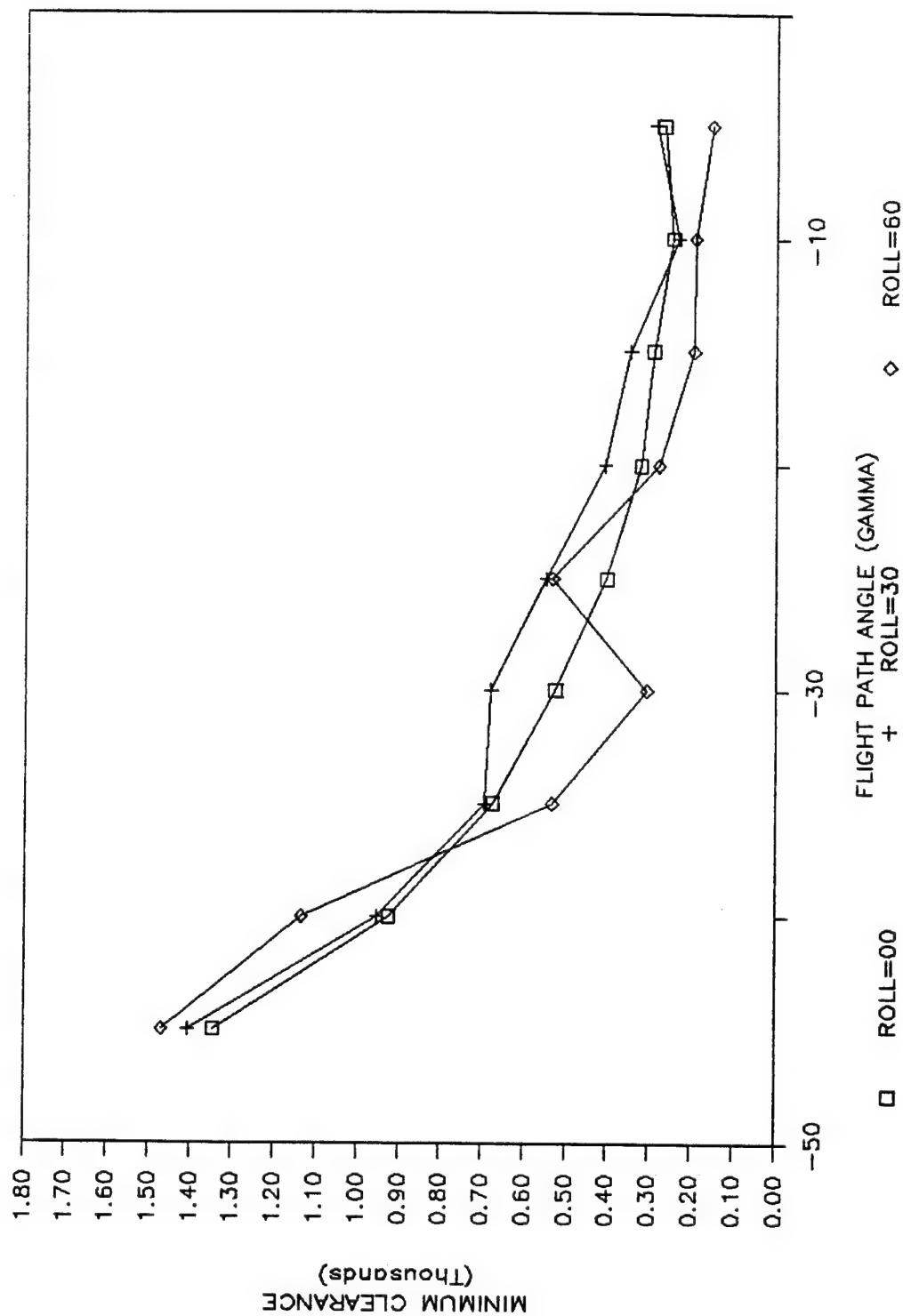


Figure 39 (a). Minimum clearance as a function of flight path angle for pilot model at slope = 15 speed = 650 wsweep = 45.

SLOPE=15 SPEED=650 WSWEEP=65

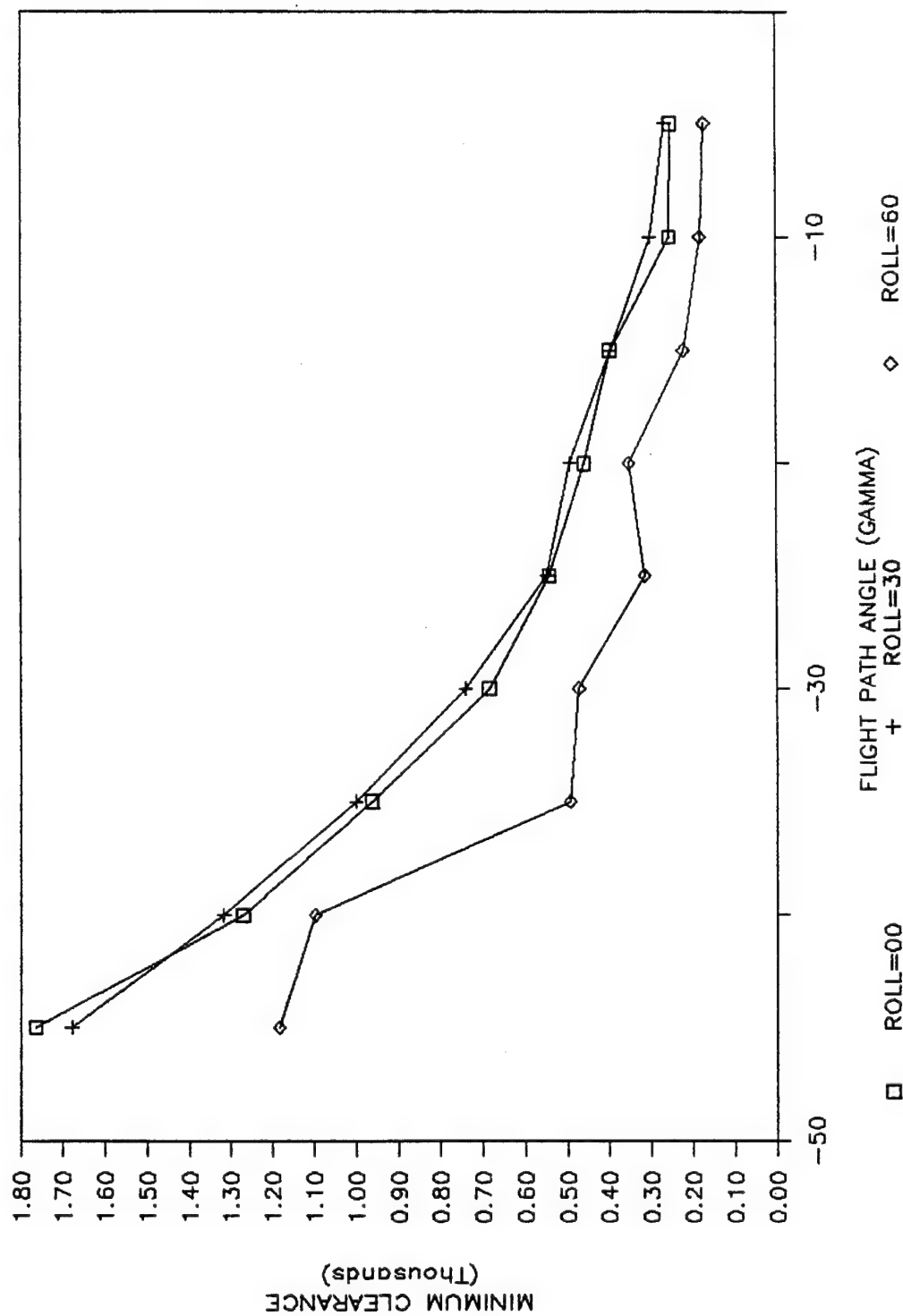


Figure 39 (b). Minimum clearance as a function of flight path angle for pilot model at slope=15 speed=650 wsweep=65.



SLOPE=18 SPEED=650 WSWEEP=45

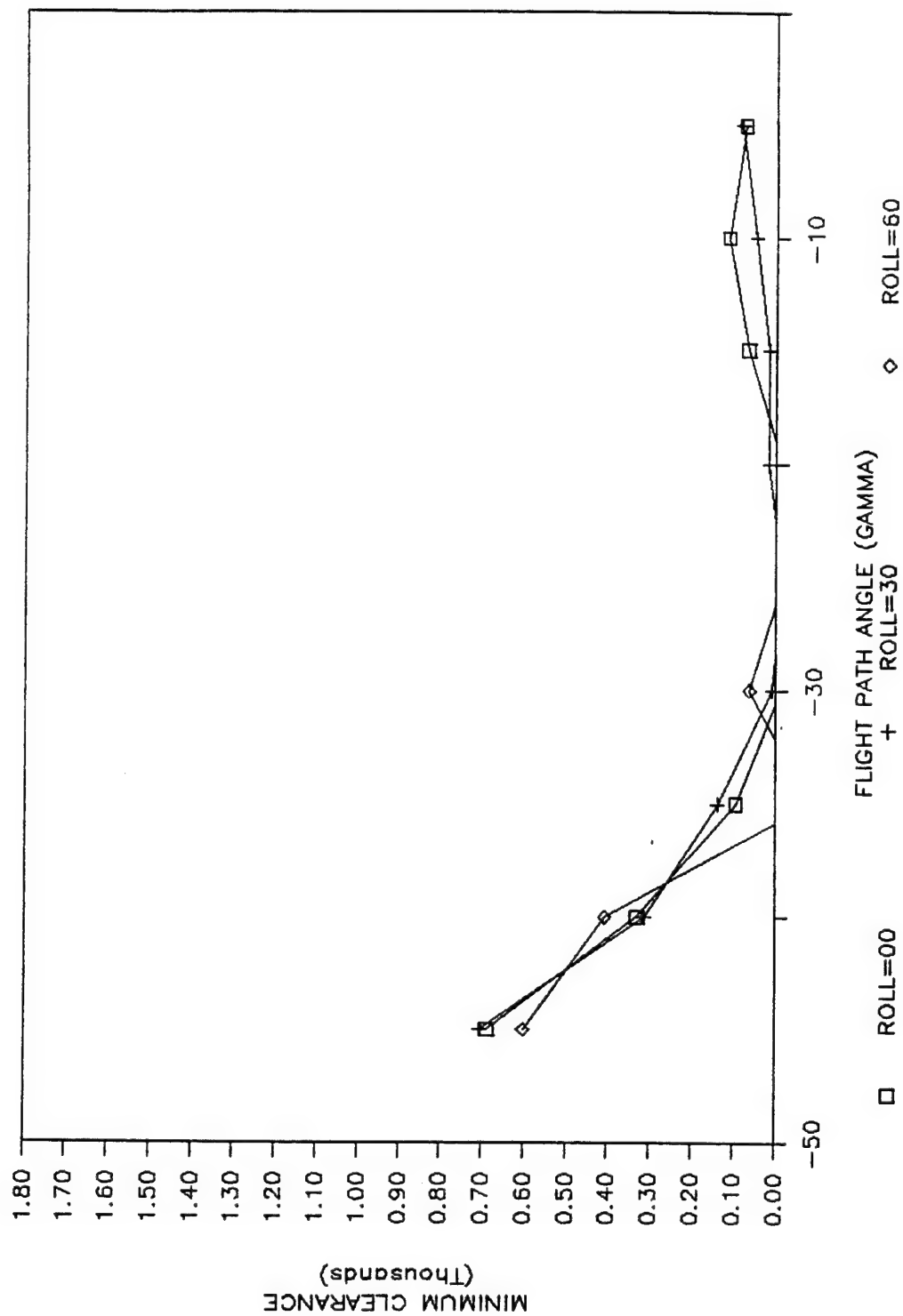


Figure 40 (a). Minimum clearance as a function of flight path angle for pilot model at slope = 18 speed = 650 wsweep = 45.

SLOPE=18 SPEED=650 WSWEEP=65

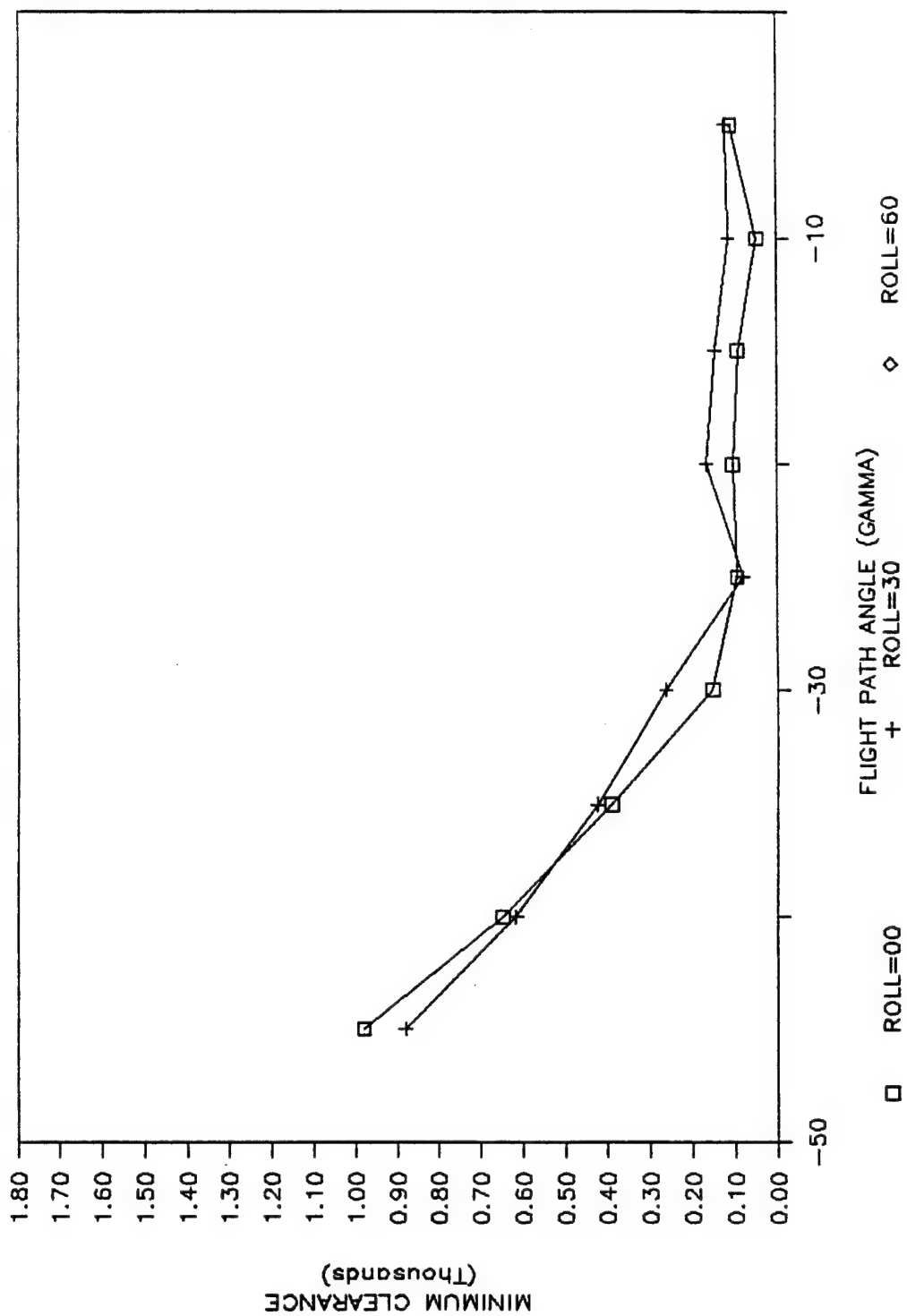


Figure 40 (b). Minimum clearance as a function of flight path angle for pilot model at slope=18 speed=650 wsweep=65.

## **Phase II Discussion**

The Phase II Evaluation employed a pilot model to test the algorithm's ability and consistency in predicting required altitude as the algorithm changed paths. Generally, the results found in this evaluation confirmed the findings from Phase I, in that shortcomings exist in the algorithm's performance under certain flight conditions.

The algorithm's ability to predict decreased under the following conditions: all rolls, high wing sweeps, and increasing flight path angle and terrain slope. These findings indicate the algorithm's insensitivity to these aircraft configurations. Obviously, the predicted functions within the paths of the subalgorithms must be refined.

At medium airspeeds, increasing terrain slope adversely affected the algorithm's ability to predict. Again, refinement of the path coefficients is necessary. The poor performance of the algorithm at high roll and wing sweep conditions for flight path angles greater than 20 degrees was the opposite of what was expected. Minimum clearance altitude should have increased rather than decrease. Two possible explanations for this occurrence exist: (1) The algorithm does not compensate for such high roll conditions at 65 degrees of wing sweep for flight path angles greater than 20 degrees; or (2) the robot pilot may have needed to compensate for the high wing sweep, high roll condition at 20 degrees of flight path angle. This action would involve increasing engine thrust as opposed to the constant thrust approach of the algorithm.

The same trend found at low and medium airspeeds was found at high airspeeds. Minimum clearance decreased at high terrain slopes. A different problem occurred at terrain slopes between six and 12 degrees. Here, the minimum clearance values were excessively high (greater than 2,100 feet) which means that the "pull-up" warning was given too soon. These warnings (nuisance warnings) are unnecessary and may increase pilot anxiety. Steps should be taken to greatly reduce these warnings.

# **PHASE III EVALUATION**

## **Phase III Introduction**

The objective of the third phase of the evaluation was to introduce the pilot factor and replicate a subset of the runs flown by the pilot model throughout Phase II, with a strong emphasis on standard flying configuration. Phase III allowed F/FB/EF-111 operational users to fly a GCAS equipped FB-111 simulator in order to evaluate and critique the most current version of the GCAS algorithm. The critique, as well as the performance and subjective results, will in turn be shared with the SPO and the designers (General Dynamics) for further modification of the algorithm.

## **Phase III Method**

### **Subjects**

Four Strategic Air Command (SAC) and four Tactical Air Command (TAC) pilots participated in the evaluation. An attempt was made to insure that the pilots were representative of the overall population by varying the age and the level of flying experience. The age of the pilots ranged from 27 to 49 with a mean of 34, and a standard deviation of nine years. F/FB/EF-111 operational flying experience varied from 150 to 1800 total hours, with a mean of 910 and a standard deviation of 609 hours. The sample of pilots represented Plattsburg, Mountain Home, McClellan and Cannon AFB.

### **Apparatus**

#### **Facility**

Refer to the Phase II Apparatus section for a description of the CSDF facility.

#### **Computer Complex**

Refer to the Phase II Apparatus section for a description of the computer complex.

#### **Simulator**

Refer to the Phase II Apparatus Section for a description of the FB-111 simulator. Added to the earlier description of the simulator was a simple Head-Up Display (HUD), shown in Figure 41, which was designed to aid the pilots in placing the simulator in the desired flight path angle configuration. The HUD also displayed a horizon line indicating ground level.

#### **Experimenter's Console**

The experimenter's console was located approximately 12 feet away from the simulator. It included a complete intercom system, with communication to and from the pilot inside the simulator. The console's displays duplicated the simulator's HUD, instruments and displays, and were used to monitor pilot and aircraft performance. Furthermore, the console's controls permitted the experimenter to start, stop and reset the simulation at any time.

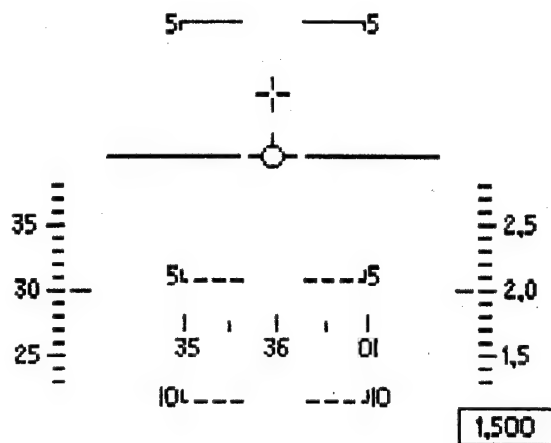


Figure 41. Head-Up Display (HUD).

#### VMU Mechanization

One warning and four caution voice messages were presented to the pilot's headset through the intercom channel. The five messages included "Pull-up," "Alpha," "Alpha Side Slip," "Autopilot" and "Autopilot Failed". The messages represented the stimulus and four distractors. In order to maintain consistency across subjects and conditions, pilots were not allowed to change the volume control setting. The warning message ("Pull-up") was mechanized in such a way that it was continuously presented to the pilot until the corrective action was completed. The warning was presented in message pairs ("Pull-up/Pull-up") with an inter-message interval of 500 milliseconds, and a delay of three seconds before the next pair of "Pull-up" messages. The caution messages, on the other hand, were also presented with an inter-message interval of 500 milliseconds, except that the messages were only repeated twice. The caution messages "Alpha," "Alpha Side Slip," "Autopilot" and "Autopilot Failed," were mechanized in such a way that they would not be presented if the GCAS warning was within 100 feet of becoming active. A more comprehensive description of the distractors may be found in the procedure section.

#### Audio Systems

The voice messages were recorded on an Amiga micro computer by a female employee of the CSDF. The employee, who had a distinctive and mature mid-western voice, presented the messages in a formal and impersonal manner. The Amiga used a high speed voice digitizer (Future Sounds), with a sampling rate of 10,000 samples per second, to convert the messages from analog to digital format. The Amiga was thereafter connected to the main frame computers using an RS-232 interface, and transmitted the messages to the pilot's headset (an ASTROCOM model number 20680 with MX-2508/A/C pads) through the intercom channel. The length of time it took to articulate the voice

message "Pullup" was approximately 420 milliseconds.

Background communication was simulated by an audio tape, on a Technics by Panasonic model number RS-263AUS tape player, and transmitted to the pilot's headset through the intercom channel.

## Design

Phase III of the evaluation was designed to compare F/FB/EF-111 pilots' performance and subjective data as a function of four independent variables. These variables were: (1) roll angle, (2) flight path angle (Gamma), (3) terrain slope and (4) airspeed. Table 11 lists the levels for each of the independent variables.

TABLE 11. Man-in-the-loop design matrix.

INDEPENDENT VARIABLES			
ROLL	FPA	AIR SPEED	SLOPE
(Degrees)	(degrees)	(Knots)	(Degrees)
0	-5	350	0
30	-10	475	6
60	-20	600	12
	-30		18
	-40		

For each airspeed condition, a different wing sweep configuration was flown. The airspeed/wing sweep combinations were 26 degrees of wing sweep for the 350 knot condition, 45 degrees for 475 knots, and 55 degrees for 600 knots. These airspeed/wing sweep combinations were considered standard flying configurations.

Also, the 350 knot airspeed condition included four flight path angles of -5, -10, -20, and -30 degrees, while the 475 and the 600 knot airspeed conditions included four flight path angles of -5, -10, -20, and -40 degrees. It was identified prior to the evaluation that some of the pilots may encounter difficulty flying the simulator at low airspeed (350 knots) with a flight path angle of -40 degrees.

Minimum clearance altitude (also referred to as the minimum recovery altitude) was considered the primary dependent variable of interest. The overall experimental design was comprised of a single run per condition/per pilot for a total of 144 test trials per pilot (three roll angles X four flight path angles X three airspeed conditions X four terrain slopes). The performance data were analyzed using the linear regression technique.

Pilots' subjective ratings (on a scale from 1 to 5; 1 being too high, and 5 being too low), on the minimum recovery altitude for each of the 144 test trials, were also analyzed using a linear regression

technique on each of the five ratings. The results of the data were used to influence the development of a subjective window of acceptability for a minimum recovery altitude as a function of vertical velocity.

Other performance data included actual pilot reaction times. Using these data, correlation coefficients were calculated for predicted versus actual reaction times. Furthermore, univariate statistics were calculated to examine trends in the data. A follow-up analysis examined the relationship of predicted reaction time with other variables such as minimum clearance, flight path angle, vertical velocity, airspeed, altitude at time of warning, and altitude loss.

Finally, a second set of subjective data were collected at the completion of the simulator evaluation. The data, relevant to such GCAS mechanization issues as the need for a redundant GCAS light to complement the voice message, most appropriate delay time between the pairs of Pullup/Pullup voice warnings, and the pilots' overall assessment of the GCAS algorithm, will be discussed in terms of preference options.

## Procedure

Prior to flying the FB-111 simulator, the pilots were given the desired aircraft parameters for each particular test trial. The evaluation simulated flying in the weather without an outside the window visual scene. However, a HUD was presented as an aid to the pilot, allowing him to place the simulator in the desired flight path angle condition without performing major mental calculations in translating from dive angle to flight path angle. Pilots' responsibilities included (1) establishing the given parameters for wing sweep, airspeed, roll angle, and flight path angle, (2) attempting to stabilize and maintain the simulator at one G until the GCAS warning was initiated and (3) recovering to climbing flight. Each test trial was terminated when the flight path angle of the simulator became greater than the angle of the terrain slope. The pilots were instructed to perform the following recovery procedure: (1) Roll to wings level ("+" or "-" 20 degrees); (2) pull to five Gs or 14 degrees AOA and (3) roll and pull simultaneously. As a means of compensating for the absence of gravitational force feedback, a light located on the right caution panel would illuminate at four Gs or 12 degrees AOA, while a second light would follow suit at six Gs or 16 degrees AOA. The pilots were also instructed to focus on the G and AOA indicators. All trials which the simulator exceeded the maximum of six Gs and/or 18 degrees AOA were repeated. At the completion of the recovery maneuver, each pilot was given feedback on the maximum G, maximum AOA, and the minimum clearance for that specific configuration, and was asked to rate minimum recovery altitude based on a five point scale (1 = too high, 2 = slightly high, 3 = about right, 4 = slightly low, and 5 = too low).

In an attempt to decrease pilots' reaction time performance biases (an anticipatory situation where the pilot knew he would eventually receive a pull-up warning that required immediate recovery), two additional factors were introduced. Throughout all the test trials, background communication was simulated by playing an audio tape of a combat mission, recorded during the Vietnam war, and transmitted to the pilot through the headset. Furthermore, four distractor voice caution messages were randomly presented to the pilot during the initial configuration set-up window. These voice messages

were "Autopilot," "Autopilot Failed," "Alpha" and "Alpha Side Slip". The distractor caution messages were presented to the pilot at an average of 10 seconds with a standard deviation of five seconds. The pilots were instructed to ignore both the background communication and the distractor voice messages, which were irrelevant to the performance of the test trial.

Each pilot flew eight practice trials, followed by three sets of 48 experimental trials, for a total of 144 test trials. A 15 minute break after the first set of trials and a one-hour lunch break after the second. At the completion of all the test trials (which lasted a total of five hours), the pilots were asked to complete a short questionnaire relevant to certain GCAS mechanization issues.

Finally, the delay between the pairs of "Pull-up/Pull-up" messages was changed from three seconds to two seconds, and eventually to one second, in order to allow the pilots to experience the different time delays and select the most appropriate one. This was not done, however, with the first pilots. All eight pilots were also shown two lights being considered by GD as redundant to the voice warning messages. The two options included either (1) a constantly illuminated red warning light (RDR ALT LOW) located below the windshield, at about eye level or (2) a constantly illuminated yellow caution light located on the left caution panel (GCAS). This GCAS caution light primarily indicated a GCAS fail condition. Either light was activated throughout the entire GCAS warning window. Again, pilots' preference data were elicited for further evaluation.

### **Phase III Results**

Four sets of data were collected throughout the man-in-the-loop simulation. The first set of data (performance data), representing minimum clearance altitude (or minimum recovery altitude) was analyzed using the linear regression model. The airspeed variable was divided into three independent, non-interacting levels, and analyzed as a function of flight path angle ( $\Gamma$ ), roll angle, and terrain slope. The second set of data, pilot reaction time, was analyzed and compared to the predicted pilot reaction time equation (RTIME) used in the GCAS algorithm. The third set of data, representing pilots' preferences on certain GCAS mechanization issues, was not formally analyzed because (1) certain mechanization options were changed in the middle of the experiment and (2) the sample size was small (only eight pilots participated in the evaluation). Finally, the third set of data (rating data), including pilots' ratings on the minimum clearance altitude, was analyzed using the linear regression model in an attempt to create some type of a window representing an acceptable minimum clearance altitude as a function of vertical velocity. The following three sections will present and discuss the three sets of data.

#### **Performance Data Results**

All the pilots' minimum clearance data were plotted as a function of the absolute value of  $\Gamma$  separately for each roll angle (0, 30, and 60 degrees) and terrain slope angle (0, 6, 12, and 18 degrees). Furthermore, the function lines based on the first order coefficients, calculated using the linear regression analysis, were also drawn on the same graph to allow the reader to extrapolate beyond



the levels of flight path angle flown during the evaluation. Finally, each plot will contain the correlation coefficient, as well as the equation for the predicted line in the form:  $y = ax + b$ , where "y" is the minimum clearance altitude, "a" is the slope of the line, "x" is the corresponding Gamma value, and "b" is the zero intercept of that line. To simplify data inspection, a description will be given for each airspeed (350, 475, and 600 knots) separately.

#### **Low Airspeed--350 Knots/26 Degrees Wing Sweep**

The plots from the low airspeed condition are shown in Figures 42 through 45. Each figure contains three plots of minimum clearance altitude as a function of Gamma. Each set of plots represents one terrain slope condition for all three roll angles (0, 30, and 60 degrees).

An inspection of the data revealed a consistent linear relationship between minimum clearance altitude as a function of Gamma. High correlation coefficients were calculated for most conditions, but seemed to decrease as a function of terrain slope. This led to the major concern regarding the GCAS algorithm's ability to calculate and extrapolate the necessary additional altitude for a safe recovery as terrain slope was increased. In regard to terrain slope, two things appeared to be happening. First, the intercept of the regression line decreased as a function of the increased terrain slope. The algorithm failed to predict the appropriate recovery altitude at the smaller flight path angles. Second, the slope of the regression line increased from zero to six degrees, but then began to decrease again at 12 degrees and nearly flattened out at 18 degrees of terrain slope.

The algorithm's ability to predict the needed additional altitude for a safe recovery as a function of roll angle was shown to be fairly consistent. Both the slopes and the intercepts of the regression lines, for all three roll angles, were closely related to each other, at the different terrain slope conditions.

SPEED=350 SLOPE=0 ROLL=0

R=0.91  $Y=-15X-17$

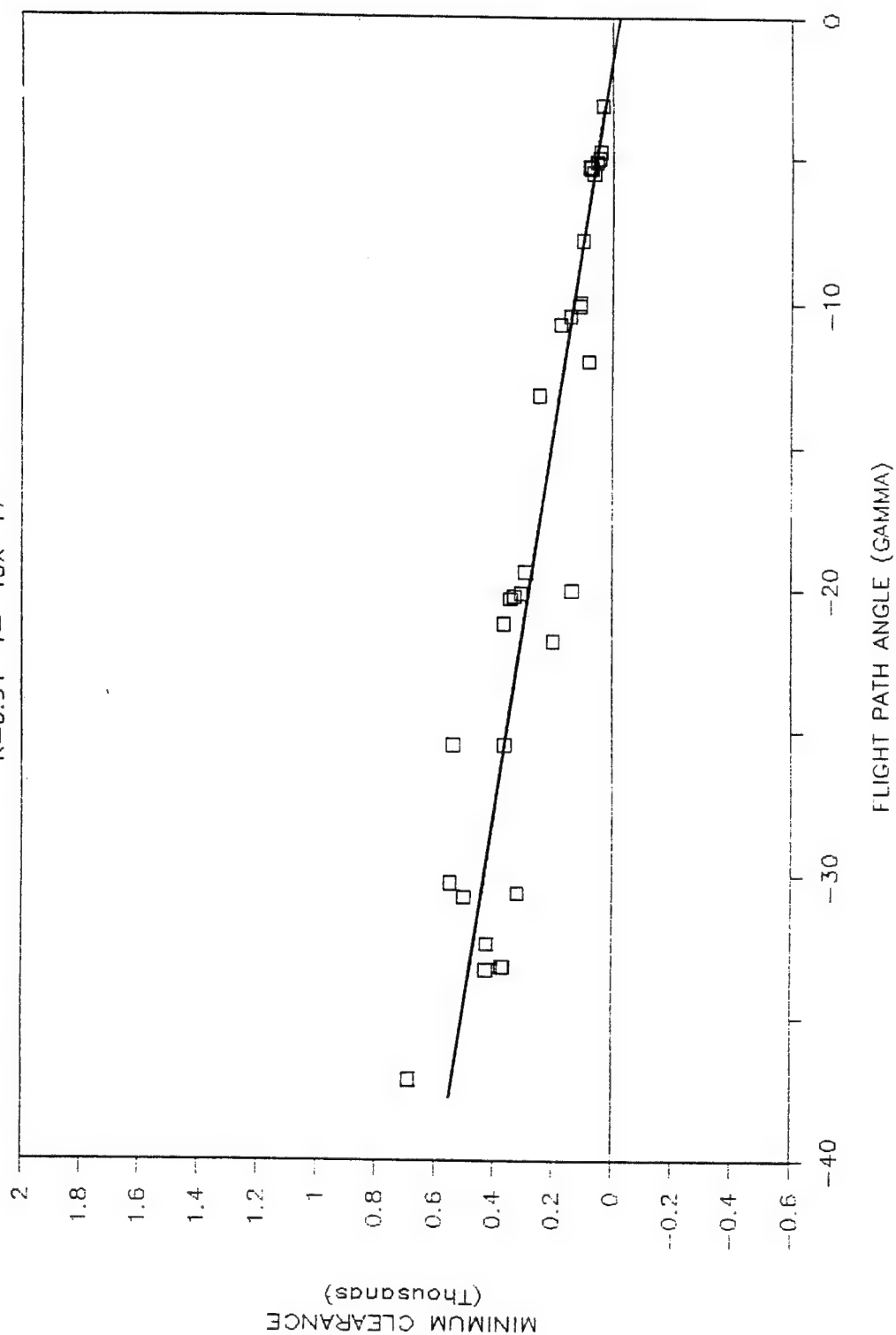


Figure 42 (a). Minimum clearance as a function of flight path angle for all pilots at speed = 350 slope = 0 roll = 0.

SPEED=350 SLOPE=0 ROLL=30

R=0.66  $Y = -8X + 48$

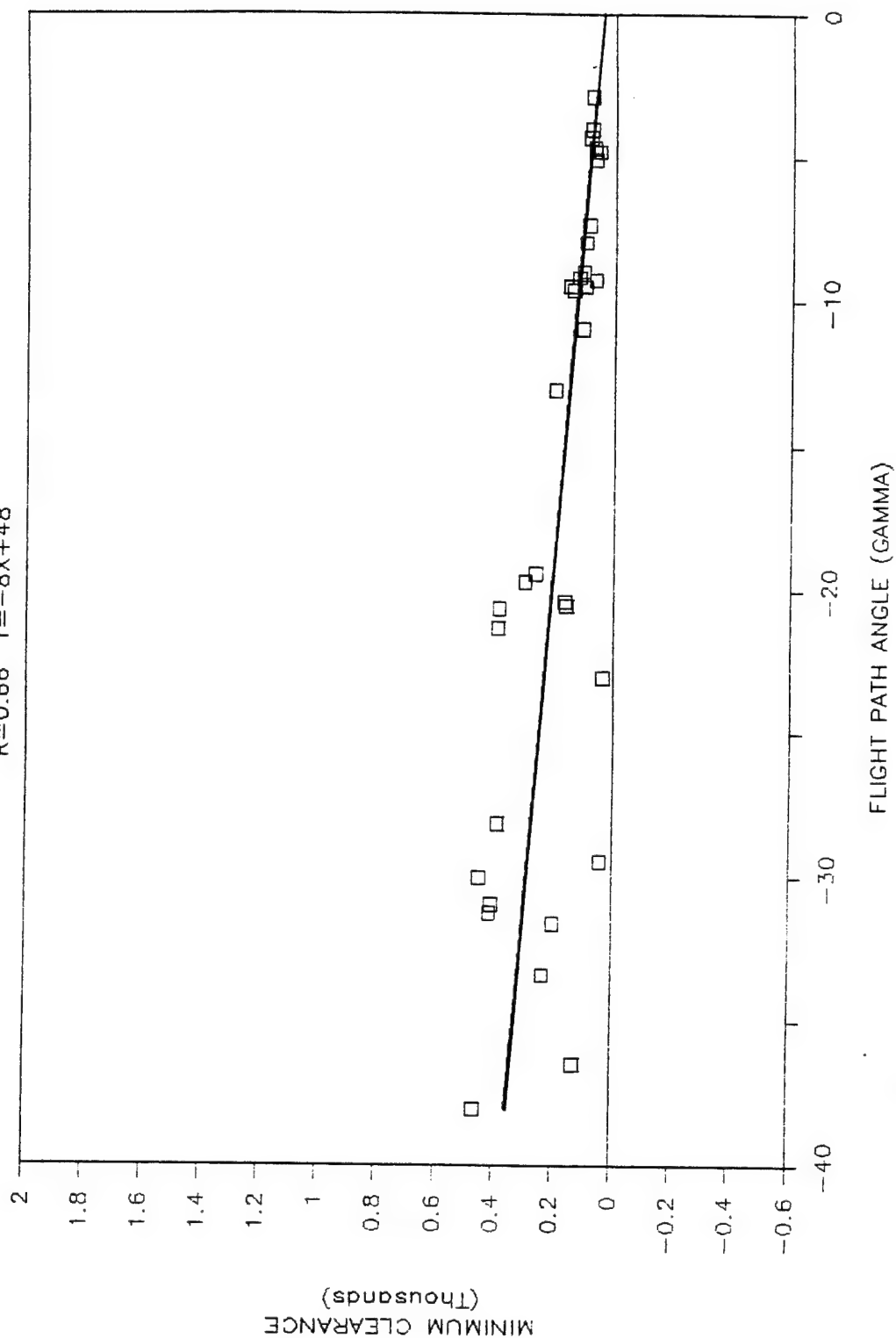


Figure 42 (b). Minimum clearance as a function of flight path angle for all pilots at speed = 350 slope = 0 roll = 30.

SPEED=350 SLOPE=0 ROLL=60

R=0.34  $Y = -7X + 67$

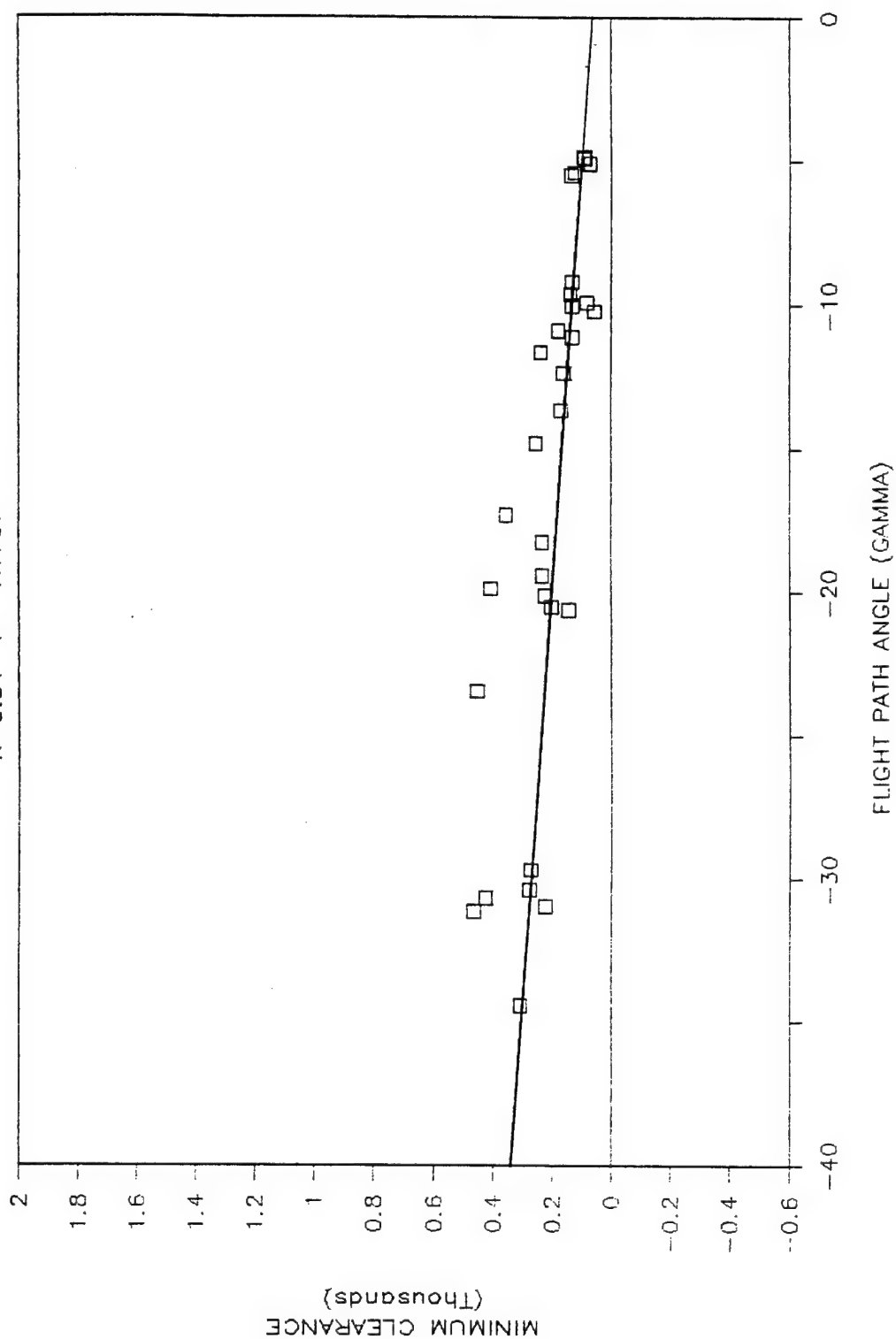


Figure 42 (c). Minimum clearance as a function of flight path angle for all pilots at speed=350 slope=0 roll=60.

SPEED=350 SLOPE=6 ROLL=0

R=0.94  $Y=-24X-187$

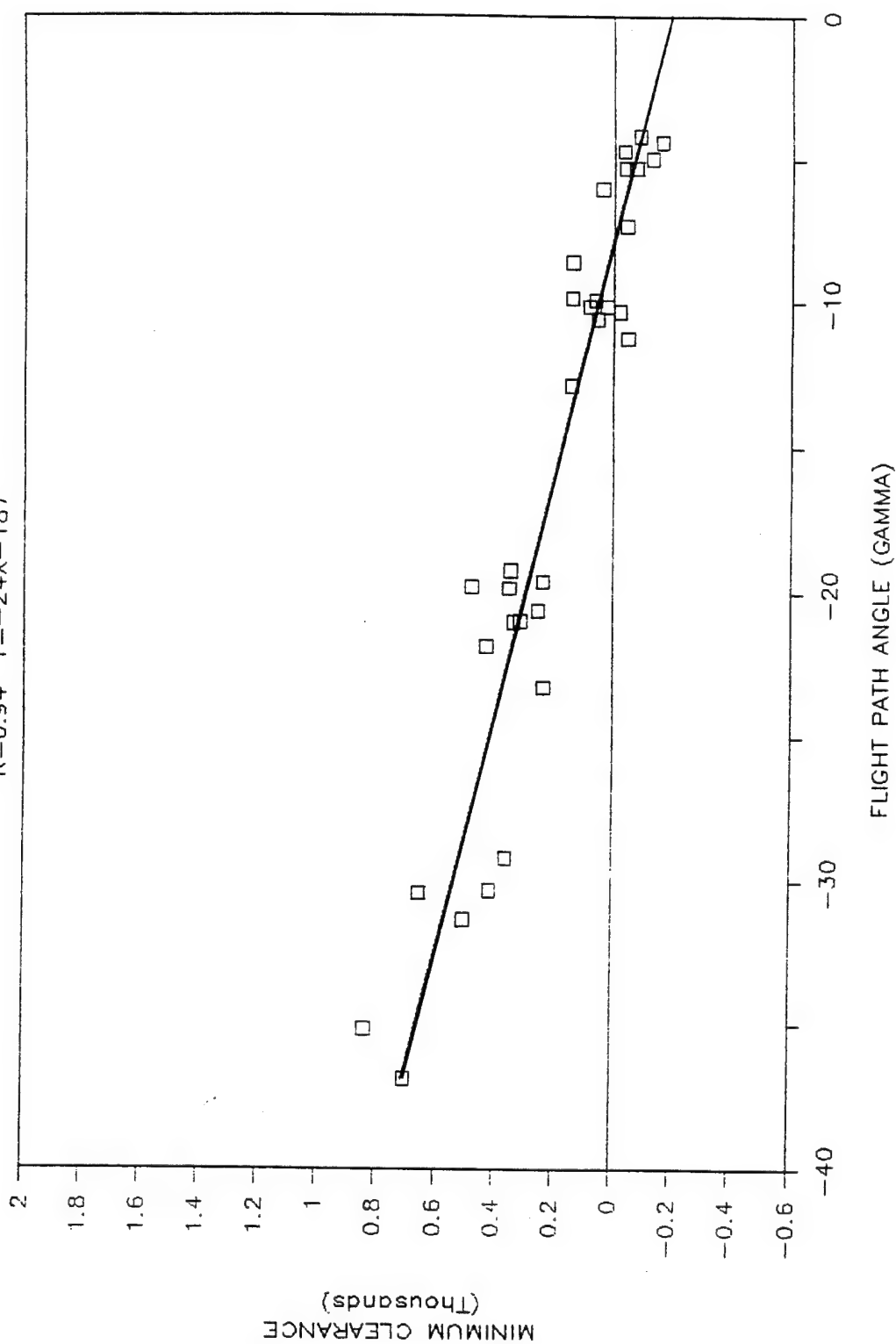


Figure 43 (a). Minimum clearance as a function of flight path angle for all pilots at speed = 350 slope = 6 roll = 0.

SPEED=350 SLOPE=6 ROLL=30

R=0.69  $Y=-21X-148$

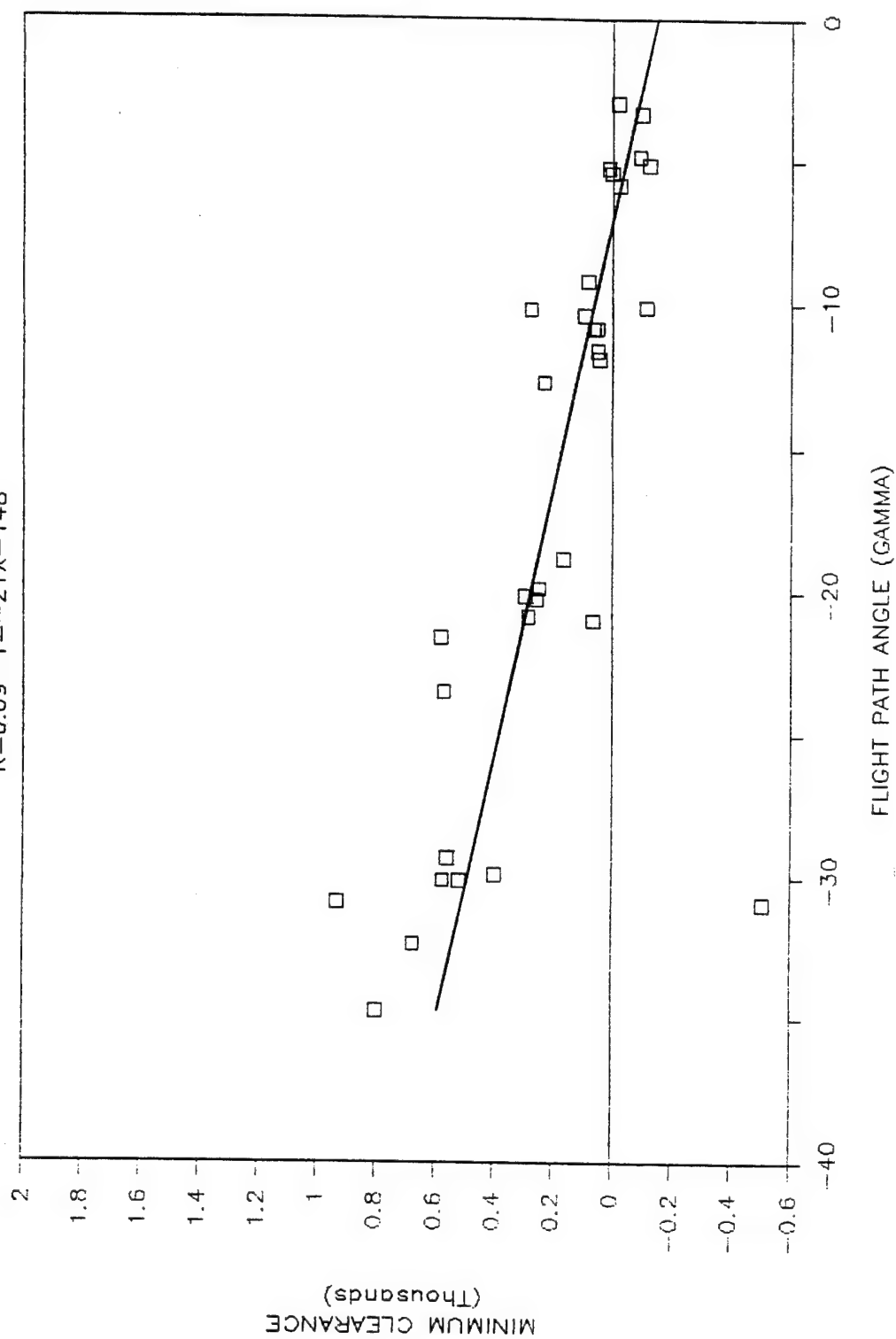


Figure 43 (b). Minimum clearance as a function of flight path angle for all pilots at speed = 350 slope = 6 roll = 30.

SPEED=350 SLOPE=6 ROLL=60

R=0.92 Y=-29X-241

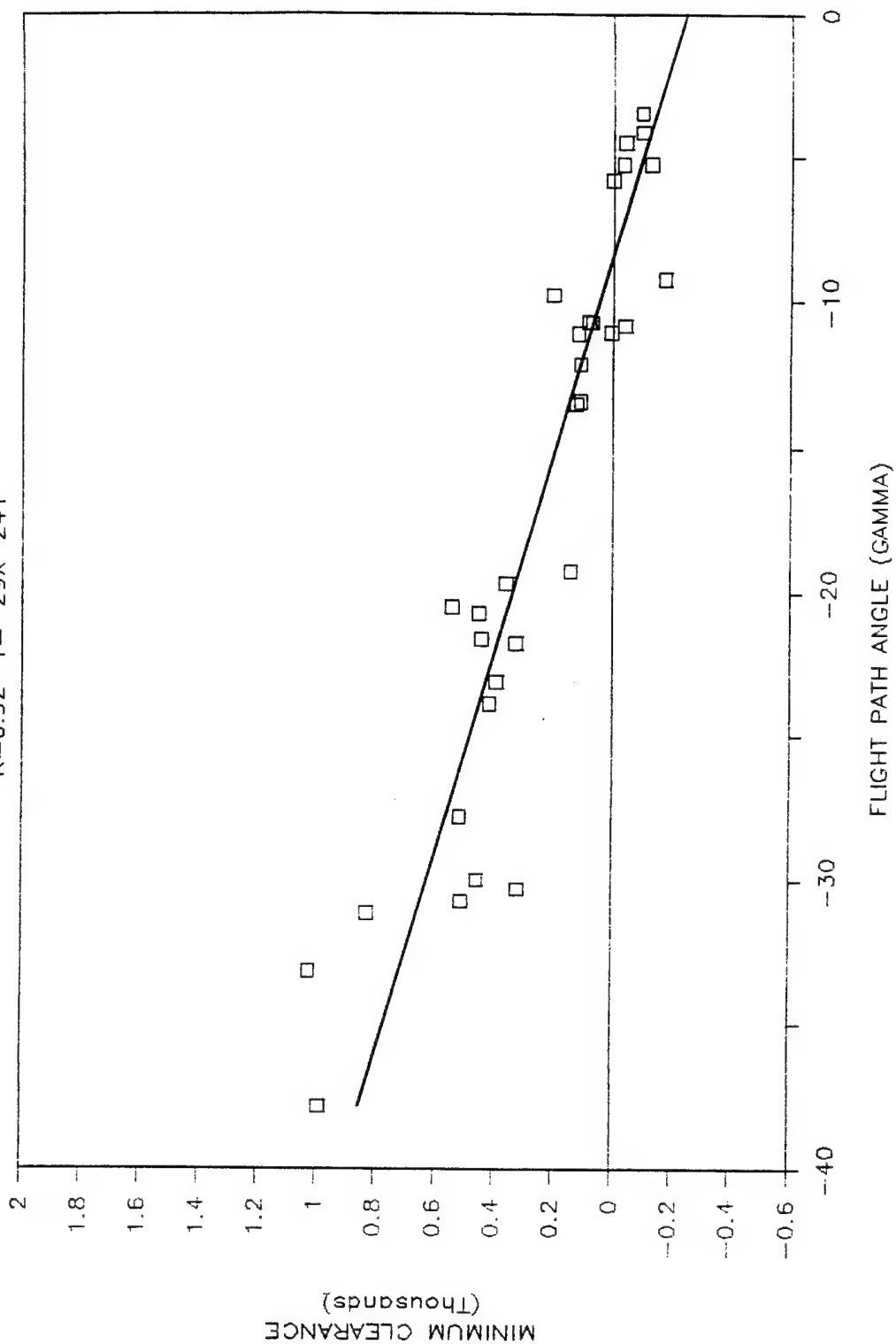


Figure 43 (c). Minimum clearance as a function of flight path angle for all pilots at speed = 350 slope = 6 roll = 60.

SPEED=350 SLOPE=12 ROLL=0

R=0.92  $Y=-17X-171$

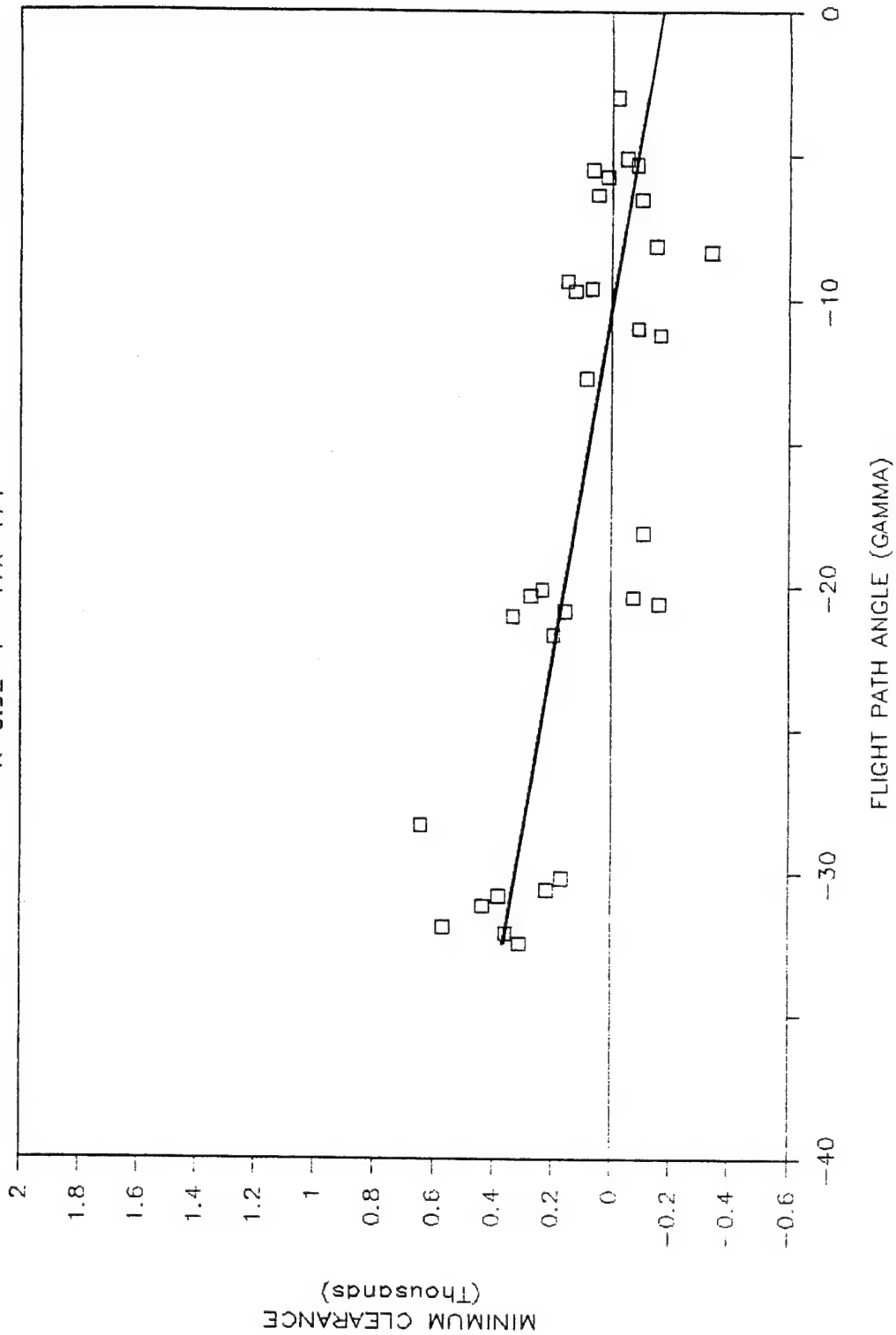


Figure 44 (a). Minimum clearance as a function of flight path angle for all pilots at speed = 350 slope = 12 roll = 0.



SPEED=350 SLOPE=12 ROLL=30

R=0.63  $Y=-16X-155$

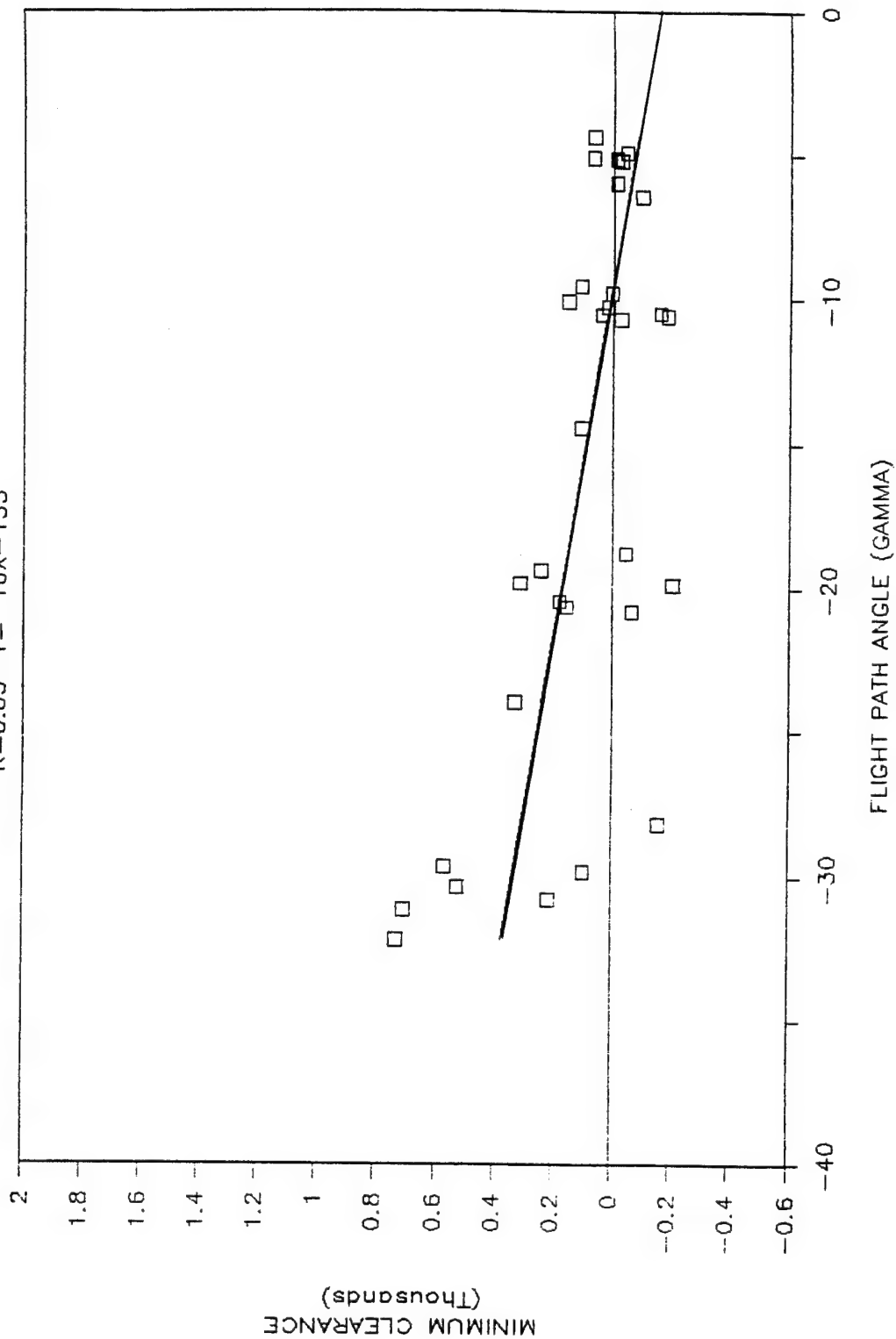


Figure 44 (b). Minimum clearance as a function of flight path angle for all pilots at speed = 350 slope = 12 roll = 30.

SPEED=350 SLOPE=12 ROLL=60

R=0.63  $Y=-19X-245$

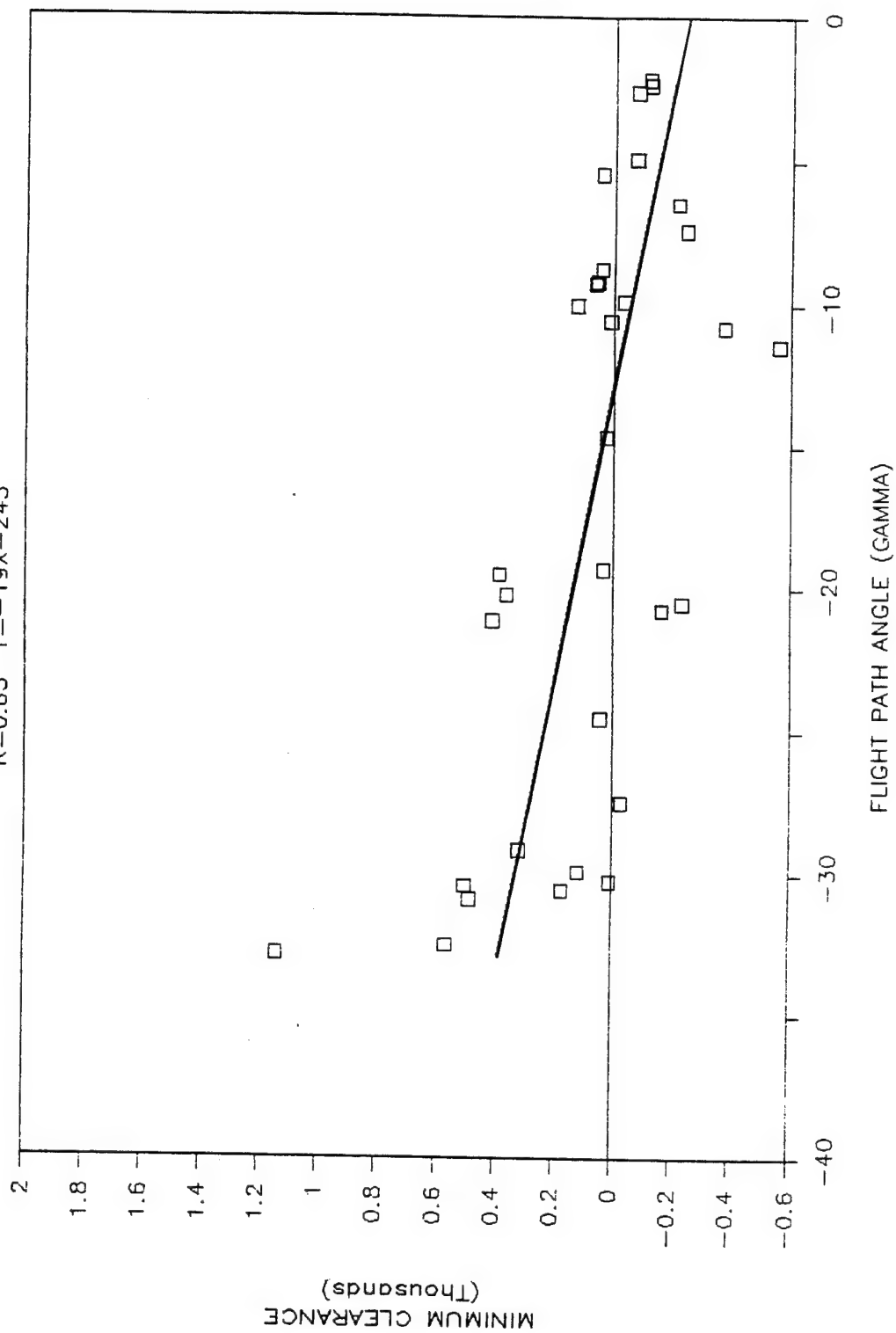


Figure 44 (c). Minimum clearance as a function of flight path angle for all pilots at speed = 350 slope = 12 roll = 60.

SPEED=350 SLOPE=18 ROLL=0

R=0.22  $Y=-5X-262$

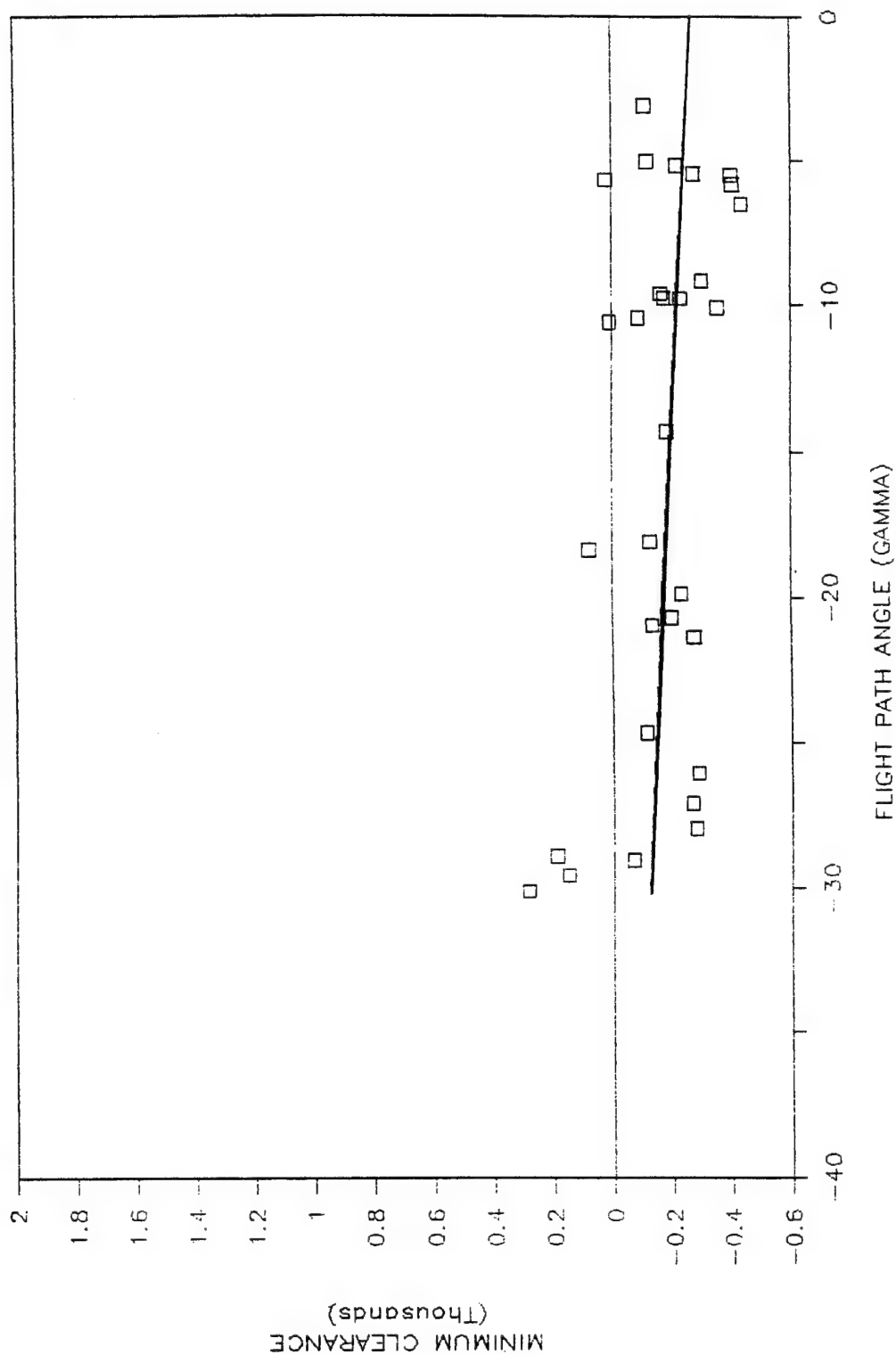


Figure 45 (a). Minimum clearance as a function of flight path angle for all pilots at speed=350 slope=18 roll=0.

SPEED=350 SLOPE=18 ROLL=30

R=0.14  $Y=-3X-287$

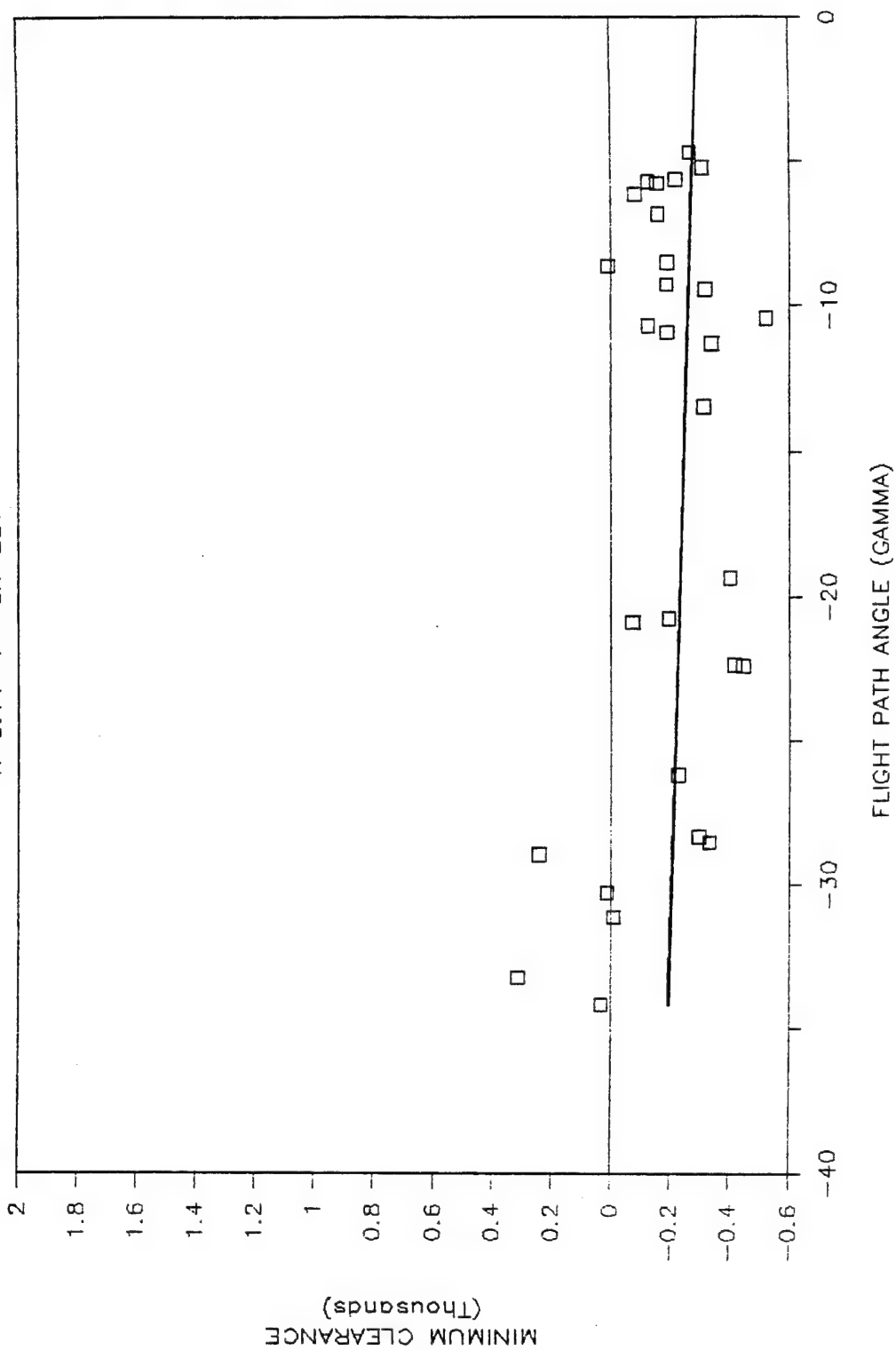


Figure 45 (b). Minimum clearance as a function of flight path angle for all pilots at speed = 350 slope = 18 roll = 30.

SPEED=350 SLOPE=18 ROLL=60

R=0.22  $Y = -7X - 407$

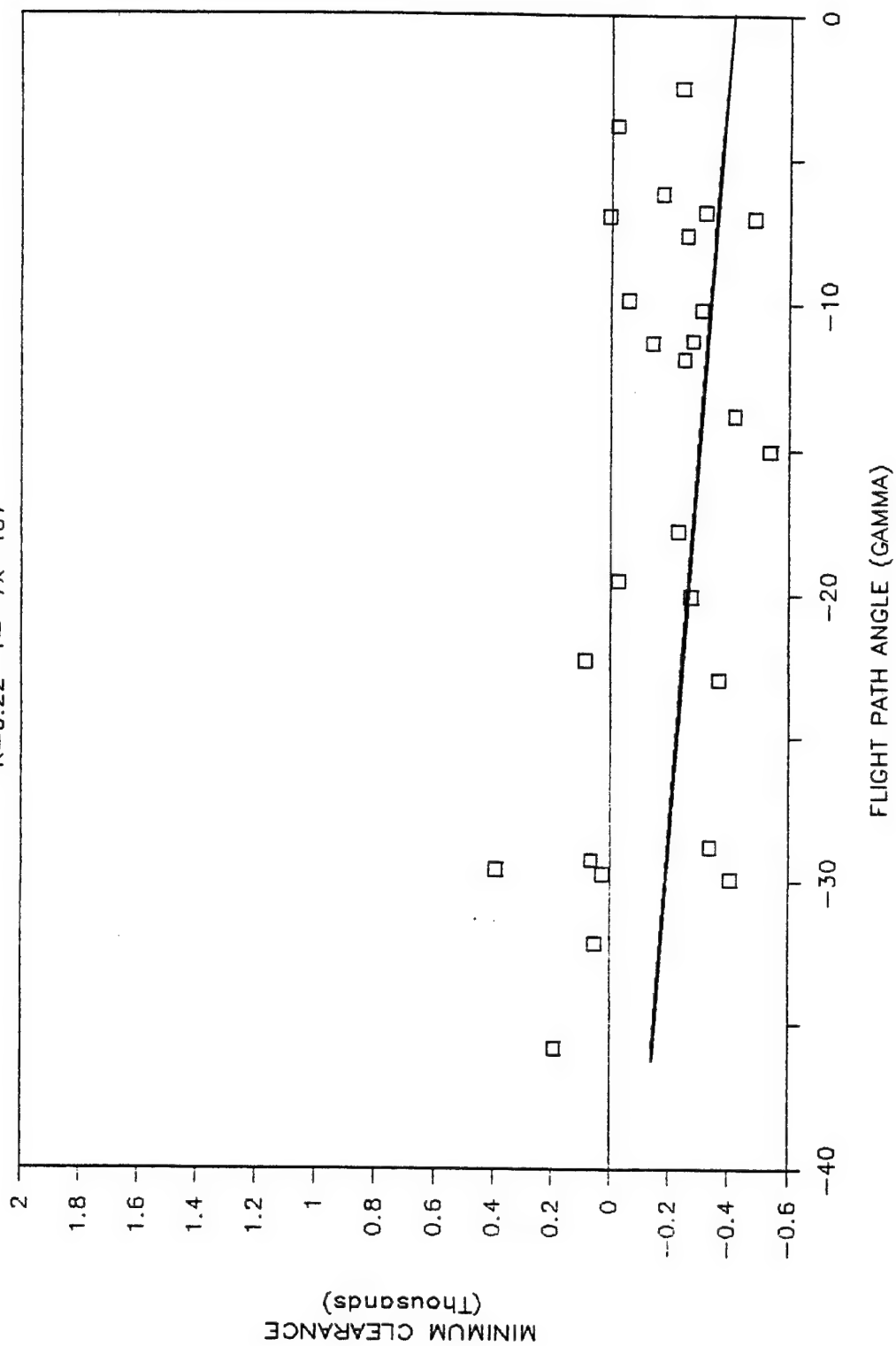


Figure 45 (c). Minimum clearance as a function of flight path angle for all pilots at speed = 350 slope = 18 roll = 60.

### **Medium Airspeed--475 Knots/45 Degrees Wing Sweep**

The plots from the medium airspeed condition are shown in Figures 46 through 49. Each figure contains three plots of minimum clearance altitude as a function of the Gamma (0 through -40 degrees). Each set of plots represents one terrain slope condition for all three roll angles (0, 30, and 60 degrees).

An inspection of the data revealed a consistent linear relationship between minimum clearance altitude as a function of Gamma. High correlation coefficients were calculated for most conditions. In regard to terrain slope however, it appears that the increase in terrain slope lead to an increase in the number of crashes at the low Gamma conditions. This was also demonstrated by an overall decrease in the intercepts of the regression lines as a function of terrain slope. However, the slopes of these predicted lines were fairly consistent across each other with a slight tendency to decrease as terrain slope increased, indicating a predictive weakness, again, at 18 degrees of terrain slope.

The roll compensation section of the algorithm (HPHI) appeared to allow more altitude as roll angle increases. The intercept of each of the regression lines increased as roll angle increased. The trend was replicated with the different terrain slopes. The results were interpreted as having the pilots clear the ground, on the average, 37 feet higher at 30 degrees of roll than at zero degrees of roll. On the same line, minimum clearance altitude was 43 feet higher at 60 degree-roll than at 30 degree-roll.

SPEED=475 SLOPE=0 ROLL=0

R=0.91 Y=-.38X-239

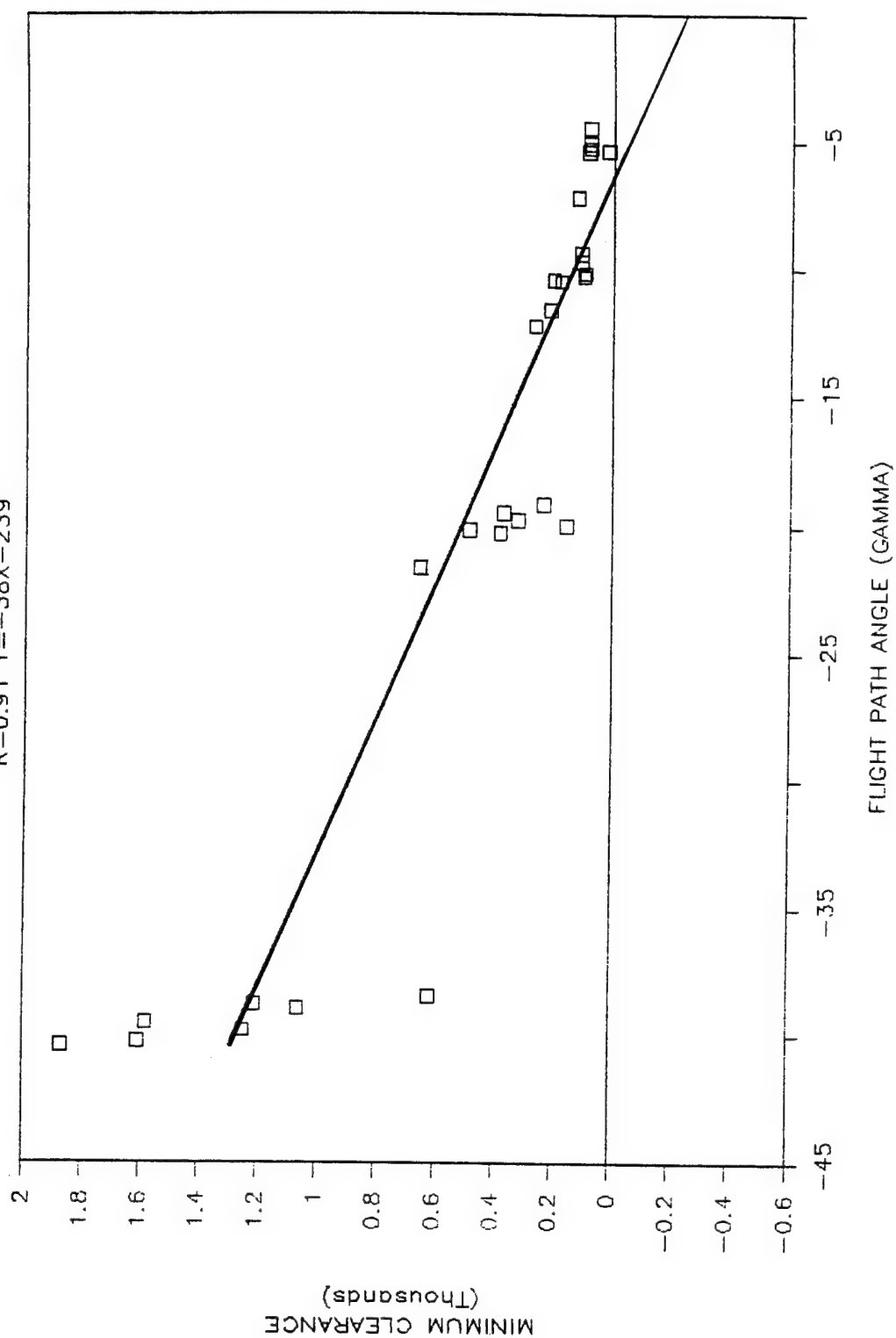


Figure 46 (a). Minimum clearance as a function of flight path angle for all pilots at speed=475 slope=0 roll=0.

SPEED=475 SLOPE=0 ROLL=30

R=0.79  $Y = -28X - 94$

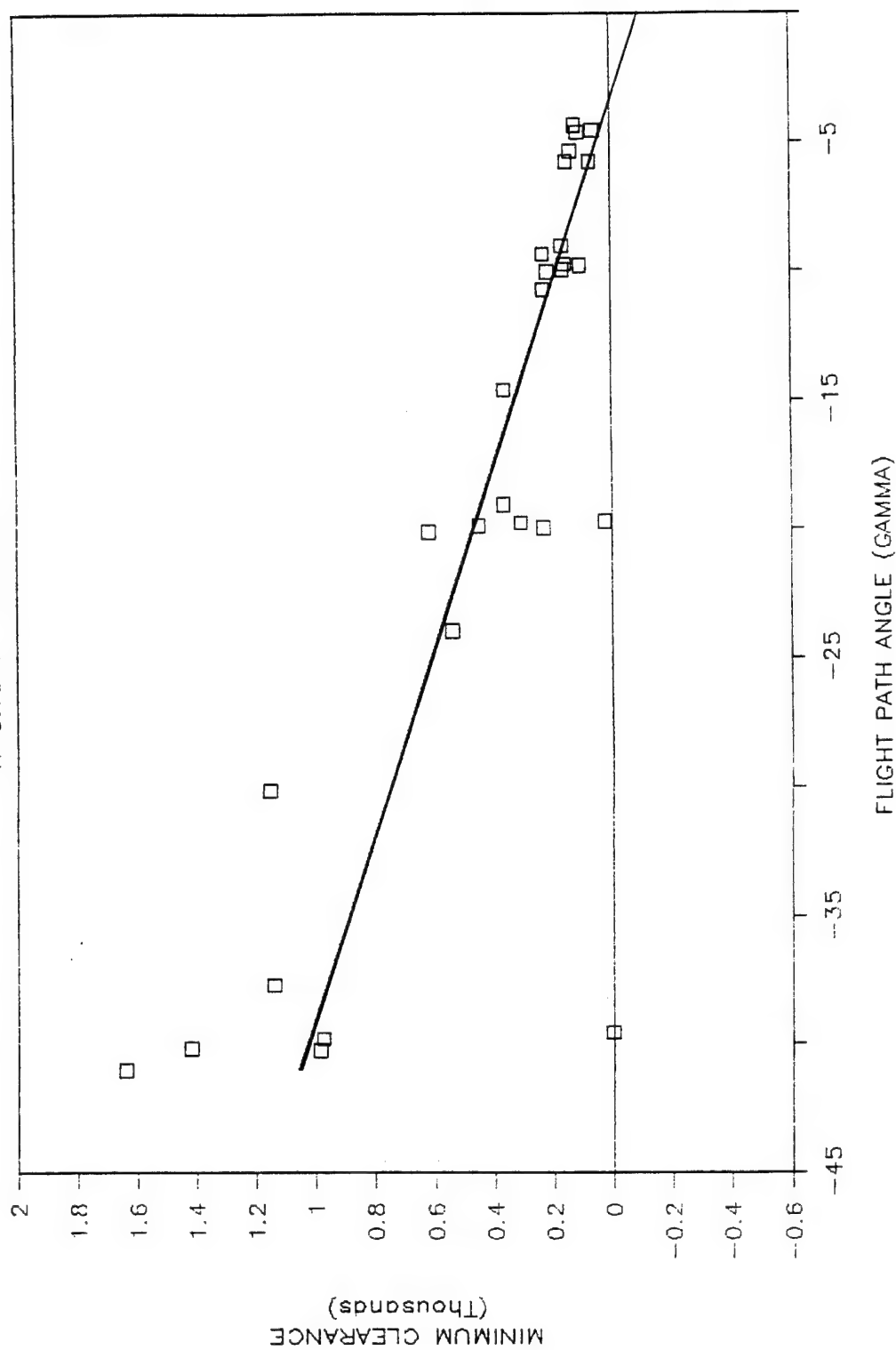


Figure 46 (b). Minimum clearance as a function of flight path angle for all pilots at speed = 475 slope = 0 roll = 30.



SPEED=475 SLOPE=0 ROLL=60

$R=0.93$   $Y=-29X-30$

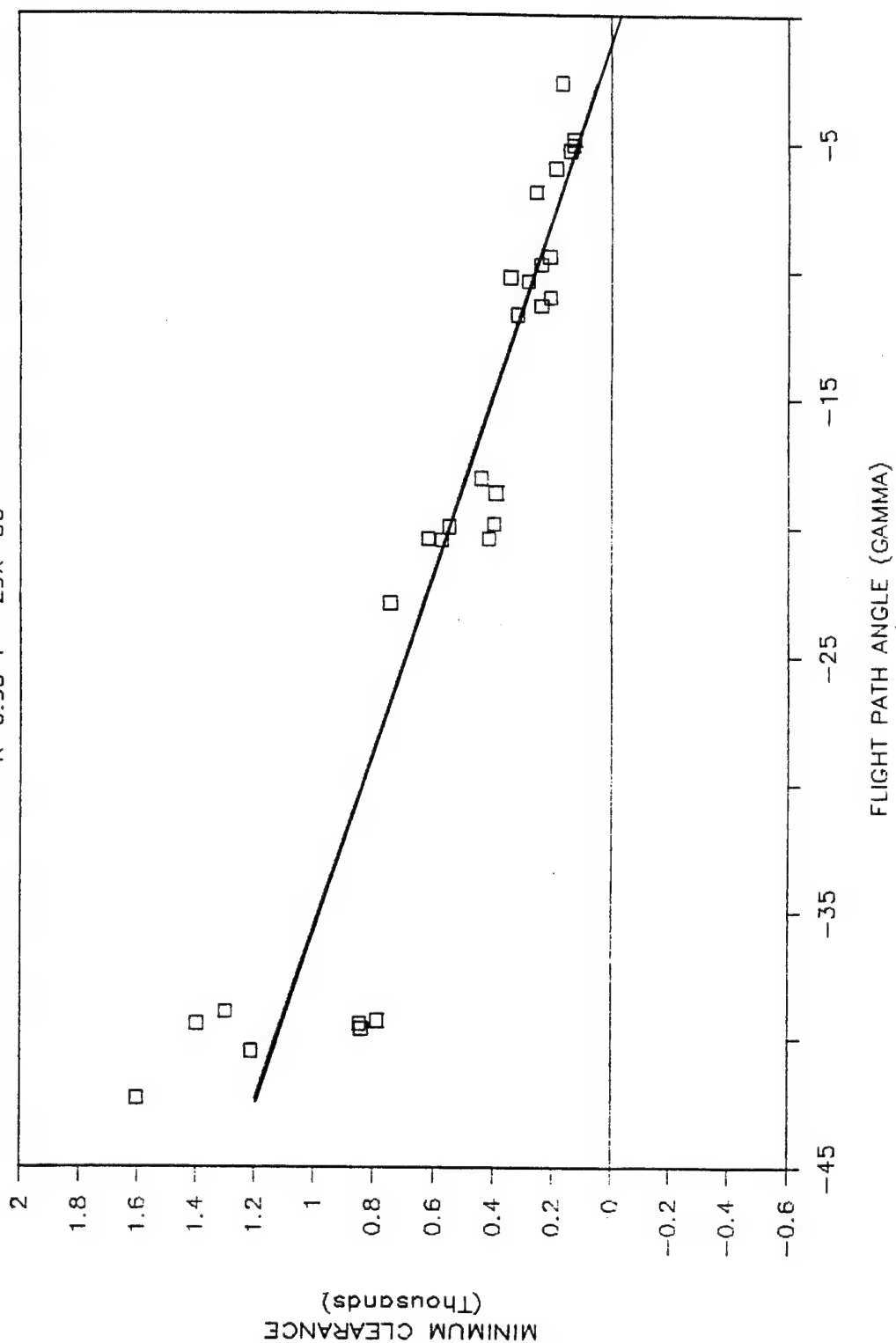


Figure 46 (c). Minimum clearance as a function of flight path angle for all pilots at speed=475 slope=0 roll=60.

SPEED=475 SLOPE=6 ROLL=0

R=0.96  $Y = -52X - 312$

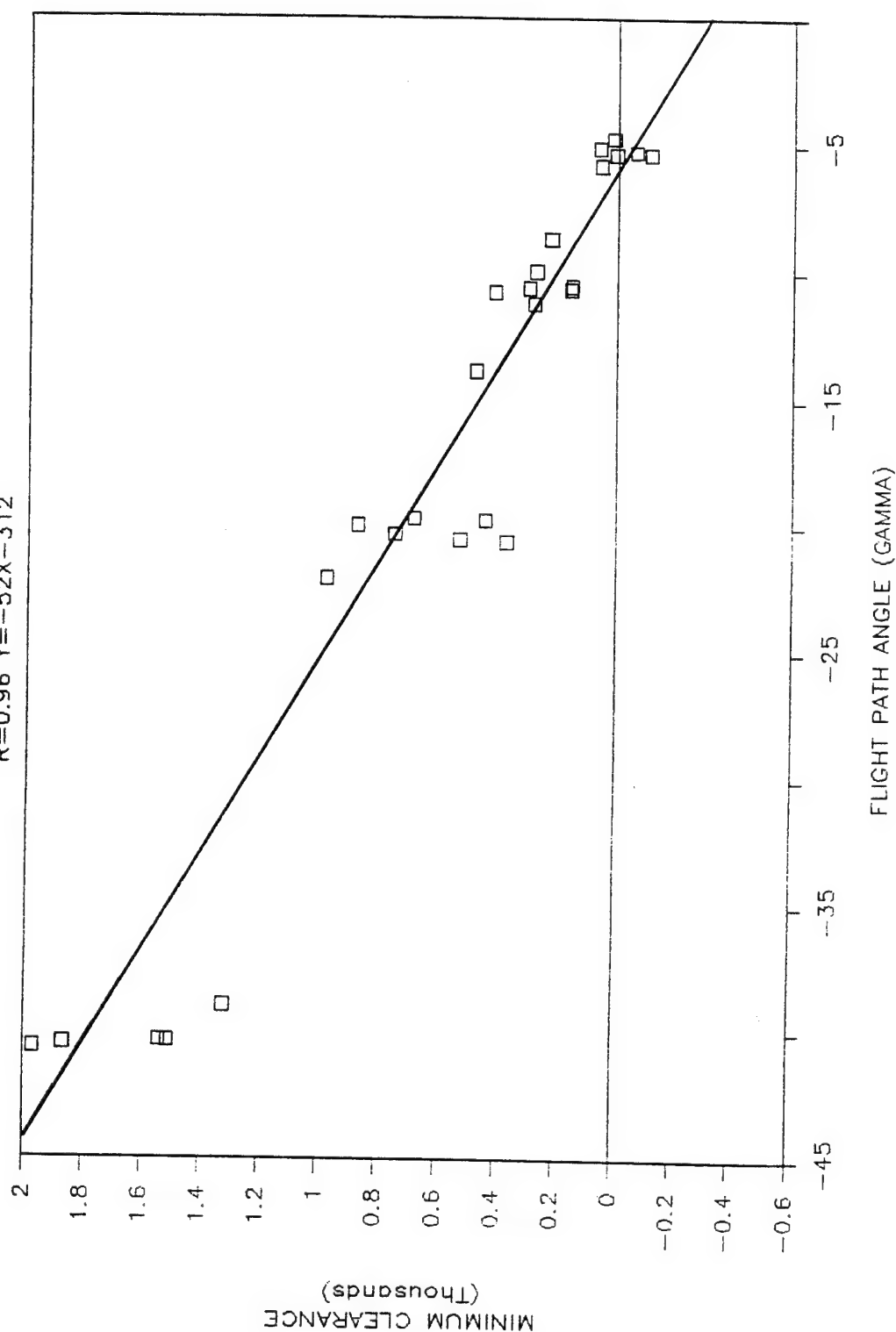


Figure 47 (a). Minimum clearance as a function of flight path angle for all pilots at speed=475 slope=6 roll=0.

SPEED=475 SLOPE=6 ROLL=30

$R=0.94$   $Y=-45X-214$

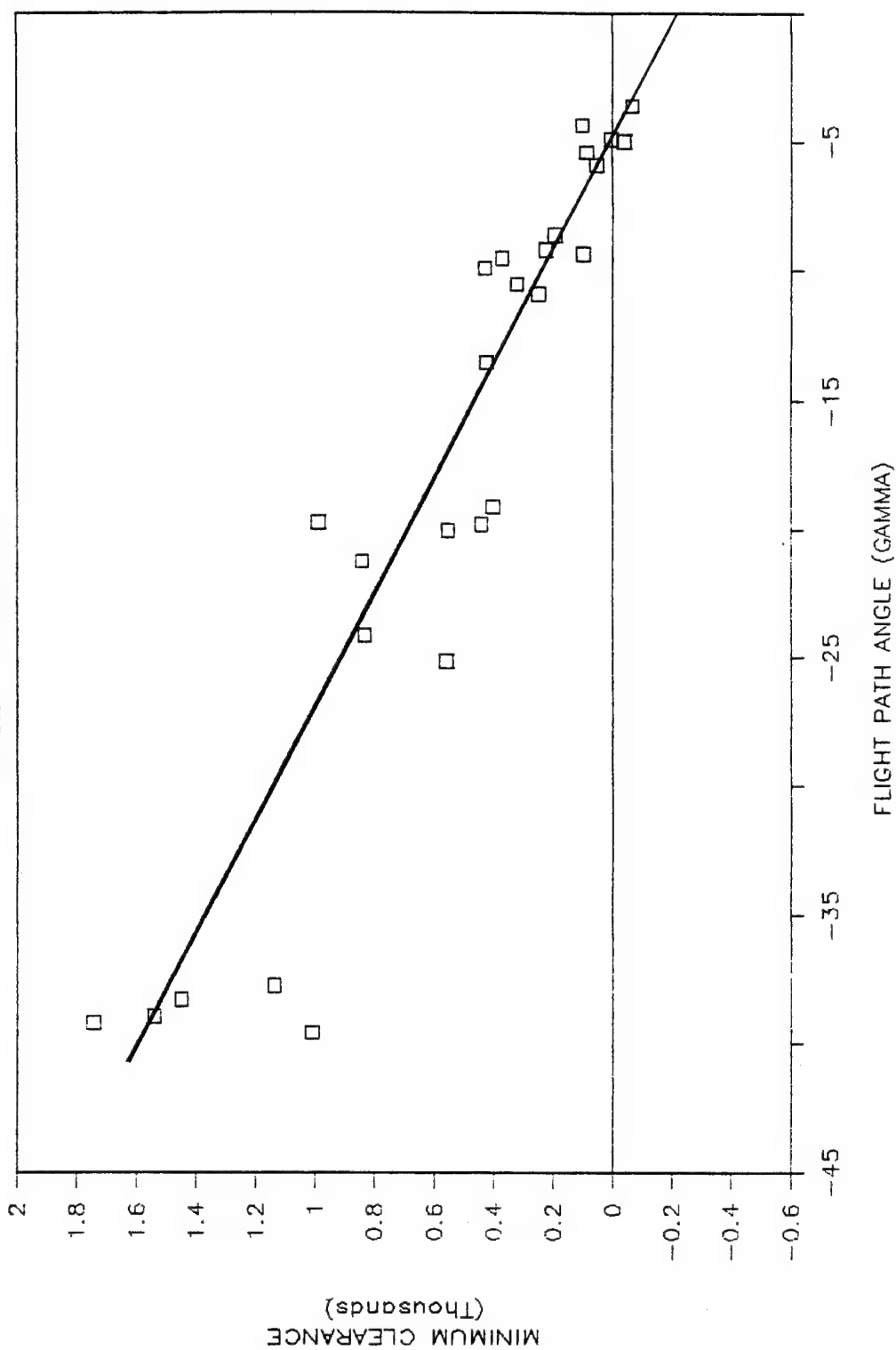


Figure 47 (b). Minimum clearance as a function of flight path angle for all pilots at speed=475 slope=6 roll=30.

SPEED=475 SLOPE=6 ROLL=60

$R=0.89$   $Y=-41X-124$

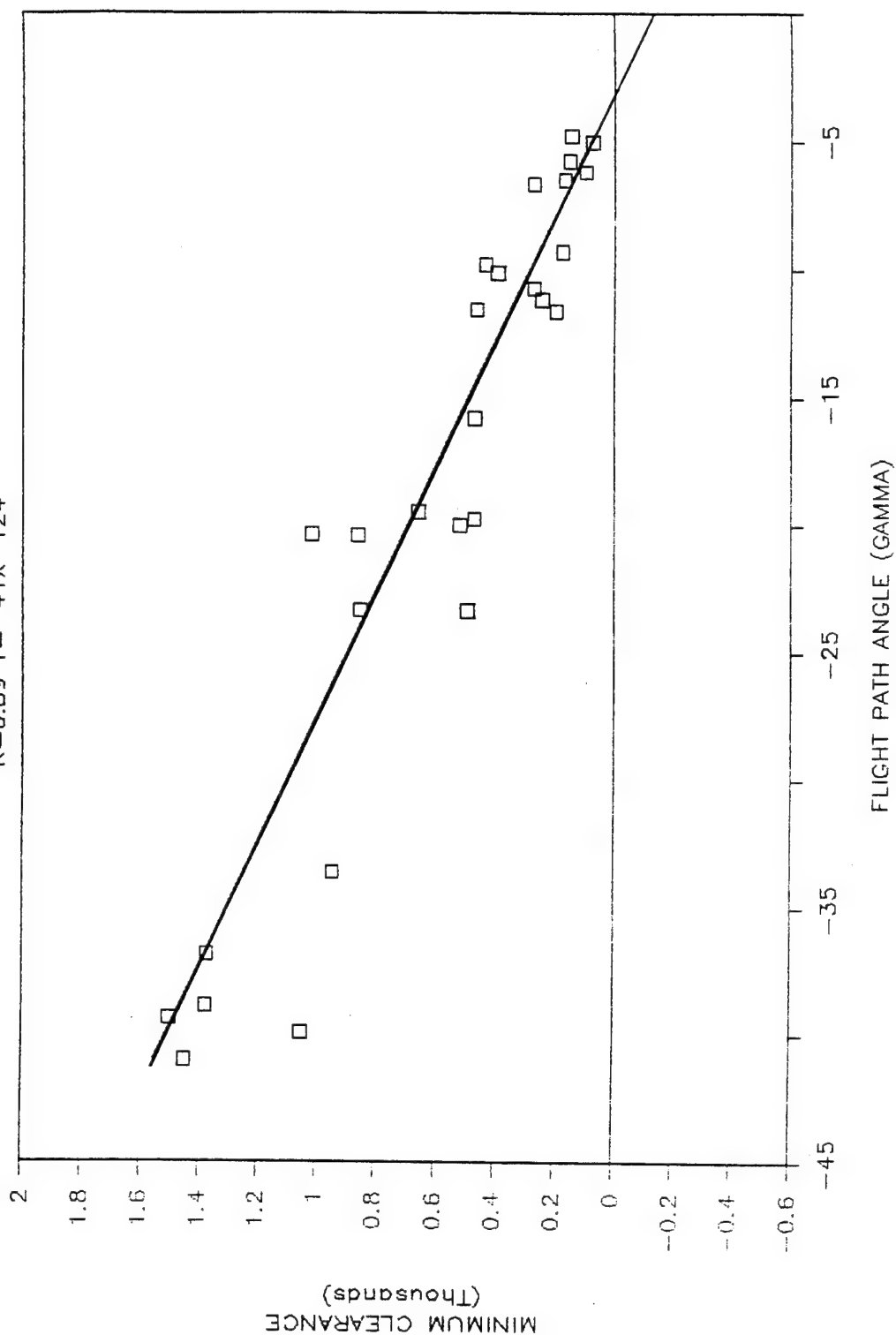


Figure 47 (c). Minimum clearance as a function of flight path angle for all pilots at speed =475 slope =6 roll =60.

SPEED=475 SLOPE=12 ROLL=0

R=0.89  $Y = -40X - 115$

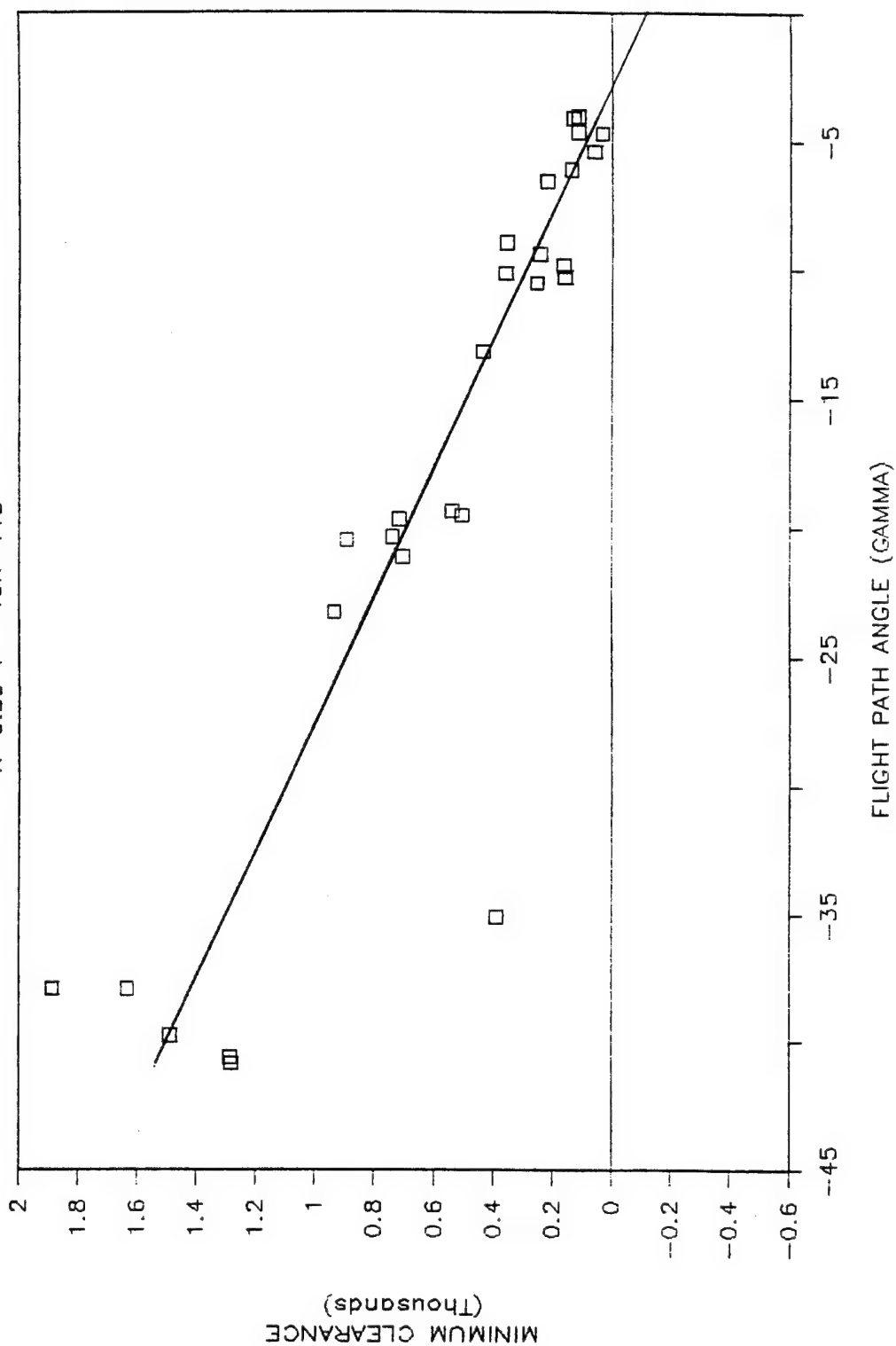


Figure 48 (a). Minimum clearance as a function of flight path angle for all pilots at speed=475 slope=12 roll=0.

SPEED=475 SLOPE=12 ROLL=30

$$R=0.91 \quad Y=-41X-175$$

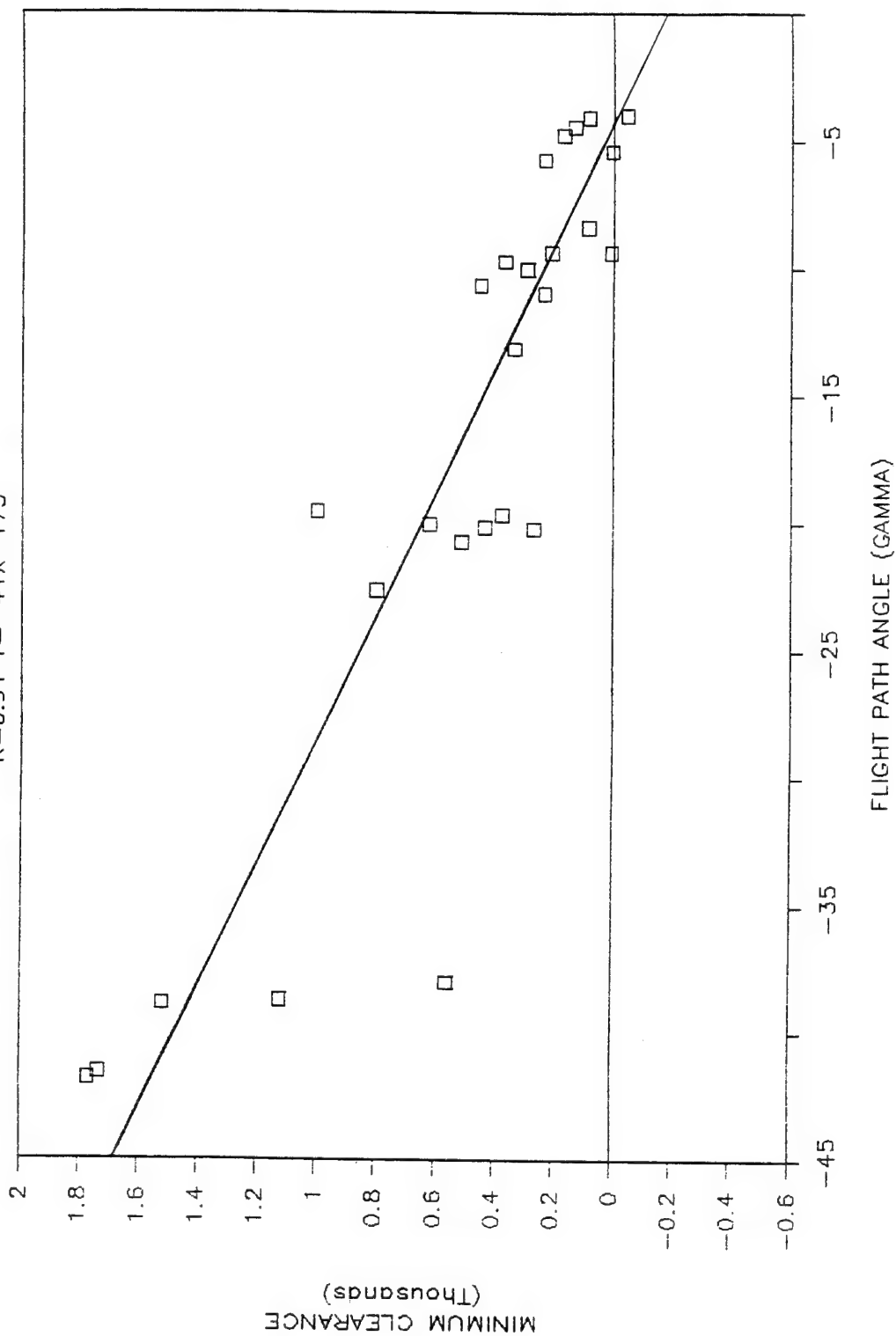


Figure 48 (b). Minimum clearance as a function of flight path angle for all pilots at speed = 475 slope = 12 roll = 30.

SPEED=475 SLOPE=12 ROLL=60

R=0.87  $Y=-.33X-81$

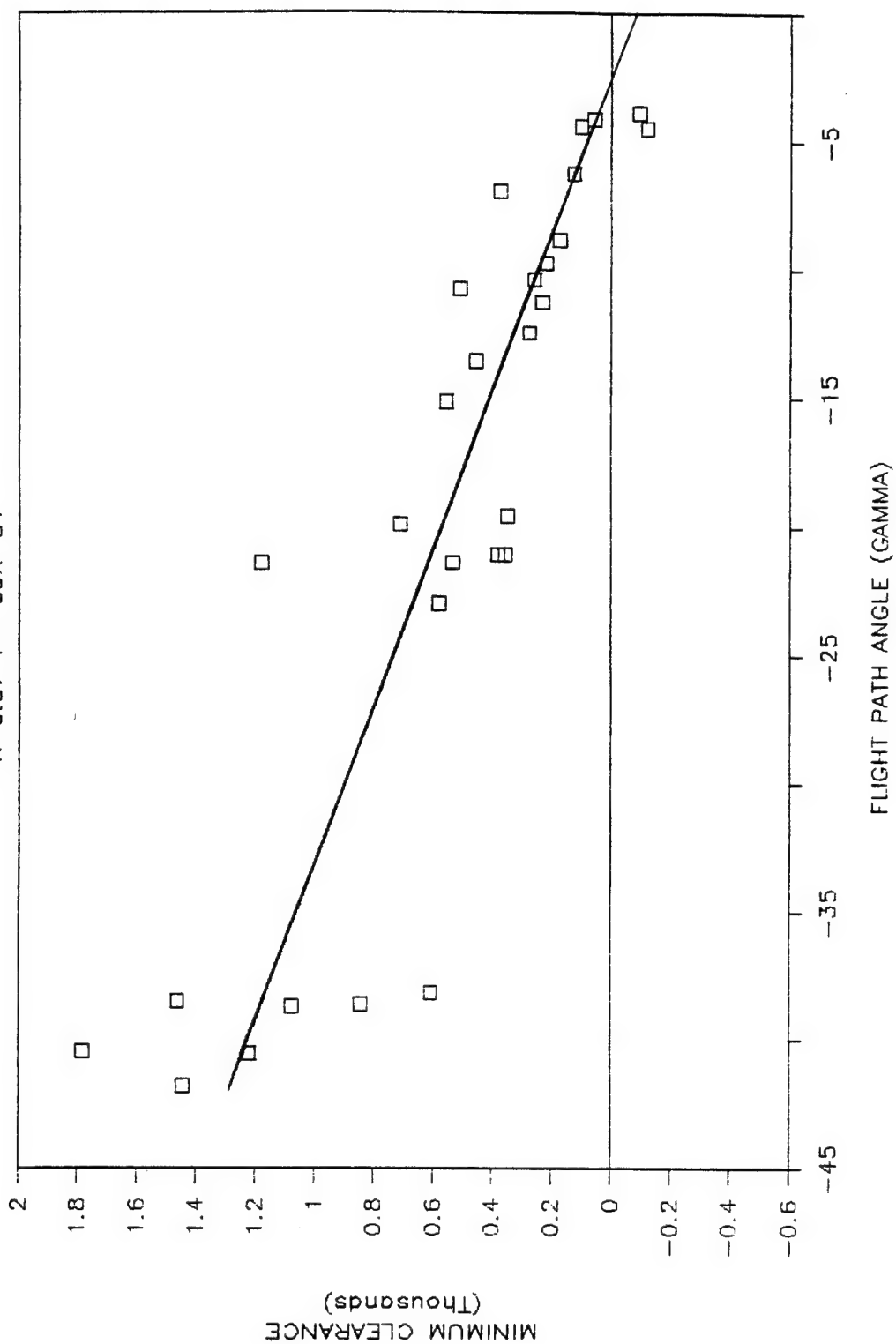


Figure 48 (c). Minimum clearance as a function of flight path angle for all pilots at speed =475 slope =12 roll =60.

SPEED=475 SLOPE=18 ROLL=0

R=0.85  $Y=-27X-207$

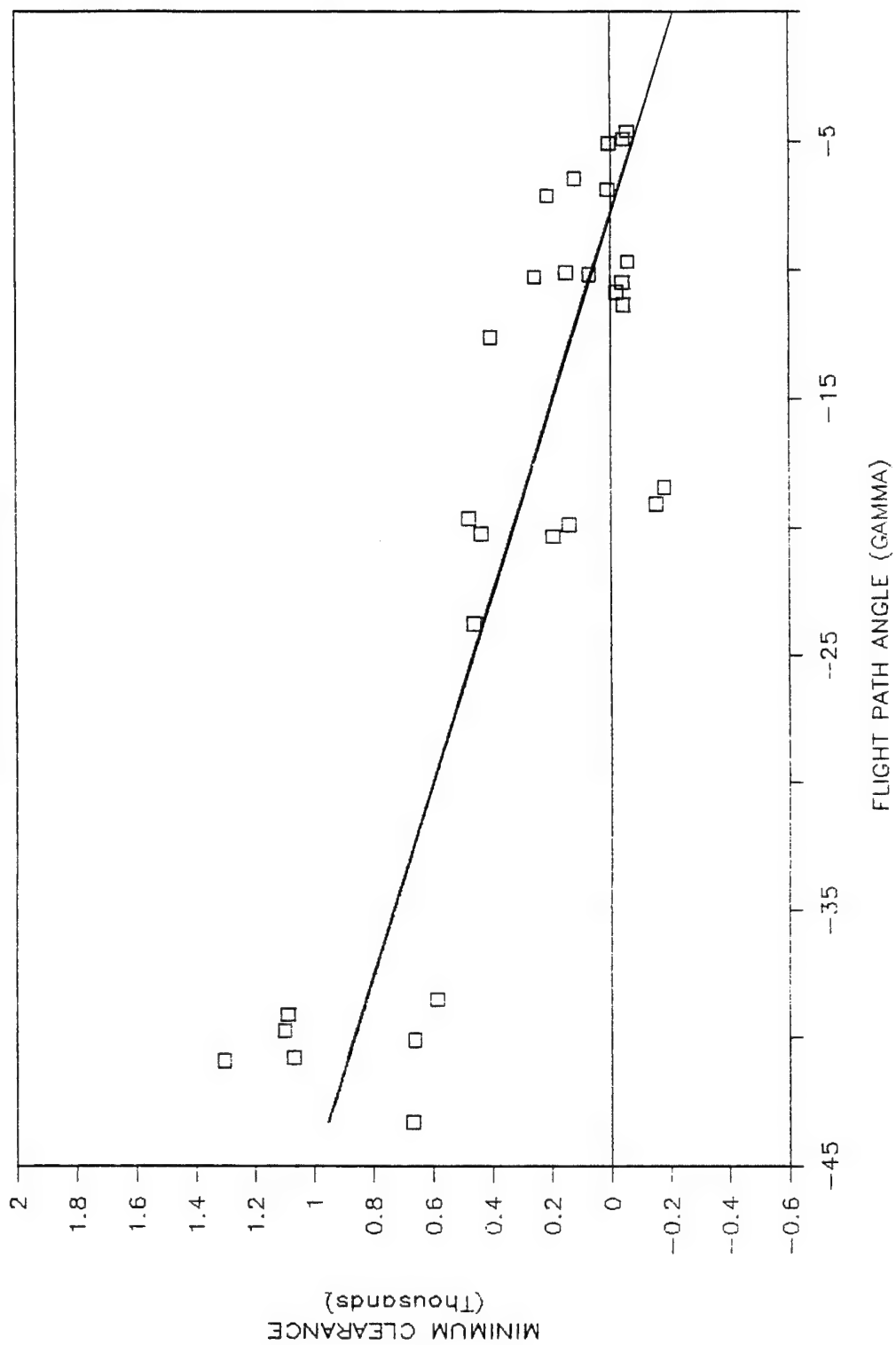
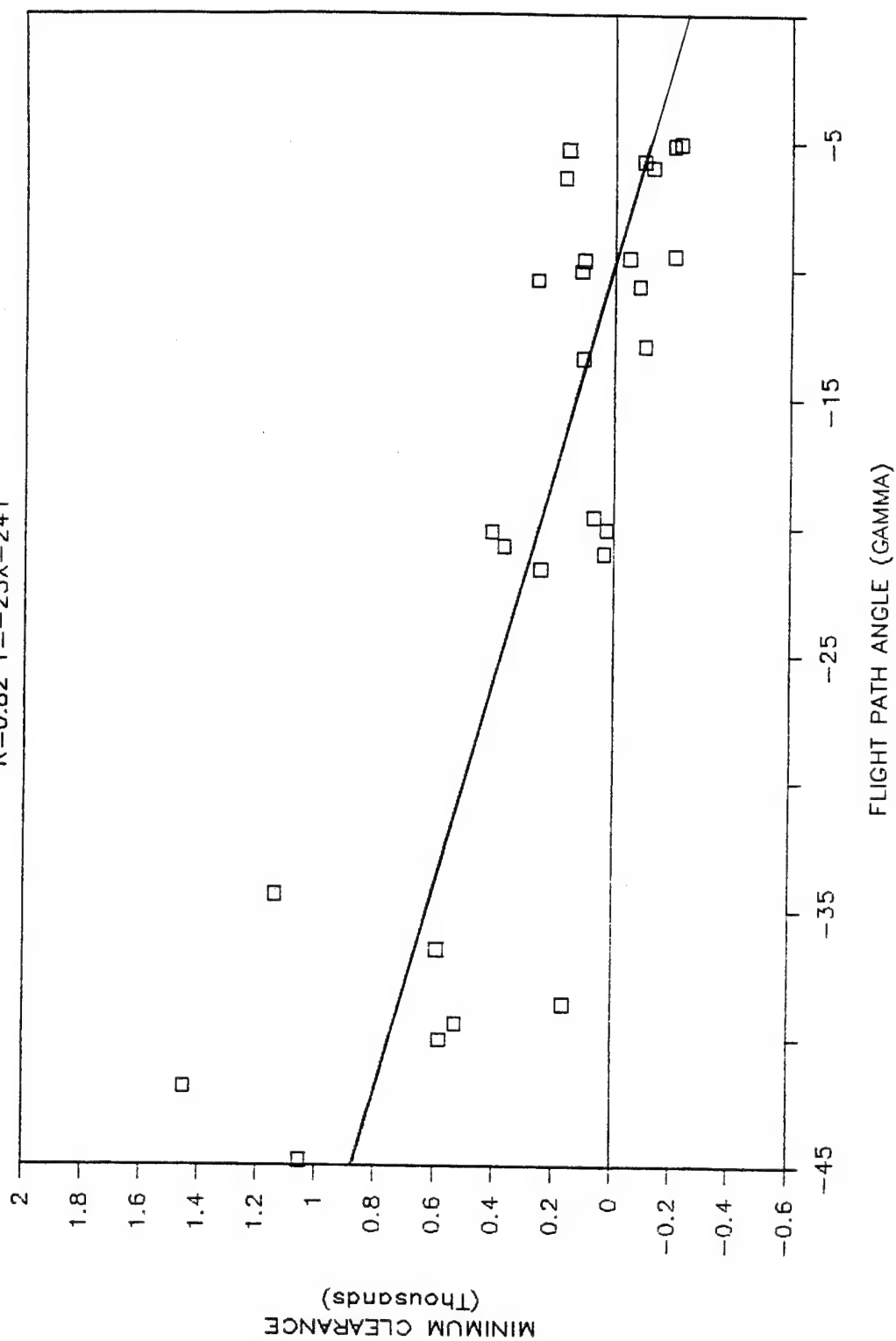


Figure 49 (a). Minimum clearance as a function of flight path angle for all pilots at speed=475 slope=18 roll=0.



SPEED=475 SLOPE=18 ROLL=30

R=0.82  $Y = -25X - 24.1$



SPEED=475 SLOPE=18 ROLL=60

R=0.64  $Y=-17X-139$

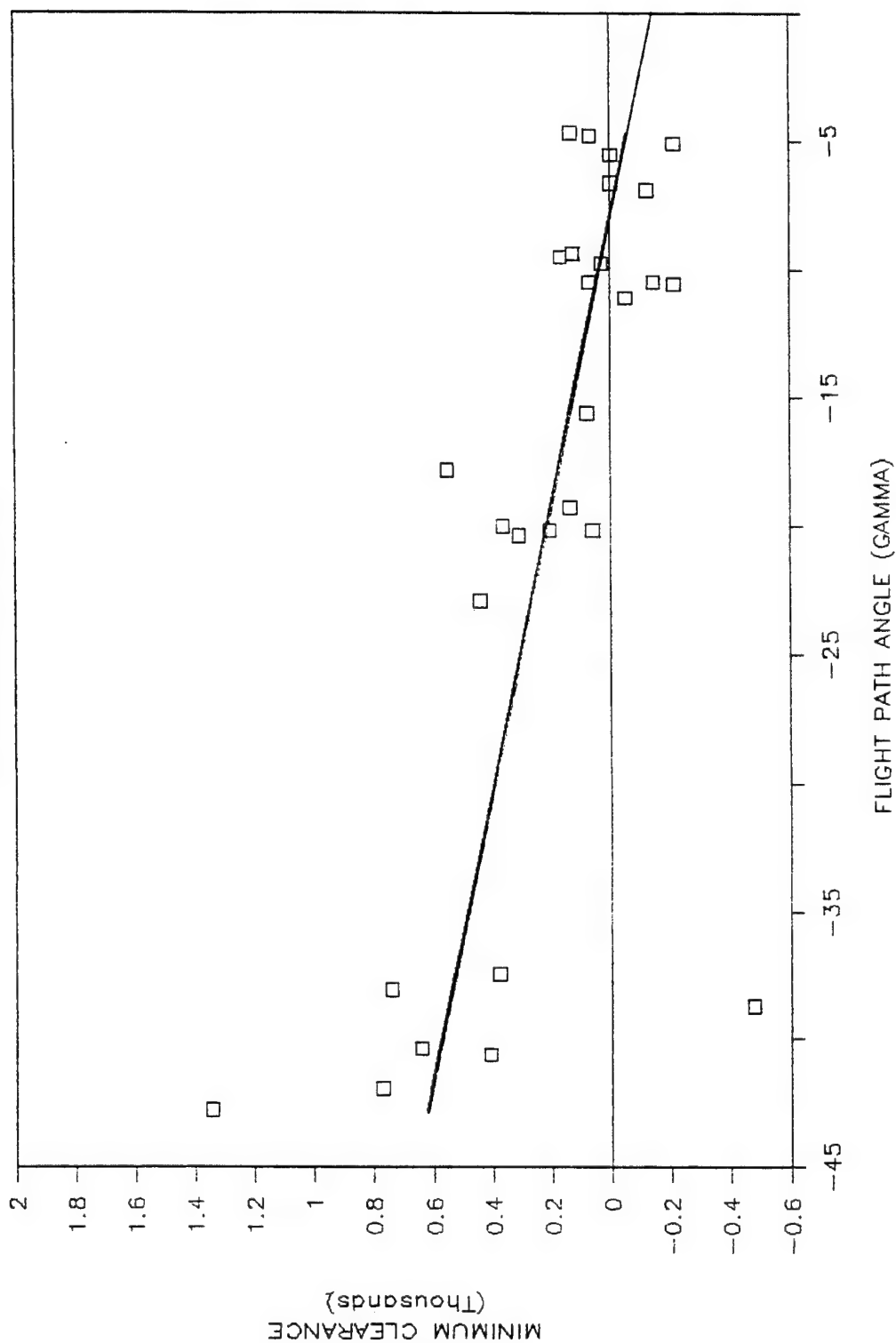


Figure 49 (c). Minimum clearance as a function of flight path angle for all pilots at speed=475 slope=18 roll=60.

### **High Airspeed--600 Knots/55 Degrees Wing Sweep**

The plots from the high airspeed condition are shown in Figures 50 through 53. Each figure contains three plots of minimum clearance altitude as a function of Gamma (0 through -40 degrees). Each set of plots represents one terrain slope condition for all three roll angles (0, 30, and 60 degrees).

An inspection of the figures suggested a consistent linear relationship between minimum clearance altitude as a function of Gamma. High correlation coefficients were calculated for most conditions. Terrain slope behaved in the same fashion as it did for the medium airspeed condition. First, the intercepts of the regression lines decreased in relationship to an increase in terrain slope, which led some of the small Gamma trials to hit the ground during terrain slope angles greater than zero. Furthermore, the slopes of the regression lines increased from zero to six to 12 degrees of terrain slope, and then decreased again at 18 degrees, thus reflecting the algorithm's inconsistency in predicting at higher Gammas during non-zero terrain slopes (such as 18 degrees).

The roll compensation section of the algorithm (HPHI) allowed more altitude to be lost as roll angle increased. The intercept of each of the lines increased as roll angle increased. This trend was replicated with the different terrain slopes. On the average, minimum clearance altitude was 52 feet higher at 30 degrees of roll than at zero degrees of roll, and 95 feet higher at 60 degrees of roll than at 30 degrees of roll.

SPEED=600 SLOPE=0 ROLL=0

R=0.82  $Y=-30X-117$

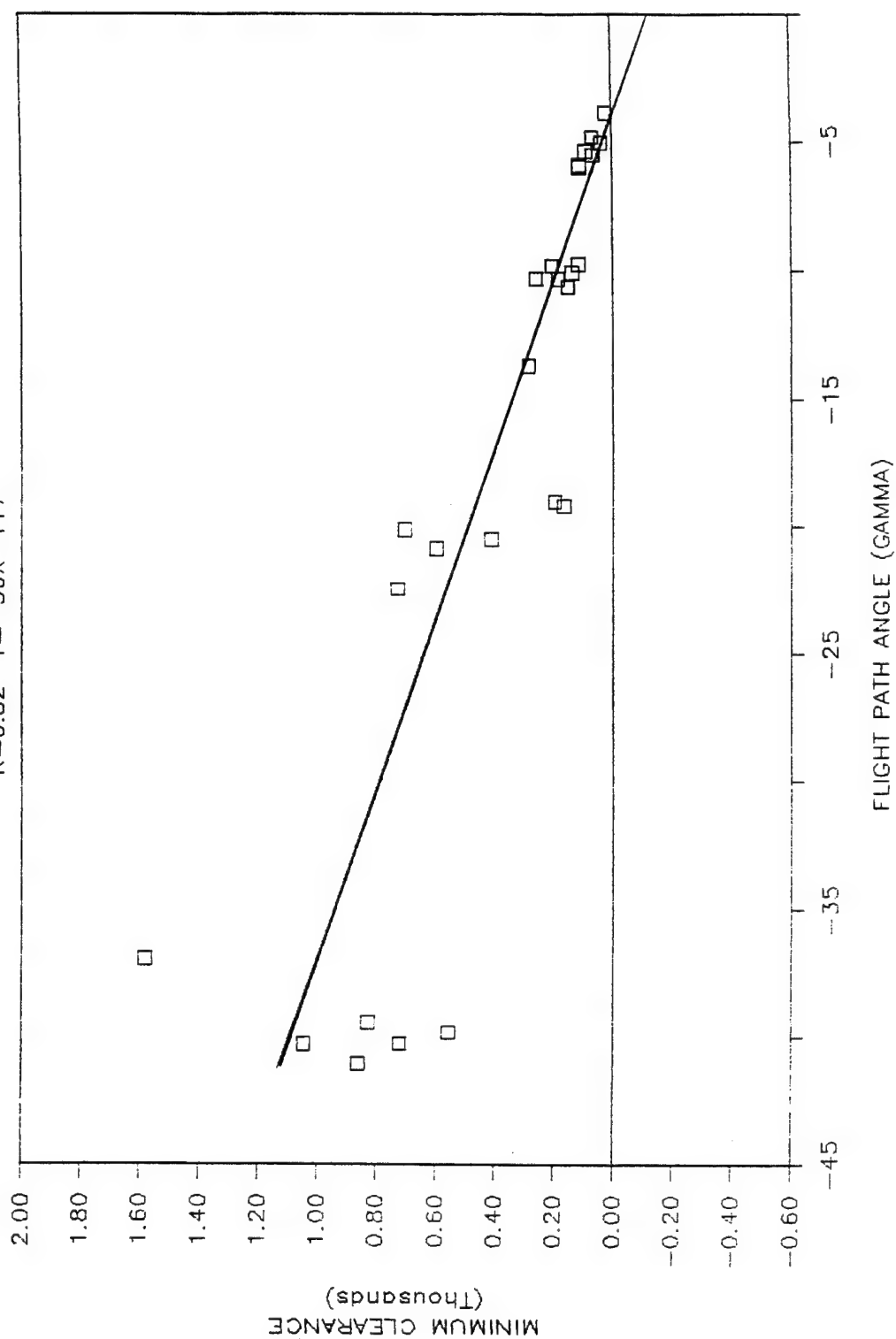


Figure 50 (a). Minimum clearance as a function of flight path angle for all pilots at speed = 600 slope = 0 roll = 0.

SPEED=600 SLOPE=0 ROLL=30

R=0.75  $Y = -25X - 55$

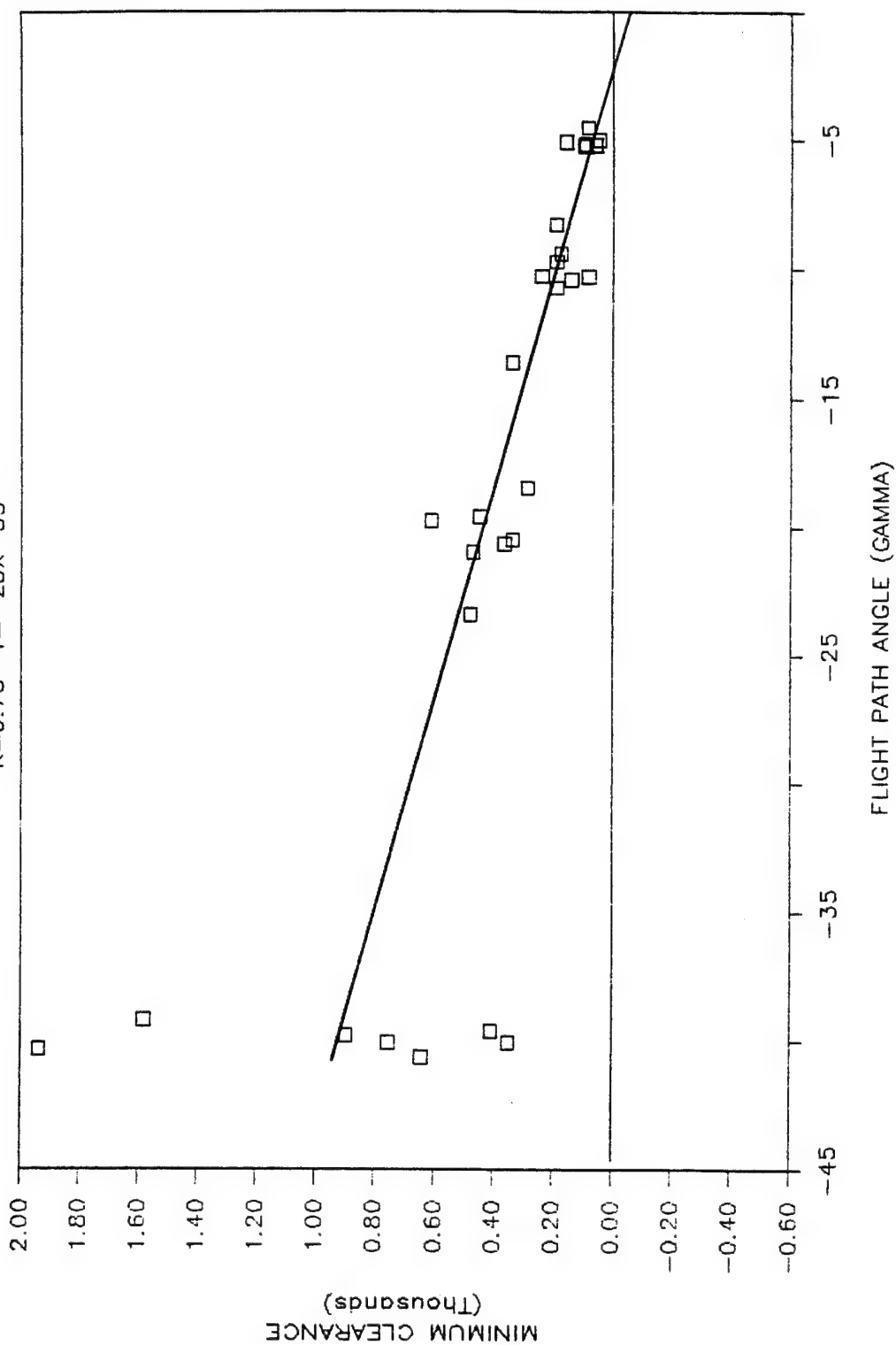


Figure 50 (b). Minimum clearance as a function of flight path angle for all pilots at speed=600 slope=0 roll=30.

SPEED=600 SLOPE=0 ROLL=60

R=0.71  $Y = -26X - 25$

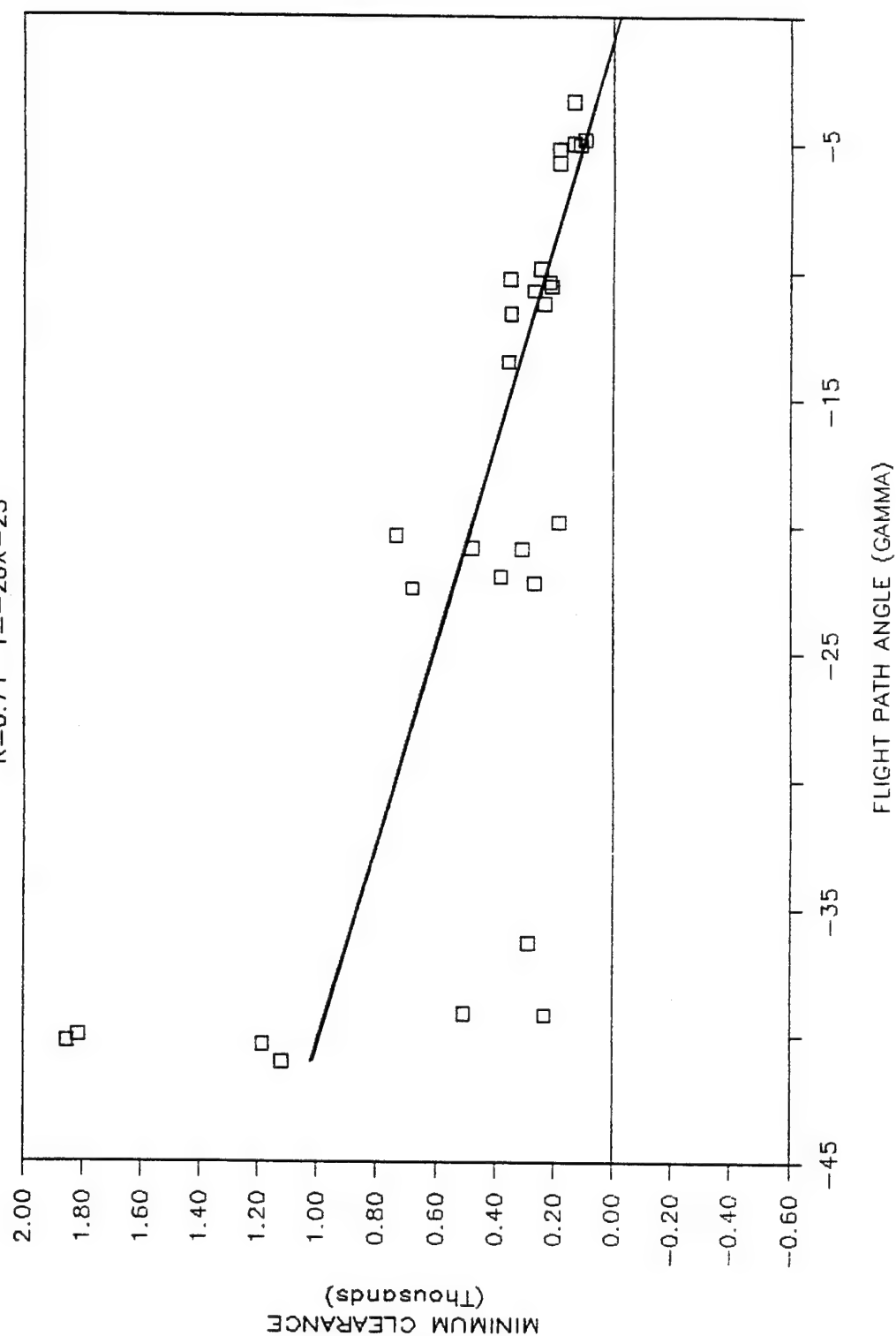


Figure 50 (c). Minimum clearance as a function of flight path angle for all pilots at speed = 600 slope = 0 roll = 60.

SPEED=600 SLOPE=6 ROLL=0

$R=0.84$   $Y=-51X-204$

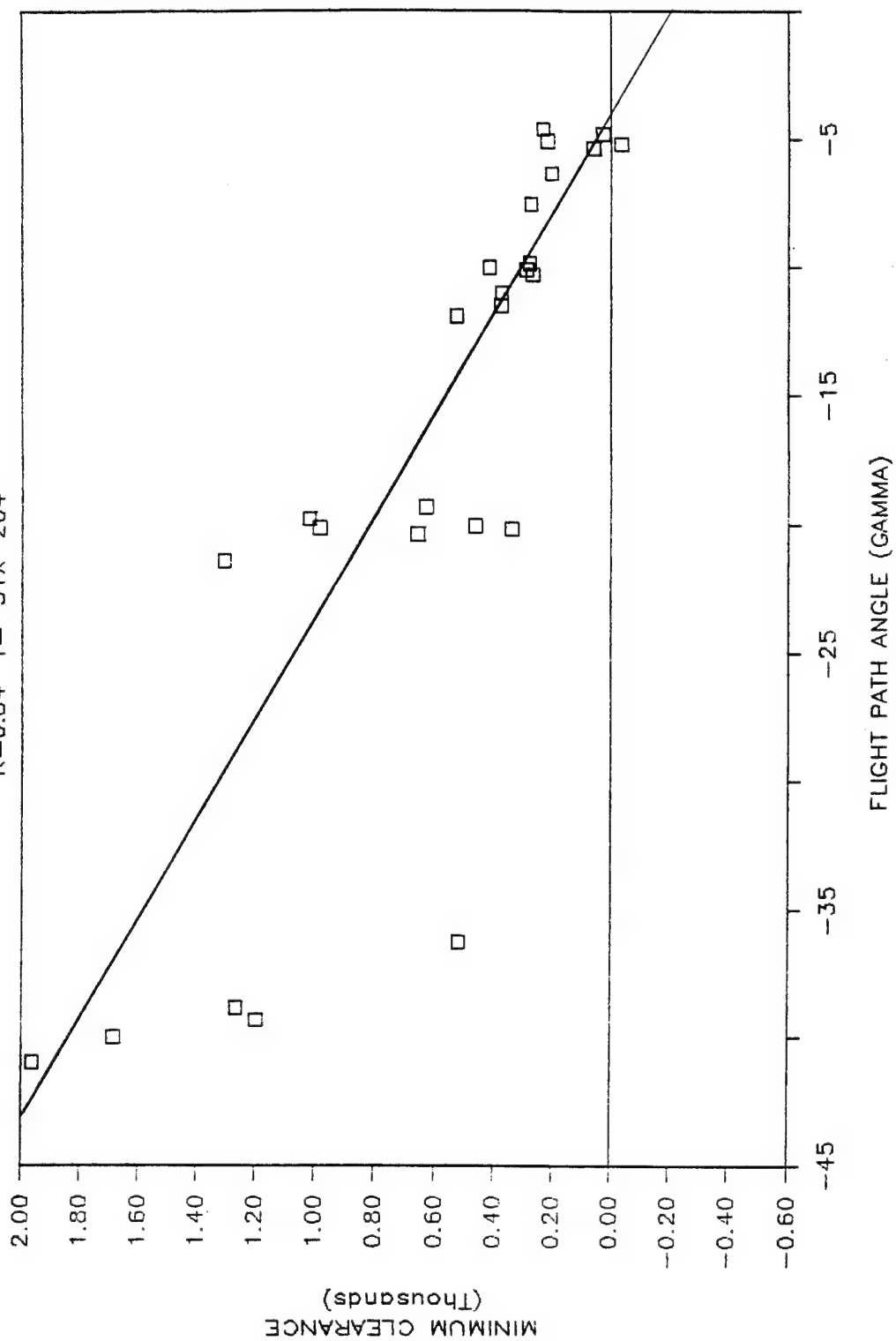


Figure 51 (a). Minimum clearance as a function of flight path angle for all pilots at speed=600 slope=6 roll=0.

SPEED=600 SLOPE=6 ROLL=30

R=0.70  $Y = -39X - 83$

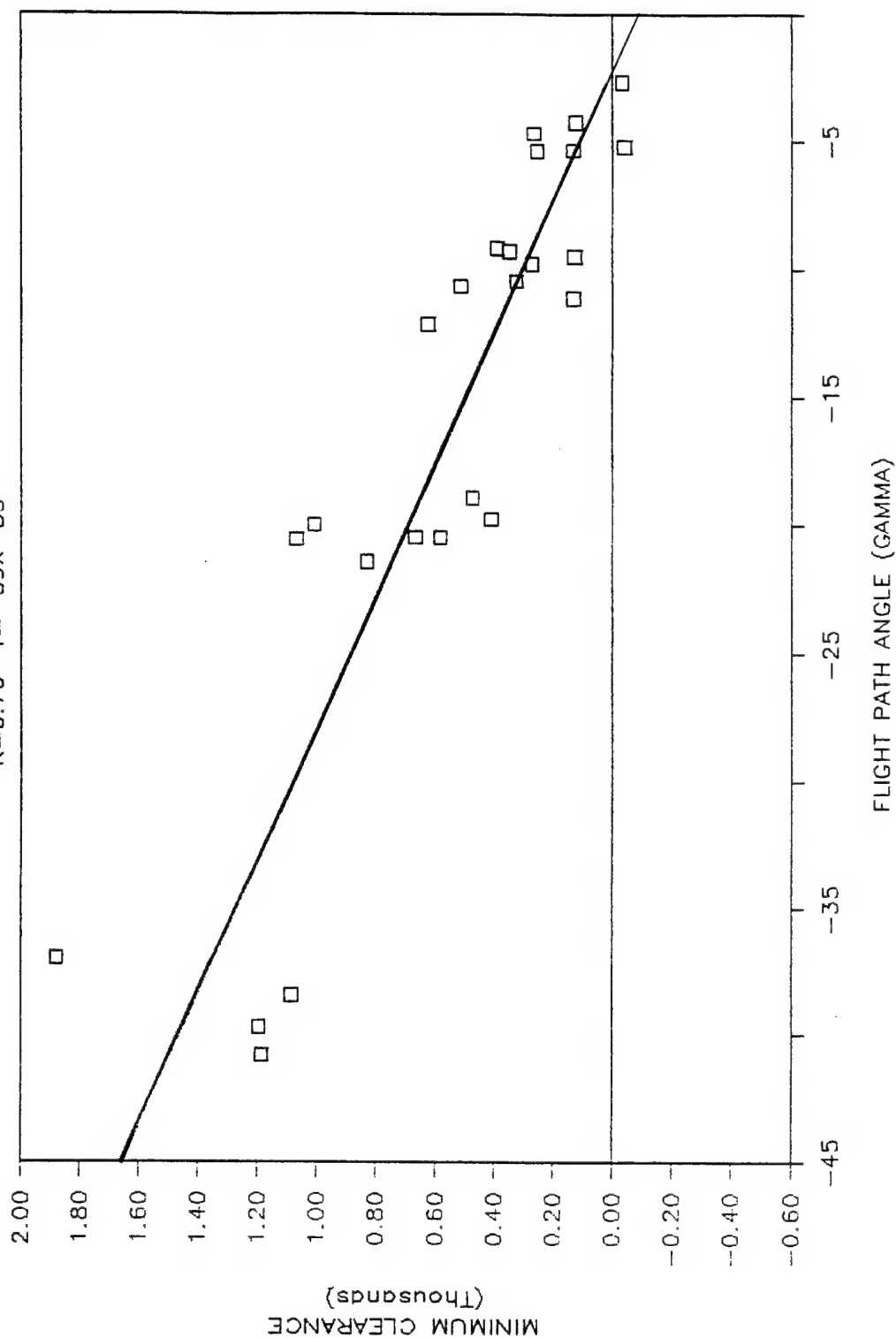


Figure 51 (b). Minimum clearance as a function of flight path angle for all pilots at speed = 600 slope = 6 roll = 30.



SPEED=600 SLOPE=6 ROLL=60

R=0.75  $Y=-.36X+6$

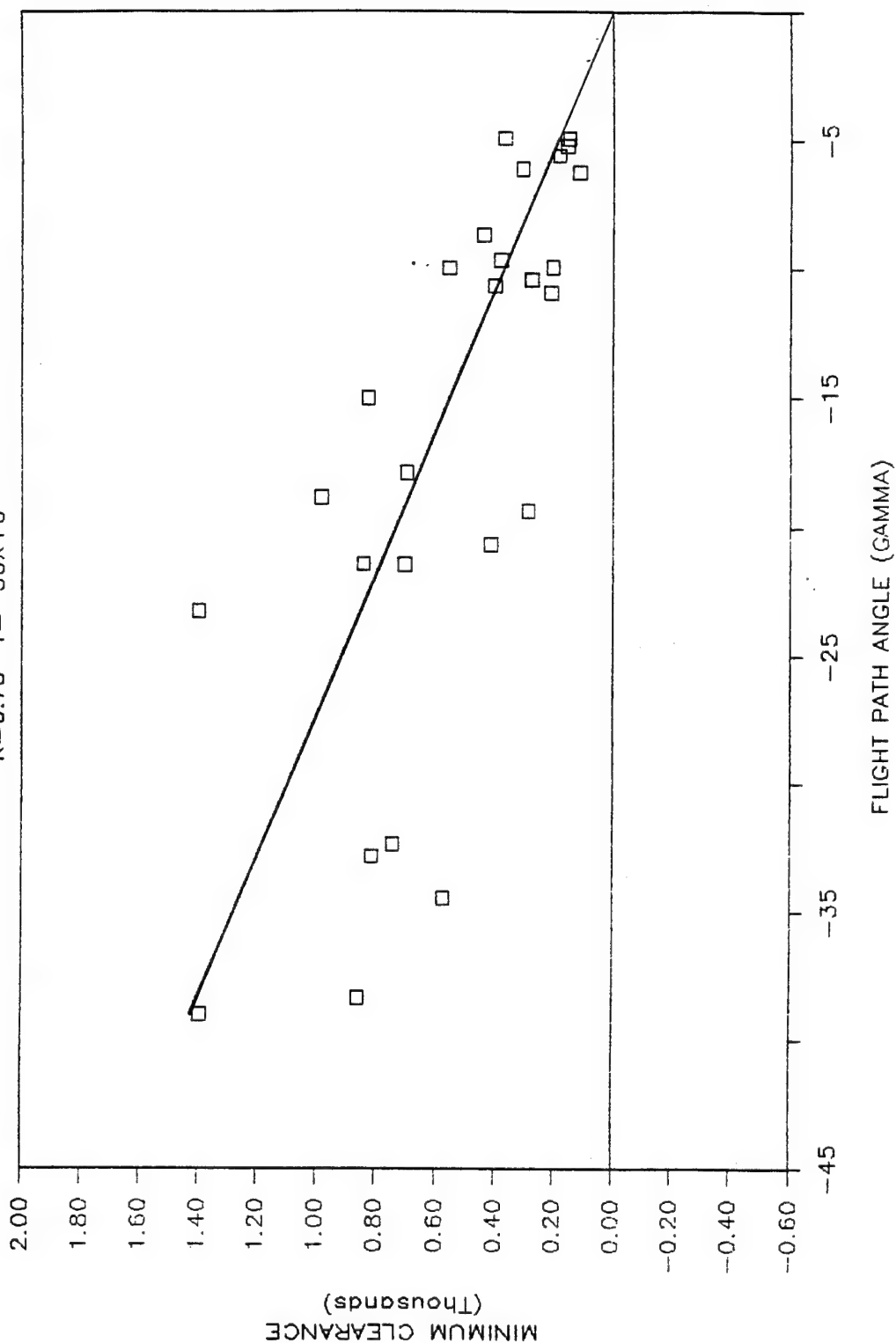


Figure 51 (c). Minimum clearance as a function of flight path angle for all pilots at speed=600 slope=6 roll=60.

SPEED=600 SLOPE=12 ROLL=0

R=0.82  $Y=-50X-183$

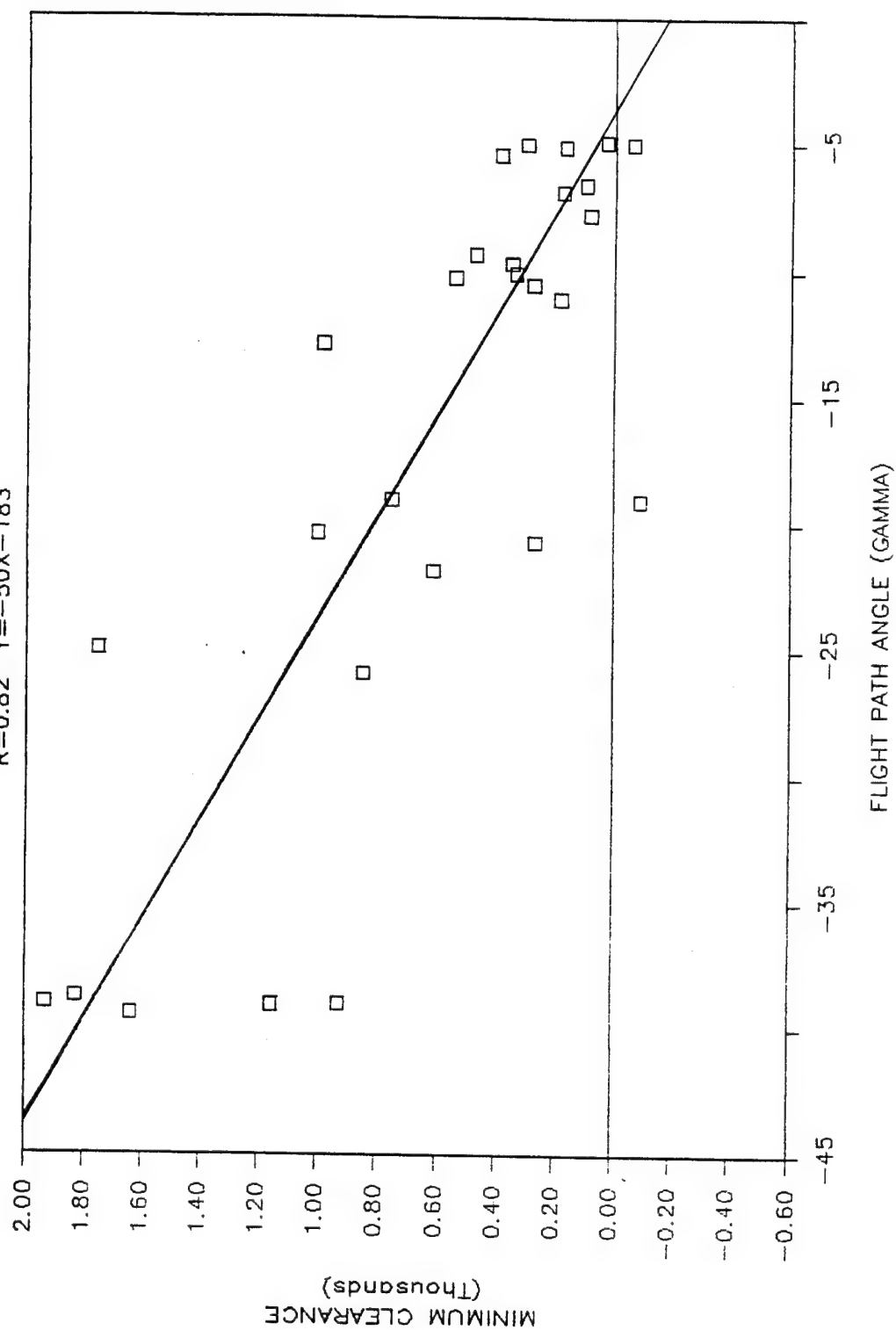


Figure 52 (a). Minimum clearance as a function of flight path angle for all pilots at speed = 600 slope = 12 roll = 0.

SPEED=600 SLOPE=12 ROLL=30

R=0.74  $Y=-43X-156$

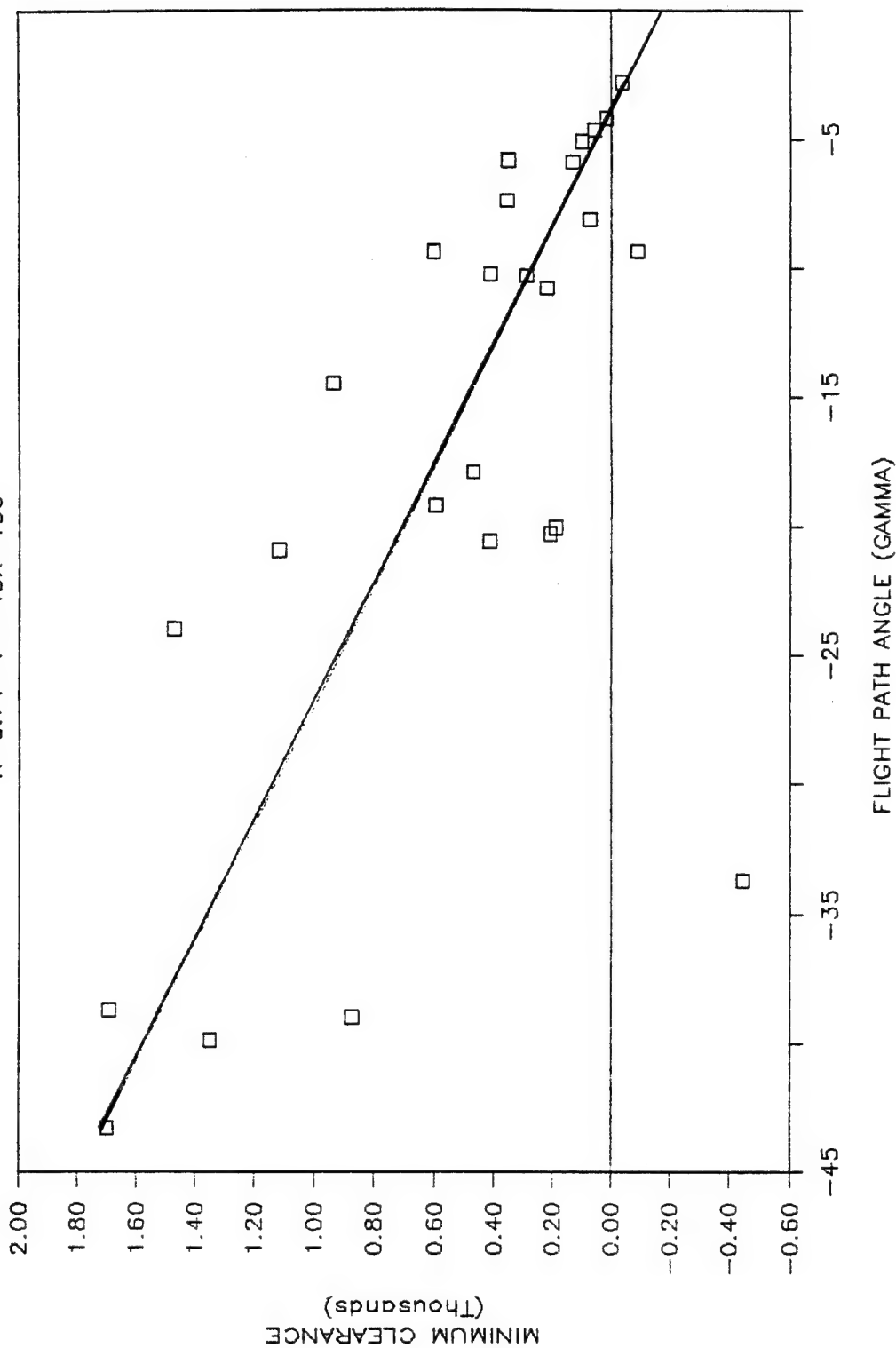


Figure 52 (b). Minimum clearance as a function of flight path angle for all pilots at speed = 600 slope = 12 roll = 30.

SPEED=600 SLOPE=12 ROLL=60

R=0.64  $Y = -34X + 25$

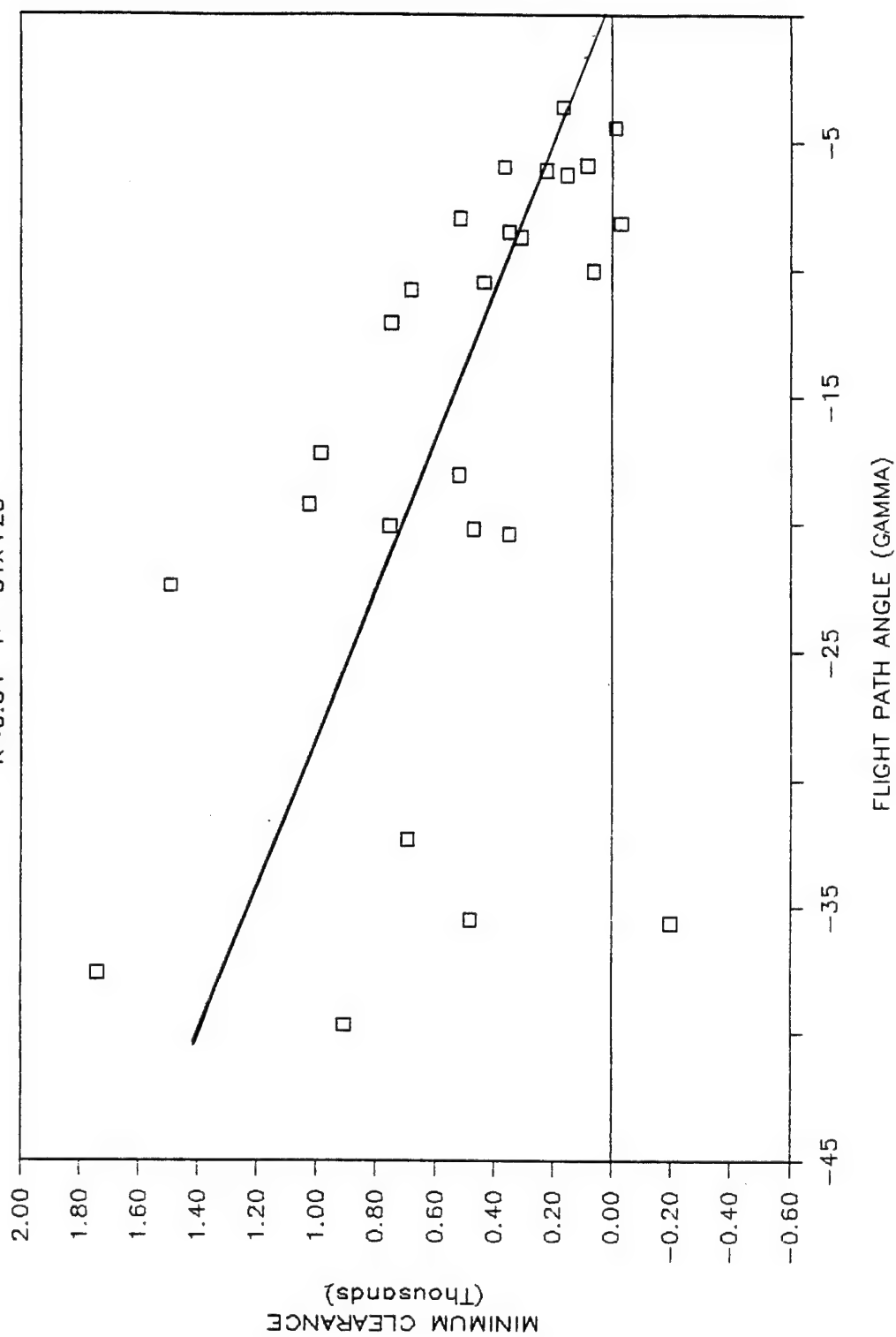


Figure 52 (c). Minimum clearance as a function of flight path angle for all pilots at speed = 600 slope = 12 roll = 60.

SPEED=600 SLOPE=18 ROLL=0

R=0.55  $Y=-25X-219$

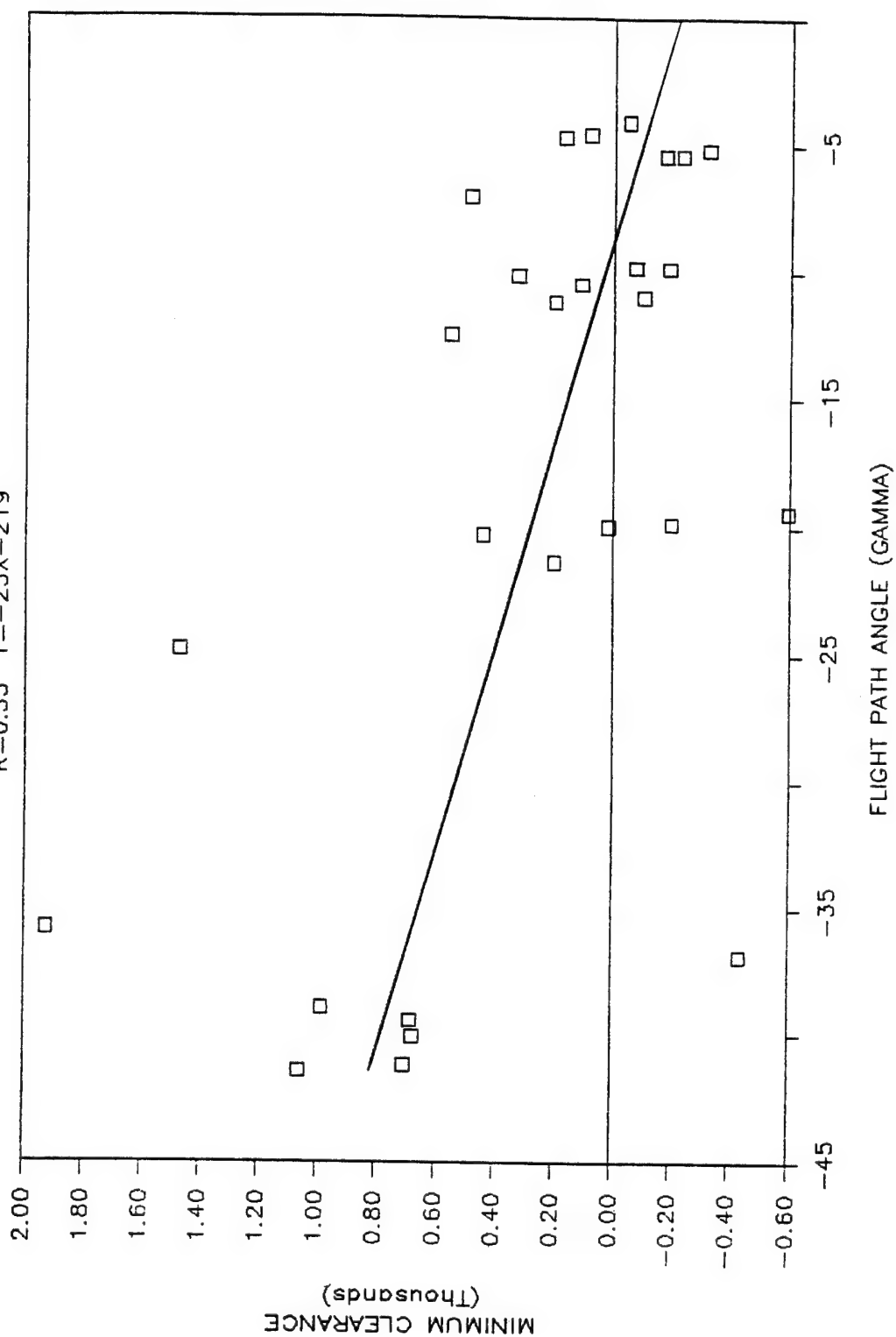
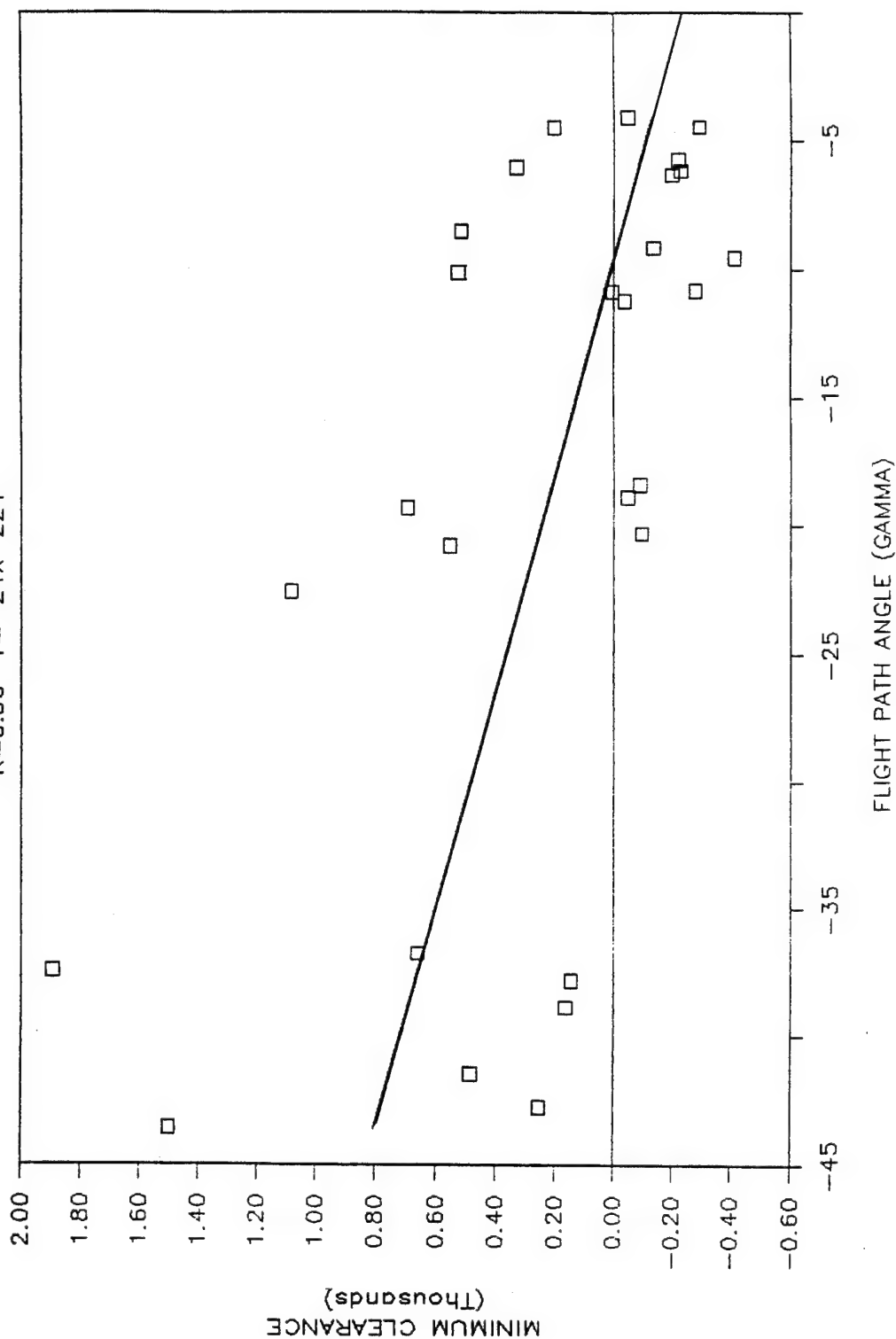


Figure 53 (a). Minimum clearance as a function of flight path angle for all pilots at speed = 600 slope = 18 roll = 0.

SPEED=600 SLOPE=18 ROLL=30

R=0.56 Y=-24X-224



SPEED=600 SLOPE=18 ROLL=60

R=0.36  $Y=-18X-141$

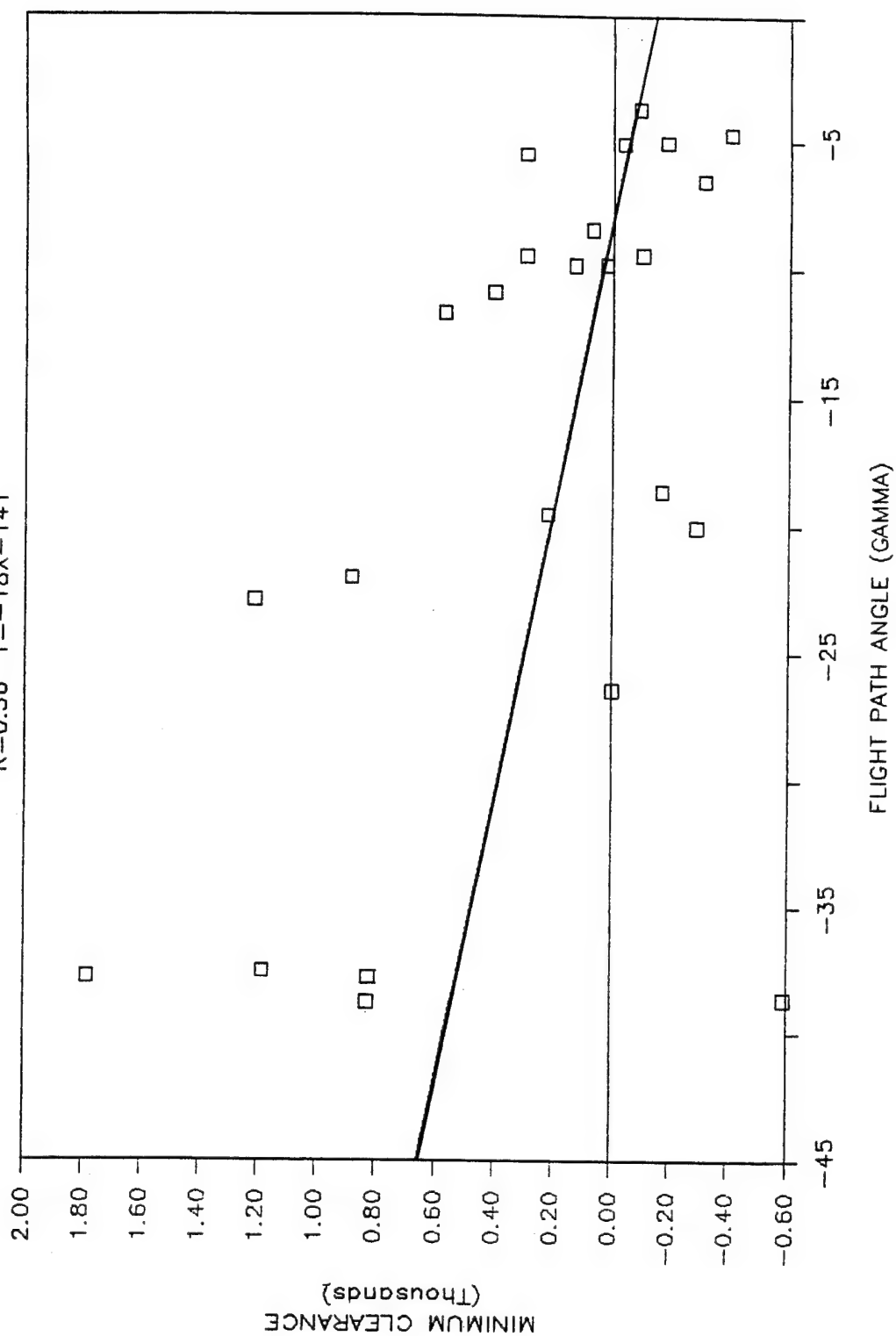


Figure 53 (c). Minimum clearance as a function of flight path angle for all pilots at speed = 600 slope = 18 roll = 60.

## Performance Data Discussion

Generally, the man-in-the-loop evaluation confirmed some of the findings from the two previous phases of the evaluation. A linear relationship existed between minimum clearance and flight path angle (gamma) for all airspeed/wing sweep conditions. As the results of the previous phases suggested, an increase in terrain slope caused crashes, particularly at low Gamma. The algorithm failed to compensate properly for increases in terrain slope. Mishaps were most prevalent at medium and high airspeed/wing sweep conditions. As expected, at high airspeed/wing sweep conditions minimum clearance was higher as a function of roll angles.

## Pilot Reaction Time Results

Upon completion of the man-in-the-loop simulation, univariate and bivariate statistics were used to note trends in the data. The frequency distribution, shown in Figure 54, depicts pilot reaction times based on 937 trials. Pilot reaction time was defined as the interval beginning with the onset of the voice warning message, until the pilot pulled the stick to a G-onset rate of one G per second. The distribution is positively skewed (+ 1.66) so the mean is not a good measure of central tendency (with a skewed distribution, the mean is drawn toward the extreme scores), hence the mode is more representative of pilot reaction time. The mode in this case was .80 seconds. Ninety percent of all reaction time data had a value smaller than 1.2 seconds, while 95 percent had a value smaller than 1.4 seconds.

For the bivariate analysis, predicted reaction times (RTIME) were plotted as a function of actual reaction times (Figures 54-1 and 54-2). Figure 54-1 indicates the actual reaction times over the entire range of predicted reaction times. Shown in Figure 54-2 are the actual reaction times and their corresponding predicted reaction times for recoveries of less than 500 feet. Correlation coefficients were calculated in an attempt to evaluate the relationship between predicted and actual reaction time (a correlation coefficient of 1.0 or -1.0 identifies a strong relationship between the variables, while a correlation of 0.0 implies no relationship at all). The results of the entire range demonstrated a correlation coefficient of -0.1. For recoveries of less than 500 feet the correlation coefficient was 0.1. The low correlation coefficients were very clear in identifying no relationship between predicted and actual pilot reaction time.

A follow-up analysis examined the relationship of predicted and actual reaction times with the following variables: (1) minimum clearance, (2) flight path angle, (3) vertical velocity, (4) airspeed, (5) altitude at time of warning and (6) altitude loss. Correlation coefficients for predicted and actual reaction time as a function of the six variables mentioned above are shown in Tables 12 and 13.



TABLE 12. Correlation coefficients for predicted and actual reaction times over the entire range of data.

	Predicted Reaction Time	Actual Reaction Time
Minimum Clearance	.44	-.24
Flight Path Angle	-.92	.10
Vertical Velocity	.80	-.14
Altitude at Warning	.73	-.07
Altitude Loass	.64	0.0

Clearly, predicted reaction time appears to be highly correlated with flight path angle. This was not a real surprise since flight path angle is one of the three variables which affect the variability of reaction time. However, when actual reaction time was correlated with the same variable, a coefficient of .10 was calculated. Altitude, which also influences the variability of reaction time, had a .73 correlation with predicted reaction time. No relationship existed between altitude and actual reaction time ( $r = -.07$ ). Vertical velocity showed a strong relationship ( $r = .80$ ) to predicted reaction time. Actual reaction time effectively showed no correlation ( $r = -.14$ ) with vertical velocity. For the same six variables listed above, correlations were calculated for predicted versus actual reaction time at altitudes lower than 500 feet. It is valuable to know the influence that the six variables have on reaction time at altitudes below 500 feet because the F-111 mission is a low-level mission.

TABLE 13. Correlation coefficients for predicted and actual reaction times for recoveries less than 500 feet.

	Predicted Reaction Time	Actual Reaction Time
Minimum Clearance	.26	-.20
Flight Path Angle	-.55	.04
Vertical Velocity	.50	-.10
Airspeed	.06	-.21
Altitude at Time of Warning	.90	.13
Altitude Loss	.52	.26

The strongest relationship shown between reaction time and any of the six variables at recovery altitude lower than 500 feet is between predicted reaction time and altitude at time of warning. Again, this was not a big surprise because altitude influences the variability of the predicted reaction time. Similar to the results over the entire range, the relationship between actual reaction time and altitude at time of warning could only demonstrate a very weak correlation ( $r = .13$ ). See Figure 54-2 which shows reaction time as a function of warning altitude.

# PILOT REACTION TIME DATA

MEAN = 0.881 SD = 0.261

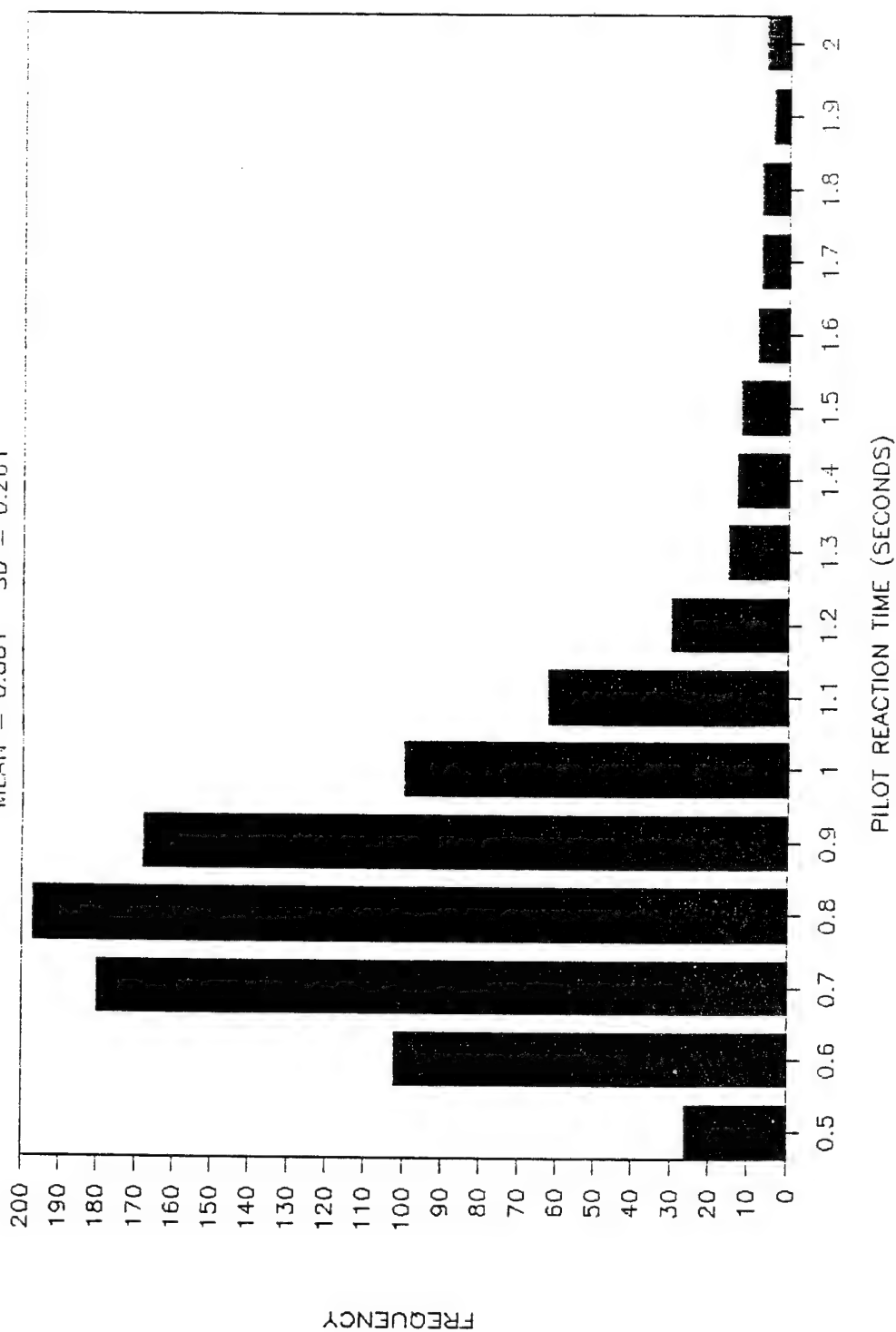


Figure 54. Frequency distribution representing pilots' reaction times to the GCAS warnings.

# REACTION TIME

GAMMA AS A FUNCTION OF HRTIME, RTIME

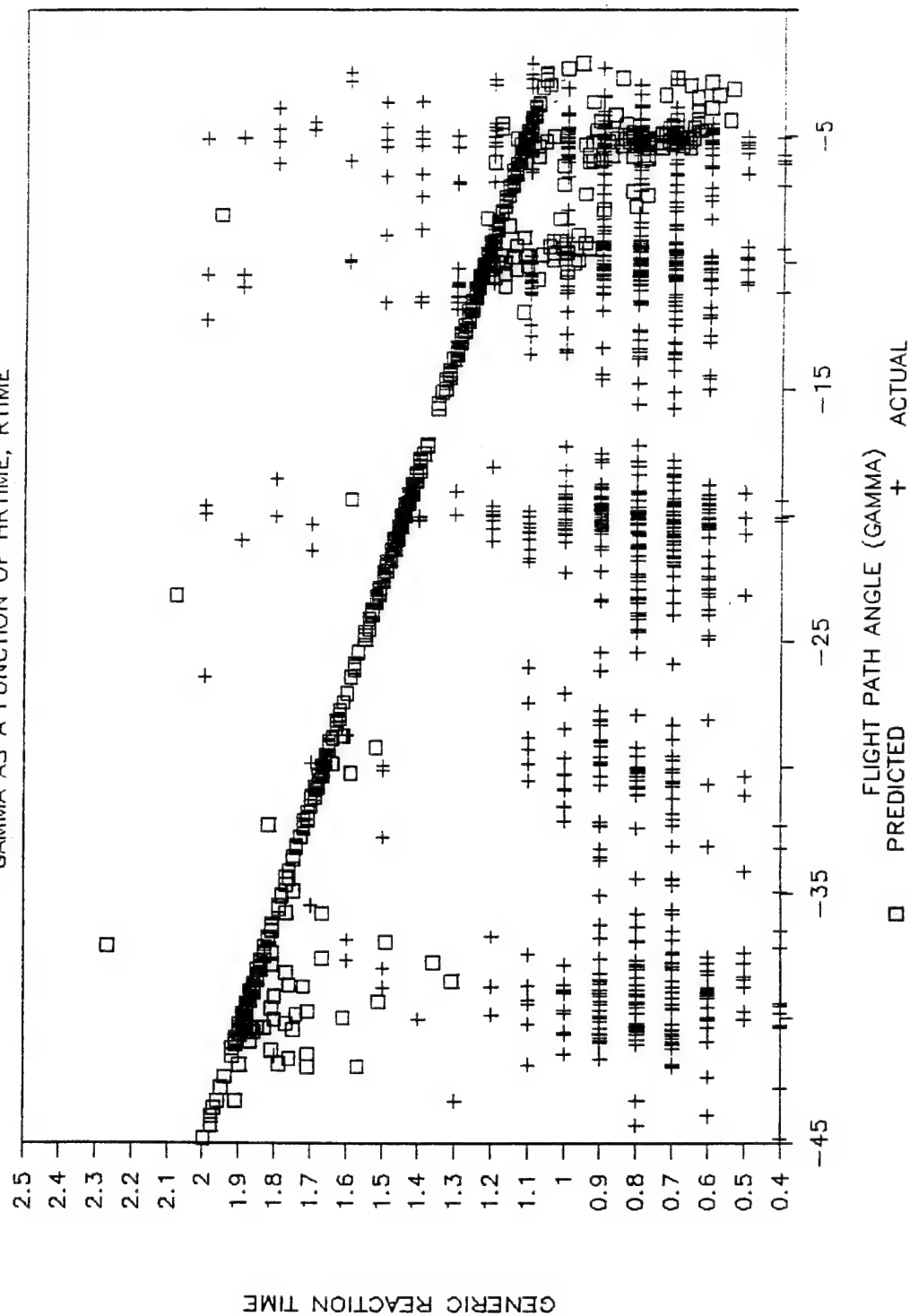


Figure 54-1. Predicted versus actual

# REACTION TIME AS A FUNCTION OF WARN ALT

FOR HRTIME AND RTIME AT < 500 FEET

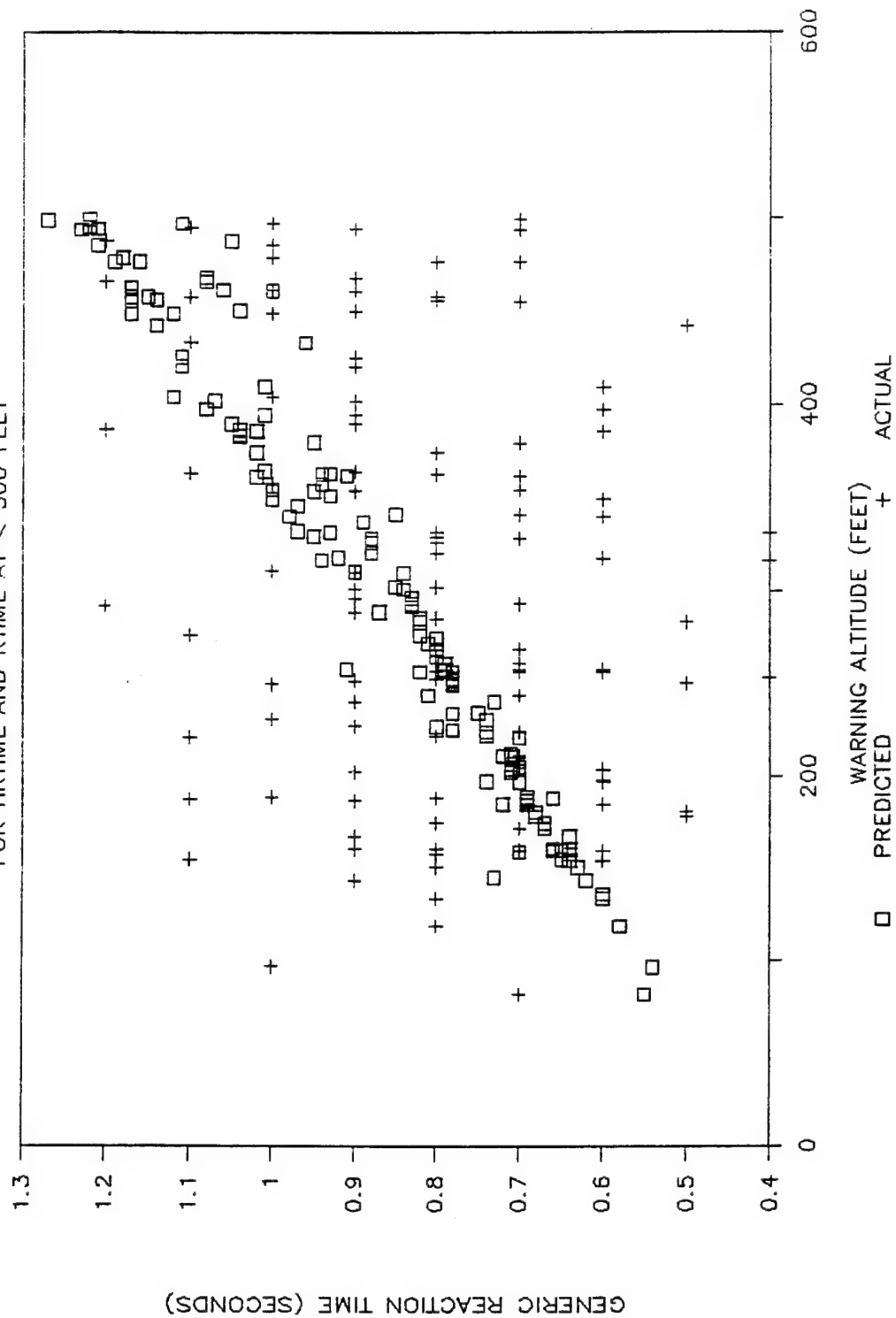


Figure 54-2. Reaction time as a function of warning altitude

### **Pilot Reaction Time Discussion**

It could be concluded from the univariate analysis that, if constant reaction time (which would include 90 to 95 percent of the population) is desirable, then a value between 1.2 and 1.4 seconds is most appropriate. The pilot's mode reaction time of .80 seconds was found to be about 200 milliseconds slower than previous data collected in an F-16 GCAS evaluation (Orr, 1986). However, while the current F/FB/EF-111 mechanization involved only a voice warning, the F-16 data were collected using multiple visual warning for pull (an "X" symbol was presented both on the HUD and two MFDs), which may have decreased pilot reaction time. Furthermore, the F-111 pilots were more careful than the F-16 pilots in pulling the stick, in that they placed more emphasis on AOA.

The predicted reaction time data used in the GCAS algorithm did not reflect the type of actual reaction time data found in the CSDF evaluation. Instead these reaction times appear to take the form of a fudge factor for flight path angle and altitude. This explains the strong relationship between predicted reaction time and flight path angle and altitude. Concerning low-level reaction times, the strongest correlation was found between altitude at time of warning and predicted reaction time.

### **Pilot Ratings Results**

Pilots' rating data were divided into five separate data sets and analyzed independently using the linear regression analysis technique. Minimum clearance altitude was considered the main dependent variable, while vertical velocity (which included two critical factors: airspeed and flight path angle) was considered the main independent variable. The five ratings corresponded to the five statements found in Table 14. The regression analyses described the relationship between minimum clearance altitude as a function of vertical velocity for each of the ratings, by calculating the correlation coefficient and the function of each line.

TABLE 14. Rating criteria for each minimum recovery (or clearance) altitude.

#### MINIMUM CLEARANCE ALTITUDE

1. TOO HIGH
2. SLIGHTLY HIGH
3. ABOUT RIGHT
4. SLIGHTLY LOW
5. TOO LOW

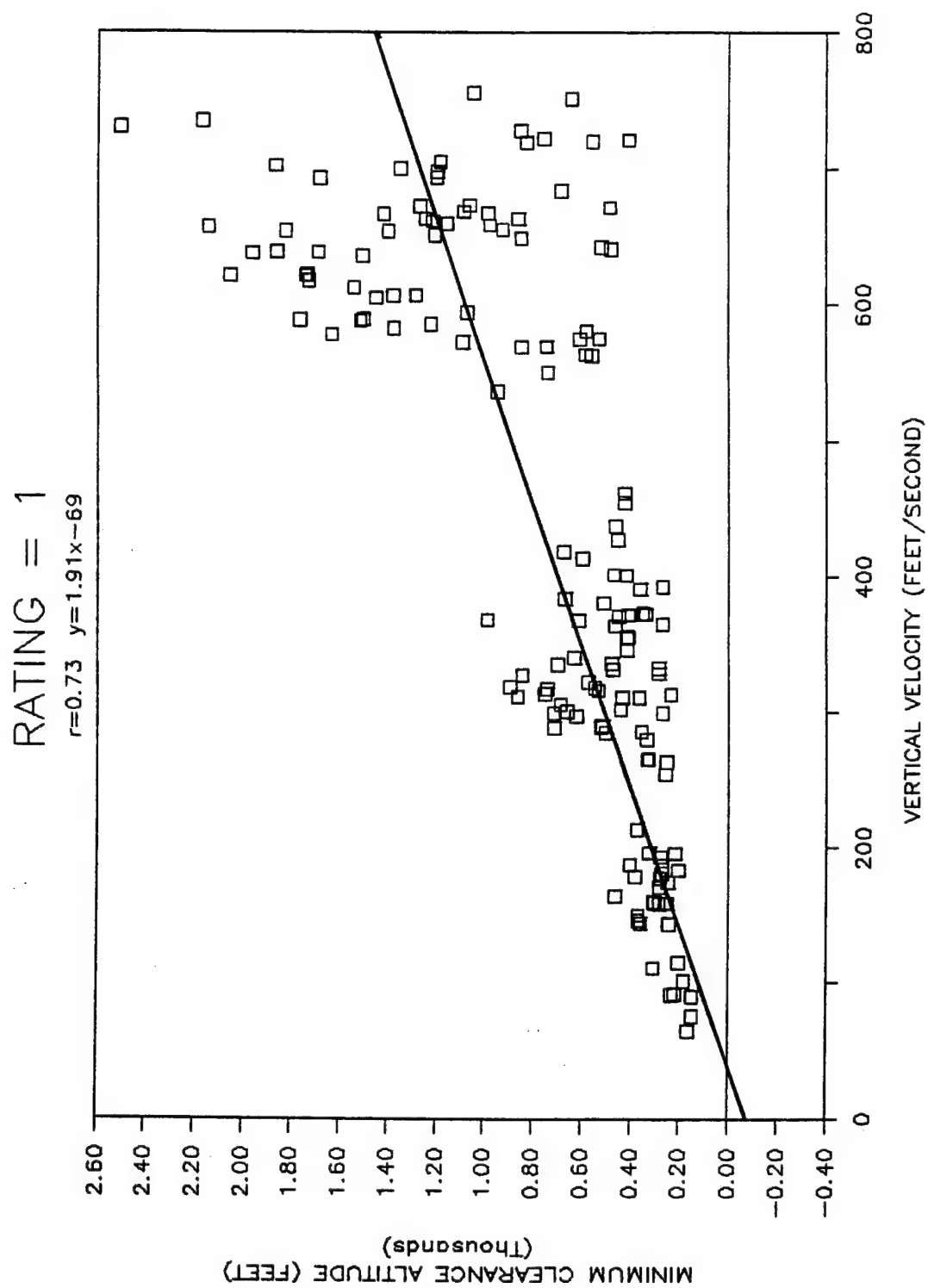


Figure 55. Minimum clearance altitude as a function of vertical velocity for pilots' subjective rating of 1 (too high).

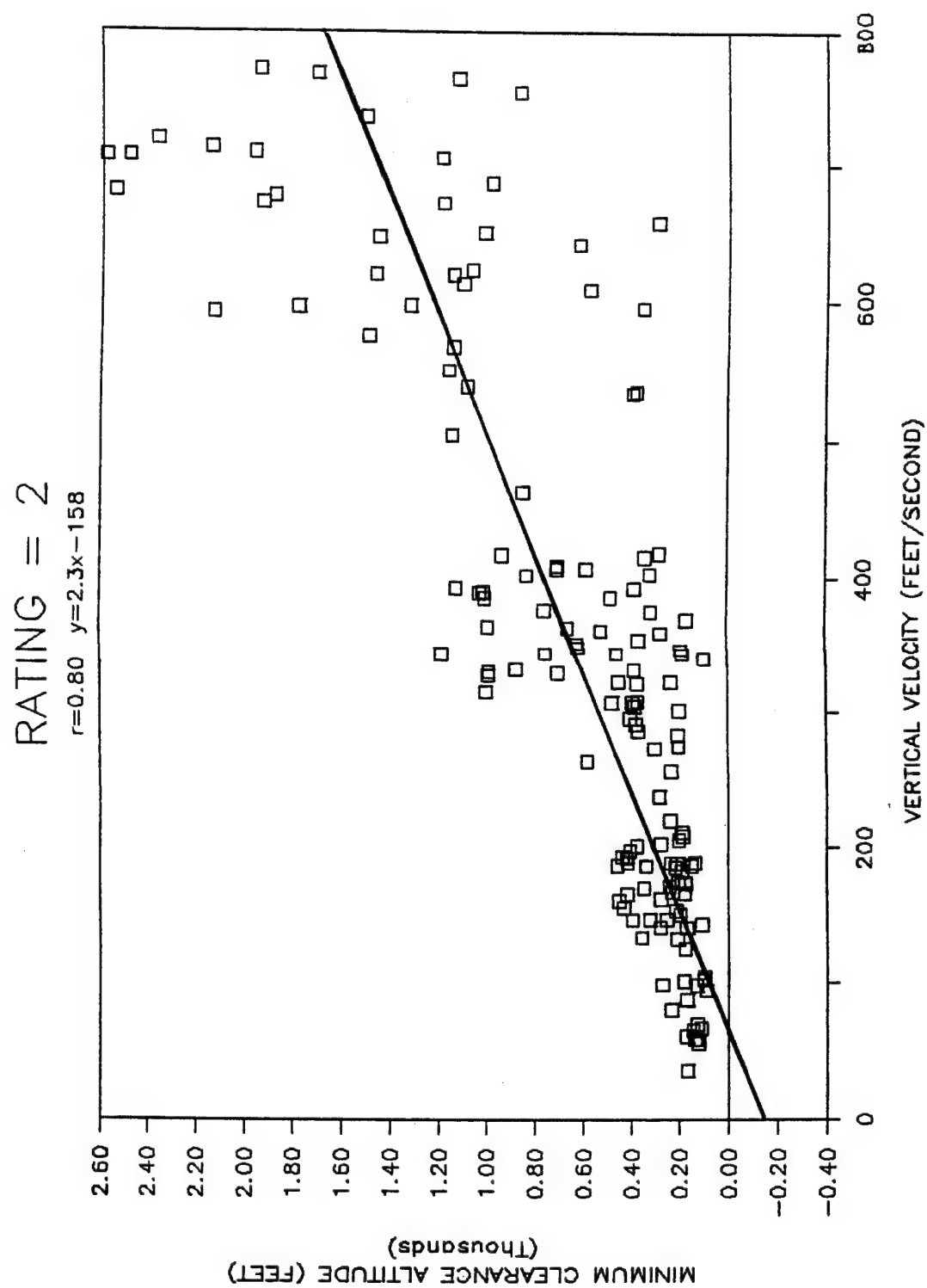


Figure 56. Minimum clearance altitude as a function of vertical velocity for pilots' subjective rating of 2 (slightly too high).

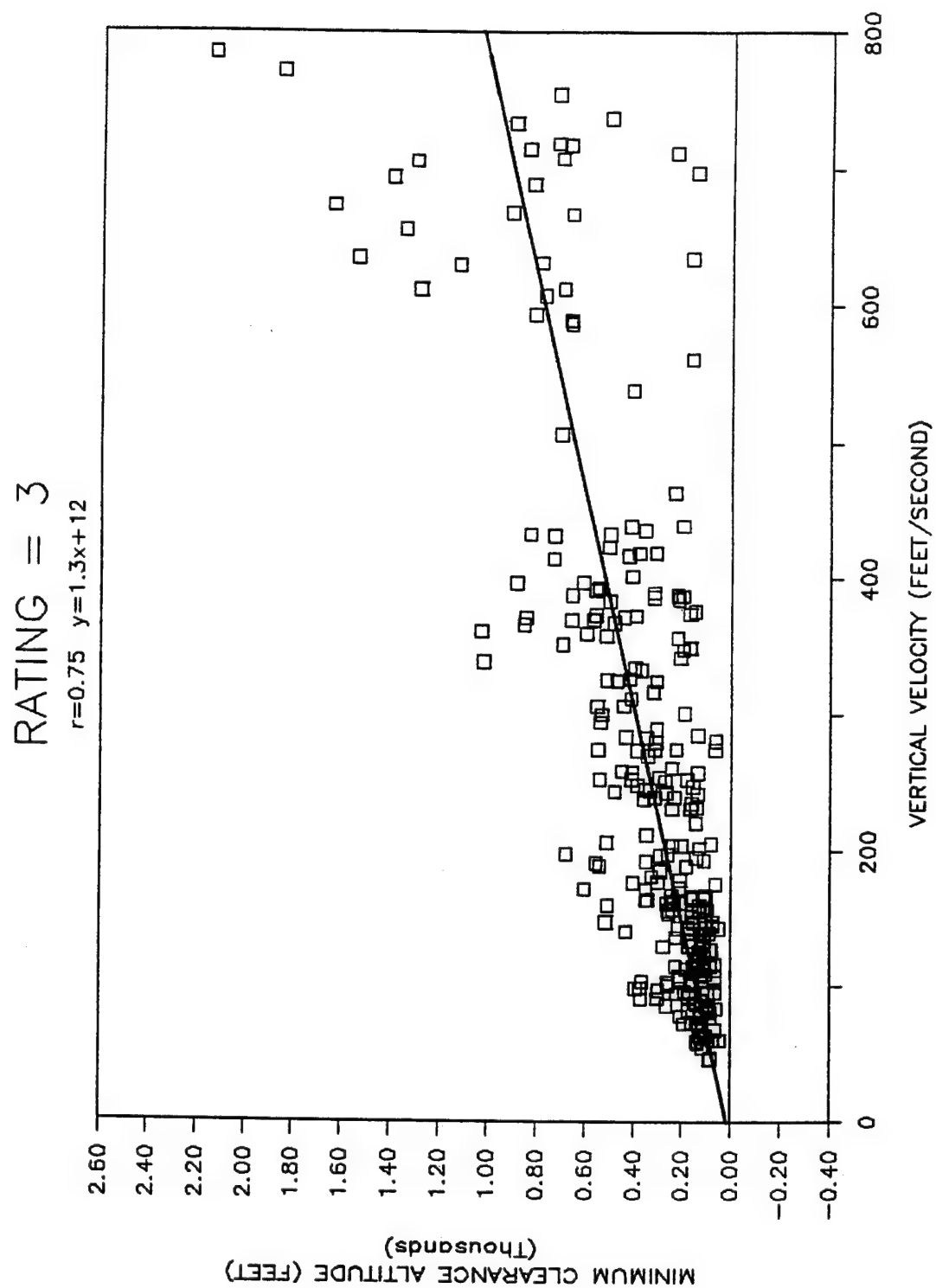


Figure 57. Minimum clearance altitude as a function of vertical velocity for pilots' subjective rating of 3 (about right).



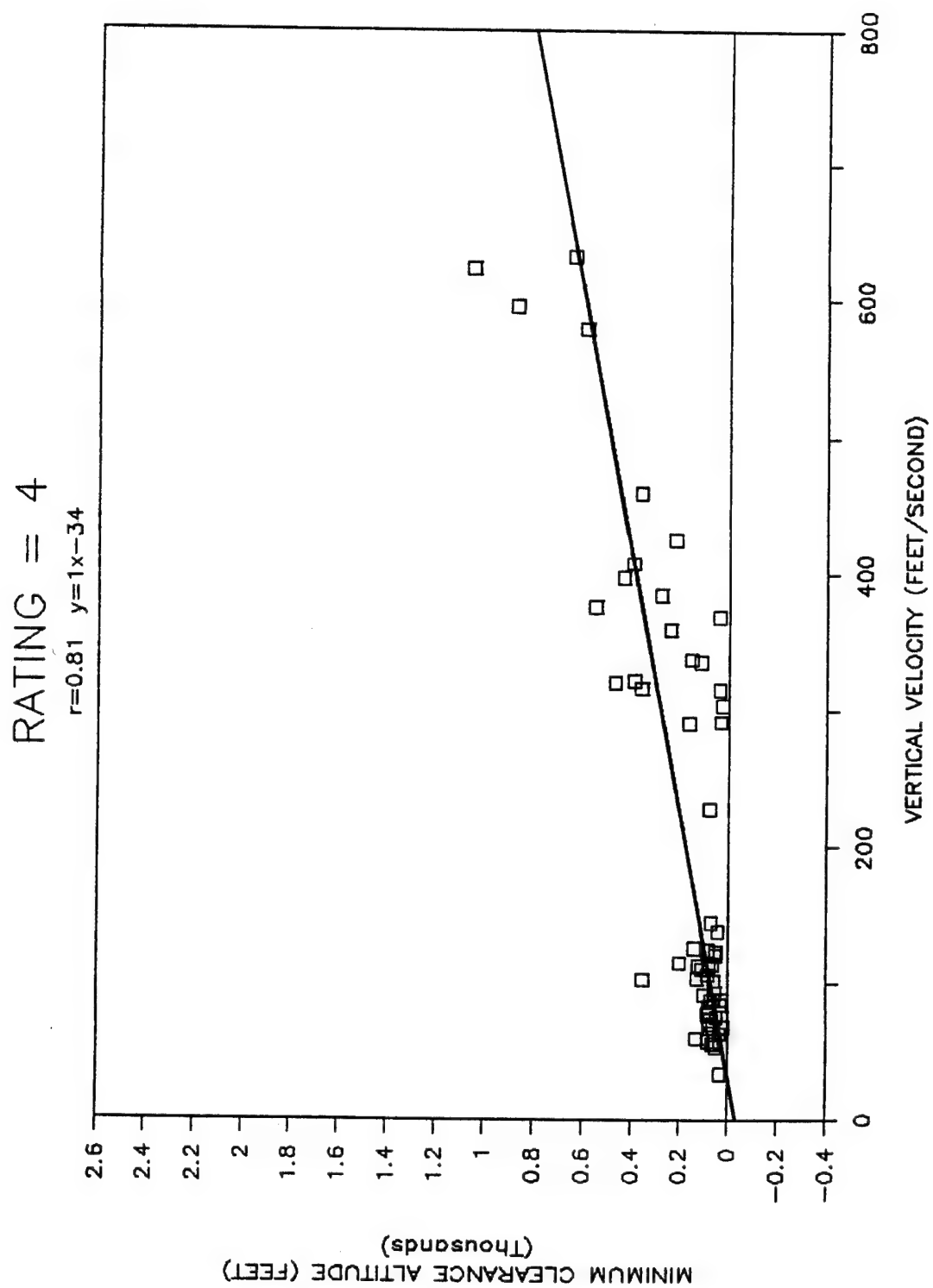


Figure 58. Minimum clearance altitude as a function of vertical velocity for pilots' subjective rating of 4 (slightly low).

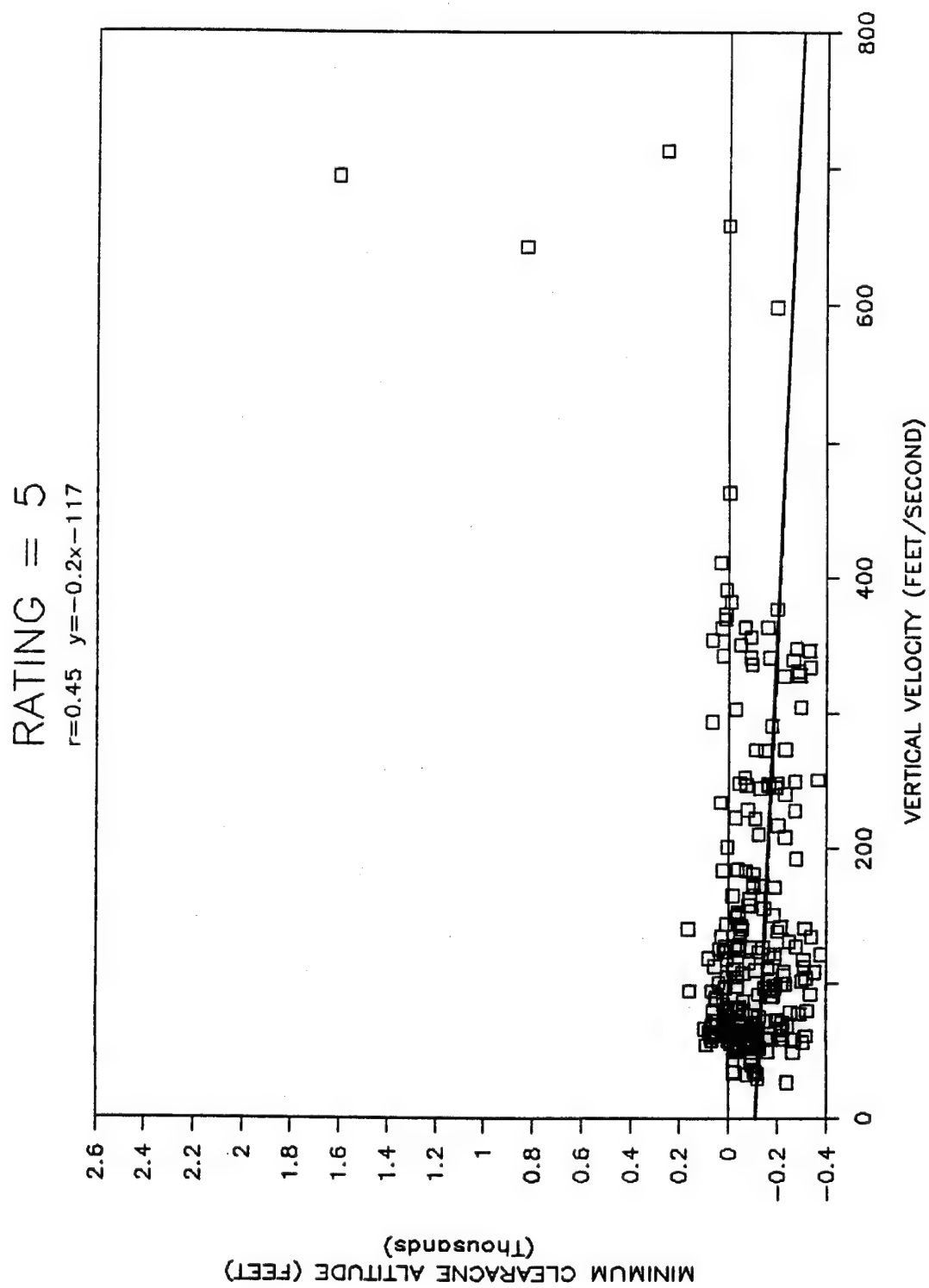


Figure 59. Minimum clearance altitude as a function of vertical velocity for pilots' subjective rating of 5 (too low).

Figure 55 contains the minimum clearance altitude as a function of vertical velocity for each trial's recovery altitude subjectively rated by the pilots as a 1 (too high). The subsequent Figures (56, 57, 58, and 59) describe the data compiled from the other four ratings. Overall high correlation coefficients indicate a strong relationship between the two variables of interest. However an inspection of Figure 60, representing the functions of each of the five ratings calculated by the regression analyses, suggested that while a distinction exists between ratings 5, 4, 3, and (1 or 2), no sensitivity was demonstrated by comparing ratings 1 versus 2. Therefore, ratings 1 and 2 were combined to form a new set of data, which is shown in Figure 61.

The regression lines from the two combined ratings (1 = too high and 2 = slightly too high) were used as the upper boundary, while the rating 4 (slightly too low) regression line was considered the lower boundary, for a pilot's subjective window of acceptability for GCAS recovery altitudes. Both regression lines were corrected in such a way that their zero-intercept points were at a recovery altitude of zero feet (as opposed to a negative value), and no minimum clearance altitude would be lower than 50 feet. Any minimum clearance altitudes that fall between the two boundaries consider the GCAS warning to be a "good" one, while values on top of the upper boundary would be considered false alarms. Any recovery altitudes lower than the lower boundary would be considered "too close for comfort."

In order to validate this acceptability window, function lines of pilots' performance data, sorted by the four terrain slopes (0, 6, 12, and 18 degrees), were calculated and plotted against the window. An inspection of Figure 63, which contains the performance data overlaid on top of the window, indicated that better than 90 percent of the recovery altitudes for terrain slope of zero fell within the acceptable window. Furthermore, terrain slopes of six and 12 degrees were acceptable for vertical velocities between 175 and 400 feet per second. At vertical velocities less than 175 feet per second, the warnings appeared to be initiated too late, while at greater than 400 feet per second the GCAS warnings were considered to be a nuisance. Finally, in accordance with the 18 degree terrain slope performance data analysis (covered in an earlier section), the majority of the GCAS warnings were initiated too late for an acceptable minimum recovery altitude.

# PREDICTED LINES FOR RATINGS 1 THROUGH 5

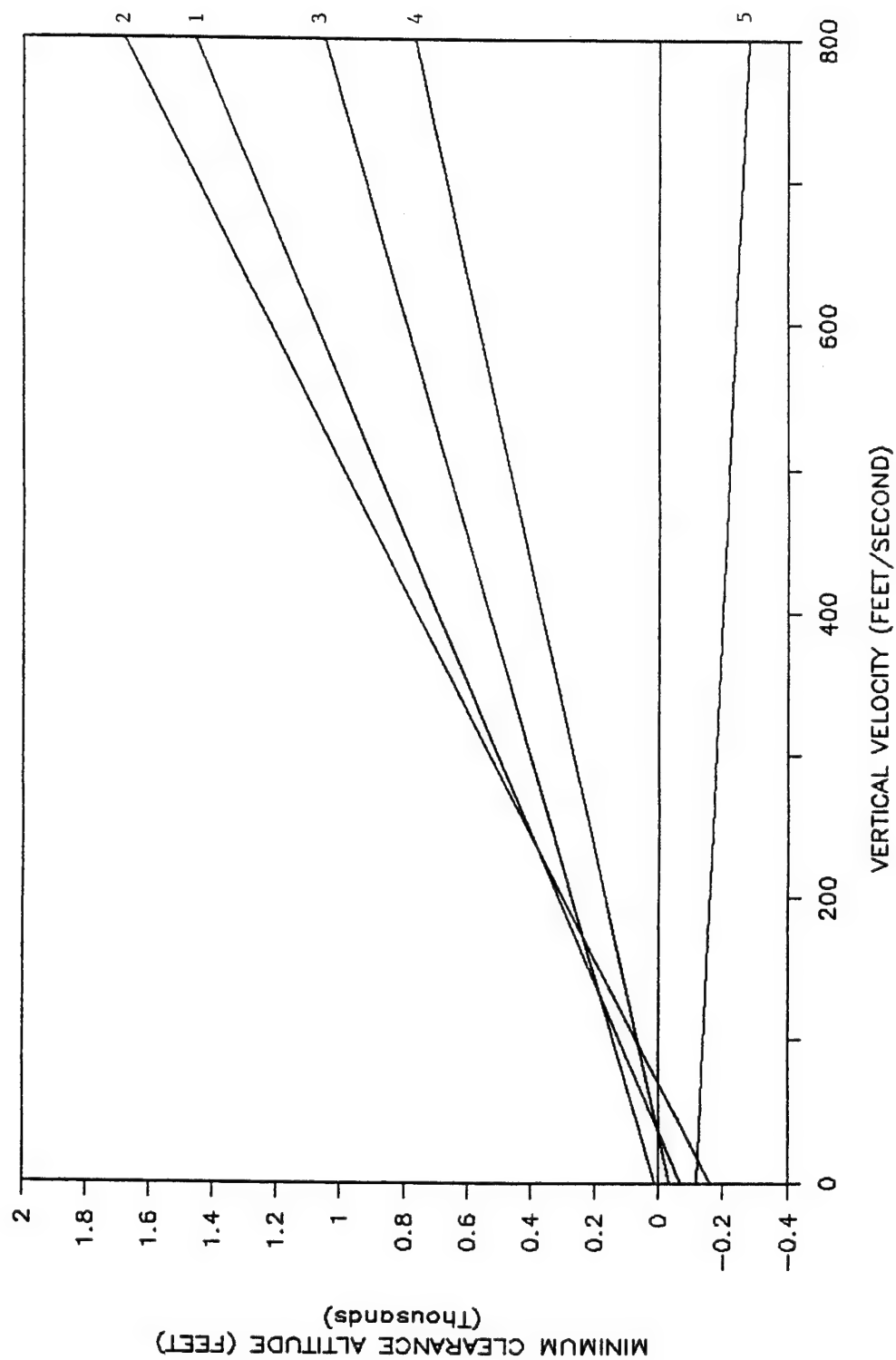


Figure 60. Predicted function lines for minimum clearance altitude as a function of vertical velocity for pilots' subjective ratings of 1 through 5.

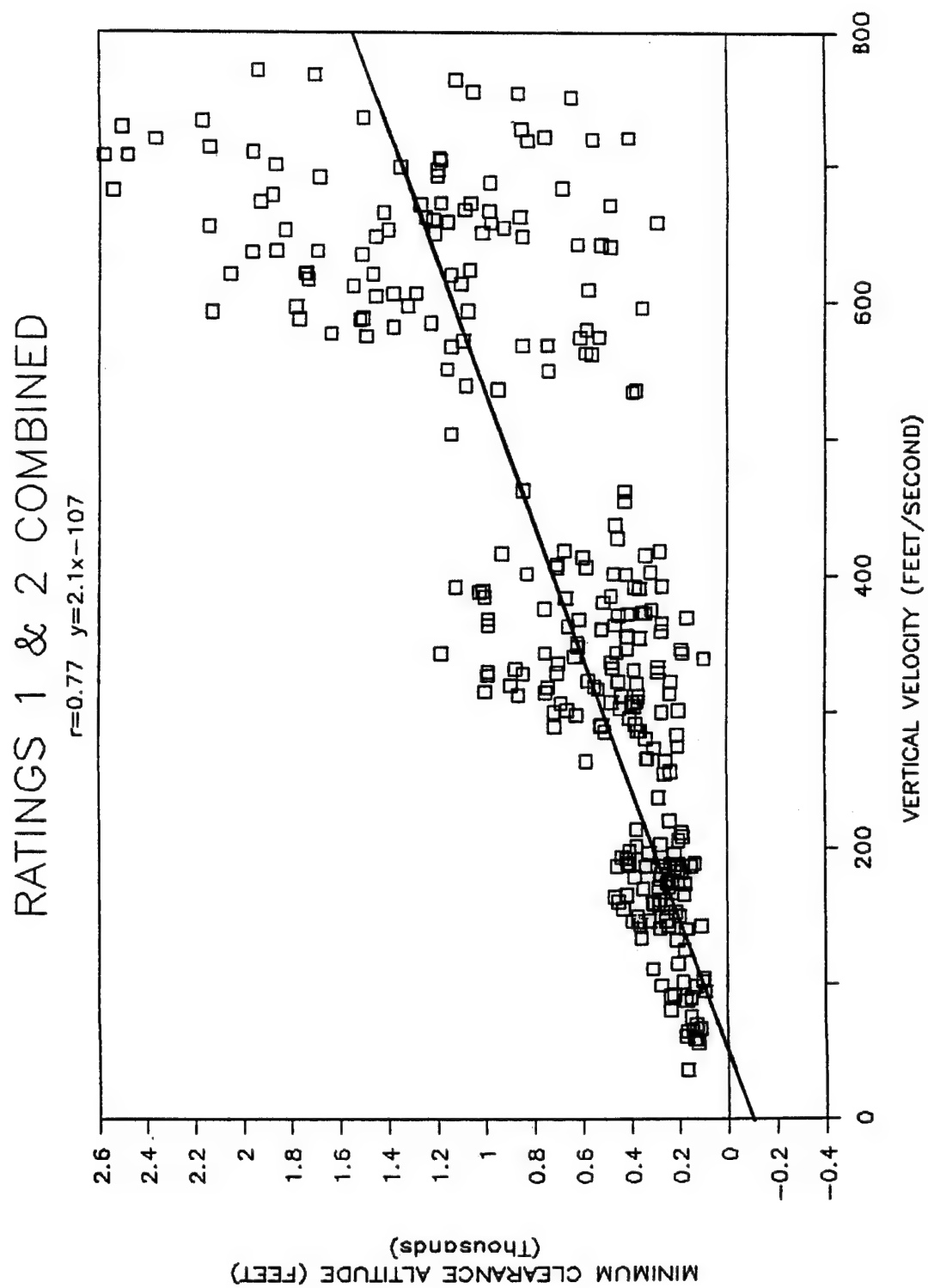


Figure 61. Minimum clearance altitude as a function of vertical velocity for pilots' subjective ratings of 1 and 2 combined.

# WINDOW OF ACCEPTABILITY

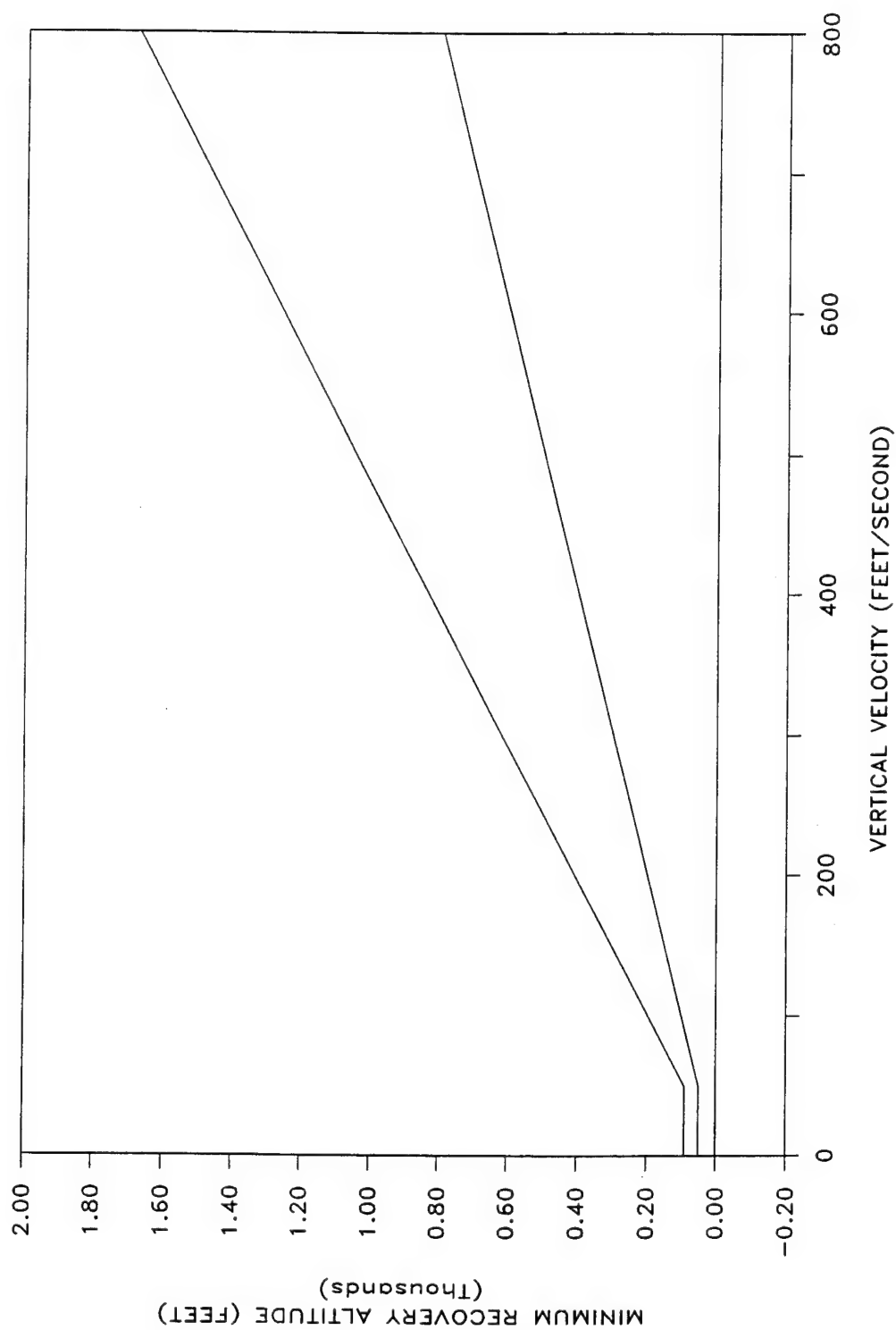


Figure 62. Pilots' Window of Acceptability based on pilots' subjective ratings.

# WINDOW OF ACCEPTABILITY

FOUR DIFFERENT TERRAIN SLOPE FUNCTIONS

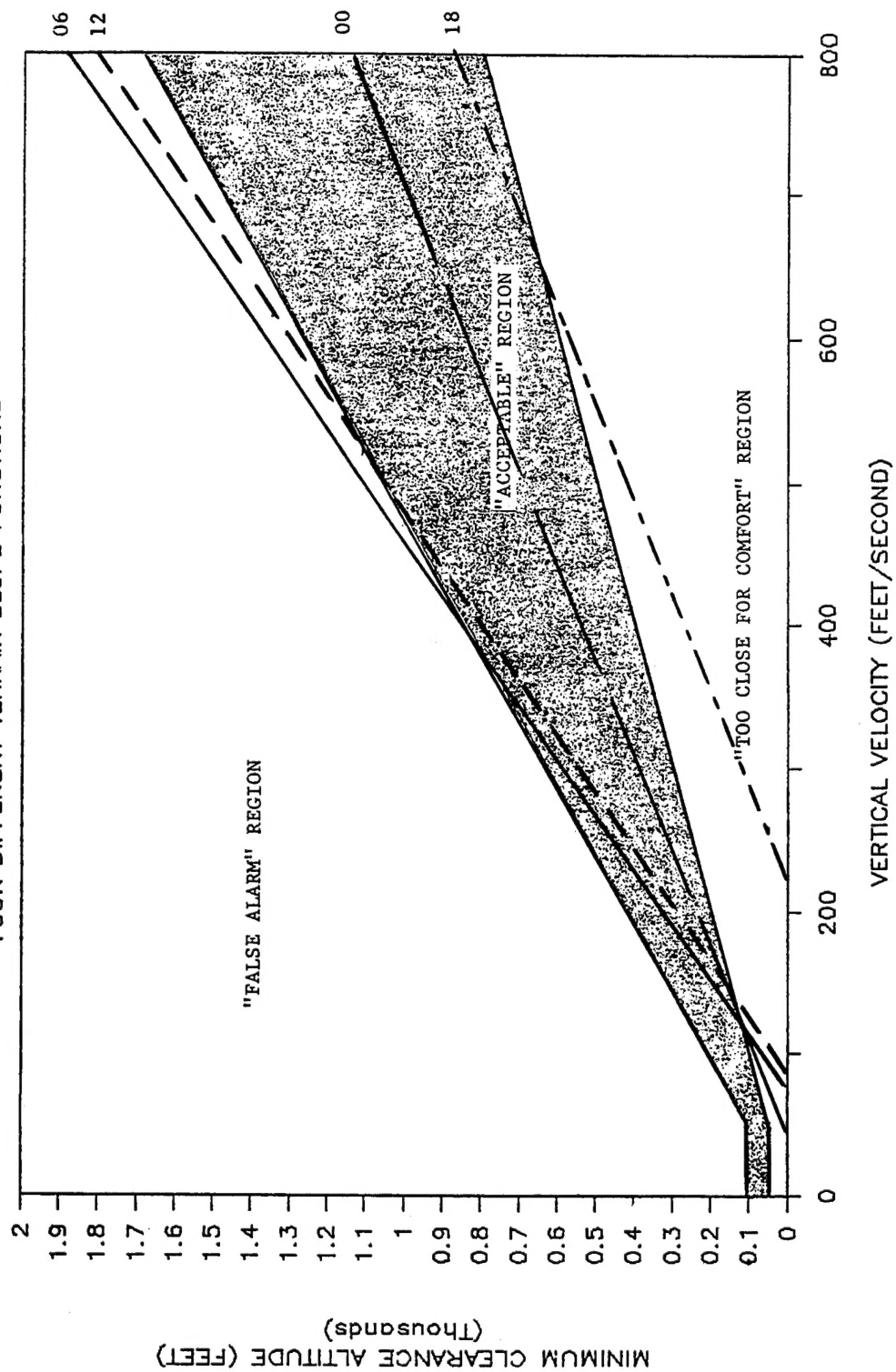


Figure 63. Function lines from the four terrain slope conditions overlayed on top of the Window of Acceptability.

### **Pilot Ratings Discussion**

This window should prove useful to the designers of the algorithm, in that it graphically describes the trend of the data and makes obvious as to which areas need additional development. Furthermore, the window will offer the SPO engineers a preliminary tool for evaluating the false alarm criteria set forth in the statement of work. The window of acceptability should be further developed by increasing the number of pilots participating in the evaluation, in order to provide a more representative subjective acceptance of pilots to GCAS warnings, and the warnings' relationships with minimum recovery altitude and vertical velocity.

### **Pilots Preferences on the Proposed GCAS Mechanization**

At the completion of the simulator trials, the pilots were presented with two different options related to the mechanization of the inter-message time of the GCAS ("Pull-up") warning. The subjects listened, while flying the simulator, to a second second and a one second inter-message presentation time in order to compare with the baseline condition used throughout the simulator evaluation (three seconds).

The last four pilots were also asked to evaluate three mechanization options associated with the presentation mode of the "Pull-up" warning. The first option involved illuminating the "RDR ALT LOW" red warning light along with the voice message. For the second option, a proposed yellow "GCAS" fail caution light located on the lower right caution panel of the FB-111 was illuminated along with the voice message "Pull-up." Finally, the third option, considered to be baseline, presented the pilots with the voice message "Pull-up" without any redundancy.

Five of the eight pilots preferred the two second inter-message-time presentation, with the other three pilots awarding two votes for the one second condition, and one vote for the baseline condition of three seconds.

All four pilots tasked to answer the second question elected the voice and "RDR ALT LOW" light as their preferred mechanization scheme. However, all four pilots commented on the fact that a flashing "RDR ALT LOW" light would be more of an "attention grabber" than the proposed steady light.

### **Discussion and Conclusion**

The GCAS algorithm was evaluated in three separate phases. Phase I attempted to verify and validate the sub-algorithms, and their relationship to HTOTAL. In Phase II, a pilot model was used to test the algorithm in the FB-111 simulator. The pilot model performed recovery maneuvers which were similar to those flown in Phase III. Phase III involved man-in-the-loop simulation. Following man-in-the-loop simulation, recommendations were made to GD regarding possible refinement of the algorithm. One of the primary difficulties encountered during the evaluation involved the unavailability



of performance criteria. Also, many questions remain which cannot be answered by the current support effort. One critical area of interest involves the usage of a window of acceptability in the evaluation of GPWSs on other aircraft (such as F-16). Can we generalize from the present results, or should a new set of data be collected on each individual aircraft? What about different pilot populations? The main argument of such a discussion is related to the fact that the response characteristics of different aircraft are not the same (for example, F-111 versus F-16). Furthermore, pilots tend to react differently based upon the type of aircraft they are flying. A comparison of F-111 and F-16 pilots would prove to be a useful evaluation in answering such concerns.

Another area of interest is the level of sophistication that could or should be exhibited by a GPWS algorithm. Current efforts have improved upon the older less sophisticated systems, which historically assumed that the world was perfectly flat all around, by attempting to predict and calculate the slope of the terrain and account for it in their calculations. Other efforts have focused on using a digital data base covering the terrain being flown over. Further research efforts, which have not been approached yet, should attempt to develop different algorithms for the type of mission or mode that the aircraft is currently flying. This type of information is currently available and could be obtained from the aircraft's own on-board computer.

## References

- DiPadua, M.A., Capt., Geiselhart, R., Gavern, J., and Lovering, P. (1988). Comparison of the General Dynamics Ground Clobber algorithm with the GCAS and Laws algorithms (ASD-TR-88-5022). Aeronautical Systems Division. Wright-Patterson AFB, Ohio.
- Cubic Defense Systems (1985). Feasibility demonstration of a Ground Collision Avoidance System (GCAS) (TR414-1). San Diego, CA.
- Orr, H., Major (1986). An evaluation of Ground Collision Avoidance System (ASD-TR-87-5040). Wright-Patterson AFB, Ohio.
- Shah, D. (1988). Ground Collision Warning Systems performance criteria for high maneuverability aircraft (ASD-TR-88-5034). Wright-Patterson AFB, Ohio.